The Tumor Suppressor RASSF1A Links Inflammation and Cancer

by

Marilyn Gordon

A thesis submitted in partial fulfillment of the requirements of the degree of

Doctor of Philosophy

in

Medical Sciences- Pediatrics

University of Alberta

Abstract

The tumor suppressor protein Ras association domain family 1A (RASSF1A) has roles in multiple signaling pathways including modulating apoptosis, the cell cycle, DNA damage, and microtubule organization. RASSF1A has been shown to be one of the most frequently epigenetically silenced genes in a variety of cancer types and thought to be one of the earliest changes in cancer development. Loss of RASSF1A has also been documented in approximately 26% of ulcerative colitis, a subset of inflammatory bowel disease (IBD) patients and 12-80% of colorectal cancer (CRC) patients. As IBD patients are known to be at an increased risk of developing colorectal cancer due to their chronic inflammatory disease, this study was to determine the molecular mechanisms whereby RASSF1A may influence the pathogenesis of inflammatory bowel disease and inflammation-associated colorectal cancer. We used acute and chronic mouse models of colitis-like inflammation and inflammation driven carcinogenesis brought on by addition of dextran sodium sulfate (DSS) in the drinking water.

Our results revealed a novel role for RASSF1A in restricting acute inflammation through inhibition of nuclear factor kappa B (NFκB) activation. Loss of *RASSF1A* resulted in exacerbated colitis symptoms and decreased survival in mice. Loss of *RASSF1A* also resulted in a novel tyrosine phosphorylation of Yes associated protein (YAP) on tyrosine 357 (pY357-YAP) to drive an aberrant transcriptional up-regulation of p73/YAP target pro-apoptotic genes, resulting in increased epithelial cell death,

inefficient epithelial repair, and poor survival of *Rassf1a*^{-/-} knockout mice following inflammation induced injury. Furthermore, under a chronic model of DSS-induced colitis-associated colon cancer, we observed that loss of *RASSF1A* accelerated tumor development/severity and poor survival of AOM/DSS treated *Rassf1a*^{-/-} mice. Loss of RASSF1A also led to dysregulation of YAP (a proto-oncogene) and YAP driven transcriptional regulation potentially contributing to the increased inflammation-driven carcinogenesis seen in AOM/DSS treated *Rassf1a*^{-/-} mice.

We propose a possible use of pY357-YAP as a biomarker of severe colitis with likely progression to colitis-associated colon cancer. In addition, the use of tyrosine kinase inhibitors (such as imatinib/gleevec) to restrict pY357-YAP and the abnormal up-regulation of pro-apoptotic genes in the absence of RASSF1A may also be beneficial in treating inflammatory diseases, especially in early onset of disease. Our observations will aid in a better understanding of the key molecular link between inflammation and cancer, the importance of the RASSF1A signaling pathway in restricting inflammation and the identification of potentially novel biomarkers of early onset disease. The identification of novel biomarkers of early onset disease will allow the rational design of useful therapeutics to reduce inflammation and interfere with inflammation driven-malignancies such as inflammation bowel disease pre-disposition to CRC.

Preface

This thesis is an original work by Marilyn Gordon. The research project, of which this thesis is a part, received research ethics approval from the University of Alberta Research Ethics Board, from ACUC:HS (Animal Care and Use Committee, Health Sciences) [Protocols AUP0000218 and AUP0000219], as well as the HREB (Human Research Ethics Board) [Protocols Pro00001523 and Pro00015569] for all studies.

The data analysis in chapters 4 and 5 as well as concluding statements are my original work, as well as the literature review in chapter 1. Portions of chapter 1 have appeared as published reviews as Gordon M and Baksh S, *RASSF1A: Not a prototypical Ras effector,* Small GTPases (2011, Jan); 2(3):148-157 [1] and Gordon M., El-Kalla M., and Baksh S., *RASSF1 Polymorphisms in Cancer*, Molecular Biology International. (2012, Jan), 1-12 [2]. For these manuscripts S. Baksh and I wrote the manuscripts and created the figures/tables. M. Kalla also aided in manuscript editing of [2]. The original research in chapter 3 of this thesis has been published as Gordon et al, *The Tumor Suppressor Gene, RASSF1A, Is Essential for Protection against Inflammation -Induced Injury* PLOS ONE, Oct 2013, vol. 8, issue 10, e75483 [3]. I was responsible for the experimental design, data collection and analysis, as well as the manuscript composition. S. Baksh was the supervisory author and was responsible for concept formation, experimental design, data analysis, and manuscript composition. N. Volodko was also responsible for manuscript editing and contributed experiments as indicated below. Additional experiments and analyses were performed by M. El-Kalla, Y. Zhao, C. Onyskiw, L. Liu, and others as indicated in the manuscript. In particular, M. El-Kalla and Y. Zhao aided in the experiments and data analysis covered in section 3.1, 3.2.1, and 3.2.2. Y. Fiteih contributed to section 3.2.4 in carrying out experiments and data analysis. N. Volodko contributed to experiments in sections 3.2.4 and 4.2.4. A. Thiesen was responsible for all histological scoring in chapters 3 and 4.

Dedication

To my family near and far- thank you for the ceaseless patience and support, without which I could not succeed.

Acknowledgments

This thesis would not be possible without the support, cooperation, and guidance of many people.

First, I would like thank Dr. Shairaz Baksh for providing support and guidance in research during my time in his laboratory. He has constantly encouraged me to think critically about scientific problems and to keep searching for the next question to continue my research. I would like to thank him especially for extra motivation when I needed it.

Next, I would like to thanks my supervisory committee members, including my co-supervisor Dr. Edan Foley, Dr. Eytan Wine, and Dr. Levinus Dieleman for guiding and supporting me during my studies. They have provided invaluable collaboration, suggestion, expertise, and resources without which my project could not have proceeded. I would also like to express my gratitude to my external examiners, Dr. Wallace MacNaughton from the University of Calgary, and Dr. Andrew Shaw from the Cross Cancer Institute, for considering my thesis. I would also like to thank all of our other collaborators, Dr. Aducio Thiesen, Dr. Richard Fedorak, Dr. Hien Huynh, and Dr. Marius Sudol for their contributions and input.

I am very grateful to have so many great friends and co-workers during my graduate study at University of Alberta. I would like to thank Mohamed El-Kalla, Yuewen Zhao, and Christina Onyskiw for helping with the initial phases of this research project. Many thanks to other past and present members of the Baksh Lab: Dr. Natalia Volodko, Yoke Fuan Wong, Jennifer Law, Tremayne Peart, Yahya Fiteih, Mohamed Salla, Ahmed Said, and Jody Bennett for your tremendous help and advice throughout my study.

Supervisory and Examining Committee:

Primary Supervisor: Dr. Shairaz Baksh, Department of Pediatrics, University of Alberta

Co-Supervisor: Dr. Edan Foley, Department of Medical Microbiology and Immunology, University of Alberta

Committee Member: Dr. Eytan Wine, Department of Pediatrics, University of Alberta

Committee Member: Dr. Levinus Dieleman, Department of Medicine, University of Alberta

Arm's length Examiner: Dr. Andrew Shaw, Department of Oncology, University of Alberta

External Examiner: Dr. Wallace MacNaughton, Department of Physiology and Pharmacology, University of Calgary

Table of Contents

List of Tables

List of Figures

List of Abbreviations

ABL	c-Abl oncogene 1, non-receptor tyrosine kinase
AKT	v-Akt murine thymoma viral oncogene homolog
ANOVA	Analysis of variance
AOM	Azoxymethane
APC	Adenomatous polyposis coli
APS	Ammonium persulfate
ASK	Apoptosis signal-regulating kinase
ATM	Ataxia telangiectasia mutated
ATP	Adenosine triphosphate
βTrCP	F-box/WD repeat-containing protein 1A
BAD	Bcl-2-associated death promoter
BAX	Bcl-2-associated X protein
BID	BH3 interacting-domain death agonist
BGS	Bovine growth serum
BH3	Bcl-2-homlogy domain 3
BME	Beta mercaptoethanol
BMDM	Bone marrow derived macrophages
bp	Base pair
BrdU	5-bromo-2'-deoxyuridine
BSA	Bovine serum albumin
C1 –	Protein kinase C conserved region 1
C19ORF5/MAP1S	Chromosome 19 open reading frame 5/microtubule-associated protein 1S
CD	Crohn's disease
cdc	Cell division control protein
cDNA	Complementary deoxyribonucleic acid
CRC	Colorectal cancer

CXCL	Chemokine (C-X-C motif) ligand
DAB	3,3'-Diaminobenzidine
DAG	Diacylglycerol
DAI	Disease activity index
DAP3	Death associated protein 3
DAPK	Death-associated protein kinase
DAPI	4'-6-Diamidino-2-phenylindole
DAXX	Death-associated protein 6
DEDD	Death effector domain-containing protein
DCF-DA	2′,7′-Dichlorofluorescin diacetate
DDB1	DNA damage-binding protein
DISC	Death inducing signaling complex
DMEM	Dulbecco's modified eagle medium
DMH	Dimethylhydrazine
DMSO	Dimethyl sulfoxide
DNMT	DNA methyltransferases
dNTP	Deoxynucleotide triphosphate - (dATP, dCTP, dGTP, dTTP)
DNA	Deoxyribonucleic acid
DSS	Dextran sodium sulfate
DTT	Dithiothreitol
ECL	Enhanced chemiluminescence
EDTA	Ethylenediaminetetraacetic acid
EGTA	Ethylene glycol tetraacetic acid
ELK	ETS domain-containing protein
ELISA	Enzyme linked immunosorbent assay
EMSA	Electrophoretic mobility shift assay
EMT	Epithelial to mesenchymal transition
EPV	Epstein Barr virus
ER	Endoplasmic reticulum

ERK1/2	AKA MAPK3/1; Mitogen-activated protein kinase, extracellular-signal-regulated kinase
GAP	GTPase activating proteins
GDP	Guanosine 5'-diphosphate
GEF	Guanine exchange factors
GI	Gastrointestinal
GM-CSF	Granulocyte-macrophage colony-stimulating factor
GRB2	Growth factor receptor-bound protein 2
GSK3	Glycogen synthase kinase
GST	Glutathione S-transferase
GTP	Guanosine-5'-triphosphate
GWAS	Genome wide association study
H&E	Hematoxylin and eosin
γH2A.X	AKA Phospho-H2A.X; H2A histone family, member X
HA	Hyaluronic acid
HAS	Hyaluronic acid synthase
HEPES	4-(2-hydroxyethyl)-1-piperazineethanesulfonic acid
HO-1	Heme oxygenase 1
HRP	Horseradish peroxidase
IAPs	Inhibitors of apoptosis
IB	Immunoblotting (Western blotting)
IBD	Inflammatory bowel diseases
IEC	Intestinal epithelial cell
IFN-γ	Interferon γ
IHC	Immunohistochemistry
IκBα	Nuclear factor of kappa light polypeptide gene enhancer in B-cells inhibitor, alpha, inhibitor of KB
IKK	Inhibitor of kappa light polypeptide gene enhancer in B-cells, kinase epsilon, IκB kinase
IL	Interleukin

IP	Immunoprecipitation
IRAK	Interleukin-1 receptor-associated kinase
JNK	c-Jun N-terminal kinase
kDa	Kilodalton
KO	Knockout
LATS	Large tumor suppressor kinase
LC3	AKA MAP1LC3A; Microtubule-associated proteins 1A/1B light chain 3A
LMP1	Latent membrane protein 1
LPS	Lipopolysaccharide
LRPPRC	Leucine-rich pentatricopeptide repeat containing
MAM	Methylazoxymethanol
MAP	Mitogen activated kinase
MAPKKK	MAP kinase kinase kinase
MCP1	Monocyte chemoattractant protein 1
MDM2	Mouse double minute 2 homolog, E3 ubiquitin-protein ligase
MEF	Mouse embryonic fibroblast
MEK	AKA MAPKK, MAP2K; Mitogen-activated protein kinase kinase
MERTK	c-Mer proto-oncogene tyrosine kinase
MMP	Matrix metalloproteinase
MOAP-1	Modulator of apoptosis 1
MPO	Myeloperoxidase
mRNA	Messenger RNA
miRNA	Micro RNA
MST1/2	AKA STK4/; Serine/Threonine kinase 4/3, mammalian sterile 20-like kinase 1/2
MTOC	Microtubule organizing center
MYC	v-Myc avian myelocytomatosis viral oncogene homolog
MyD88	Myeloid differentiation primary response gene

NaPP	Sodium pyrophasphate (Na4O7P2)
NE	Nuclear extract
NFκB	Nuclear factor of kappa light polypeptide gene enhancer in B-cells
NMR	Nuclear magnetic resonance
NOD	Nucleotide-binding oligomerization domain receptor
NORE	Novel ras effector
NOS	Nitric oxide synthase
NQO1	NAD(P)H dehydrogenase [quinone] 1
PAGE	Polyacrylamide gel electrophoresis
PAM	Petidylglycine α-amidating monooxygenase
PARP	Poly ADP ribose polymerase
PAWR	PRKC apoptosis WT1 regulator
PBS	Phosphate buffered saline
PDCD10	Programmed cell death 10
PCNA	Proliferating cell nuclear antigen
PCR	Polymerase chain reaction
PKB	Protein kinase B
PKC	Protein kinase C
PI3K	Phosphatidylinositol-3-kinase
PML-NBs	Promyelocytic leukemia protein nuclear bodies
PMSF	Phenylmethylsulfonyl fluoride
PRKC	Protein kinase C
PRR	Pathogen pattern recognition receptors
PTK	Protein tyrosine kinase
PTPN	Protein tyrosine phosphatase non-receptor type
PUMA	AKA BBC3, BCL2 binding component 3, p53 up-regulated modulator of apoptosis
PVDF	Phenylmethylsulfonyl fluoride

RA	Ras association domain
RAC	Ras-related C3 botulinum toxin substrate
Raf	v-Raf-1 murine leukemia viral oncogene homolog
RAPL	Regulator of adhesion and polarization enriched in lymphocytes
Ras	Rat sarcoma
RASSF1A	Ras association domain family member 1 isoform A
RIPK2	AKA RICK Receptor-interacting serine/threonine-protein kinase 2
RNA	Ribonucleic acid
RNAse	Ribonuclease
ROS	Reactive oxidative species
RPM	Revolutions per minute
RT-PCR	Reverse transcription-polymerase chain reaction
RUNX	Runt-related transcription factor
SAPK	Stress-activated protein kinase
SARAH	Salvador/RASSF/Hippo domain
SDS	Sodium dodecyle sulphate
SHC	Src homology 2 domain containing
SNP	Single-nucleotide polymorphism
SOS	Son of sevenless
TAE	Tris-acetate-EDTA
TAK	Transforming growth factor beta-activated kinase
Taq	Thermus aquaticus DNA polymerase
TBS	Tris buffered saline
TCF1	AKA HNF1 Homeobox A, transcription factor
TEAD	TEA domain family member
TGF	Transforming growth factor
TLR	Toll-like receptors
TMB	Tetramethylbenzidine

TNBS	2,4,6-trinitrobenzenesulfonic acid
TNF-α	Tumor necrosis factor alpha
TNFR1	TNF-α receptor 1
TNK2	AKA ACK1, Tyrosine kinase, non-receptor, 2
TP53	Tumor protein P53 (p53)
TP73	Tumor protein P73 (p73)
TUNEL	Terminal deoxynucleotidyl transferase dUTP nick end labeling
TRAIL	TNF-related apoptosis-inducing ligand
TRAF	TNF receptor associated factor
UC	Ulcerative colitis
UV	Ultraviolet
qPCR	Real time PCR
WNT	Wingless-type MMTV integration site family, member
WT	Wild type
XPA	Xeroderma pigmentosum, complementation group A
YAP	YES associated protein
YES	v-Yes-1 Yamaguchi sarcoma viral oncogene homolog

Chapter One: Introduction

1-1 Inflammatory Bowel Diseases and Colorectal Cancer

Inflammation is defined as " a protective tissue response to injury or destruction of tissues, which serves to destroy, dilute, or wall off both the injurious agent and the injured tissues. The classical signs of acute inflammation are pain (dolor), heat (calor), redness (rubor), swelling (tumor), and loss of function (functio laesa)" [4].Molecularly, inflammation is characterized by hyperactivation of transcription factors such as nuclear factor kappa B (NFκB), and elevated production of pro-inflammatory cytokines and chemokines upon activation of surface receptors [5-8]. NFκB signaling pathways regulate immunity and inflammation, and dysregulated and constitutive NFκB signaling has been implicated in several cancers in addition to inflammatory diseases [9-11].

NFκB dependent transcriptional activity can be induced by activation of pathogen pattern recognition receptors (PRRs), which may be membrane bound, such as Toll-like receptors (TLRs), or may be cytosolic intracellular receptors such as nucleotide-binding oligomerization domain receptors (NODs) [9,11-13]. TLRs may be expressed in the external cell membrane (TLRs 1, 2, 4, 5, 6, 11, and 12), or intracellularly in endosomal membranes (TLRs 3, 4, 7, 8, 9, and 13) [14]. PRRs recognize bacterial components and thus serve as our primary defense against pathogen invasion. In the canonical NFκB pathway, ligand activated TLRs, IL-1R, or TNFR1 activate NFκB p50/RelA transcription by transducing their activation signal through the MyD88 adaptor protein, which in turn directs IRAK proteins to complex with TRAF proteins. These in turn activate IKK to phosphorylate IκBα, which normally sequesters NFκB in the cytoplasm to prevent its transcriptional activation. Phosphorylation of IκBα targets it for degradation, thereby releasing the NFκB complex, allowing it to translocate to the nucleus and effect transcription [9,11,12].

An alternate NFκB pathway, termed the non-canonical NFκB pathway, is activated by a subset of TNFR receptors such as B-cell activation factor (BAFFR), CD40, receptor activator for nuclear factor kappa B (RANK), and lymphotoxin β-receptor (LTβR). Activation of any of these receptors leads to phosphorylation and activation of IKKα by NFκB inducing kinase (NIK). IKKα then phosphorylates p100 leading to polyubiquitination of p100 and its subsequent proteasomal processing to p52. p52 can then bind RelB, translocate to the nucleus, and activate transcription of NFκB target genes [9,11]. Finally, a third method of NFκB activation, termed the atypical NFκB pathway, exists, whereby activated NOD2 activates NFκB by binding to RIPK2 (aka RICK or RIP2, herein referred to as RIPK2), which in turn causes activates IKK/NEMO, and NFκB is freed from IκBα in the same manner as described above [11,13] (Figure 1.1). In the case of inflammatory bowel disease (IBD), it is thought that the initial activation of NFκB driven inflammation is through epithelial PPR sensing of a microbial breach of the mucosal layer.
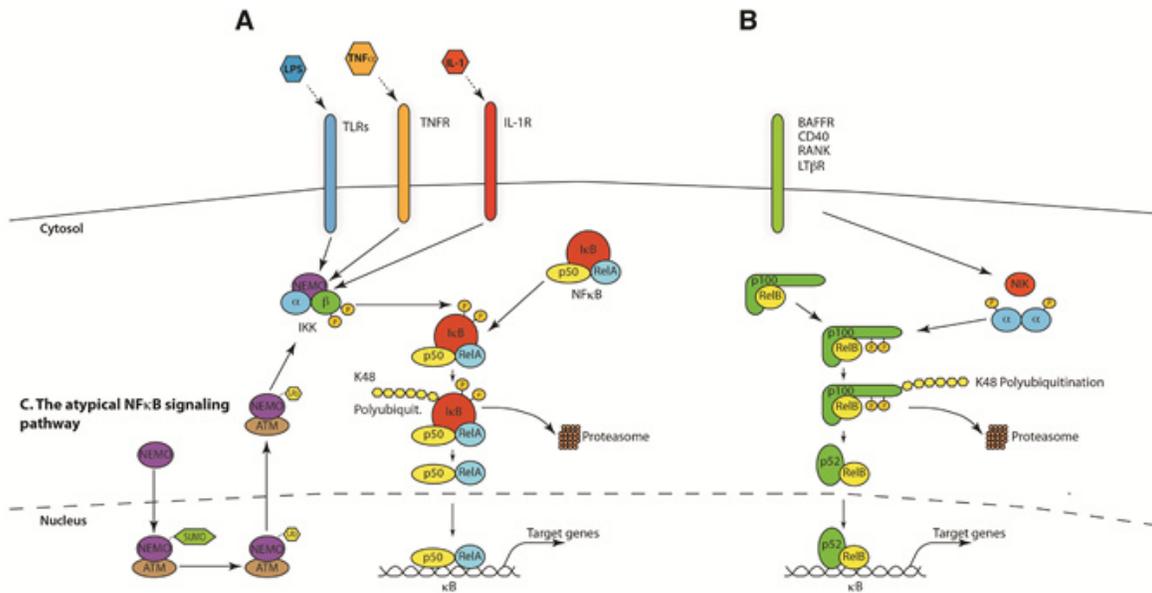
Figure 1.1: The canonical, non-canonical and the atypical NFκB signaling pathway. (A) In the canonical NFκB signaling pathway lipopolysaccharides (LPS), tumor necrosis factor α (TNFα) or interleukin-1 (IL-1) activate Toll-like receptors (TLRs), tumor necrosis factor receptor (TNFR) and interleukin-1 receptor (IL-1R), respectively. Through a variety of adapter proteins and signaling kinases this leads to an activation of IKKβ in the IKK complex, which can then phosphorylate IκBα on Serine residues S32 and S36. This phosphorylation is a prerequisite for its subsequent polyubiquitination, which in turn results in proteasomal degradation of IκBα. NFκB homo- or heterodimers can then translocate to nucleus and activate target gene transcription. **(B)** In the non-canonical NF-κB signaling pathway, activation of B-cell activation factor (BAFFR), CD40, receptor activator for nuclear factor kappa B (RANK) or lymphtoxin β-receptor (LTβR), leads to activation of IKKα by the NFκB-inducing kinase (NIK). IKKα can then phosphorylate p100 on serine residues S866 and S870. This phosphorylation leads to polyubiquitination of p100 and its subsequent proteasomal processing to p52.p52-RelB heterodimers can then activate transcription of target genes. **(C)** In the atypical NFκB signaling pathway, genotoxic stress leads to a translocation of NEMO to the nucleus where it is sumoylated and subsequently ubiquitinated. This process is mediated by the ataxia telangiectasia mutated (ATM) checkpoint kinase. NEMO and ATM can then return to the cytosol where they activate IKKβ. From Hoesel and Schmid Molecular Cancer 2013 12:86 doi:10.1186/1476-4598-12-86 (11)

Although normally beneficial, persistent inflammation can cause cellular damage resulting in the development of inflammatory diseases as well as several cancers. It has been documented that about 1/3 of all cancer cases are preceded by chronic inflammation [15-19], including chronic inflammatory bowel disease leading to colorectal or colon cancer. NFκB signaling in particular has been associated with inflammation-related cancers [9,11,20], and prolonged nuclear localization of NFκB may lead to anti-apoptotic and pro-proliferative signaling. Individuals suffering from IBD also have an increased risk of developing colorectal cancer later in life, although the exact mechanism for the progression from IBD to colorectal cancer is unknown. Inflammation has been shown to be associated with the development of cancer for several general reasons, including cellular damage causing release of reactive oxygen species (ROS), DNA damage promoting oncogenic mutations, growth factor release to promote proliferation, altered vascular permeability and angiogenesis, and the commandeering of immune cells to enhance tumor growth and prevent the normal identification and destruction of neoplastic cells [7,8,15,21-23].

Inflammatory bowel diseases (IBD) include Crohn's disease (CD) and ulcerative colitis (UC), and are chronic intestinal diseases affecting both pediatric and adult populations. IBD involves an excessive inflammation of the GI tract resulting in severe symptoms including weight loss, abdominal pain, rectal bleeding, diarrhea, and a general reduction in overall quality of life [24-28]. Crohn's disease is characterized by transmural inflammation that may occur anywhere along the gastrointestinal (GI) tract, from the mouth to the anus. Inflammatory involvement at the terminal ileum and the ileocecal junction is frequent in CD patients [29-31]. Stricturing, a narrowing of the intestine, often occurs in CD patients. CD patients tend to have patchy areas of inflammation, termed "skip lesions" which cause a "cobblestone" like appearance of the GI tract upon endoscopic examination [29,31-35]. Inflamed lesions in CD patients often also show organized infiltrative macrophage aggregates, termed granulomas, upon histological examination. Granulomas contain high levels of lymphocytic cells and neutrophils, occurring in chronic and sustained inflammation that has not been

effectively eradicated [34-37]. Crohn's disease can also be further classified by disease location, classified as: ileal, colonic, ileocolonic, and presence or absence of isolated upper disease, as well as general characteristics of the patient's disease: non-stricturing and non-penetrating, stricturing, penetrating, and presence or absence of concominant perianal disease. Together with age at diagnosis, these desriptive characteristics comprise the "Montreal Classification: for CD [38,39].

While UC is also a chronic inflammatory disease, for an unknown reason UC patients do not typically show granuloma formation as part of disease pathogenesis. While UC shares general symptomology with CD, inflammation is typically restricted to the rectum and large bowel. Ulceration in UC is continuous and shallow, often showing significant infiltrates of lymphocytes and neutrophils, and stricturing of the colon is not observed [36,37]. The pathogenesis of IBD has been shown to involve a disruption in the normal immune response, and therefore IBD patients often endure systemic symptoms of inflammation in addition to gastrointestinal symptoms, as the inflammatory and immune systems in the patient become further disordered. Systemic symptoms include skin rashes, joint inflammation and development of arthritis, eye inflammation, and mouth sores, and pediatric onset may result in growth retardation and delay in puberty [40-44].

Like CD, UC is also commonly organized into descriptive subtypes using the Montreal Classification. UC patients are classified first by inflammatory involvement: ulcerative proctitis (rectal involvement only), proctosigmoiditis (rectal and sigmoid colon involvement), left-sided UC (inflammation from the rectum to the splenic flexure), and pan-colitis (involvement of the entire large bowel); and then by disease severity: mild UC (diarrhea with or without blood less than four times a day), moderate UC (diarrhea with or without blood more than four times a day), and severe UC (bloody diarrhea more than six times a day, fever, and low iron) [38,39]. UC subtype diagnosis also contains a descriptor of the severity of the disease based on time: acute self-limiting colitis (usually

only applicable for enterocolitis caused by bacterial infection), colitis in remission, and long-standing colitis. These descriptive diagnostic categories help physicians determine the best treatment course for each patient.

IBD are highly prevalent in North America, particularly in Canada. Within Canada Nova Scotia and Alberta have the highest incidences of IBD [45], and Canada wide occurrences are continuing to increase [27]. In North America, incidence rates for IBD range from 2.2 to 14.3 cases per 100 000 person/year for UC and from 3.1 to 14.6 cases per 100 000 person/year for CD. In Alberta, the incidence rate for CD and UC is 16.5 and 11 cases per 100 000 person/year respectively [45,46]. IBD are particularly concerning chronic diseases as, unlike other chronic conditions, IBD often affects pediatric and young adult patients, whereas typical chronic inflammatory diseases do not occur until later in life. Research has also shown a significantly decreased quality of life for IBD patients due to illness burden, fatigue, cost burden, and a decreased ability to participate in social activities such as school and work [24-26,47]. Current standard therapy is extensive and often involves lifelong immunomodulating therapy [48-50].

Currently, the causes of IBD are unknown, but research suggests that IBD is caused by a combination of genetic predisposition, environmental influences (e.g. climate, diet), intestinal microbial disruptions, and immunologic dysfunction [33,35,37,49,51]. As a robust incidence of IBD among family members has been observed, it is unsurprising that genetic mutations have been shown to predispose individuals to IBD development [52,53]. Over 160 susceptibility genes have been identified as risk loci for IBD patients using genome wise association studies (GWAS) [52,54]. Unsurprisingly, the majority of identified genes are involved in immunomodulation, microbial sensing, epithelial restitution and barrier function, stress responses, and most recently, autophagic signaling [52]. However, genetic predisposition alone is not sufficient for development of disease as penetrance is never 100%, with even identical twins

showing parallel development of IBD in only 10-35% of cases where at least one twin has IBD [52].

Environmental influences may include factors such as geographic location, diet, exposure to pollutants, exposure to tobacco products, medications (antibiotics and oral contraceptives), and general hygiene to name a few [55,56]. Some environmental factors such as diet, hygiene, and geographic location may be linked to microbial influences, as changes in such factors may lead to a change or imbalance in the gut microbiota with pathogenic consequences. Some studies have suggested that IBD is more prevalent in the developed world, and particularly in urban areas, however this association is somewhat controversial [56,57]. Some medications such as oral contraceptives and inappropriate antibiotic use have also been associated with increased development of IBD [56,58,59]. Other environmental influences, such as pollutants and tobacco product exposure, are thought to contribute to disease development by irritating the colonic epithelium, which leads to ulceration and disruption of intestinal homeostasis [56,60,61]. Interestingly, tobacco use has been identified as a risk factor in CD patients, but appears to be protective in UC patients. Despite this, tobacco use is still not recommended due to other serious health detriments [52,56,62].

Intestinal homeostasis is crucial to the normal function of the bowel, and of particular importance is the makeup of the gut microbiota. A healthy population of typical gut microbiota, such as *Bacteroides*, *Enterococci*, *Lactobacilli*, and *Bifidobacterium*, add a layer of protection to the host by out-competing pathogenic bacteria in the colonization of a normal gut [63,64]. The gut microbiota also play key roles in nutrient absorption and metabolism, particularily in the conversion of dietary fibre into essential short-chain fatty acids. Gut microbiota also aid in the removal of toxic metabolic by-products and the metabolic breakdown of dietary lipids [63,64].

Dysbiosis, a dramatic alteration of the normal microbial population in the gut, has previously been associated with development of IBD [56,65-67]. IBD patients tend to have lower levels of gut *Firmicutes* and increased levels of *Bacteroidetes*, and may also have increased levels of pathogenic *Proteobacteria*. Pathogenic variants of *E. coli* have been associated with some cases of IBD, but are not necessary for disease pathogenesis [56,65,67]. It has been noted that overall, IBD patients tend to have higher levels of aerobic bacteria as opposed to the normal dominance of anaerobic bacteria in the gut population, leading some to pose an "oxygen theory" that changes in gut oxygen status may favor a shift from anaerobic to aerobic bacterial populations [67]. Dysbiosis has also been implicated in the development of colorectal cancer, with increased levels of *Bacteroides*, *Fusobacterium*, and *Campylobacter* species in CRC patients, along with decreased levels of *Faecalibacterium* and *Roseburia* [68]. Indeed, because the majority of our natural microbiota reside in the colon, it is unsurprising that major changes in normal microbe composition easily lead to diseases such as IBD and CRC. Early changes in microbiota composition lead to host responses that result in altered metabolism, altered tissue architecture, and altered immune signaling, all of which can result in disease states when persistant [64].

Normal intestine has a robust mucosal defense mechanism with three components: pre-epithelial, epithelial and post-epithelial [69,70]. The pre-epithelial barrier is a mucous layer composed primarily of mucins. This barrier acts as a barrier between host epithelial tissue and gut microflora, and acts as the primary defense against epithelial damage. The second barrier is the epithelial cell layer itself. The intestinal epithelium is composed of columnar epithelial cells tightly associated by tight junctions and adherens junctions. Tight junctions are composed of claudins and cytoskeletal actins, and adherens junctions are comprised of cadherins, a family of transmembrane proteins that bind intracellular catenins, which in turn bind to the actin cytoskeleton [69-71]. The last barrier layer is the lamina propria, which is located beneath the basement membrane and contains immune cells, including macrophages, dendritic cells, plasma cells, lamina propria lymphocytes and neutrophils [69-71]. IBD patients have been shown

to have reduced mucosal barriers, allowing microbes and other irritants to breach the epithelial barrier and activate an immune response [69,70,72,73]. IBD patients have also been shown to have alterations in their immune response systems which cause hyperactivation of the inflammatory reaction, and failure to properly restrict this reaction leads to disease pathogenesis [70,74,75].

Colon cancer, like IBD, shows dramatic changes in tissue architecture which cause changes in organ function. Early dysplastic changes in colon cancer include the appearance of aberrant crypt foci (abnormal clusters of small tube-like glands in the colonic epithelium) and polyps (tubular, tubulovillous, and villous- small projecting benign growths of epithelium), and generalized crypt hyperplasia. Later progression to adenocarcinoma appears as dense glandular tissue with highly condensed nuclei in the epithelial layer of the gut, while invasive carcinoma shows this dense glandular tissue encroaching into the mucosa and underlying muscle layers. Invasive colon carcinoma also often shows large necrotic bodies within the lumen of the cancerous glands as a defining feature [76]. Development of CRC may or may not present with symptoms such as blood in stools, dramatic changes in bowel habits, and bowel cramps. As these symptoms are also common in IBD CRC screening by endoscopy especially crucial for these patients [77].

Colon cancers and colorectal cancers (CRCs) are one of the leading causes of death in North America and Canada in particular [78-80]. While IBD associated CRCs oly comprise 1-2% of all colon cancer cases, having IBD is one of the highest risk factors for developing CRC besides having family history [77,81]. Colon cancer deaths account for 10-15% of IBD patient deaths, and therefore expanding our understanding of how these diseases are link in order to improve predicting and preventing CRC development in IBD patients is crucial [77,81]. In particular, a more aggressive inflammatory course of disease appears to be correlated with increased likelihood of dysplastic and neoplastic lesion development. This appears to be due to the increased accummulation of

oxidative damage at inflammed sites, which in turns causes an accumulation of DNA damage and a high level of cancer initiating mutations in an area with high epithelial cell turnover [77,81-83].

Another reason that we require a more in depth understanding of IBD-related CRC is that IBD-CRC shows a distinctly different molecular pattern of pathogenic alterations leading to full CRC development. In sporadic CRC, mutations of the APC gene are typically the earliest initiating change, followed by chromosomal aneuploidy and global methylation changes, K-Ras mutations, mutations in DCC, and lastly mutations in p53. In IBD-CRC, these changes occur in a different order: aneuploidy, methylation changes, and p53 mutations are the earliest detectable changes, followed by mutations in DCC, then mutations in K-Ras, and mutations in APC are one of the last observed events in IBD-CRC [77,84,85]. These major molecular differences between IBD-CRC and sporadic CRC illustrate the need to consider these cancers as separate diseases which need to be treated differently in affected patients.

In terms of IBD subtypes, UC patients tend to be at an overall higher risk for developing IBD-CRC than CD patients. UC patients having approximately up to a 9 fold increased risk of CRC, or up to a 23 fold increased risk in UC patients with pancolitis [81]. UC patients who also have primary sclerosing cholangitis (PSC), another inflammatory disease affecting the live bile ducts, are at a further 5 fold increased risk of developing CRC compared with the rest of the UC population, highlighting the inflammatory drivers behind IBD-CRC [81,86]. While the risk of IBD-CRC in CD patients overall remains controversial and is though to be negligable, it has been reported that patients with long-standing CD may be at similar risk for CRC development as UC patients [81]. CD patients are also at an increased risk for developing IBD-related small bowel cancer, with up to a 12 fold increased risk compared to the general population [81].

Pediatric onset of IBD particularly increases risk for colonic neoplasia later in life, as colorectal cancer risk in IBD patients increases approximately five percent for every ten years a patient has had IBD, with pediatric IBD patients having an average age of CRC onset at 40-50 years old, compared with 60-70 years of age in the general population [16-19]. According to Canadian Cancer Statistics, colorectal cancer is the 4th overall most common cancer in Canada, both in new cases per year and overall cases. Colorectal cancer is also the 2nd most lethal cancer in Canada [78,80]. Colorectal cancer most commonly develops in patients over the age of 70, but can develop in pediatric patients as well [16]. Although the predisposition to cancer has been well documented, the exact mechanism(s) involved are unknown.

IBD has a susceptibility locus at 3p21- the location of RASSF1A, our gene of interest [87]. One study has identified up to 26% of ulcerative colitis patients having lost RASSF1A expression through promoter hypermethylation [88]. These patients represented a small sample size of 19 UC patients undergoing routine endoscopy, with four females and fifteen males, with fourteen subjects under the age of 50 years and four subjects over the age of 50 years old. Subjects showing RASSF1A methylation were all under 50 years of age, and consisted of four men and one woman. One patient had early signs of dysplastic changes, however the other four patients appeared histologically normal and one patient reported a family history of IBD [88]., Loss of RASSF1A is well documented in a variety of cancers, including colon cancers [89-91], and for this reason, we chose to examine whether RASSF1A plays a role in inflammatory signaling, and whether RASSF1A function may provide a molecular link between chronic inflammatory diseases and the development of cancer. For our research, we used animal models of chemically-induced colitis and inflammation-associated colon cancer that recapitulate many of the symptoms and pathological changes seen in human IBD and CRC. An in depth review of several animal models of colitis and colitis-associated CRC are presented in the next chapter, followed by an introduction to the complex signaling protein RASSF1A.

1-2 Animal Models of Inflammatory Bowel Disease and Colorectal Cancer

Because the etiology of IBD and inflammation driven colon cancers is not yet fully understood, no one *in vivo* or *in vitro* model system exactly replicates any of the IBD diseases. In fact, due to the variety of potential genetic influences and environmental pressures, one single model will likely never be able to reflect the many facets of IBD. However, several animal models have been in use for the last 25 years which appear to mirror the symptoms, the pathological manifestations, and share some of the molecular signaling pathways important in contributing to inflammatory bowel disease states. While the exact cause(s) of IBD are not fully understood, it is generally recognized that a complex combination of genetic, environmental, immune, and microbial factors are at play, and it is therefore not surprising that the three most commonly used animal models of IBD are genetic, environmental, and microbial in nature.

Although rodent models of disease are exceptionally useful and have led to significant advances in our understanding of a variety of pathologies, we must keep in mind that every model system has its limitations. While there are numerous similarities between mammalian model systems and human physiologies, there will also always be species specific differences to account for. In particular, while retaining overall similar gastrointestinal and immune systems to humans, mice do have several important differences that must be taken into account when attempting to translate lessons learned in mouse models to human disease [92,93]. Human blood has a higher proportion of circulating neutrophils compared to lymphocytes, while mice have significantly higher proportions of circulating lymphocytes, with comparatively few neutrophils [93,94]. Anti-pathogenic peptides known as defensins are an important part of the initial innate immune response in both mice and humans in the GI tract and elsewhere, however, most defensins are produced by neutrophils in humans but by Paneth cells in mice [95].

Mouse neutrophils do not produce defensins at all, and while over 20 different types of defensins are produced by murine Paneth cells, only two are produced in the human equivalent [93,96,97].

Toll-like receptors, in particular TLRs 2,3,4, and 9 show different expression patterns in myeloid cells between humans and mice [93,98-100]. Murine macrophages do not express CD4 or MHC class II peptides while human macrophages do, and murine T cells and endothelial cells also lack MHC class II expression [93,101-104]. Activation of natural killer (NK) cells also appears to differ between the two species [92,93,105]. These differences suggest significant differences in how mouse and human immune systems deal with antigen sensing [93,106,107]. Several cytokine and chemokine differences also exist, with IFN having slightly different activating properties between species, and several chemokines being exclusive to either humans or mice, with no orthologous equivalent in the other species [93,108-111]. Nevertheless, while it is important to keep these immunological differences in mind, mouse models of inflammatory disease have proved invaluable to molecular studies and therapeutic investigations.

Genetic Models of IBD

There are a multitude of genetic rodent models of IBD at present, most of which utilize knockouts of genes known to be involved in pathogen sensing, inflammatory responses, immune regulation, and autophagy. It is not surprising that key molecules involved in inflammation and the immune response are key contributors to the development of overactive inflammatory disease. Knockout genetic models have been created in cytokines (e.g. IL-2, IL-10), in pathogen recognition receptors (e.g. NOD2, TLR2/4), and molecules involved in the activation of the adaptive immune response (e.g. TCR) [112-116]. Dysfunction of these factors have been identified in IBD patients in GWAS as well as genetic screening studies, lending to their credence of their use as

animal model systems, either alone (spontaneous disease), or in combination with chemical or microbial models [112,113,117-119].

One of the most commonly used genetic mouse model of inflammatory bowel disease is the *IL-10* knockout strain of mice. These mice were first described in 1993, and develop spontaneous colitis as early as three weeks old [120]. Interleukin-10 is an anti-inflammatory molecule produced by Th2-type cells as well as macrophages, B-cells, and keratinocytes, and down-regulates NFκB transcriptional activity and therefore restricts the inflammatory response [114,121-123]. IL-10 targets macrophages to down-regulate IL-12 production and also stimulates B-cell proliferation and antibody production in order to mount a humoral immune response [120,124]. IL-10 had previously been identified as a probable factor in the pathology of IBD, as IL-10 levels are frequently elevated in IBD patients, and mutations in both IL-10 and the IL-10R receptor have been identified in IBD patients, particularly UC patients, in genome wide association studies (GWAS) [125-127]. Additionally, IL-10 therapeutics have been somewhat effective in treating some IBD patients and reducing their overactive inflammatory response, although this effect was somewhat minimal [128-130].

IL-10$^{-/-}$ mice show normal B-cell and T-cell development and function with a normal antibody response, although they have some growth retardation and anemia compared to wild-type mice. Major organ systems in these mice appear to be normal with the exception of the GI tract and the hematopoietic organs. The *IL-10*$^{-/-}$ murine model most closely resembles human CD pathogenesis. Spontaneous inflammation of the GI tract occurs in the colon and small intestine in these animals, with areas of polyp-like hyperplasia as well as areas of dramatic ulceration, and progresses to an advanced state which is usually fatal around 30 weeks of age [120,114,124]. At 3 weeks of age approximately 69% of *IL-10*$^{-/-}$ mice show spontaneous inflammation, and by the age of 3 months, 100% of mice show spontaneous disease [114,123]. At 3 months of age 25% of *IL-10*$^{-/-}$ mice also show colonic adenocarcinoma, with 60% showing adenocarcinoma

development by the age of 6 months [114,123]. The growth retardation and anemia in these mice is thought to be due to an inability to properly absorb nutrients due to the excessive enterocolitis, and, combined with lack of proper nutrition, is thought to be the reason for the early mortality seen in these mice. Histological examination of the GI tracts of these mice shows inflammatory infiltrates and excessive fibrosis similar to human IBD patients, thus making these mice a genetic model for studying IBD [120,,124]. Interestingly, when *IL-10*$^{-/-}$ mice are raised in a germ-free environment, their spontaneous disease is diminished. Importantly, while a microbial trigger seems to worsen disease, *IL-10*$^{-/-}$ mice still develop spontaneous colitis in germ free conditions, highlighting that lack of IL-10 and the resulting normal immune response is the primary cause of disease in these mice [120,124,131].

Importantly, while IL-10 deficiency is certainly a strong driver of spontaneous colitis in this rodent model, there is evidence that other genetic pressures may also contribute to the appearance of disease in these mice. When *IL-10*$^{-/-}$ mice were generated on three different genetic backgrounds, differences in disease penetrance was seen at 3 months of age: *IL-10*$^{-/-}$ mice on the 129/SvEv background showed the most severe disease with 100% of mice showing severe colitis and 67% showing colorectal adenocarcinoma, *IL-10*$^{-/-}$ mice on the BALB/c background had 100% of mice with colitis and 29% with adenocarcinoma, *IL-10*$^{-/-}$ on the (original) 129/Ola 3 C57BL/6 background showed 100% of mice with disease and 25% with adenocarcinoma, and finally *IL-10*$^{-/-}$ mice on the C57BL/6 background showed the least severe disease with 57% of mice showing spontaneous colitis and none with adenocarcinoma [123]. This finding further illustrates the complex multi-factorial pressures that contribute to an environment permissive to colitis development.

IL-10$^{-/-}$ mice show an overactive Th1 immune response, with intestinal epithelial cells (IEC) recovered from these mice showing an excess of IFN-γ and IL-12 cytokines and an absence of IL-4, creating an over-enriched CD4+ Th1 and macrophage cell

population [114,122,123]. As the normal function of IL-10 is to down-regulate pro-inflammatory cytokines such as IL-1, IL-6, TNF-α, and NOS once an inflammatory response is no longer needed [121-123], it appears that the development of CD-like IBD in these mice is due to an inability to shut down pro-inflammatory signaling by the enriched Th1 cells and a lack of Th2 cells [114,122,123]. Additionally, increased levels of IFN-γ has been associated with increased gut permeability or "leaky gut", so it has been suggested that after an initial inflammatory response is mounted in response to a microbial insult, *IL-10^-/-* mice may also develop increased gut permeability as IFN-γ levels increase. As gut permeability increases, so too does the immune system's exposure to microbial insults, further perpetuating the inflammatory response and contributing to a pathogenic IBD phenotype [73,123,131]. A similar inappropriate immune response to intestinal microflora has also been seen in IBD patients [72,123,132]. Overall, the *IL-10^-/-* mouse genetic model of IBD has been especially useful in elucidating how the response and regulation of the immune system contribute to the development and resolution of IBD.

Chemical Models of IBD and CRC

In addition to the genetic pressures and predispositions that may contribute to the pathogenesis of IBD, there is also evidence for environmental influences. These may include factors such as geographic location, diet, exposure to pollutants, exposure to tobacco products, medications such as antibiotics and oral contraceptives, and general hygiene to name a few [52,55,56,133]. Some environmental factors such as diet, hygiene, and geographic location may be linked to microbial influences, as changes in such factors may lead to a change or imbalance in the gut microbiota with pathogenic consequences. Some medications such as oral contraceptives and antibiotics may also alter microbial balances as a side-effect [56]. Other environmental influences, such as pollutants and tobacco product exposure, are thought to contribute to disease development by irritating the colonic epithelium, which leads to ulceration and disruption

of intestinal homeostasis [55,56,134]. Chemical models of IBD and inflammation driven CRC work in a similar manner, primarily by evoking an inflammatory response by irritating the intestinal lining with erosive chemicals.

The most common means of chemically inducing colitis in rodents is the use of either 2,4,6-trinitrobenzenesulfonic acid (TNBS) or dextran sodium sulfate (DSS). TNBS causes epithelial ulcerative and necrotic damage, production of reactive oxidative species (ROS), and increased epithelial permeability [117,135,136]. TNBS has been successfully used as an acute model of colitis in mice, rats, and rabbits, all showing similar symptoms and histopathology to human IBD, in particular CD [137]. TNBS is administered by rectal injection, with doses between 0.5 and 6 mg per mouse, usually with a single dose being enough to induce acute local colitis. Similar to the genetic models of IBD, strain background differences reveal difference susceptibilities to TNBS treatment, with SJL/J mice showing the most severe disease, BALB/c mice showing disease susceptibility, and C57BL/6 mice having relative resistance and require a higher dosage to see colitis symptoms [138]. Due to the disease severity of the TNBS model, TNBS is typically used as an acute model of one inflammatory event [138] although chronic protocols have occasionally been used as well [113,139,140].

While the initiation of TNBS induced colitis is primarily due to the erosive nature of the TNBS/ethanol treatment and the resulting increased epithelial permeability, different gut microbiota and immune responses contribute to the disease progression [113]. For example, if protective microbes are present that produce polysaccharide A, such as *Bacteriodes fragilis*, they will induce IL-10 production and an anti-inflammatory response and rodents are more protected against TNBS-induced colitis [113,141]. There has also been evidence that one of the other mechanisms by which TNBS initiates inflammation and colitis like symptoms is through haptenation, whereby the TNBS reacts with host proteins to create reactive allergenic antigens and evoke an immune response [137,138,142]. As the hypersensitivity reaction continues, the mucosal T cells

appear to lose tolerance to normal mucosal antigens, further exacerbating the hypersensitivity immune response and furthering inflammation [119]. TNBS-induced colitis is a cheap and easy to reproduce chemical model of colitis.

Another common model of chemically-induced colitis is the commonly used DSS model system. DSS is a sulfated polysaccharide irritant that initiates inflammation by disrupting intestinal barrier function, not only directly irritating the mucosa but also increasing intestinal permeability and allowing microbes to cross the epithelial barrier [117,143-145]. The use of DSS in mice as a model for IBD was first described in 1990 by Okayasu et al [145] and has since become one of the most widely used model systems for studying the biochemical subtleties of IBD. Colitis is induced in mice by dissolving 1-5% DSS in the sole source of rodent drinking water, and colitis-like symptoms such as diarrhea, rectal bleeding, weight loss and general moribund posture can be seen as early as day three post application [145-148]. While the DSS model system has typically been thought to most closely resemble UC, several features of DSS induced colitis are also reminiscent of CD; therefore it is more accurate to describe DSS as a model of general IBD [113,147]. Features of DSS-induced colitis that are more consistent with CD than UC include the cytokine profile, the appearance of patchy focal lesions, the appearance of colonic granulomas, and fissuring ulcers [113,147].

As with other models described above, strain variety causes differing susceptibilities to DSS-induced colitis, with strains on the C3H/HeJ and Swiss Webster backgrounds [149] being the most severe, BALB/c mice and C57BL/6 mice being moderately severe, and 129/SvJ or Sv/Pas strains being relatively resistant [113,145-147,150]. An acute model of intestinal inflammation using DSS is typically generated by 5-7 days administration of DSS in drinking water and 2-7 days of recovery on regular drinking water, with the percentage of DSS and duration of exposure differing slightly between strains [145,147,148]. DSS is available in a variety of molecular weights, ranging from approximately 5-500 000 kDa. Different molecular weights have been shown to

have different effects on the severity of induced colitis, with mid-range (approximately 30 000-60 000 kDa) preparations inducing the most potent inflammatory response, and higher molecular weights showing no inflammatory induction. Low molecular weight DSS elicits a milder inflammatory colitis, and high molecular weight DSS does not appear to induce colitis [147,151,152]. One of the most beneficial features of the DSS model system is the ease with which a chronic model can be adapted from the acute model, which more accurately represents the fluctuating nature of human disease. Okayasu et al. first suggested exposure to DSS for one week followed by 10 days of regular drinking water, repeated for five cycles [145]. This protocol successfully resulted in the appearance of chronic intestinal inflammatory disease similar to human IBD, and other similar models have been developed by alternating periods of DSS exposure with periods of regular water for recovery [148,153-155].

The chronic DSS model of colitis is useful not only for studying chronic and recurring colitis, but also eventually results in inflammation-driven colonic carcinogenesis [145,146,154], making this an ideal model to study how inflammation can drive cancer development in the GI tract [113,137,148]. The use of DSS alone in a chronic model will result in adenocarcinoma development eventually, however latency varies vastly between strains, and is easily affected by DSS percentage and the exposure protocol followed [145,146,148,156,157]. Because tumor latency may be up to a year or more, when inflammation-driven carcinogenesis is a desired outcome, exposure to a known pro-carcinogen has been shown to accelerate time to tumor appearance as well as the number of lesions observed [146,148,156-158] The most commonly used carcinogen is azoxymethane (AOM), a metabolite of dimethylhydrazine (DMH) (another carcinogen used to induce colonic tumors), which is administered to the mice by IP injection at a dosage of 6-12 mg/kg [156]. A single injection of AOM is sufficient to accelerate tumorigenesis if administered prior to DSS exposure, and multiple injections of AOM do not appear to accelerate this effect [156-158]. AOM injection alone does not appear to generate significant colonic tumors when not followed with DSS treatment [157]. It has been shown that the active NFκB activity promoted by the DSS-induced inflammation

directly contributes to the development of CRC in the presence of AOM [156,159]. This has been successfully demonstrated to driven malignancy in a variety of wild type and genetic knockout animals.

DSS induced inflammation results in colonic ulceration, loss of goblet cells, infiltration of inflammatory cells into the lamina propria, and destruction of tissue crypt structure [145,147,148]. Inflammatory changes can be seen as early as Day 1 post DSS administration, with the loss of epithelial tight junctions and integrin expression as well as induction of pro-inflammatory cytokines [148,151,160,161]. As the epithelial barrier is destroyed, disease pathogenesis appears to be exacerbated by potential imbalances between apoptosis and proliferation, which can in turn increase epithelial layer permeability and allow further microbes to cross the gut barrier [3,147,162]. A recent study by Laroui et al. [163] demonstrated that DSS reacts with medium-chain- length fatty acids to form vesicles capable of fusing with colonic epithelial cells. A high fat diet increased the amount of medium-chain-length fatty acids available to form this DSS vesicle complex, illustrating that a high fat diet could aggravate the severity of DSS-induced colitis [163].

Both Th1 and Th2 cytokine profiles have been associated with DSS-induced inflammation [155]. Typically, acute DSS-inflammation is dominated by Th1-type cytokines (e.g. IL-1, IL-2, IL-12, IL-18, IFN-γ, TNF-α), moving toward more Th2 cytokine expression (e.g. IL-4, IL-5, IL-6, IL-10, IL-13, GM-CSF) as the condition becomes more chronic, although maintaining some Th1 cytokine expression [147,148,155,164]. While adaptive immune T and B cells have been shown to be dispensable for the development of DSS-induced colitis [165-167], new research highlights that the adaptive immune response, and T cells in particular, may play an important role in how DSS-induced colitis progresses, giving further relevance to the DSS system as a model for human IBD [147,168-170].

AOM requires metabolic activation prior to becoming actively carcinogenic. AOM is metabolically activated through hydroxylation [171-173], to produce its reactive metabolite, methylazoxymethanol (MAM), which is capable of methylating guanine to create mutagenic DNA adducts, and alkylating other molecules in the GI tract [156,171-174]. This metabolic activation has been shown to be primarily undertaken by cytochrome P450 enzymes such as CYP2E1, however, recent studies have implicated that other enzymes are also likely involved in the metabolism and activation of AOM [172,174,175]. AOM/DSS inflammation driven colon carcinogenesis pathologically resembles human CRC development with frequent K-ras mutations, mutations in β-catenin signaling molecules, cyclin D1 dysregulation, and c-MYC dysregulation. Unlike sporadic CRC, AOM/DSS mice rarely show APC or p53 mutations [156,175-178]. Dysplasia progression is similar to human colorectal tumor development, progressing through aberrant crypt foci to microadenomas, tubular adenomas, and finally full invasive carcinomas [156,179]. Additionally, tumors from mice exposed to AOM/DSS also show similar changes in the methylation status of many genes shown to be aberrantly methylated in human CRC [156,178,180-183].

Overall, the ease, versatility, and reproducibility of chemically induced models of colitis have made them a favorite among researchers. The acute and chronic DSS models in particular provide an excellent comparative model against which to further examine the effects of genetic and microbial factors.Chemical models of colitis are however limited in recapitulating human disease, as the primary mode of colitis induction is via direct epithelial injury. For this reason, chemically-induced models of colitis are considered to primarily model the wound repair response and inflammation resulting from epithelial injury. and will not fully model all aspects of human IBD.

Microbial Models of IBD

A complication that has been observed in all currently used mouse models of IBD is that inflammatory severity appears to be tied to microbial influences. Strain backgrounds have been noted to have differing penetrance to all IBD models, and while this is partially a genetic influence, it has also been shown that differing microbiota profiles between strains contribute as well [51,134,149,184,185]. Other evidence for the strong microbial pressures driving murine IBD can be seen in fecal transplant models, whereby exposure to feces/microbiota from sick mice transmits disease and/or exposure to feces/microbiota from healthy mice can cure sick mice [51,186]. Additionally, prebiotic (promoting the growth of healthy gut microbiota) and probiotic (live dietary microorganisms providing health benefits) therapies aimed at shifting gut microflora from a "pathogenic" state to a "healthy" or homeostatic state have also proved effective [187-192]. Likewise, in human IBD, there have been many documented cases of traditional and opportunistic pathogen contribution to enteric infection and development of IBD [193-195].

Two microbial models of IBD used in mice are infection with Gram-negative bacteria: *Citrobacter rodentium* (formerly *freundii*), or infection with *Salmonella typhimurium* [196-200]. Interestingly, infection of mice with *Salmonella* was successful in eliciting inflammatory disease only if the normal microbiota of the mice was first disrupted by pre-treatment with antibiotics, allowing the *Salmonella* to colonize the microbial cleared gut [196,201-204]. The *Salmonella* also need to exhibit pathogenic features in order to successfully colonize and infect mice: bacteria lacking a flagellum were unable to infect mice and create an inflammatory response [196,199]. In humans, *Salmonella* infection is more commonly associated with acute self-limiting enterocolitis rather than IBD, although an increased risk for developing IBD has been connected to *Salmonella* infection [196,200]. Because there is no direct implication of *Salmonella* in the

development of IBD, the *Salmonella* infection model is more useful for studying the effects of rapid onset pathogenic infections on gut physiology [196].

Oral infection of mice with *Citrobacter rodentium* has been reported to result in inflammation-related colonic hyperplasia and a Th1 immune response [198,205-208]. *C. rodentium* are inoculated into mice via oral gavage and rectal swabbed prior to inoculation and throughout the experiment to monitor infection. *C. rodentium* infection in mice closely resembles pathogenic *Escherichia coli* (EHEC and EPEC) infection in humans, with bacteria secreting a peptide called Tir (intimin) which allows adhesion to the host epithelial surface through the creation of attaching and effacing lesions [196,197,205,207]. The creation of attaching and effacing lesions involves destruction of the surface microvilli insertion of the Tir protein into the host epithelial cell and subsequent cytoskeletal rearrangements [197,205,207]. *E. coli* infection has been associated in some cases of IBD, and the molecular mechanisms underlying the *C. rodentium* model mirror those seen in human IBD [197,205,209]. Post-infection, colitis like symptoms such as diarrhea, rectal bleeding, and weight loss, can be seen in mice within several days, and histological evidence of inflammation such as inflammatory cell infiltrates, crypt destruction, and significant crypt hyperplasia are present [197,205,205].

In a similar manner to other rodent models of IBD, there are strain penetrance differences, with Swiss Webster mice showing infection and hyperplasia but little accompanying inflammation, and other strains showing significant inflammatory changes [198,208,210-212]. *C. rodentium* also elicits an NFκB pro-inflammatory response, with sustained elevated activation of NFκB throughout infection [198,206]. Not surprisingly, TLR4, a pathogen sensing receptor that is activated by LPS secreted by Gram-negative bacteria, and MyD88, an adaptor protein that activates NFκB upon TLR4 activation, have shown to be important in the induction of an inflammatory response in the C. rodentium model [198,213,214]. Similar to the DSS model, infection with *C. rodentium* has also been shown to cause increased gut permeability and disruption of tight junctions,

further perpetuating the inflammatory response and likely contributing to the extreme diarrhea often seen in infected mice [198,215-217]. An important difference that is seen in the *C. rodentium model* in comparison to the DSS model of colitis is that due to the inflammatory cause being primarily bacterial, an adaptive immune response with T and B cell involvement is crucial in *C. rodentium* pathogenesis. Infection by *C. rodentium* to mice deficient in T or B cells is therefore fatal, highlighting the importance of the adaptive immune response in the *C. rodentium* model [198,218-220]. The *Citrobacter rodentium* model is an easy to use system that is excellent for studying host responses to pathogenic bacteria and the contribution of these bacteria to the development of colitis.

For our research, we elected to use the DSS model of colitis in order to study whether the signaling protein RASSF1A played any part in regulating intestinal inflammation. Furthermore, as RASSF1A is a known tumor suppressor protein frequently lost via epigenetic promoter hypermethylation in cancers, we also utilized the AOM/DSS model of inflammation-driven carcinogenesis in order to determine if and how RASSF1A may provide a molecular link between chronic inflammatory disease and the development of cancer. The next chapter provides an in depth summary of our current understanding of the many functions of RASSF1A.

1-3 RASSF1A: A Complex Signaling Molecule

Disclaimer: The reviews in this chapter has been previously published elsewhere as "Gordon M and Baksh S, *RASSF1A: Not a prototypical Ras effector,* Small GTPases (2011, Jan); 2(3):148-157" [1] and "Gordon M., El-Kalla M., and Baksh S., *RASSF1 Polymorphisms in Cancer*, Molecular Biology International. (2012, Jan), 1-12" [2].

"RASSF1A: Not a prototypical Ras effector"[1]

A Short History of Ras Signaling

The Ras superfamily of proteins contains over 100 members that are GTP-regulated molecular switches for signaling pathways involving cellular processes as diverse as proliferation, migration, cell death and differentiation. The Ras signaling pathway has been the subject of intense investigation since it was first characterized in 1993 [221]. Shortly after this discovery it was determined that this pathway is highly conserved in *Drosophila*, *S. cerevisiae* and *C. elegans*. Three main Ras GTPase isoforms exist in mammals that are commonly targeted for germline mutations in several cancers: H-, N-, K-Ras (isoforms 4A and 4B). Other prominent members of the Ras GTPase superfamily include Rap1 (involved in integrin signaling), Rho (involved in neuronal signaling) and the Rac family of GTPases (the latter of which have additional roles in cytoskeleton reorganization) [222]. Activating mutations in the Ras oncogenes account for about 30% of germ-line mutations in human cancers. In addition, it is known that abnormal Ras signaling, resulting from genetic changes in Ras oncogenes and Ras upstream activators or downstream effectors, can contribute to the origin of about 70% of all human cancers. Therefore, an understanding of Ras signaling is of vital importance to the origin of cancer and in designing new targets for treating human malignancies.

Ras proteins are strategically positioned at the inner surface of the plasma membrane, at the endoplasmic reticulum (ER) and there is recent evidence for Ras activation at the Golgi complex [222]. It is now well established that membrane association of Ras is a requirement for its biological activity regulated by membrane proximal events involving the molecular switch of Ras-GDP to Ras-GTP (Figure 1.2). Extracellular signals promote the GTP loading of Ras2 by recruiting and activating the Ras guanine exchange factors (GEFs). Reversal of Ras activation is achieved by the actions of the Ras GTPase activating proteins (GAPs). GTP-Ras undergoes a conformational change in switch regions I and II in order to promote the association of downstream effectors [222]. Growth factor receptors such as the prototypical epidermal growth factor function primarily to promote this conformational change in Ras in order to initiate a signal cascade to the cytoplasm and eventually to the nucleus.

Growth factor stimulation results in the auto-phosphorylation of the cytoplasmic domain of these receptors that functions to prime the recruitment of signaling molecules SHC, Grb2 and the GEF SOS (Figure 1.2). SOS functions to switch Ras-GDP to Ras-GTP and activated Ras can in turn activate the serine/threonine kinase, Raf, the first characterized downstream effector of Ras. Raf then activates downstream kinases such as the mitogen activated kinase kinase kinase (MAPKKK) to continue the signal cascade to mitogen activated kinase kinases (MEK1 and MEK2) and then to the MAP kinases, extracellular regulated kinases (p44/ERK 1 and p42/ERK2). ERKs then translocate to the nucleus to activate transcription factors such as ELK-1 allowing them to acquire DNA binding competency. Once activated, ELK-1 can drive transcription of genes important to growth and proliferation. Collectively, the components above are part of the well studied Ras-Raf-MAPK pathway, a highly conserved universal growth signaling pathway.
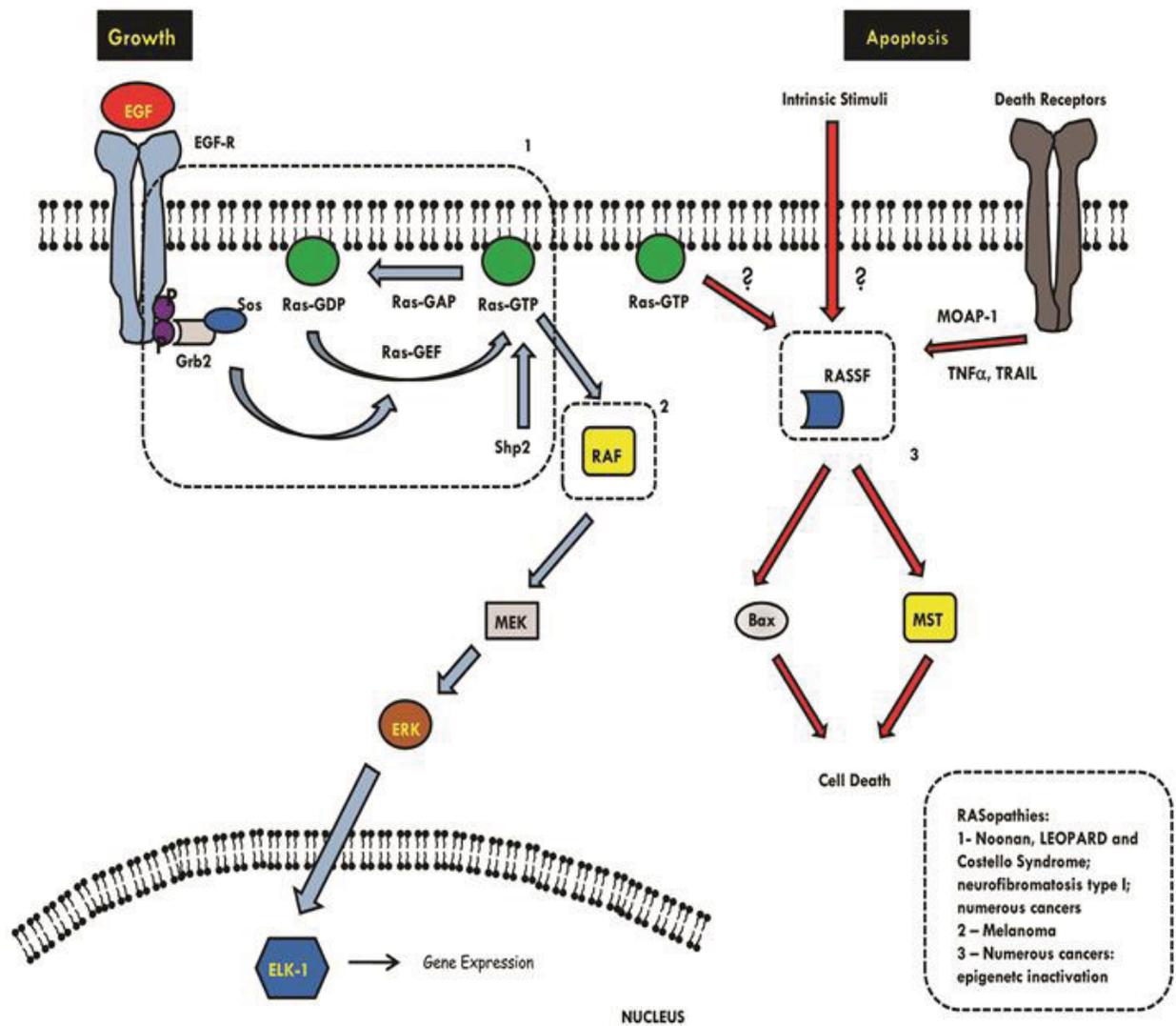
Figure 1.2: A simplified model of Ras signaling. Ras signaling pathways originate from growth factor binding and activation of its receptor such as the epidermal growth factor [EGF] binding to its receptor, EGF-R. The activation of the EGF-R by EGF primes the autophosphorylation of the cytoplasmic domain of EGF-R (P) and the recruitment of adapter proteins, Grb2 and Sos. Sos is a primary Ras-GEF that will promote GTP loading of Ras and subsequent Ras activation. Ras can then continue the signaling cascade to Raf-MAPKK (MEK)-MAPK (ERK) and eventually to the activation of the transcription factor Elk-1. Once activated by phosphorylation, Elk-1 can then acquire DNA binding competency to activate gene transcription to drive proliferation. Elk-1 is just one of many transcription factors modulated by Ras signaling and is only shown here for simplicity. There is evidence for Ras activation of cell death and it is thought to proceed through the RA SSF family of proteins. In the bottom right corner of this figure is a limited list of diseases that are a direct result of abnormal Ras signaling (the RASopathies).

27

The RAS opathies: diseases resulting from abnormal Ras signaling.

The Ras-Raf-MAPK pathway functions as one of the main effector pathways of Ras to regulate growth. As such, this pathway is also one of the primary targets for genetic changes resulting in the RASopathies, syndromes caused by abnormal Ras signaling [222-224].These syndromes are well characterized as melanomas (B-Raf mutations and loss of RASSF1A expression), lung and pancreatic cancers (mutations in K-Ras and loss of RASSF1A expression), Noonan syndrome (mutations in PTPN11, K-Ras, SOS and Raf-1), LEOPARD syndrome (a syndrome similar to Noonan syndrome having mutations in PTPN11 and Raf-1), neurofibromatosis (NF) type 1 (mutations in the NF1, a Ras-GAP), Costello syndrome (mutations in H-Ras) to mention a few [223,224]. PTPN11 encodes the non-receptor protein tyrosine phosphatase SHP-2, a phosphatase that is required for activation of Ras and other signaling cascades such as the Jak/Stat and insulin receptor pathways [225].

Mutations in H-Ras and N-Ras are also very prevalent in numerous human cancers that can effectively promote uncontrolled Ras-dependent activation. As such, there has been and continues to be considerable interest in searching for a "drugable" target within the Ras-Raf-MAPK pathway that may suppress or inhibit the growth promoting effects of these mutations. To date, most efforts have failed to specifically target this pathway without toxic side effects. The major limiting factor has been target specificity for the tumor cell while avoiding inhibiting a functional Ras-Raf-MAPK pathway in surrounding normal cells. Ras function is complicated in that it is involved in numerous biological processes; regulated by multiple growth factors, GEFs and GAPs; activated in different membrane compartments (plasma membrane, ER, Golgi complex) and by multiple isoforms of Raf, MEK and ERK leading to the activation of numerous transcription factors. The combined permutations of these variables produce very distinct Ras signaling pathways that, if dysregulated, can result in the occurrence of the RASopathies (Figure 1.2).

Ras and Apoptosis: An Unresolved Debate

There is no debate as to the significant role that Ras plays in growth control and proliferation and how this is important for the appearance of malignancy. It is well documented that sustained activation of active Ras is required for tumor development and for tumor cells to avoid apoptosis [226]. Over-expression studies, the presence of Ras mutations and mouse genetic knockouts of Ras family members have all proven that Ras has a robust role in growth control. However, considerable debate remains as to the importance of Ras in cell death or apoptosis, a concept that is counter-intuitive to its role in promoting cellular growth. It has been reported that, depending on the cell type and environment, Ras can be anti-apoptotic or pro-apoptotic. There is speculation that in normal cells Ras may be up-regulated to promote protective pro-apoptotic responses in order to prevent tumorigenesis. Ras can mediate an anti-apoptotic effect by the activation of phosphatidylinositol 3-kinase (PI3K) and AKT/PKB that will in turn phosphorylate BAD and sequester BAD to 14-3-3. Bad is a pro-apoptotic member of the Bcl-2 family of apoptotic regulators. This event will relieve the BAD inhibition of Bcl2 or Bcl-xL resulting in an anti-apoptotic response [227,228]. In addition, the activation of AKT/PKB can also phosphorylate IκBα kinase (IKK) and subsequently activate NFκB to promote survival. This is mainly carried out by promoting the transcription of anti-apoptotic proteins such as inhibitors of apoptosis (IAPs). Therefore, AKT/PKB and NFκB pathways activated by Ras will promote survival and thus provides examples of how Ras can intersect with signaling pathways to provide an anti-apoptotic role.

Several reports suggest that upon growth factor withdrawal Ras can promote apoptosis via a Ras/Raf/MEK/ERK pathway [228]. This has been observed for IL-3 withdrawal in the pro-B cell BaF3 [229] and serum rich media withdrawal in 3Y1 rat fibroblasts [230]. Furthermore, in T-lymphocytes, IL-2 or antigen receptor stimulation can activate Ras and drive cellular proliferation. However, if proper co-receptor stimulation

does not occur, Ras activation can lead to apoptosis [231]. Furthermore, over-expression of activated Ras in T-cells can lead to increased expression of Fas ligand and increased cell death most likely via autocrine stimulation of Fas ligand [227,232]. Thus, both excessive Ras activation and growth factor withdrawal can promote cell death in a Ras dependent manner. This may suggest that under conditions of abnormal homoeostasis, Ras functions in a "protective" manner to remove the cell by apoptosis in order to prevent the inheritance of abnormality. These examples illustrate the controversial nature of the influence of Ras signaling on apoptosis and how little is known about the molecular mechanisms that link Ras to cell death.

The RASSF family of proteins brought excitement to an aspect of Ras signaling that needed some answers, that is, the role of Ras in apoptosis. As mentioned earlier, the RASSF family of proteins have an RA domain that can potentially associate with Ras. However, unlike most Ras effectors, the RASSF family of proteins lack catalytic activity and function as adaptor proteins that can regulate multiple signaling pathways including two (and maybe more) apoptotic signaling pathways. The association of Ras with RASSF family of proteins suggested that we had finally found a Ras effector that required Ras association in order to promote apoptosis. Ten family members exist that contain an RA within the N-terminal (RASSF7–10) or C-terminal region (RASSF1–6) of the primary sequence [233,234]. RASSF5A was initially named novel Ras effector 1 (NORE1) and RASSF5B is a splice variant of RASSF5 that was independently identified as RAPL, regulator of adhesion and polarization enriched in lymphocytes [235]. RASSF9 was originally named P-CIP1, petidylglycine α-amidating monooxygenase (PAM) C-terminal interactor 1 as it associated with the C-terminus of PAM.

Reports from numerous laboratories suggest that the RA domain may not be utilized equally by all RASSF family members. We have summarized the Ras association studies with RASSF family members in Table 1.1. What is revealing is that there are contradictory reports of Ras association with RASSF1A. If this association

does occur it is with active K-Ras indirectly through heterodimerization with RASSF5A [236]. We have not observed RASSF1A association with N-, H-, K- or R-Ras association either with wild type or active mutants of these Ras proteins (unpublished observations). We support the studies by Ortiz-Vega et al. (2002) [236] suggesting that Ras association with RASSF1A is indirect and weak. In contrast, convincing data does exist for the ability of RASSF2, 4, 5 and 6 to associate with the active forms of H-Ras and K-Ras (Table 1.1) [237]. For these associations, Ras proteins aid in the ability of the RASSF proteins to induce cell death, reduce colony formation (and thus growth stimulating potential) and reduce tumor formation in nude mice. RASSF9 is the only N-terminal RASSF family member that has been shown to associate with N-Ras, K-Ras and R-Ras by co-immunoprecipitation experiments [237]. The ability of the other N-terminal RASSF members to associate with Ras has yet to be tested.

Table 1.1: Summary of what is known about Ras association with the RASSF family of proteins

RASSF family member	Associated RAS isoform	Cell type and condition	References
RASSF1A	H-Ras G12V: only in the presence of RASSF5A/ Nore1A K-Ras V12 association promotes RASSF1A/MOAP-1 association K-Ras WT associates very weakly with RASSF1A and this was lost with the K-Ras V12/Y40C mutant R-Ras can associate with RASSF1A	(1) COS-7 cells, over-expressed Flag-RASSF1A and GST H-RasG12V (2) 293-T cells, over-expressed HA-RASSF1A, Myc-MOAP-1 and Ha-K-Ras 12V or HA-K-Ras 12V/Y40C	Vos et al. (2006)[248] Rodriguez-Vician et al. (2004)[237] Disputed in Ortiz-Vega et al. (2002)[236]
RASSF1C	H-Ras (G12V) but not with H-Ras (E37G) or Ras (C186S)	(1) 293-T cells, over-expressed RASSF1C and H-Ras G12V; (2) In vitro: MBP-1C (RA) and H-Ras (GTP) form	Vos et al. (2000)[551] Disputed in Ortiz-Ortiz-Vega et al. (2002)[236]
RASSF2	K-Ras 4B (G12V)	293-T ells, over-expressed HA K-Ras 4B (G12V) and Flag-RASSF2	Vos et al. (2000 and 2003)[551, 230] Donninger et al. (2010)[288]
RASSF3, 7, 8, 10	Not tested		
RASSF4	K-Ras G12V	293-T cells, over-expressed FLAG-RASSF4 with HA-K-Ras G12V	Eckfeld et al. (2004)[552]
RASSF5A/Nore1A	H-Ras (G12V) >>> Ki-Ras No H-Ras N17 association Ki-Ras, R-Ras, M-Ras, R-Ras3, Rap2A H-Ras G12V K-Ras G12V	(1) COS-7, over-expressed Flag-RASSF5A and GST-H-Ras G12V (2) Yeast-two hybrid (3) 293-T and COS-7 cells, over-expressed RASSF5A and H-Ras G12V (4) Rassf5a-/-/K-Ras G12V mice	Ortiz-Vega et al. (2002)[235] Vos et al. (2003)[230] Stieglitz et al (2008)[243] Park et al. (2010)[245]
RASSF5B/RAPL	Rap1 G12V	Over-expressed EGFP-RASSF5B with FLAG-Rap1 G12V	Fujita et al. (2005)[235]
RASSF6	K-Ras G12V No association to K-Ras G12V/Y40C Note: Association with K-Ras V12 promotes RA SSF1A/MOAP-1 association H-Ras G12V >> K-Ras G12V = MRas G12V >>> N-Ras G12V	(1) 293-T cells, over-expressed FLAG-RASSF6 and HA K-Ras G12V (2) COS-7 cells, over-expressed Ras isoforms were used in pull-down experiments with MBPRASSF6	Allen et al. (2007)[389] Ikeda et al. (2007)[253]
RASSF9	N-Ras > K-Ras >> R-Ras	293-T cells with GST-Ras proteins co-transfected with Myc-tagged RASSF9 RA domain	Rodriguez-Vician et al. (2004)[237]

RASSF1A: A complex tumor suppressor regulating apoptosis and cell cycle control.

RASSF1A, the founding member of this family, has now been shown to be one of the most methylated genes in human cancers. Not only is it commonly silenced, but it is thought to be one of the earliest detectable changes in tumorigenesis [90,238]. RASSF1A contains several domains within its primary sequence that may be important for its role as a tumor suppressor protein (Figure 1.3). Some of these have been characterized and demonstrated to be important for death receptor association (the C1 zinc finger domain) [239], DNA damage repair of double strand breaks (the ATM phosphorylation site) [240] and for association with pro-apoptotic kinases MST1 and MST2 (the SARAH domain) [241]. Although important for death receptor association, it is unclear if the potential diacylglycerol (DAG) C1 domain may play a role in membrane lipid binding similar to how the C1 domain of protein kinase C binds to membrane lipids. No function has been assigned to the potential SH3 binding PxxP motif on RASSF1A (Figure 1.3).

The NMR solution structure of RASSF5A/Nore1A revealed a surprising intramolecular association between the C1 domain of RASSF5A and the RA [242]. Interestingly, Ras can disrupt this association and promote a more "open" conformation of RASSF5A [242]. We have modeled the C1 domain of RASSF1A based on the NMR structure of RASSF5A and found surprising similarity between the two [239]. RASSF5A, the closest family member, has 60% amino acid identity to RASSF1A [234]. We speculate that the C1 domain of RASSF1A may associate with the RA of RASSF1A in an intramolecular complex. However, since RASSF1A binds very weakly to Ras, we hypothesize that the RA of RASSF1A may associate with a yet unknown GTPase that may, in a similar manner to RASSF5A, displace the C1 domain to aid in further downstream signaling.

What is known about the RA of RASSF5A is that it is not sufficient to promote Ras association but may require an extended region spanning amino acids 203–219 on RASSF5A [243]. Furthermore, RASSF5A requires part of the switch region II of Ras in order to have maximal association with Ras in contrast to most Ras effectors that require only switch region I. Stieglitz et al. (2008) [243] have elegantly worked out the kinetic parameters of the Ras/RASSF5A association to show that Ras stays bound to RASSF5A for 10 seconds versus 60–250 milliseconds for Ras/PI3K or Ras/Raf associations. In addition, the Ras/RASSF5A RA complex has a surface area of contact at 1,546 $Å^2$ versus 1,331 $Å^2$ for Ras/Raf RBD and the Ras/RASSF1A complex had an association constant 33 times weaker than that of Ras/RASSF5A. These structural studies provide evidence for bona fide Ras association with some family members. Again, RASSF1A does not associate to classical Ras GTPases and any associations with Ras are indirect and most likely mediated through heterodimerization with RASSF5A, the only RASSF family member that can heterodimerize with RASSF1A [236].
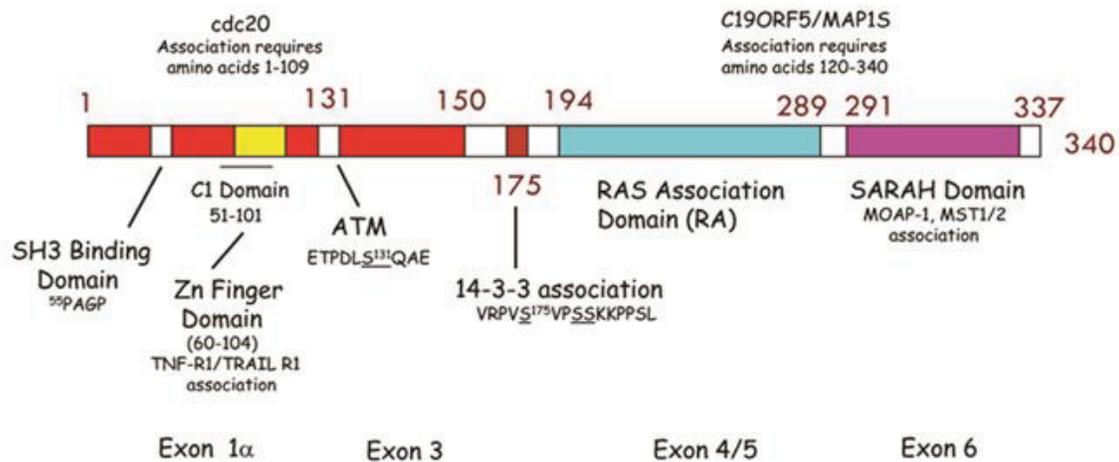
Figure 1.3: Schematic of RASSF1A. The SH3 binding domain of RASSF1A has the sequence PAGP that is conserved in mouse and human forms of RASSF1A and found as PQDP in RASSF5A. The ATM (Ataxia telangiectasia mutated) phosphorylation site is underlined with surrounding residues shown. ATM is a serine/threonine protein kinase that is a DNA damage sensor activated upon double strand breaks (DSBs), apoptosis or the addition of genotoxic stresses such as ultraviolet A light (UVA). The binding sites for several RASSF1A effector proteins are shown. The Ras association domain (RA) may potentially associate with the Ras family of oncogenes. The SARAH domain modulates heterotypic associations with the sterile-20 like kinases, MST1 and MST2. Approximate positions of exons and amino acids are also indicated as well as the identification of several polymorphisms to RASSF1A. Adapted from El-Kalla et al. (2010).(277) See text for details on the other functional domains.

The RASSF apoptotic signaling pathways: keys to tumor suppressor function.

As mentioned earlier, considerable excitement was generated when the RASSF family of proteins was first identified. RASSF5A demonstrated robust associations with Ras [236], the ability to promote apoptosis in the presence of active Ras [244] and the ability to reduce the transforming ability of Ras in a mouse xenograft model [245]. Apoptotic function of RASSF2 and RASSF6 were also demonstrated to be augmented in the presence of active Ras, reinforcing the importance of the RASSF family in linking Ras signaling to apoptosis. RASSF1A, however, does not appear to strongly associate with Ras to promote apoptosis, suggesting that it no longer requires Ras and may utilize an as yet unidentified GTPase in order to promote apoptosis.

The majority of the pro-apoptotic function of RASSF5A is through the associations with mammalian sterile 20-like kinases, MST1 and MST2 (Figure 1.2). MST is a cytosolic class II germinal center serine/threonine kinase that shows similarity to MAPKK and can be activated by both intrinsic and extrinsic stimuli. MST1 and MST2 share 76% sequence identity and contain an N-terminal catalytic domain followed by an autoinhibitory segment and a coiled-coil Salvador/Rassf1a/Hippo (SARAH) domain that mediates hetero- and homo-dimerization [246,247]. Both MST1 and MST2 have been shown to undergo a caspase-3 (at DEMD326 of MST1) and caspase 6/7 (at TMTD349 of MST1) dependent cleavage following apoptotic stimulation [248]. This results in an enhanced kinase activity and ability to translocate to the nucleus in order to phosphorylate histone H2B at serine-14. This phosphorylation event functions to possibly target H2B for endonuclease attack, promoting DNA fragmentation and subsequent cell death [249].

Regulating the activity of MST1/2 are a limited number of non-catalytic adapter proteins including RASSF family members that can associate through their SARAH

domain [248,250]. Although important for associations with MST1/2, the SARAH domain of RASSF5A was demonstrated by Aoyama et al. (2004) [251] to be dispensable for its growth suppressive properties in A549 lung cancer cells. Therefore, it remains to be determined if MST1/2 are the only downstream effectors of the Ras/RASSF5A signaling pathway linked to the SARAH domain.

Similar to RASSF5A, RASSF1A can utilize its SARAH domain to associate with and activate both MST1 and MST2 in order to drive apoptosis and subsequent translocation of MST1 and MST2 to the nucleus [241,250]. It has been demonstrated that recombinant RASSF1A can inhibit the kinase activity of MST1 whereas over-expressed RASSF1A can activate MST1 in response to Fas/FasL stimulation [252] suggesting that the *in vivo* regulation of MST1 by RASSF1A involves more than the simple association of the two proteins. RASSF2 [236] and RASSF6 [253] can also form a complex with MST1/2 in order to activate the kinase activity of MST1/2. RASSF3 [248] was found to associate with MST in a yeast two hybrid screen suggesting that several RASSF family members may be physiological binding partners to MST1 and MST2. Curiously, the SARAH domain is absent from N-terminal RASSF family members suggesting that they may have lost the ability to associate with MST1/2 and instead most likely associate with a unique spectrum of interacting proteins. Furthermore, it is uncertain if MST1 and MST2 associate with RASSF family members while they are associated with the microtubular network. In summary, the RASSF/MST associations function to regulate MST catalytic activity *in vivo* and may direct MST to sites of activation and promote associations with endogenous substrates in order to induce apoptosis.

In addition to their roles in cell death, MST1 and MST2 have recently been shown to be involved in several aspects of biology ranging from regulation of organ size via Yes-associated protein (YAP) [254], modulating hypertrophic responses in both cardiomyocytes and fibroblast cells of the heart [255] and regulation of actin cytoskeleton integrity by the activation of the JNK pathway [256]. Furthermore, MST1/2 can be

activated by death receptor stimulation, IGF/AKT stimulation [257] and non-physiologically with okadiac acid [248]. Recently, the *Mst1*^{-/-}*Mst2*^{-/-} double knockout mouse was generated [258] that revealed that single loss of either gene was well tolerated and normal organ development was observed. However, the loss of both MST1 and MST2 resulted in the *in utero* death at approximately embryonic day 8.5. The *Mst1*^{-/-}*Mst2*^{-/-} embryos exhibited severe growth retardation, failed placental development, impaired yolk sac/embryo vascular patterning and primitive hematopoiesis, increased apoptosis in placentas and embryos and disorganized proliferating cells in the embryo proper [258]. These findings indicate the essential roles for these two sterile 20-kinases in early mouse development, cell proliferation and survival. Recently, van der Weyden et al. demonstrated that the combined loss of *Rassf1a* and *Runx2* promoted the formation of oncogenic YAP1/TEAD transcriptional complexes to promote tumorigenesis, highlighting a previously unknown role for RASSF1A in regulating YAP signaling pathways [259].

We have also defined some of the molecular mechanisms of apoptotic regulation by RASSF1A that is MST-independent [239,260,261]. Ectopic expression of RASSF1A (and not RASSF5A) enhanced death receptor-evoked apoptosis stimulated by TNF-α and TRAIL [239]. In contrast, knockdown (by RNA interference) or knockout cells to either RASSF1A or modulator of apoptosis-1 (MOAP-1, a downstream target to RASSF1A) have significantly reduced caspase activity, defective cytochrome c release, BAX translocation and impaired death receptor dependent apoptosis [260]. Intrinsic pathway dependent cell death does not rely on death receptor stimulation but can promote increased mitochondrial permeability, enhanced cytochrome c release and subsequent cell death. This pathway does not appear to be significantly lost in *Rassf1a*^{-/-} cells and is reduced in *Moap-1*^{-/-} cells (unpublished observations). Our current model of RASSF1A mediated cell death in described in Figure 1.4.

Death receptor stimulation primarily drives the activation of RASSF1A to complex with TNFR1/MOAP-1 at membrane proximal sites. This allows RASSF1A to expose the BH3-like domain of MOAP-1 to associate with and conformationally change BAX in order to drive BAX activation and localization to the mitochondrial membrane [239,261]. BAX can then proceed to promote cytochrome c release, activation, nuclear and cytoplasmic breakdown resulting in the demise of the cell [260]. Consistent with our model, the absence of MOAP-1 in H1299 non-small cell lung cancer cells resulted in the inability of RASSF1A to associate with TNF-R1 but association returned once MOAP-1 expression is re-established [239]. Importantly, robust RASSF1A/MOAP-1 association does not require the presence of active K-Ras contrary to what was observed by Vos et al. [262]. We currently do not have an explanation for this but have observed RASSF1A/MOAP-1 associations in several cell types (including the ones utilized by Vos et al. [2006] [262]) without the need to over-express K-Ras or other GTPases. Reduced antibody efficiencies for the immunoprecipitations may explain these differences in addition to clonal differences in the cell type utilized. We believe that RASSF1A/MOAP-1 interactions are highly dynamic associations that are dependent on death receptor activation [260] and the ability of RASSF1A to promote apoptosis is dependent on the presence of MOAP-1.

More recently, additional roles for RASSF1A have been revealed. Jung et al. revealed an additional mechanism whereby RASSF1A can regulate microtubule stability, showing that RASSF1A suppresses the tubulin deacetylase histone deacetylase 6, and loss of this suppressive action resulted in increased cell motility [263]. Additionally, Verma et al. showed that RASSF1A interacts with Rap1A in order to regulate microtubule dynamics [255].

A particular role for RASSF1A in regulating cardiac stress has also emerged in recent years. When *Rassf1a*^{-/-} mice were subjected to cardiac pressure overload they developed enlarged hearts as well as enlarged cardiac myocytes [264]. Over-expression

of RASSF1A in cardiac myocytes inhibited this growth by promoting apoptosis. Alternatively, in cardiac fibroblasts, RASSF1A restricted NFκB activity, highlighting the importance of RASSF1A in regulating a variety of cardiac functions [255].
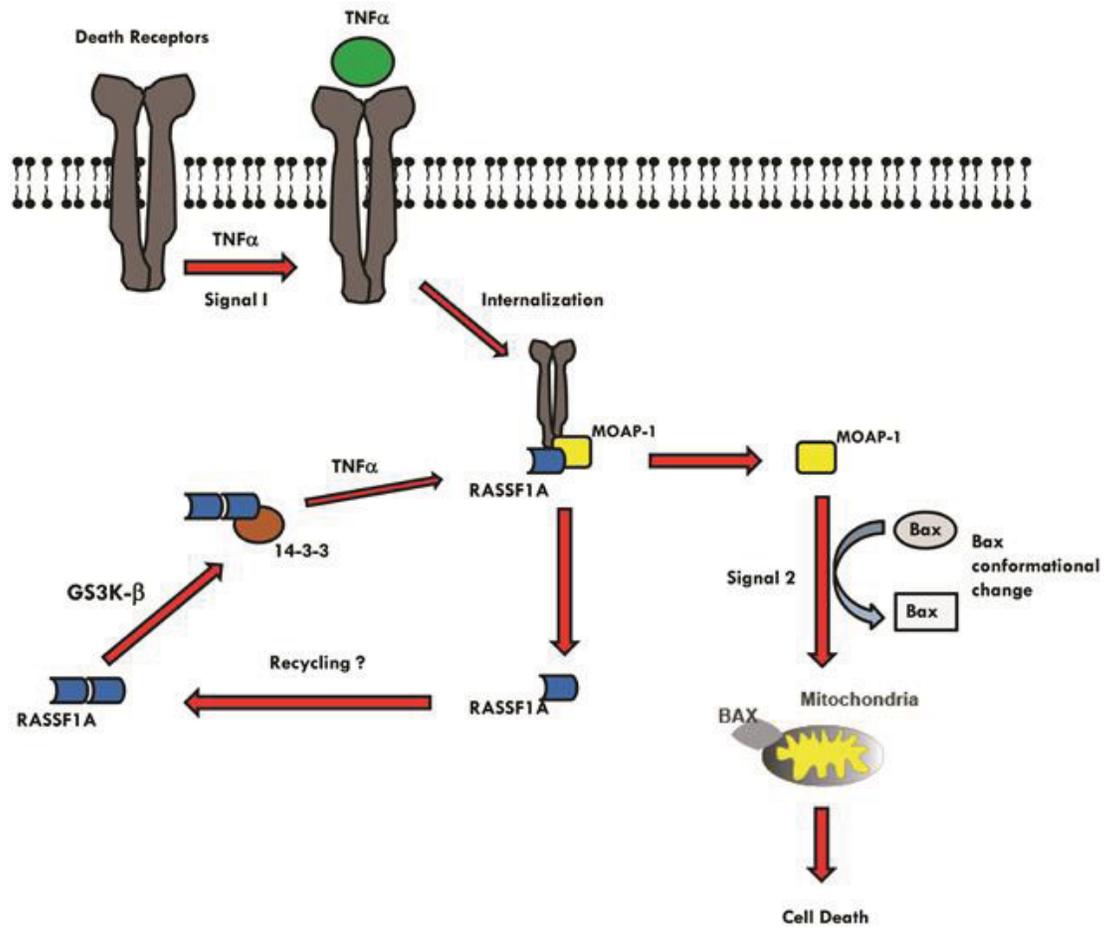
Figure 1.4: Model for RASSF1A modulated apoptosis. Death receptor-induced cell death (TNF-α is used as an example) can result in the recruitment of protein complexes to activate BAX and promote apoptosis. Basally, RASSF1A is kept complexed with 14-3-3 by GSK-3 β phosphorylation in order to prevent unwanted recruitment of RASSF1A to death receptor and uncontrolled stimulation of BAX and apoptosis. Once a death receptor stimuli has been received (TNF-α as shown above), the TNFR1/MOAP-1/RASSF1A complex promotes the "open" form of MOAP-1 to associate with BAX. This in turn results in BAX conformational change and recruitment to the mitochondria to initiate cell death. Following release from TNF-R1/MOAP-1 complex, RASSF1A may re-associate with 14-3-3 to prevent continued stimulation of this cell death pathway.

Regulation of RASSF1A

The pro-apoptotic function of RASSF1A can be regulated on many levels. (1) Basal inactivation of RASSF1A is achieved by RASSF1A self association [239,261], and via 14-3-3 interactions (to isoforms σ and ε) at serine 175/178/179 of RASSF1A [261], (2) TNF-α stimulation functions to promote MOAP-1 recruitment to TNF-R1, disrupt RASSF1A self association and association with 14-3-3 and promote the recruitment of RASSF1A to TNF-R1/MOAP-1 [239,260]. As previously mentioned, if MOAP-1 is absent RASSF1A does not associate with TNF-R1; and lastly, (3) the possible re-association with 14-3-3 may occur in order to prevent continued stimulation of this cell death pathway (unpublished results and see Figure 1.4). The 14-3-3 family of proteins function as molecular scaffolds to restrict the localization, stability and/or molecular interactions of their target proteins such as BAD, BAX and apoptosis signal regulated kinase (ASK) 1 [265]. In addition, both c-Raf and Raf-1/B-Raf can also be modulated by 14-3-3 associations [266,267]. 14-3-3 recognizes the phosphorylated serines at residues 175, 178 and 179 on RASSF1A. Mutation of these residues resulted in increased basal cell death in H1299 cells providing evidence that associations with 14-3-3 are important to provide basal inhibition of TNF-α-dependent cell death linked to RASSF1A [261].

We further demonstrated that basal phosphorylation of RASSF1A is carried out by the canonical WNT signaling pathway multifunctional serine/threonine kinase, GSK-3β. This adds an interesting dimension to the regulation of RASSF1A with links to the WNT/β-catenin signaling pathways, an important pathway in neuronal development, embryogenesis and cancer [268]. What drives GSK-3β phosphorylation of serine 175 and possibly serine 178/179 of RASSF1A is an interesting question. In addition to GSK-3β, RASSF1A can also be regulated by phosphorylation by ATM [240], PKC [269] and the cell cycle kinases (Aurora kinases) [270]. These phosphorylations have been demonstrated to be important for the biology of RASSF1A with respect to cell cycle control and DNA damage response [240]. Continued analyses of the role these phosphorylation events

play in the biology of RASSF1A will yield a wealth of information of how the tumor suppressor properties of RASSF1A are regulated.

It was recently shown that the RASSF1A promoter has a p53 binding site upstream from the ATG transcription start codon, and that p53 was able to bind to the RASSF1A promoter and inhibit RASSF1A expression via promoter methylation [271]. p53 binds to the RASSF1A promoter, recruits DAXX and DNMT1, and inactivates RASSF1A by inducing promoter methylation [272]. Finally, an emerging field of RASSF1A regulation is through microRNA regulation. miR-7 and miR-218 have been shown to epigenetically regulate RASSF1A, while miR-602 has been shown to directly down-regulate RASSF1A expression [273,274].

RASSF1A Polymorphisms: Key to Unknown Functions

Somatic mutations of RASSF1A are uncommon but several somatic polymorphisms have been detected in tumors (mainly lung, breast, kidney and nasopharyngeal carcinomas) and in a few cell lines [275] that can be mapped to these functional domains (Figure 1.3). The population distribution and significance of these alterations in tumorigenesis remains to be determined. Two RASSF1A polymorphisms have been demonstrated to lose microtubule association (C65R and R257Q) [276,277] and two failed to induce cell cycle arrest by inhibiting cyclin D1 accumulation (A133S and S131F) [278]. The ATM site polymorphisms, especially A133S is the most common RASSF1A polymorphism identified to date with two others also indentified to this region- a S131F and I135T change. Recently, it was demonstrated that S131 of the ATM site can be phosphorylated upon gamma radiation and phosphorylation of S131 is required to signal to p73, induce cell death and suppress colony formation [240,278]. The importance of these changes within the ATM phosphorylation site of RASSF1A is not currently known but we speculate that these changes may perturb the tumor suppressor

properties of RASSF1A. As such, patients harboring the ATM site polymorphisms to RASSF1A may be resistant to radiation based chemotherapy. If this is true, one must not only determine if RASSF1A is present in cancer patients but if they have a polymorphic form of RASSF1A.

We have also characterized the importance of several polymorphisms in modulating the stability of tubulin and RASSF1A tumor suppressor function—C65R, E246K and A133S [277]. Interestingly, the C65R polymorphism acquires a nuclear localization and does not have the ability to promote cell death (unpublished observations). The majority of the other polymorphisms of RASSF1A localize to microtubules in a similar manner to wild type RASSF1A (unpublished observations and [256]). In addition, we have preliminary evidence from a mouse xenograft assay to suggest that the SARAH domain polymorphisms (A33T and Y325C) and RA localized polymorphisms (V211A and R257Q) are transforming, suggesting that functional SARAH and RA domains are required for the tumor suppressor function of RASSF1A (unpublished observations). The biological role of these alterations in tumorigenesis remains to be determined and a detailed analysis of the role of RASSF1A polymorphisms to the biology of RASSF1A is warranted.

Other Roles for RASSF Family of Proteins

Regulating cell death and cellular proliferation are common themes for the RASSF family of proteins. These functions have been well documented, interacting partners are being identified, and the importance of Ras binding for their function is becoming clearer. As we gain more knowledge of the biology of the RASSF family of proteins, we are beginning to realize that their role stretches beyond cell death and cell cycle regulation. RASSF1A has been demonstrated to be involved in the recovery from hypertrophic injury [264] and RAPL/RASSF5B is an important component of lymphocyte

adhesion and homing [235]. RASSF1A, RASSF5A, RASSF7 and RASSF10 have been shown to associate and localize to microtubules or to centromeres [233] while RASSF8 is an important part of adherens junction and may have a role in cellular migration [234]. Microtubule associations are very commonly observed amongst the RASSF family of proteins that may allow for the stability of tubulin, proper formation of the mitotic spindle and aid in sister chromatid separation during mitosis [234]. RASSF1A has also recently been shown to associate with C19ORF5/MAP1S complex and to localize to the microtubule-organizing center to anchor RASSF1A to the centrosomes [279,280]. Furthermore, C19ORF5/MAP1S can associate with LC3, an important component of the autophagosome and with the mitochondria-associated protein, leucine-rich PPR-motif containing protein (LRPPRC) [281,282]. These associations may be important for autophagy involving proteins from both the microtubule and mitochondrial network.

Autophagy, or self digestion, is a major mechanism that occurs during starvation to reallocate nutrients from unnecessary biological processes to more urgent ones. It is a process that involves the formation of the autophagosome in order to rid the body of unwanted material through the lysosomal machinery. It may also be an important component of the tissue repair pathway allowing for efficient membrane fusion following injury. We have substantial evidence for the role of RASSF1A in regulating intestinal inflammation and possibly in the repair process following colonic epithelial cell damage [3]. We are currently exploring how RASSF1A may be involved in regulating inflammation and epithelial tissue repair and we speculate that the role of RASSF1A in intestinal epithelial repair may involve associations with the microtubule and autophagy related proteins. These are just some examples of the diverse roles of the RASSF family of proteins have in physiology. Several members of the RASSF family of proteins are frequent targets for promoter specific methylation and inactivation in cancer. Detailed analyses of the molecular mechanisms and identification of their molecular partners is warranted in not only cancer but other disease groups. Surprising discoveries are on the horizon for this gene family and we have only begun to understand their importance in biology [1].

Introduction

Cancer is a disease affecting 1 in 3 adults worldwide and is considered to be the second leading cause of death in both Canada and the United States behind heart disease [79,283]. It is thought that cancer arises due to the occurrence of 2–5 genetic events to potentiate tumor formation and sustain abnormal growth [85]. These genetic changes occur in passenger genes (to support the cancer phenotype) and driver genes (to promote the cancer phenotype) [84]. About 10% of driver genes code for oncogenes that promote accelerated growth. However, about 90% of the driver genes code for tumor suppressor genes that inhibit accelerated growth [85], suggesting that tumor suppressor genes play an integral part in the origin of cancer. Evidence also suggests that the mutation rates of tumor suppressor genes are much higher than oncogenes supporting their importance in cancer formation [84,85,284].

In 2000, Hanahan and Weinberg systematically described several key features or "hallmarks" of cancer that defined the behavior of a cancer cell [285]. These defining features of a cancer cell included the unique properties of limitless replicative potential, evasion of apoptosis, ability to stimulate neo-vascularization, invasion and metastasis, inhibition of suppressor pathways, and sustained proliferation. As described in their seminal paper, the aforementioned hallmarks are acquired through a "multistep process" that allows the cancer cells to acquire key survival traits while avoiding the watchful eye of established molecular "checkpoints" to inhibit abnormal growth [286]. It was around this time that the RASSF1 was identified as a potential tumor suppressor gene on chromosome 3, at 3p21.23 [234,287]. Now more than a decade later, RASSF1A has been demonstrated using numerous approaches to be a tumor suppressor gene and an important driver gene in cancer influencing/intersecting with many of the

hallmarks of cancer [1,234]. It is epigenetically silenced in the majority of cancers by promoter specific methylation, resulting in loss of expression of the RASSF1A protein [288]. Although expression loss of RASSF1A by methylation occurs frequently in cancer, nucleotide changes by somatic mechanisms have also been detected in patients from several cancer subtypes. Several studies have tried to elucidate the importance of these polymorphic changes and how it may affect the tumor suppressor function of RASSF1A. They have also revealed interesting and surprising influences on numerous aspects of biology.

The Origin of RASSF1A Polymorphisms

The RASSF1 gene consists of eight exons alternatively spliced to produce 8 isoforms, RASSF1A-H, that have distinct functional domains including the Ras association (RA) domain [241,287]. Of these, RASSF1A and RASSF1C are the predominant ubiquitously expressed forms in normal tissues [287,288]. RASSF1C has been demonstrated to be perinuclear in appearance in NCI H1299 lung cancer cells [289], nuclear in HeLa cells with translocation to the cytosol upon DNA damage [290], and localized to microtubules in a similar fashion to RASSF1A in 293T cells [291,292]. Thus, the localization of RASSF1C is varied and controversial. This is not the case for RASSF1A as it has been demonstrated by our group and several others to be a microtubule binding protein having a microtubule like localization and functioning to stabilize tubulin in a taxol like manner [277,292,293].

To date, a crystal structure for RASSF1A or RASSF1C has not been identified, but Foley et al. [239] provided a molecular model of the N-terminal C1 domain containing four zinc finger motifs which is very similar to the one found on RASSF5A/Nore1A [242]. The zinc finger motifs have now been demonstrated to be involved in death receptor associations and possible associations with other receptors or signaling components

[239]. In addition to the C1 domain, RASSF1A has been noted to have a sequence specificity motifs to associate with SH3 domain (PxxP); motifs for 14-3-3 associations; a Ras association (RA) domain (although association is weak or indirect for K-Ras) [1]; associations with the anaphase promoting complex protein cdc20 and the autophagy protein C19ORF5/MAP1S; and heterotrophic associations with the Hippo pro-apoptotic kinase (MST1/2) and the BH3-like protein modulator of apoptosis 1 (MOAP-1) through the Salvador/RASSF/Hippo (SARAH) domain (both reviewed elsewhere in this issue) (please see Figure 1.5 for schematic summary of RASSF1A protein associations).

RASSF1A polymorphisms have been identified in several cancers as listed in Table 1.2 and can be mapped to specific protein interaction domains (Figure 1.5). These polymorphisms have been found in tumors from numerous cancer patients and cell lines [294]. The population distribution and significance of these alterations in tumorigenesis remain to be determined but do vary from 9% to 33% of the specific cancer population. The majority of RASSF1A polymorphisms have been confirmed using several approaches as outlined by the 1000Genome project (http://www.1000genomes.org/), HapMap project (http://hapmap.ncbi.nlm.nih.gov/) and submitted by multiple sources (Table 1.2 and NCBI SNP database [http://www.ncbi.nlm.nih.gov/projects/SNP/snp_ref.cgi?showRare=on&chooseRs=coding&go=Go&locusId=11186] and University of Maryland SNP database [http://bioinf.umbc.edu/dmdm/gene_prot_page.php?search_type=gene&id=11186,NP_009113]). Recently, a comprehensive study of 400 lung, renal, breast, cervical, and ovarian cancers by Kashuba et al. [294] revealed frequent loss of genetic material on chromosome 3p in 90% of the tumors investigated. Furthermore, they determined that the mutation rate in cancer for RASSF1A was 0.42 mutation frequency/100 base pair whereas in the "normal" population was about 0.10 mutations/100 base pairs. They speculate that RASSF1A has a 73% GC content within exons 1–2 which may explain the high mutation rate of RASSF1A within cancer cells. Within cell lines, RASSF1A was found to carry 0.7 mutations/100 bp in the Burkitt's lymphoma-derived cell lines, BL2 and RAMOS, whereas it was 0.14 in the renal carcinoma cell line KRC/Y and, with each

division of the BL2 lymphoma line, transitional mutations were observed. Interestingly, codon changes in RASSF1A were also observed in 15 normal human hearts that included two nucleotide changes (CTA to CTG and GTA to GTG) but no amino acid changes [294]. They speculate that RASSF is simply located in an area that is "extensively damaged" and susceptible to mutational pressures in 90% of epithelial cancers [294].

The most common polymorphism is the alanine (A) to serine (S) at amino acid 133 (A133S) located within the ATM DNA damage checkpoint kinase site (please see below sections). This has single nucleotide germ line polymorphism (SNP) on both alleles in some breast cancer patients and is significantly associated with BRCA1/2 mutations. Patients with wild-type BRCA1/2 and RASSF1A A133S have a +15-year better survival period than those harboring both BRCA1/2 mutations and RASSF1A A133S [295,296]. The RASSF1A A133S SNP has been found in 20.6% of patients with breast carcinomas [295,296], 19.8% in lung cancer [296,297], 11.1% in head and neck cancer, 6.9% in colorectal cancer, 14.3% in esophageal cancer, 24.3% in patients with fibroadenoma, and in 2.9%–10% of healthy controls [295,297]. Interestingly, Gao et al. (296) also revealed the presence of the A133S polymorphism in brain and kidney cancer patients and Bergqvist et al. (2010) detected the presence of the A133S SNP in 18.4% of the white British female population [298]. The high percent obtained for the latter is surprising and requires further validation. The prevalence of the rest of the RASSF1A polymorphisms has not been determined yet, and functional studies to systematically determine influence of these polymorphisms on RASSF1A biological function are yet to be done. However, in this section we will only summarize what has been carried out already to ascertain the consequences of polymorphisms to RASSF1.
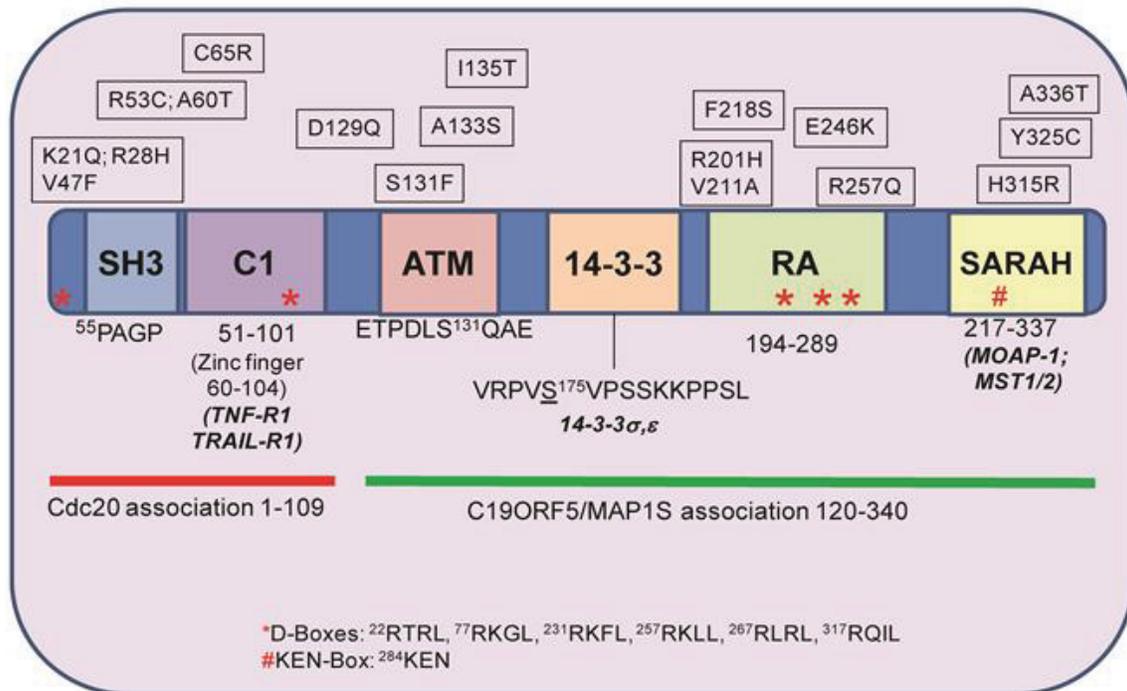
Figure 1.5: Schematic of RASSF1A with location of identified polymorphisms. Location of identified RASSF1A polymorphisms is indicated with respect to amino acid location, changed amino acid, and exon location. A potential binding sequence to an SH3 domain has been identified with a PxxP motif. The ATM phosphorylation site is underlined with surrounding residues shown. The docking sites for several RASSF1A effector proteins are shown including the location of potential D- and KEN-boxes for protein association (D1 to D6). The latter boxes are thought to be important for associations with APC/cdc-20 [12]. The Ras association domain (RA) is present in RASSF1A but has not been convincingly demonstrated to associate with the Ras family of oncogenes [10]. The SARAH domain modulates hetero-typic associations with the sterile-20-like kinases, MST1 and MST2 (adapted from El-Kalla et al. (2010)) (277) and Gordon and Baksh (2011) (1).

50

Table 1.2: RASSF1A single nucleotide polymorphisms

Several RASSF1A polymorphic changes have been identified as outlined in Table 1. SNP sites consulted to draft this table include NCBI (at http://www.ncbi.nlm.nih.gov/projects/SNP/snpref.cgi?showRare=on&chooseRs=coding&go=Go&locusId=11186) and DMDM (at http://bioinf.umbc.edu/dmdm/gene prot page.php?search type=gene&id=11186).

Polymorphism	Tissue or Cell Line Origin	SNP ID and Other Information	References
K21Q (AAG → CAG)	Breast (Tumor) Kidney (renal carcinoma cell TK10 and KRC/Y) Lung (Non small cell Lung cancer cell line)	rs4688725	Schagdarsurengin et al (2005)[295]; Dammann et al. (2000)[334]; Agathanggelou et al. (2001)[343], Burbee et al. (2001)[553]
R28H (CGT → CAT)	Breast (Tumor) Lung (Non small cell Lung cancer cell line)	Presence in Lung carcinomas are rare	Schagdarsurengin et al (2005)[295]; Dammann et al. (2000)[334;] Burbee et al. (2001)[553]
V47F (GTC → TTC)	Not listed	rs61758759	NCBI
R53C (CGC → TGC)	Breast (Tumor) Lung (Non small cell Lung cancer cell line)	Q9NS23	Schagdarsurengin et al (2005)[295]; Dammann et al. (2000)[334]; Burbee et al. (2001)[553]
A60T (GCA → ACA)	Breast	No SNP ID found	Agathanggelou et al. (2001)[343]
C65R (TGC → CGT)	Breast (Tumor)	No SNP ID found	Dallol et al. (2004)[276]
S131F (TCT → TTT)	Breast (Tumor) Kidney (Wilm's Tumor)	No SNP ID found	Schagdarsurengin et al (2005)[295]; Dammann et al. (2000)[334]
A133S (GCT → TCT)	Breast (Tumor, Fibroadenomas), 33% Kidney (Wilm's Tumor), 21% Brain (medulloblastoma), 9% Muscle (Rhadomyosarcoma), 19% Lung (Non small cell Lung cancer cell line)	rs52807901 and rs2073498 Association with BRAC1/2 mutations; Homozygous in Breast cancer; 21% of kids with germ line mutation, maternal in origin	Schagdarsurengin et al (2005)[295]; Dammann et al. (2000)[334]; Bergqvist et al. (2010)[298]; Gao et al. (2008)[296], Burbee et al. (2001)[553]; Lusher et al., (2002)[554]
I135T (ATT → ACT)	Lung (Non small cell Lung cancer cell line) Breast (Tumor cell line)	No SNP ID found	Dammann et al. (2000)[334;] Agathanggelou et al. (2001)[343]
V211A (GTC → GCC)	Breast	No SNP ID found	Agathanggelou et al. (2001)[343]
R201H (CGC → CAC)	ENT (nasopharyngeal carcinoma)	In 23 tumor samples, 34 other polymorphisms were detected (not listed in this table) with 30 transitions, 2 transversions and 2 deletions (6 in SH3/C1 domain and 6 in RA domain)	Zhi-Gang Pan et al. (2005)[555]
E246K (GAA → AAG)	Breast (Tumor)	No SNP ID found	Agathanggelou et al. (2001)[343]
R257Q (CGG → CAG)	Breast (Tumor) Lung (Non small cell Lung cancer cell line	No SNP ID found	Schagdarsurengin et al (2005)[295]; Dammann et al. (2000)[334;] Agathanggelou et al. (2001)[343]; Dallol et al. (2004)[276]
H315R (CAC → CGC)	NCBI SNP database, source unknown	rs52792349 and rs12488879	Geoffery Clark (personnel communication)
Y325C (TAT → TGT)	Breast (Tumor) Lung (Non small cell Lung cancer cell line	No SNP ID found	Schagdarsurengin et al (2005)[295]; Dammann et al. (2000)[334;] Burbee et al. (2001)[553]
L270V (CTG → GTG)	Cervical (Tumor)	No SNP ID found	Schagdarsurengin et al (2005)[295]; Dammann et al. (2000)[334]
A336T (GCC → ACC)	Lung (Non small cell Lung cancer cell line	No SNP ID found	Dammann et al. (2000)[334]

RASSF1A: A Key Element in Cellular Stability

One of the most striking features of RASSF1A is its appearance as a microtubule associated protein. Microscopy of numerous tagged versions of RASSF1A have all revealed similar microtubule-like appearance as seen in MCF-7 breast cancer cells in Figure 1.6. This appearance has been observed in many other cell lines with similar appearances. It has also been determined that both N- and C-terminal residues of RASSF1A are required for the microtubule appearance of RASSF1A [277,292]. Several groups have characterized the appearance and function of the microtubule localization of RASSF1A. It has been demonstrated that the microtubule localization of RASSF1A mainly functions to stabilize tubulin both in interphase and in mitosis even in the presence of the microtubule destabilizer, nocodazole [276,277,299,300].

To date, RASSF1A has not been demonstrated to co-localize to actin or intermediate filaments. RASSF1A associations function to stabilize tubulin in a paclitaxel (taxol)-like manner [276,291] especially during mitosis allowing sister chromatid segregation. This function is governed by associations with γ-tubulin at spindle poles and centromeric areas during metaphase and anaphase and near the microtubule organizing center (MTOC) where microtubules emerge and nucleate [301-303]. If the microtubule spindle complex is not properly formed, cell death proceeds to prevent inheritable aneuploidy. In the absence of cell death pathways chromosomal mis-segregation and inheritable aneuploidy arise which can lead to malignancy. Several of the effects on microtubule biology have been observed in mouse embryonic fibroblasts (MEFs) obtained from *Rassf1a*$^{-/-}$ mice developed by two separate groups [287,304].

Rassf1a$^{-/-}$ mice are viable, fertile and retain expression of isoform 1C. However, by 12-16 months of age they have increased tumor incidence, especially in the breast, lung, and immune system (gastrointestinal carcinomas and B-cell-related lymphomas)

[287,304]. These data suggest a tumor suppressor function specific for the RASSF1A isoform. MEFs obtained from *Rassf1a*$^{-/-}$ mice are more susceptible to nocodazole-induced microtubule depolymerization suggesting a protective effect of RASSF1A on microtubule stability similar to what has been observed using tissue culture approaches [287].

It has now been demonstrated that RASSF1A disease associated polymorphisms may affect the function of RASSF1A as a microtubule stabilizer. It was demonstrated that the S131F mutant of RASSF1A continued to maintain the ability to promote tubulin stability as determined by immunofluorescence microscopy and acetylation status of tubulin [291]. Furthermore, it was demonstrated by Vos et al. [291] that RASSF1C could not function in a similar manner to RASSF1A to stabilize tubulin. This provided one of the first evidences for differential function for these two prominent isoforms of the *RASSF1* loci. A comprehensive analysis of several other RASSF1A polymorphisms was carried out by Liu et al. [305]. They demonstrated that polymorphisms around the ATM phosphorylation site (A133S, S131F, and I135T) maintained the microtubule appearance of RASSF1A. A second comprehensive study revealed that the C65R and R257Q polymorphisms of RASSF1A resulted in "atypical localizations" of RASSF1A away from a microtubular appearance [276]. Furthermore, both C65R (a residue within the C1 domain) and R257Q (a residue within the RA domain) promoted enhanced BrdU incorporation into NCI-H1299 nonsmall cell lung cancer cells suggesting loss of tumor suppressor function.

Recently, we have also observed a complete loss of the microtubule localization of RASSF1A in the presence of a C65R change and "oncogenic" properties of this polymorphism in a classical xenograft assay in athymic mice [277]. The C65R polymorphism acquired a nuclear localization for unexplained reasons and also failed to stabilize tubulin in the presence of the microtubule depolymerizing agent nocodazole [277]. It clearly lost the tumor suppressor function of RASSF1A in a xenograft assay and

can robustly drive enhanced growth [277]. Similarly, both the A133S and E246K mutants maintained microtubule localization and lost tumor suppressor function but not to the level of the C65R polymorphism (xenograft assays were carried out in HCT116 colon cancer cells) [277]. We are currently characterizing many of the other polymorphisms in Table 1.2 for their ability to behave as tumor suppressor, inhibit abnormal growth, and affect microtubule stability and protein interaction with established RASSF1A effectors.

Interestingly, it has been reported that Epstein-Barr virally encoded protein, latent membrane protein 1 (LMP1) can function to transcriptionally decrease RASSF1A levels and promote tubulin depolymerization and mitotic instability in human epithelial cells (HeLa and HaCaT) [306]. Punctate structures of tubulin were observed in the cytoplasm indicative of tubulin depolymerization [306]. Decreased RASSF1A levels resulted in increased phosphorylation of IκBα and elevated NFκB activity. Cause and effect of changes in NFκB activity were not fully elucidated. However, we have evidence that the loss of RASSF1A can lead to enhanced NFκB activity [3] suggesting that the decreased expression of RASSF1A induced by LMP1 production may have resulted from the loss of the ability of RASSF1A to restrict NFκB function. Epstein-Barr virus (EBV) infection is closely related to the appearance of nasopharyngeal cancers and we speculate that a precondition characterized by enhanced NFκB activity (and hence inflammation) may promote tumorigenesis and the appearance of nasopharyngeal cancers upon EBV infection. We are currently exploring the role of RASSF1A as a molecular link between inflammation and tumorigenesis.
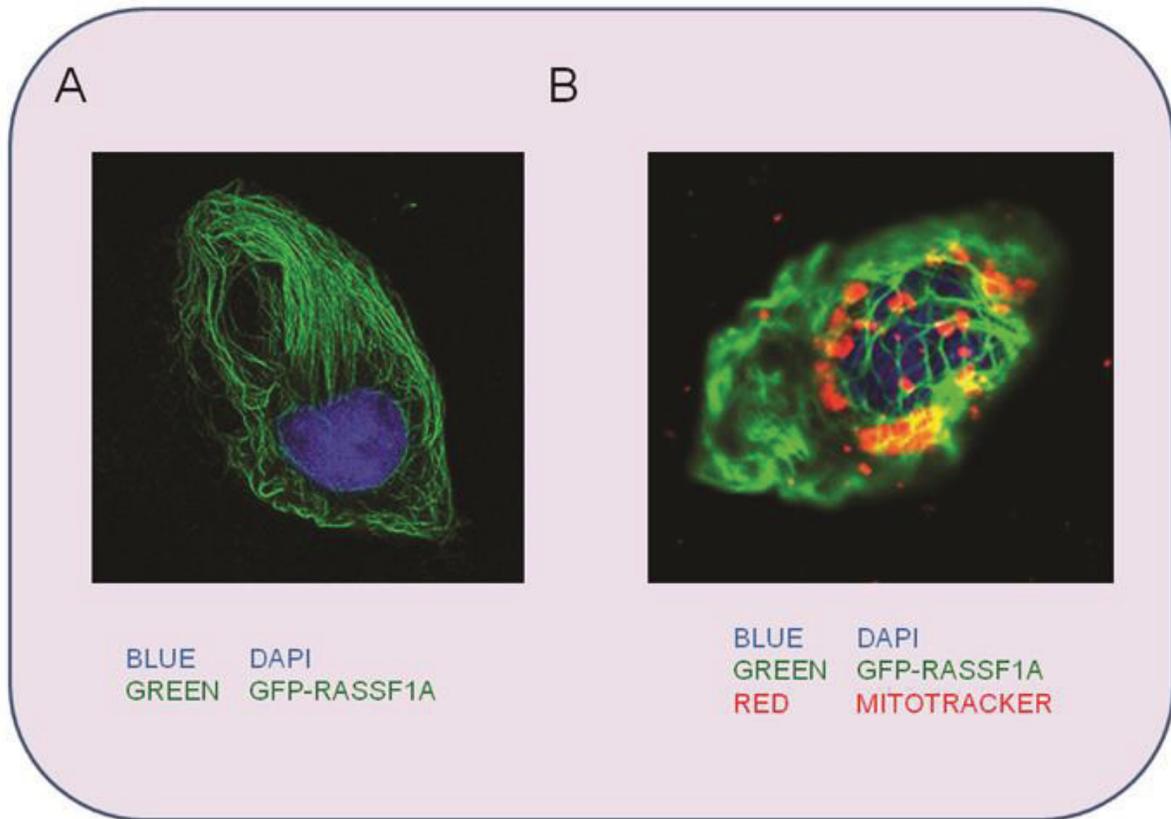
Figure 1.6: Microtubule localization of RASSF1A. GFP-RASSF1A was expressed in U2OS osteosarcoma cells (A and B) and co-stained with DAPI to reveal the nucleus **(A and B)** and with mitotracker red to reveal mitochondrial localization **(B)**. Areas of yellow reveal co-localization and all images were acquired using confocal microscopy using a Zeiss system and a 63x oil immersion lens.

RASSF1A: Linking Extrinsic Death Receptor Stimulation to BAX Activation

Every cell has an inherent ability to die under abnormal conditions. This ability has been programmed by nature into every cell and follows a defined series of events. Apoptosis is critical for multiple physiological processes, including organ formation, immune cell selection, and inhibition of tumor formation [307]. Two types of signaling pathways promote apoptosis using the mitochondria. The "intrinsic" pathway is activated by noxious factors such as DNA damage, unbalanced proliferative stimuli, and nutrient or energy depletion. Components of intrinsic-dependent apoptosis are still unclear, although Bcl-2-homlogy domain 3 (BH3) proteins are required. In contrast, the "extrinsic" pathway is stimulated by specific death receptors (e.g., TNF-α receptor R1 (TNF-R1), TNF-α-related apoptosis-inducing ligand receptor (TRAIL-R1) or Fas (CD95)) [308-310]. Molecular mechanisms modulating programmed cell death (apoptosis) impinge on growth and immune cell function. We speculate that these cellular processes may be regulated in part by tumor suppressor pathways, pathways frequently inactivated in several disease states (such as cancer and autoimmune/inflammatory disorders).

RASSF1A is one element involved in death receptor-dependent cell death that is epigenetic-silenced in numerous cancers. In the majority of these studies, RASSF1A epigenetic silencing strongly correlates with the epigenetic silencing of three other genes—p16INK4a, death associated protein kinase (DAPK), and caspase 8 [311-314]. Two of these genes are involved in pro-apoptotic pathways, DAPK and caspase-8 [309,315,316]. DAPK is a unique calcium/calmodulin activated serine/threonine kinase involved in several cell death-related signaling pathways including tumor necrosis factor α receptor 1 (TNF-R1) cell death and autophagy [316,317]. It is a tumor suppressor protein [316] that has also been demonstrated to be involved in associations with and the regulation of pyruvate kinase, a key glycolytic enzyme that may be influential in the link between metabolism and cancer [318]. We have evidence to demonstrate association of RASSF1A and DAPK (Baksh et al., unpublished observations) and RASSF1A has two

potential phosphorylation sites for DAPK within the RA domain at 193GRGTSVRRRTSFYLPK [319]. Curiously, these sites have also been demonstrated to be sites for protein kinase C [269] and aurora kinases [320]. In the presence of S197A or S203A mutant of RASSF1A, PKC failed to phosphorylate RASSF1A resulting in the loss of microtubule organization in COS-7 cells. Similarly, Aurora B kinase failed to phosphorylate RASSF1A in the presence of S203A resulting in a failed cytokinesis [320]. The physiological importance of these potential DAPK phosphorylation sites remains to be determined.

Caspase 8 is cysteine-dependent aspartate-directed protease and an initiator caspase, and targeted activation of caspase 8 is driven by the death inducing signaling complex (DISC) [309,315]. DISC-dependent activation of caspase 8 triggers a series of events resulting in the cleavage of Bid and insertion of Bid on the outer mitochondrial membrane, the release of small molecules (such as cytochrome c) from the mitochondria into the cytosol, and the activation of downstream effector caspases (such as caspase-3) [321]. Intrinsic pathway stimulation also leads to cytochrome c release and effector caspase activation. Once activated, effector caspases cleave several proteins (such as poly(ADP-ribose) polymerase (PARP)) and activate specific DNA endonucleases resulting in nuclear and cytoplasmic breakdown [322].

Our research group was the first to define and continues to define some of the molecular mechanisms of death receptor-dependent apoptotic regulation by RASSF1A [239,260,261]. Ectopic expression of RASSF1A (but not RASSF1C) specifically enhanced death receptor-evoked apoptosis stimulated by TNF-α that does not require caspase 8 activity or Bid cleavage [239,260]. We have also shown that RASSF1A does not influence the intrinsic pathway of cell death [260]. Furthermore, we demonstrated that microtubule localization was required for association with death receptors and for the role of RASSF1A in apoptosis [239,277]. In contrast, RASSF1A knockdown cells (by RNA interference) and *Rassf1a*⁻/⁻ knockout mouse embryonic fibroblasts (MEFs) have

significantly reduced caspase activity, defective cytochrome c release and BAX translocation (but not BID cleavage), and impaired death receptor-dependent apoptosis [260]. These data suggest a direct link of death receptor activation of BAX through RASSF1A. Our current model of RASSF1A-mediated cell death is described in Figure 1.7. Death receptor stimulation functions to bring RASSF1A (and not RASSF1C or RASSF5A/Nore1A) and modulator of apoptosis 1 (MOAP-1) to TNF-R1 in order to promote a more "open" MOAP-1 to subsequently associate and promote BAX conformational change and translocation to the mitochondria to activate cell death (Figure 1.7) [239,260-262]. We have evidence that the 14-3-3 may keep RASSF1A in check and inhibit it from promoting cell death or associating with other unexplored signaling components [261]. We are currently characterizing the primary and secondary signals required for MOAP-1 induced BAX conformational change and the apoptotic regulation of MOAP-1 by ubiquitination (please see [387]).

To date, very little is known about the cell death properties of numerous RASSF1A polymorphisms. Dallol et al. demonstrated that both C65R and R257Q promoted enhanced BrdU incorporation into NCI-H1299 non-small cell lung cancer cells suggesting loss of tumor suppressor function and possible loss of cell death properties [276]. We have observed partial activation of apoptosis in the presence of several RASSF1A polymorphisms (such as C65R, A133S, I135T, and A336T) suggesting importance to death receptor-dependent apoptosis via ATM site and SARAH domain associations (unpublished observations). Further analysis is warranted to explore how RASSF1A polymorphisms may affect death receptor-dependent apoptosis.

Although not discussed in great detail here, RASSF1A can also promote cell death utilizing the autophagic protein, C19ORF5/MAP1S, [276,280,299] the Hippo pathway components MST1/2 and possibly Salvador [241,323], and, in melanoma cells, influence Bcl-2 levels and activate apoptosis signal regulating kinase 1 (ASK-1) [324]. Min et al. [299] demonstrated that the ability of RASSF1A to efficiently inhibit APC/cdc20 activity

during mitosis (please see next section) is dependent on the recruitment of RASSF1A to spindle poles via C19ORF5/MAP1S. C19ORF5/MAP1S was also shown to regulate mitotic progression by stabilizing mitotic cyclins in a RASSF1A-dependent manner. Recently, C19ORF5/MAP1S was demonstrated by Lui et al. [280] to associate with a component of the autophagosome, LC3, and the mitochondria-associated leucine-rich PPR-motif containing protein (LRPPRC) protein. These associations suggest that C19ORF5/MAP1S may serve as a potential link between autophagic cell death, mitochondria, and microtubules and appears to require RASSF1A. It will be essential to determine associations of RASSF1A polymorphisms with key cell death mediators, such as MOAP-1, TNF-R1, DAPK, C19ORF5/MAP1S, and MST1/2 in order to ascertain their importance in influencing the tumor suppressor function of RASSF1A.
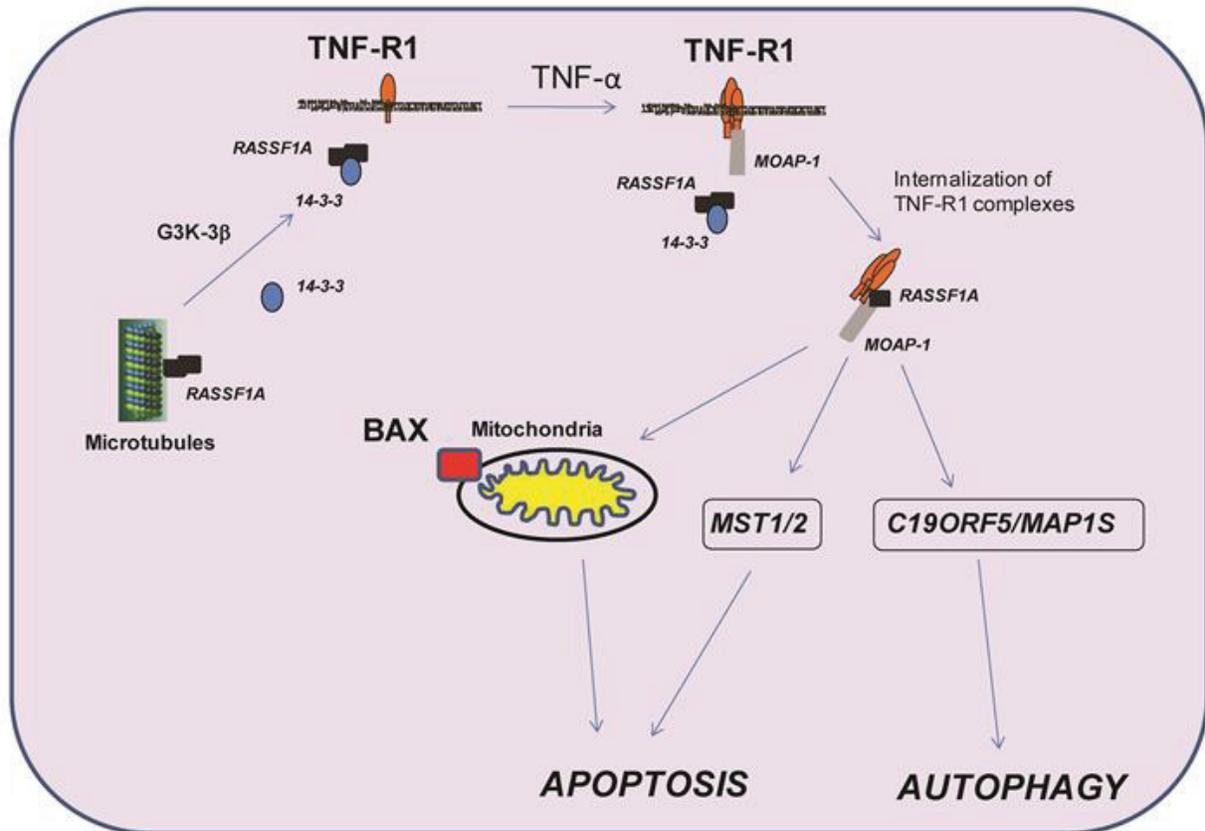
Figure 1.7: Model for the RASSF1A/MOAP-1 proapoptotic pathway. Death receptor-induced cell death (TNF-α is used as an example) can result in the recruitment of protein complexes to activate BAX and promote apoptosis. Basally, RASSF1A is kept complexed with 14-3-3 by GSK-3β phosphorylation in order to prevent unwanted recruitment of RASSF1A to death receptor and uncontrolled stimulation of BAX and apoptosis. Once a death receptor stimuli have been received (TNF-α as shown above), the TNF-R1/MOAP-1/RASSF1A complex promotes the "open" form of MOAP-1 to associate with BAX. This in turn results in BAX conformational change and recruitment to the mitochondria to initiate cell death. Following release from TNF-R1/MOAP-1 complex, RASSF1A may re-associate with 14-3-3 to prevent continued stimulation of this cell death pathway.

Cell Cycle Control Pathways Influenced by RASSF1A

As mentioned previously, RASSF1A is a microtubule binding protein that co-localizes with α- and β-tubulin, and with γ-tubulin on centromeres [301-303]. RASSF1A is thought be an important component of mitotic spindles and can influence the separation of sister chromatids at the metaphase plate. This observation has held true five years later and reinforced the findings of Song et al. [320,325] of the possible involvement of RASSF1A in cell cycle control. Although, very limited knowledge of the cell cycle effects of polymorphic forms of RASSF1A are known, several lines of evidence do suggest a role in cell cycle control. In 2004, RASSF1A was identified as an interacting protein with the anaphase promoting complex (APC)/cdc20 and prevented the ability of APC/cdc20 to degrade cyclins A and B in order to exit mitosis [325]. In the absence of RASSF1A, cyclins A and B were rapidly degraded due to increased ubiquitination of the cyclins to allow exit from mitosis.

Whitehurst et al. [326] supported this role for RASSF1A and further identified β-TrCP as associating with RASSF1A and functioning to restrict the role of APC-cdc20 in mitotic progression. β-TrCP is an IκBα E3 ligase and negative regulator of the β-catenin/WNT signaling pathway. Although Liu et al. could not find evidence for a RASSF1A-APC/cdc20 association [327], the influence of RASSF1A on APC/cdc20 was once again demonstrated by Chow et al. in 2011 [328]. They not only demonstrated an association with APC/cdc20, but also clearly showed that a "RASSF1A-APC/cdc20 circuitry" was in place in HeLa cells to regulate mitosis. RASSF1A associates with APC/cdc20 via two D boxes at the N-termini (DB1 and DB2) and keeps it inhibited until there is mitotic activation of the serine/threonine kinases Aurora A/B. Phosphorylation of RASSF1A by Aurora A/B on T202 or S203 subsequently labels RASSF1A as a target to the E3-ubiquitin ligase activity of APC, ensuring that mitosis proceeds by degrading RASSF1A and suppressing its mitotic inhibitor function [329]. They speculate that this

occurs before spindle body formation and sister chromatid separation. Their results are intriguing and reveal the complex signaling world that RASSF1A is part of.

Beyond a RASSF1A-APC/cdc20 molecular control of mitosis, research has continued into a potential role of RASSF1A during cell cycle progression. This has led to several observations suggesting RASSF1A G1/S regulation of cyclin D1 [278,324,326] in melanoma and HeLa cells (respectively.), interaction with the transcriptional regulator p120E4F at the G1/S phase transition resulting in inhibition of passage from G1 [330], DNA damage control regulation by ATM and by the DNA damage binding protein 1 (DDB1) that can associate with RASSF1A linking to the E3-ligase cullin 4A during mitosis [331]. The p120E4F transcription factor was determined to be involved in inhibiting the transcription of cyclin A, resulting in the failure of cyclin A to associate with CDK2 to allow for progression through S phase. RASSF1A cooperates with p120E4F to repress cyclin A expression by enhancing its binding at the promoter region [330]. ATM and DDB1 are important DNA damage control elements during ultraviolet and gamma irradiation which have evolved to repair damage.

Shivakumar et al. revealed that in both H1299 non-small cell lung cancer and in the human mammary epithelial telomerase immortalized (HME50-hTERT) cell line over-expression of RASSF1A wild-type expression construct can reduce BrDU accumulation and cyclin D1 expression [278]. The ability of RASSF1A to inhibit growth, and cyclin D1 expression was lost in the presence of the A133S and S131F ATM site mutants of RASSF1A suggesting an important role in tumor suppression [278]. Other polymorphic forms of RASSF1A have not been explored with respect to their abilities to regulate mitosis. What these studies reveal is how highly regulated RASSF1A is, not only in interphase cells, but especially in cells undergoing active cell division. It can then be appreciated how devastating the functional consequence of the loss of RASSF1A would be resulting in an unregulated and unwanted increase in mitotic cyclins, accelerated mitosis, enhanced growth and tumor formation. It would be interesting to speculate that

they may result in the loss of the ability of RASSF1A to properly regulate mitosis and inhibit unwanted proliferation. It is imperative that we understand completely how polymorphic changes in RASSF1A may influence the important role of RASSF1A in mitosis and other biological pathways (Figure 1.8).
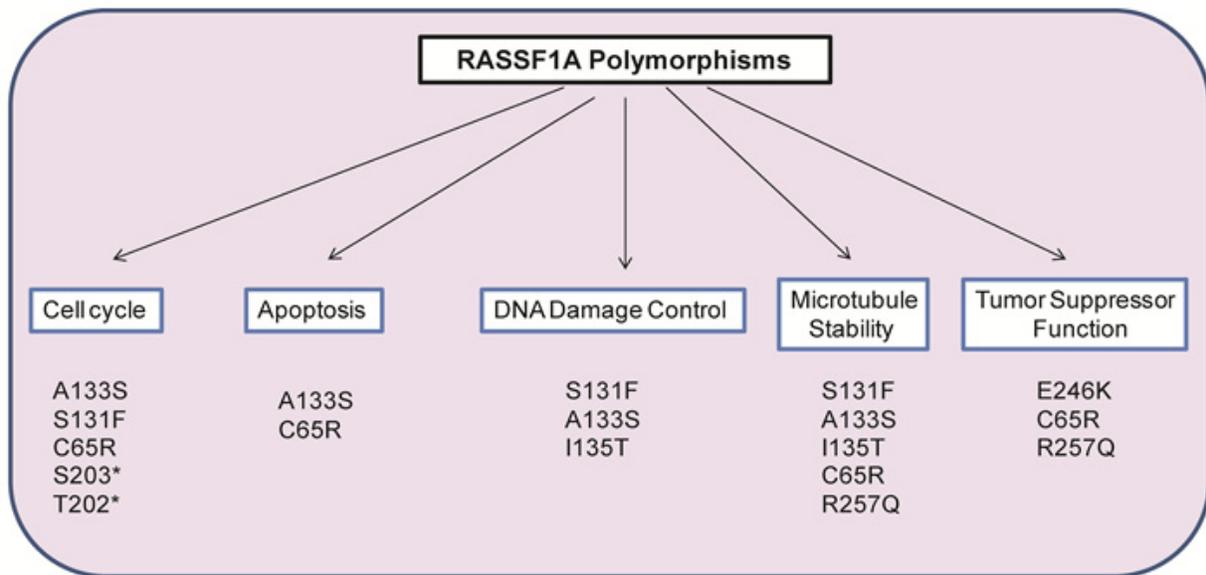
Figure 1.8: Identified biological roles for RASSF1A polymorphisms. Several polymorphisms have been identified for RASSF1A over the past decade since it was first cloned. Biological analyses of the *in vivo* role have identified the importance of RASSF1A over numerous pathways. This figure summarizes what is known about RASSF1A polymorphisms. *denotes a non-polymorphic but mutational change. This change does not naturally exist in the cancer patient population to our knowledge.

The DNA Damage Connection

One of the first motifs identified on RASSF1A was the phosphorylation site for the DNA damage serine/threonine kinase Ataxia telangiectasia mutated (ATM). ATM is usually activated and recruited in response to double strand breaks. It is part of a DNA damage checkpoint that ensures that damaged DNA is repaired in a timely and efficient manner. RASSF1A has been shown by several groups to be phosphorylated by ATM and the ATM site polymorphisms are present in several cancer types [240]. Although not currently well defined, RASSF1A is believed to have an important role in DNA damage control as evidenced by associations with xeroderma pigmentosum complementation group A (XPA) [332] and phosphoregulation by ATM [240,333]. XPA is involved in nucleotide excision repair and association with RASSF1A has only been identified in a yeast two-hybrid screen [334]. Hamilton et al. [240] elucidated a novel pathway linking ATM-dependent phosphorylation of RASSF1A in response to gamma irradiation on serine-131 followed by MST/LATS activation resulting in Yes-associated protein (YAP)/p73-dependent transcriptional program to promote cell death. The S131F mutant of RASSF1A lacked the ability to carry out the transactivation of YAP/p73.

Curiously, RASSF1C has been demonstrated to be constitutively anchored to the death domain-associated protein (DAXX) in the nucleus and is released upon UV-induced DNA damage [290]. Localization with DAXX occurs on pro-myelocytic leukemia-nuclear bodies (PML-NBs). DNA damage promotes the degradation and ubiquitination of DAXX, release of RASSF1C to allow the nucleo-cytoplasmic shuttling of RASSF1C to cytoplasmic microtubules, and the activation of the SAPK/JNK pathway in HeLa cells. RASSF1A was shown to only associate weakly with DAXX suggesting a specific role for RASSF1C [290]. Recently, it was demonstrated that the E3 ligase, Mule, can ubiquitinate RASSF1C under normal conditions, and both Mule and β-TrCP can ubiquitinate RASSF1C under UV exposure [335]. These studies and others have continued to demonstrate the diverse role that the splice variants of RASSF1 may function in biology.

RASSF1C: The Other RASSF1 Isoform

Very little is known about the biological role for the other major splice variant of the RASSF1 gene family. Several lines of evidence suggest that RASSF1C may be a tumor suppressor gene in prostate and renal carcinoma cells but not in lung cancer cells [336]. In fact, it has been demonstrated by Amaar et al. that the loss of RASSF1C actually results in the loss of proliferation of lung and breast cancer cells suggesting a pro-survival (not tumor suppressor) role for RASSF1C [337,338]. Furthermore, RASSF1C can associate with the E3 ligase β-TrCP via the SS18GYXS19 motif (where X is any amino acid and numbers correspond to amino acid sequence in RASSF1C) at the N-terminus (i.e., not present in RASSF1A) [339] and promote the accumulation and transcriptional activation of β-catenin [339]. Activation of β-catenin would result in enhanced proliferation by transcriptional up-regulation of genes such as cyclin D1, MYC, and TCF-1. Thus, either the lack of RASSF1A expression or the over-expression of RASSF1C perturbs β-TrCP E3 ligase/β-catenin homeostasis and WNT signaling pathways.

Unlike RASSF1A, RASSF1C has not been found to be significantly epigenetically silenced in cancer. Polymorphisms to RASSF1C have not been uncovered yet, but a C61F mutation in RASSF1C (equivalent to the S131F mutation in RASSF1A) resulted in the failure of RASSF1C to protect microtubules against nocodazole-induced depolymerization [291]. This would again suggest importance of serine residue within the ATM site found on both RASSF1A and 1C. Recently, it has been suggested that a possible pathogenic role for RASSF1C in cancer may exist as its expression was more than eleven-fold greater in pancreatic endocrine tumors than in normal tissue [340]. It remains to be determined the exact biological role for RASSF1C, but the ability of RASSF1C to function as a tumor suppressor is cell specific and remains to be further investigated and confirmed.

The Future of Understanding RASSF Polymorphisms

Knudson stated in 1971 that cancer is the result of accumulated mutations to the DNA of cells and that multiple "hits" to DNA were necessary to cause cancer [341]. It is generally known that the loss of function in a tumor suppressor protein typically requires the inactivation of both alleles of its gene in contrast to proto-oncogenes which promote tumorigenesis due to dominant acting mutations affecting one gene copy. Similar to what Knudson discovered for retinoblastoma, the RASSF1A tumor suppressor may become inactivated by the epigenetic loss by promoter specific methylation of both allele or by a combination of epigenetic silencing and loss of function polymorphic changes. Most cancers investigated to date have >50% of the disease population containing epigenetic silencing of RASSF1A [275,288]. However, numerous cancers such as cervical, head and neck, myeloma, and leukemia have <25% of the disease population containing epigenetic silencing of RASSF1A. It may be speculated that polymorphic changes to RASSF1A may exist in the latter patients that, in agreement with the Knudson two hit hypothesis, resulting in the loss of function of the RASSF1A tumor suppressor and causing cancer. A systematic and functional analysis of RASSF1A polymorphism is therefore necessary to allow physicians to carry out personalized medicine on patients harboring polymorphic changes to RASSF1A [2].

1-4 Research Project Overview and Specific Aims

Rationale:

IBDs includes Crohn's disease (CD) and ulcerative colitis (UC), affecting both pediatric and adult patients. IBD is characterized by an intense inflammation of the GI tract resulting in severe symptoms including weight loss, abdominal pain, rectal bleeding, and diarrhea. About 1/3 of all cancer cases are preceded by chronic inflammation, including chronic IBD leading to colorectal or colon cancer [15-19]. Although the predisposition to cancer has been well documented, the exact mechanism involved is unknown. NFκB signaling pathways regulate immunity and inflammation, and dysregulated and constitutive NFκB signaling has also been implicated in several cancers [9,159].

RASSF1A, is a tumor suppressor gene located on chromosome 3, at 3p21.3. RASSF1A has been known to act in many signaling pathways regulating cellular apoptosis, the cell cycle, and microtubule localization within the cell [2,3,234,277,342]. Loss of RASSF1A expression and subsequent activity results in tumor formation and dysregulation of the cell cycle [238,334,343,344]. RASSF1A expression is often lost due to epigenetic methylation of the promoter region of the gene. Subsequently, no mRNA transcript produced leading to loss of RASSF1A protein and loss of tumor suppressor function. The RASSF1A locus has been shown to be methylated in a high percentage of cancers, including 20-60% of colorectal cancers, and may also be methylated in non-cancer stage IBD patients [90,345-349].

Yes associated protein (YAP1) is a transcription factor co-activator traditionally thought of as a proto-oncogene regulating cell proliferation and organ size [350-353]. YAP is a part of the Hippo signaling pathway, a kinase cascade regulated by cell-cell

68

contacts. MST1/2 (the mammalian ortholog of Drosophila Hippo), when activated, phosphorylates LATS1/2, which in turn phosphorylate YAP at S127, causing YAP to be cytoplasmically retained through association with 14-3-3 complexes. Loss of cell contact inhibition inactivates the Hippo pathway, allowing the nuclear translocation of YAP and binding to TEAD proteins and activating pro-proliferative transcription [350,354-356]. In many cancers, including colorectal cancer, the Hippo pathway is dysregulated and YAP accumulates in the nucleus to promote uncontrolled growth [351,354,357]. RASSF1A has also been shown to be able to activate MST1/2 and suppress YAP proliferative activity by preventing MST1/2 desphosphorylation [287,323,354,355,358,359]. Additional pro-proliferative roles for YAP have been identified in the Wnt and TGF-β signaling pathways, by associating with β-catenin/TBX5/TCF4 and SMAD transcription factors, respectively. Increased YAP transcriptional activity in both the Wnt and TGF-β pathways has been seen in colorectal cancers [353,360-363]. Following DNA damage, YAP has been shown to be tyrosine phosphorylated at Y357 by the ABL1 tyrosine kinase, causing YAP to accumulate in the nucleus and bind p73 as a transcriptional co-activator to induce pro-apoptotic transcription [364,365], illustrating a dual role for YAP as a potential tumor-suppressor protein in certain contexts. Recently, interest in how RASSF1A may regulate YAP signaling has grown, suggesting that RASSF1A may play a pivotal role in regulating YAP activity [259,323,354,355,358,365].

IBD has a susceptibility locus at 3p21- the location of RASSF1A [87]. Inflammation has been shown to be associated with the development of cancer for several reasons, including cellular damage causing release of reactive oxygen species (ROS) resulting in DNA damage, and cytokine release including growth factors to promote tissue regeneration via cell proliferation [7,8,21-23]. RASSF1A is known to regulate DNA damage due to ROS, as well as regulate apoptosis and the cell cycle [260,270,324,366] and may therefore be an important regulator of pathways leading to abnormal inflammation and predisposition to cancer.

The objective of this research was to molecularly characterize how loss of expression of RASSF1A may restrict inflammation in a mouse model of IBD, and how the loss of RASSF1A can promote colonic inflammation induced dysplasia. RASSF1A expression may provide a novel molecular link between chronic inflammation and eventual cancer development. Understanding how RASSF1A functions to regulate inflammatory signaling will elucidate putative new IBD biomarkers for disease diagnosis and treatment. My research validated some of our novel targets by analyses of mouse and human colonic sections. In addition, we propose potentially novel biomarkers/targets for IBD to foster the design of new therapeutics to improve disease outcome in patients, identify novel molecular links between chronic inflammation and cancer, and offer better prognostics for cancer development later in life for IBD patients.

We hypothesized that RASSF1A is critical for restricting colonic inflammation by shutting down the nuclear factor kappa B (NFκB) signaling pathway, as well as restricting pro-apoptotic signaling programming driven by p73 bound tyrosine phosphorylated Yes-associated protein (YAP). As YAP can also drive tumorigenesis when bound to transcriptional co-activators other than YAP, dsyregulated YAP signaling as a result of the loss of RASSF1A is a likely molecular link between inflammation and cancer development. Therefore, we propose that RASSF1A is a key signaling protein that regulates inflammatory signaling and the progression of inflammatory disease to cancer.

Research Aims:

1. Molecularly characterize how RASSF1A may regulate intestinal inflammation and how loss of RASSF1A may contribute to exacerbated colitis. Our research indicates that RASSF1A may regulate intestinal inflammation in mice through inhibition of NFκB activity as well as inhibition of tyrosine phosphorylation of YAP (pY-YAP). The latter

would otherwise drive an abnormal pY-YAP/p73 transcriptional program to promote uncontrolled cell death of intestinal epithelial cells, colonic damage, and inefficient epithelial repair.

2. Characterize how RASSF1A and YAP signaling is dysregulated in an inflammation-driven model of carcinogenesis. As we have evidence that loss of RASSF1A is driving abnormal and unrestricted YAP/p73 driven apoptosis, we would like to characterize this phenomenon in a chronic model of inflammation known to result in accelerated inflammation-driven carcinogenesis. As part of this aim, we intend to determine how abnormal YAP signaling may contribute to molecular switching from pro-apoptotic to pro-tumorigenic signaling.

3. To translate our research observations in mice to human IBD. We will utilize biopsy samples from human IBD patients in order to identify novel biomarkers of IBD that may be useful for diagnostic and prognostic testing in IBD patients and may help predict the likelihood of IBD-related cancer development. The goals of my project will allow us to identify new therapeutic targets for more personalized prediction of IBD disease severity. We are currently exploring the use of pY-YAP as a molecular biomarker in IBD patient biopsy samples as well as epigenetic loss of RASSF1A. YAP protein tyrosine kinases (PTKs) may be novel targets for IBD therapies in patients exhibiting the pY-YAP biomarker.

Chapter Two: Materials and Methods

2-1   Mouse lines

This project will utilize a mouse model of colitis and a mouse model of inflammation-driven carcinogenesis in order to understand the role of RASSF1A in inflammation and inflammation-related cancers. For our experiments, we used 12-14 week old wild type and $Rassf1a^{-/-}$ mice [287,304]. All animals (except for the $Rassf1a^{IEC-KO}$ and $Rassf1a^{IEC-WT}$) were on the C57BL/6 background. $Rassf1a^{IEC-KO}$ and $Rassf1a^{IEC-WT}$ were on the C57BL/6-129 background. Although the loss of $Rassf1a$ can lead to tumor formation, the loss of $Rassf5a$ ($Rassf5a^{-/-}$ mice) have not been documented to display an overt phenotype or tumor formation as they age. We therefore used the $Rassf5a^{-/-}$ mice as a related control [245] for experiments in chapter three. Wild type C57BL/6 mice were obtained from Charles River, $Rassf1a^{-/-}$ mice were obtained from Louise van der Weyden (Cambridge University), and Villin-Cre transgenic mice [B6.SJL-Tg(Vil cre)997Gum/J] were obtained from Jackson Laboratories. All colonies are currently maintained at the University of Alberta.

2-2   Chemicals, Reagents, Kits, and Antibodies

Chemicals:

Acetic acid: Fisher BioReagents BP2401C-212

Acrylamide: Invitrogen 15512-023

Agarose: Invitrogen 16500-500

Amidinophenylmethanesulfonyl fluoride hydrochloride (APMSF): Calbiochem 178281

Ammonium persulfate (APS): BioRad 161-0700

Aprotinin: Fisher BioReagents BP2503-10

Azoxymethane: Sigma Aldrich A5486

β-mercaptoethanol: Sigma Aldrich M6250

Betaine: Sigma Aldrich B2629

Bis-acrylamide crosslinker: BioRad 161-0201

Bovine serum albumin (BSA): Sigma Aldrich A9647

Bradford protein assay reagent: BioRad 500-0006

Bromophenol blue Sigma Aldrich B6131

CpG Methyltransferase: New England Biolabs M0226S

Dextran sodium sulphate (DSS), 36 000-50 000 MW: MP Biomedicals 160110

Dithiothreitol (DTT): Millipore 3860

DirectPCR Lysis Reagent: Viagen Biotech 102-T

DNA ladder 100bp: Genedirect DM001-R500

dNTP mix: Qiagen 201901

E-64 inhibitor: Calbiochem 324890

Eosin: Fisher BioReagents E514-25

Ethidium bromide: BioRad 161-0433

Ethylenediaminetetraacetic acid (EDTA): Millipore EX0539-1

Ethylene glycol tetraacetic acid (EGTA): Calbiochem 324626

Ethanol: Commercial Alcohols P016EAAN

Glycerol: Anachemia 43567-360

Glycine: Fisher BioReagents BP3815

Harris modified method hematoxylin: Fisher BioReagents SH26-500D

Horse serum: Gibco 16050-122

Hydrochloric acid: Fisher Chemical A144C-212

Hydrogen peroxide 30% (H_2O_2): Fisher BioReagents H323

Imatinib mesylate: Selleck Chemicals 51026

Isoflurane: Baxter 1001936060

Isopropanol: Fisher Chemical A451

Leupeptin: Calbiochem 108975

Luminol: Sigma Aldrich A8511

Methanol: Fisher Chemical A452

N-alpha-tosyl-L-lysinyl-chloromethylketone (TLCK): Calbiochem 616382

p-Coumaric acid: Sigma Aldrich C9008

Pepstatin A: Calbiochem 516481

Permount: Fisher Chemical SP-15

PCR grade sterile water: Fisher BioReagents BP561

Phenylmethylsulfonyl fluoride (PMSF): Thermo Scientific/ Pierce 36978

Phosphoramidon: Calbiochem 525276

Polyvinylidene fluoride (PVDF) membrane: Millipore

Potassium acetate: Fisher Chemical 580130

Potassium chloride: Caledon Laboratories 5920-1

Potassium chloride solution: Fisher BioReagents SP138-500

Potassium phosphate monobasic: Fisher Chemical P285

Precision Plus Protein Dual Color Standard: BioRad 161-0374

Protein A Sepharose GE Healthcare

Protein G Sepharose GE Healthcare

Proteinase K: Promega V3021

RNAlater RNA stabilization reagent: Qiagen 76106

RNAlater ICE: Life Technologies AM7030

RNAse Out: Invitrogen 1077-019

Skim milk powder: Great Value Foods

Sodium acetate: Calbiochem 567418

Sodium azide: Fisher BioReagents BP922I-500

Sodium citrate dihydrate: Fisher Chemical S279

Sodium chloride: Fisher BioReagents BP358-212

Sodium dodecyle sulphate (SDS): BioRad 161-0302

Sodium hydroxide 5N: Fisher Chemical SS256

Sodium hyperchlorate 4%: Sigma Aldrich 239305

Sodium orthovanadate: Calbiochem 56740

Sodium phosphate dibasic heptahydrate: Fisher BioReagents BP-331

Sodium pyrophosphate: Sigma Aldrich 221368

SsoAdvanced Universal SYBR Green Supermix: BioRad 172-5271

SuperSignal West Dura Chemiluminescent Substrate: Thermo Scientific/ Pierce 34075

Taq Polymerase: New England Biolabs M0273

Tosyl phenylalanyl chloromethyl ketone (TPCK): Calbiochem 616387

T-PER Lysis Reagent: Thermo Scientific/ Pierce 78510

Tris base: Invitrogen 15504-020

Triton X-100: VWR VW3929-2

TUNEL Enzyme: Roche 11767305001

TUNEL Label: Roche 11767291910

Tween- 20: Fisher Bioreagents Whatman Chromatography paper Fisher Scientific BP337

Vectashield Mounting Medium with DAPI: Vector Laboratories H-1200

Vectastain Elite ABC Kit, Vector Laboratories PK-6100

Xylenes: Fisher Chemical X5

Xylene cyanol: Amresco 0819

Z-fix: Anatech 170

ELISAs and other Kits

AllPrep DNA/RNA Mini Kit: Qiagen 80204

Epitect Bisulfite Kit: Qiagen 59104

High-Capacity cDNA Reverse Transcription Kit: Applied Biosystems 4368814

Hyaluronan Enzyme-Linked Immunosorbent Assay: Echelon K1200

IL-18 Mouse ELISA Kit: Life Technologies KMC0181

Metal-enhanced DAB Substrate Kit: Thermo Scientific/ Pierce 34065

Mouse Cytokine Array / Chemokine Array 32-Plex Panel: Eve Technologies

Mouse IL-1 beta ELISA Kit: Thermo Scientific/ Pierce EM2IL1B

Mouse IL-6 ELISA Kit: Thermo Scientific/ Pierce EM2IL6

Mouse IL-10 ELISA Kit: Thermo Scientific/ Pierce EM2IL10

Mouse IL-12 (p70) ELISA Kit: Thermo Scientific/ Pierce EMIL12

Mouse IFN gamma ELISA Kit: Thermo Scientific/ Pierce EM1001

Mouse MCP-1 Ultra-Sensitive Kit: MSD Meso Scale Discovery K152AYC-1

Mouse Pro-Inflammatory 7-Plex Ultra-Sensitive Kit: MSD Meso Scale Discovery K15012C-1

Mouse TNF alpha ELISA Kit: Thermo Scientific/ Pierce EMTNFA

MPO Mouse, ELISA kit: Hycult Biotech HK210-02

NE-PER Nuclear and Cytoplasmic Extraction Reagent: Thermo Scientific/ Pierce 78835

PyroMark Q24 Advanced CpG Reagents: Qiagen 970922

PyroMark CpG Assay Mouse Rassf1a: Qiagen PM00416290

PyroMark PCR Kit: Qiagen 978703

PyroMark Wash Buffer: Qiagen 979008

TGF-β1 Multispecies ELISA Kit: Life Technologies KAC1688

Reagents/ Buffers:

4X Separating Buffer: 1.5 M Tris, 0.4% SDS, pH to 8.7 with HCl

4X Stacking Buffer: 0.4 M Tris, 0.4% SDS, pH to 6.58 with HCl

5X DNA loading buffer: 3% Bromophenol blue, 3% xylene cyanol FF, 30% glycerol

5X EMSA Binding Buffer: 50 mM Tris pH7.6, 50% glycerol, 5 mM DTT, 2.5 mM EDTA

10X Phosphate Buffered Saline (PBS): 1.347 M NaCl, 0.027 M KCl, 0.043 M Na_2HPO_4, 0.014 M $KH_2PO_4 \cdot \bullet 7H2O$, pH to 7.4 when diluted

10X Running Buffer: 0.125 M Tris, 0.96 M Glycine, 0.5% SDS, pH to 8.3 when diluted

10X Tris Buffered Saline (TBS): 1.5 M NaCl, 0.5 M Tris, pH to 7.4

Acrylamide/Bis 30:0.8: 30% Acrylamide, 0.8% Bis-acrylamide

Kinase Activity Buffer: 30 mM HEPES pH 7.1, 10 mM $MgCl_2$, 2 mM $MnCl_2$, 5 mM DTT, 10% glycerol, 0.2 mM sodium orthovanadate

Sample Buffer for SDS-PAGE: 26% Glycerol, 5% SDS, 0.174 M Tris, pH to 6.8 with HCl, 0.02% Bromophenol blue, add fresh 0.04% β-mercaptoethanol

Semi-Dry Transfer Buffer: 50 mM Tris, 380 mM Glycine, 0.1% SDS, 20% Methanol

SL Protease Inhibitor Cocktail: 0.1% aprotinin, 0.05% phosphoramidon, 0.1% TLCK, 0.2% TPCK, 0.1% APMSF, 0.1% E-64, 0.05% leupeptin, 0.02% pepstatin A, in 100% ethanol

Stripping Buffer: 52 mM Tris pH 6.8, 2% SDS

TBS-Tween Buffer: 500 mM Tris pH 7.4, 100 mM NaCl, 0.05% Tween-20

Tris-acetate-EDTA (TAE) Buffer: 400 mM Tris-acetate pH 8.5, 2 mM EDTA

Wet Transfer Buffer: 0.025 M Tris, 0.192 M Glycine, 20% Methanol

Antibodies

4G10 Platinum Anti-Phosphotyrosine, Millipore 05-1050, 1:5000 IB, 0.5ug IP

c-ABL1 (K-12), Santa Cruz Biotechnology sc-131, 1:200 IB

BAX YTH-5B7, Trevigen 2280-MC-100, 1:500 IB, 1:200 IHC

BAX (N-20), Santa Cruz Biotechnology sc-493, 1:500 IB

β-catenin, Cell Signaling 9562, 1:1000 IB

E-cadherin (24E10), Cell Signaling 3195, 1:500 IB, 1:100 IHC

N-cadherin, Cell Signaling 4061, 1:1000 IB, 1:100 IHC

ERK1 (C-16), Santa Cruz Biotechnology sc-93, 1:5000 IB

ERK2 (C-14), Santa Cruz Biotechnology sc-154, 1:5000 IB

GSK3β (27C10), Cell Signaling 9315, 1:500 IB

Phospho-GSK3β (Ser9), Cell Signaling 9336, 1:500 IB

Phospho-H2A.X (Ser139), Millipore 05-636, 1:500 IB (aka γH2A.X)

IκBα, Cell Signaling 9242, 1:1000 IB

Phospho IκBα (Ser32/36) (5A5), Cell Signaling 9246, 1:200 IB

Lamin B, Invitrogen 33-2000, 1:500 IB

c-MYC (9E10), Santa Cruz Biotechnology sc-40, 1:200 IB

Tp53 (PAb 1801), Abcam ab28, 1:1000 IB

Tp73 (H-79), Santa Cruz Biotechnology sc-7957, 1:500 IB

PARP, Cell Signaling 9542, 1:1000 IB

pan-Ras (FL-189), Santa Cruz Biotechnology, 1:200 IB

RASSF1A (M304), from Dr. Gerd Pfiefer in house, 1:200 IB

β-tubulin (TUB2.1), Sigma-Aldrich T5201, 1:1000 IB

YAP (H-125), Santa Cruz Biotechnology sc-15407, 1:500 IB

Phospho-YAP (Ser127), Cell Signaling 4911, 1:500 IB

Phospho-YAP (Tyr357), Sigma Aldrich Y4645, 1:200 IB, 1:500 IHC

Anti-Mouse HRP, GE NA931V, 1:7000 IB

Anti-Rabbit HRP, GE NA934V 1:7000 IB

Anti-Mouse Biotin, Jackson Labs 711065152, 1:500 IHC

Anti-Rabbit Biotin, Jackson Labs 715065150, 1:500 IHC

2-3   Acute Mouse Model of Inflammation

Intestinal colitis can be modeled in mice by the addition of 3% dextran sodium sulfate (DSS) in drinking water for 7 days (acute treatment) to induce injury, followed by regular drinking water for recovery. DSS irritates the colonic mucosa, resulting in epithelial wall breakdown, microflora invasion activating TLR-expressing epithelial cells, and mucosal injury [367-369]. DSS-induced colitis mimics the symptoms of human IBD and is considered a model of epithelial damage and repair.

Animals were administered 3% w/v DSS in the drinking water for 7 days followed by recovery for 7 days. They were monitored for: piloerection, bloatedness, tremors, lack of movement, rectal bleeding and weight loss (all on a scale of 0–5 with 5 being very severe, adapted from Madsen et al. [187]). Animals were euthanized once rectal bleeding became grossly apparent. For weight loss, a score of 0 for no weight loss, 1 for <5% loss, 2 for 5–10% loss, 3 for 10–15% loss, 4 for 15–20% loss and a score of 5>20% loss in initial body weight. Disease activity indices (DAI) were the sum of all individual scores (Table 2.1). Animals were sacrificed at various points (Figure 2.1) and blood, colon, kidney, and liver samples collected for molecular analysis. Colon lengths were also measured at each time point to determine colonic shortening due to inflammatory damage.

2-4   Chronic Mouse Model of Inflammation-Induced Carcinogenesis

For our inflammation-driven carcinogenesis model mice were exposed to one injection (8 mg/kg) of the pro-carcinogen azoxymethane (AOM) followed by 3 cycles of 2% DSS and water in order to mimic human IBD 'flare ups' with intermittent recovery periods [146,157,158] (Figure 2.1). Mice were monitored over time for weight changes as well as clinical symptoms of colitis such as rectal bleeding and diarrhea. Together, these symptoms and body weight changes were assigned a disease activity index (DAI) score (Table 2.1). Due to the high mortality of *Rassf1a-/-* mice exposed to 3% DSS, in our chronic model animals were administered 2% w/v DSS in the drinking water for 5 days followed by recovery for 7 days. Animals were sacrificed at various points (Figure 2.1) and blood, colon, kidney, and liver samples collected for molecular analysis.
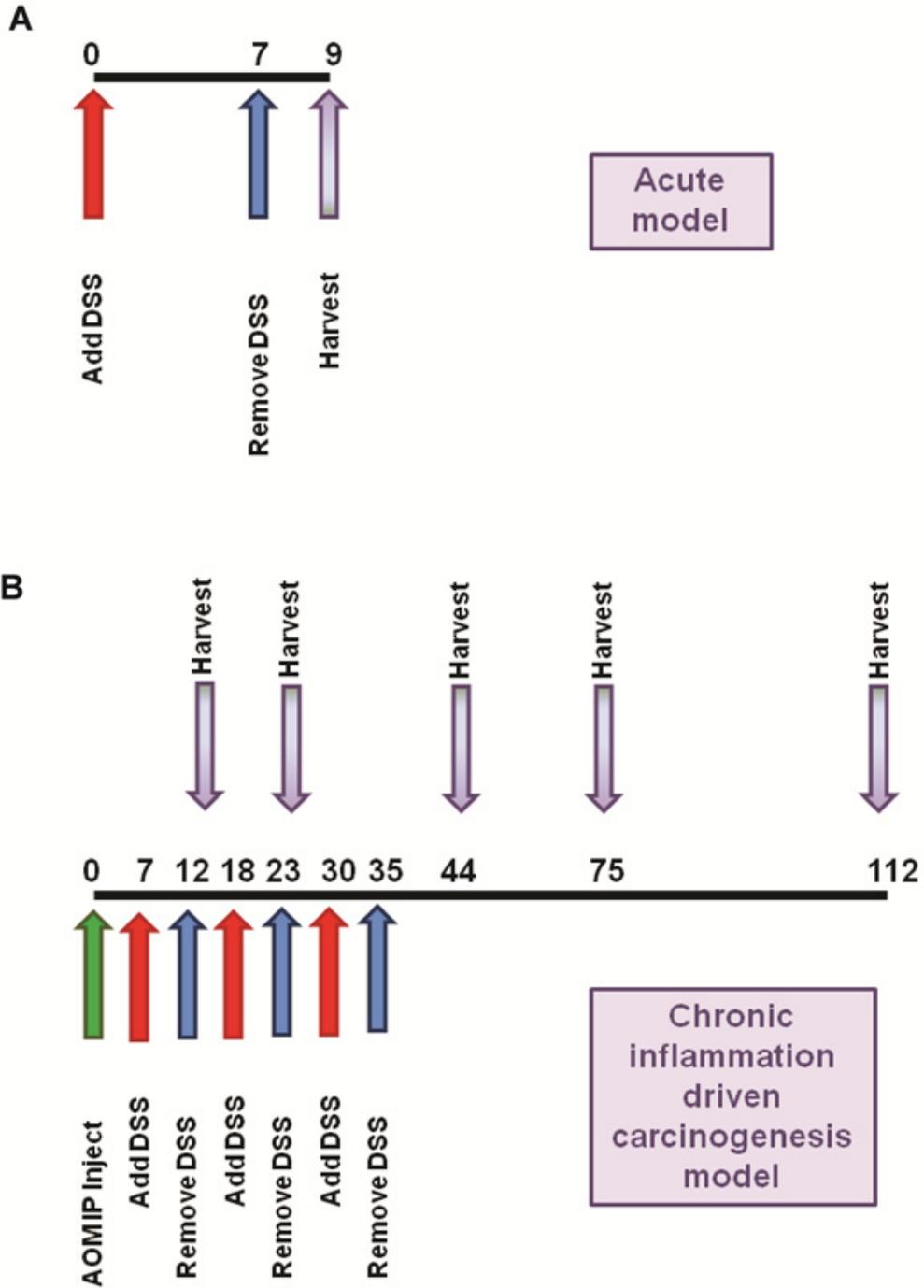
Figure 2.1: Diagrammatic representation of mouse models used in this study. (A) An acute model represents a single incidence of chemically induced colitis flare-up with one exposure to DSS in drinking water for seven days, followed by one day of recovery. **(B)** A chronic inflammation-driven carcinogenesis model using exposure to a pro-carcinogen (azoxymethane) followed by exposure to inflammation inducing DSS in the drinking water for three cycles, representing recurring inflammatory flare-ups, followed by inflammatory recovery and subsequent development of inflammation-related carcinogenesis

Table 2.1: Disease Activity Index (DAI) Scoring Parameters [modified from 187]

Piloerection: Score 0 (none)- 5 (severe)	**Rectal bleeding**: Score 0 (none)- 5 (severe)
Bloat: Score 0 (none)- 5 (severe)	**Movement**: Score 0 (normal)- 5 (very slow/none)
Tremors: Score 0 (none)- 4 (severe)	**Pussed eyes**: Score 0 (none)- 4 (severe)
% Body Weight Change: 1-5% loss- Score 1 6-10% loss- Score 2 11-15% loss- Score 3 >15% loss- Score 4	

2-5 Cardiac Puncture and collection of serum samples

Cardiac puncture was used to obtain whole blood samples from mice at the time of harvest as a terminal procedure. Mice were sedated to surgical plane using isoflurane, which was confirmed using the toe-pinch test [370]. Mice were placed dorsally with the ventral surface facing up. A 1 mL syringe fitted with a 23 G needle was inserted just below the xiphoid process through the diaphragm into the heart and blood gently aspirated. Collected whole blood was placed immediately into a 1.5 mL eppendorf tube on ice and allowed to coagulate for 1.5 hours. Samples were then spun in a 4°C microcentrifuge at 16 000g for 10 min. Cleared serum supernatant was collected and stored at -80°C for cytokine analysis.

2-6 Tissue Handling

Colon, kidney, and liver samples collected were for molecular analysis. Samples intended for nucleic acid analyses were immediately submerged in RNA-later post excision and allowed to incubate at 4°C for 24 hours in order to fully permeate the tissues. At this point samples were removed from RNA-later and stored at -80°C until use. RNA was isolated from colon tissue using the Qiagen AllPrep DNA/RNA spin column nucleic acid extraction kit according to the manufacturer's directions. Nucleic acid concentration was determined using the Thermo Scientific Nanodrop.

Colon samples intended for molecular protein analysis were excised from the mouse, flushed with 1X PBS to remove fecal matter, and immediately submerged in 1 mL ice-cold T-PER lysis buffer (Pierce) with fresh 0.1% aprotinin, 0.2% phenylmethanesulfonylfluoride or phenylmethylsulfonyl fluoride (PMSF), 0.1% sodium pyrophasphate (NaPP/ Na_4O7P_2), 1% sodium orthovanadate (Na_3VO_4), and 0.2% SL protease inhibitor cocktail in a 2 mL eppendorf tube. Samples were then homogenized

using a Fisher PowerGen handheld homogenizer and centrifuged at 4°C at max speed for 10 min. The soluble protein supernatant was collected and stored at -80°C until use. Protein concentration was determined using a Bradford protein assay.

2-7 Crypt cell isolation

Intestinal crypt cells were isolated as outlined previously [371]. Briefly, colons were flushed with cold 1× PBS, cut open longitudinally and then soaked in 1X PBS with gentle shaking for 20 minutes. The colons were cut into small pieces and incubated with 0.04% sodium hypochlorite for 30 min with gentle shaking in a 10 cm^2 Petri dish. Following incubation, the colon pieces were removed and allowed to shake continuously at room temperature for 30 minutes in a solution containing 1X PBS/1 mM EGTA/1 mM EDTA. Cells were then dislodged by pipetting the tissue up and down using a 25 mL serological pipette until the solution became cloudy. The supernatant was removed (containing the crypt cells) and centrifuged at 3000 rpm for 10 minutes to collect the crypt cells. The cells were washed in 1X PBS, transferred to an eppendorf tube, pulse spun to pellet the cells followed by nuclear extraction as previously described [371]. Generally, one crypt cell preparation for nuclear extraction was obtained from two colons. Crypt isolation was confirmed visually using a light microscope.

Isolation of crypt cells using chelating agents is primarily achieved by disrupting the calcium based cell-cell contacts, and therefore cells isolated using this method show reduced metabolic activity and increased susceptibility to apoptosis over 24 hours [372,373]. An alternative method (not used in this study) is to obtain colonic crpyt cells by manual tissue scrapings, however this method also has the drawback of causing mechanical stress to epithelial cells.

2-8   Isolation of bone marrow derived macrophages

Mice were euthanized by CO_2 asphyxiation and sprayed down with 70% ethanol before dissection. Femurs were dissected out, attached muscle and fibers removed, and transferred to a sterile petri dish containing DMEM media with 10% bovine growth serum (BGS). Bone marrow cells were flushed from femurs using a 1 mL syringe fitted with a 30 G needle using DMEM media and the resulting cell suspension filtered through a 4 μm cell strainer before centrifugation at 16 000 g for 5 min. After pouring off the supernatant, 5 mL of red cell lysis buffer was added to the pellet and 1 mL of BGS added directly to the bottom of the 15 mL conical tube and incubated for 5 min at room temperature. Cells were centrifuged again at 16 000g for another 5 min, washed in 1 mL of sterile PBS, and transferred to a 1.5 mL eppendorf tube before final centrifugation at max speed for 1 min to pellet cells. Supernatant was removed and the dry pellet was stored at -80°C for future use [374].

2-9   Preparation of nuclear extracts

Nuclear extracts were obtained from crypt cell and BMDM pellets using the NE-PER nuclear and cytoplasmic fraction kit from Pierce Scientific according to the manufacturer's directions. Purity of the resulting nuclear and cytoplasmic fractions was confirmed using Western blotting for β-tubulin and lamin B, with the cytoplasmic fraction expected to have plentiful tubulin and no lamin B, and the nuclear fraction expected to have plentiful lamin B and little to no tubulin. Fractions were stored in 1.5 mL eppendorf tubes at -80°C until use.

2-10   Tissue histology and immunohistochemistry

Colon samples were isolated, fixed in z-Fix (Anatech Ltd) and paraffin-embedded. All inflammation scores were obtained utilizing blinded scoring by a gastrointestinal pathologist (Dr. Aducio Thiesen) based on infiltration of enterocytes, neutrophils, lamina propria cellularity, crypt structure and epithelial hyperplasia (scored as 0-2 where 2=maximal injury)[187]. Dysplasia scoring assessed the presence or absence of dysplasia/neoplasia and indicated the degree of dysplasia based on a numerical score similar to tumor grading (Table 2.2, adapted from [187] and [375]).

Immunohistochemistry (IHC) and hematoxylin and eosin (H&E) staining were carried out using standard techniques. Formalin fixed, paraffin embedded sections were de-paraffinized and re-hydrated as described previously [376]. Antigen retrieval was done by boiling in sodium citrate buffer as previously described. Endogenous peroxidase activity was quenched with 3% H_2O_2. Sections were blocked in 2% BSA + 2% donkey serum for one hour at room temperature, and incubated in primary antibody as indicated overnight at 4°C. Sections were incubated in 1:500 biotinylated secondary antibody for 1 hour at room temperature and signal amplification and detection was done using the VECTASTAIN Elite ABC Kit and the Metal Enhanced DAB Substrate Kit. Counterstaining was done using Harris' modified hematoxylin.

Table 2.2: Summary of Histological Scoring Criteria (modified from 187 and 370)

Inflammation Histological Scoring Parameters	
Enterocyte Injury: Score 0-3	*Epithelial hyperplasia:* Score 0-3
Lamina propria lymphcytes: Score 0-2	*Lamina propria neutrophils:* Score 0-2
Dysplasia/Neoplasia Scoring Parameters	
Normal: Score 0	*Abberant crypt foci*: Score 1 • Epithelial cell pleomorphism • Gland malformation (splitting/infolding)
Moderate dysplasia: Score 2 • Polyploidy hyperplasia/dysplasia • Early cellular and nuclear atypia • Piling and infolding • Projection into lumen • Loss of normal glandular, mucous, or goblet cells	*Adenomatous/sessile hyperplasia/dysplasia*: Score 3 • Gastrointestinal intraepithelial neoplasia or carcinoma in situ • Dysplasia confined to mucosa • Frequent and bizarre mitoses
Intramucosal carcinoma: Score 4 • Extension of severely dysplastic regions into muscularis mucosae	*Invasive Carcinoma:* Score 5 • Submucosal invasion • Any demonstrated invasion into blood or lymphatic vessels or nodes • Other metastases

2-11 <u>Immunoblotting</u>

Discontinuous denaturing sodium dodecyl sulfate polyacrylamide gel electrophoresis (SDS-PAGE) was used to separate proteins from protein samples. Generally, a 10% polyacrylamide separating gel with a 5% stacking gel was used for most proteins; however, a 12.5% separating gel with a 5% stacking gel was used for proteins smaller than 37 kDa. 40 µg of total protein was loaded per lane, with the exception of nuclear fraction samples, where 10 µg of total protein was loaded per sample. Gels were run using vertical electrophoresis using the CBS Scientific system, generally at 150 V for approximately 1.5 hours. Proteins were transferred to methanol activated polyvinyl difluoride (PVDF) membrane using a wet transfer for large proteins (100 V for 1.5 hours) and semi-dry transfer for proteins smaller than 37 kDa (460 mA for 2 hours). Membranes were rinsed in ddH_2O, blocked in 10% milk in 0.01% TBS-Tween for 30 min at room temperature and transferred to primary antibody in 2% milk in 0.01% TBS-Tween at 4°C overnight with rocking. After primary antibody incubation, membranes were rinsed in 0.01% TBS-Tween for 5 min three times, and transferred to secondary antibody in 2% milk in 0.01% TBS-Tween for 2 hours. Membranes were then rinsed again for 5min three times before incubation with enhanced chemiluminescence (ECL) detection reagent (in house) or SuperSignal West Dura Extended Duration Substrate (Thermo Scientific). Signal detection was captured using X-ray film or the Alpha Innotech imaging system.

Where applicable, membranes were stripped using stripping buffer with fresh BME at 60°C for 5 min, rinsed in ddH_2O three times, and rinsed in 0.01% TBS-Tween for 5 min three times. Blocking and antibody incubation followed normally. For antibodies against tyrosine phosphorylated proteins 5% bovine serum albumin in 0.01% TBS-Tween was used in substitution for all steps using milk. Where fold changes are indicated, all samples have first been normalized to their respective ERK1/2 loading controls, and then fold changes calculated as compared to baseline wild-type animals.

2-12   Enzyme linked immunosorbent assays (ELISA)

Cytokine levels were assessed in diluted serum samples or *ex vivo* cellular supernatant extracts using ELISA and carried out in accordance with manufacturer's instructions. Final absorbances at 450 nm were read using a VICTOR X4 Multilabel Plate Reader from Perkins Elmer.

Briefly, serum or tissue samples were diluted using the provided diluents and added to a 96-well microplate pre-coated in antibody specific to the protein of interest. Samples were allowed to incubate at room temperature for 1-2 hours in order to allow antibody-protein binding, at which point the microplate was washed with PBS-T and a solution containing a biotin-labelled second antibody against the protein of interest for 1-2 hours at room temperature. After a second wash, the microplate was incubated with a solution containing HRP-labelled streptavidin which bound to the biotin labelled secondary antibody for 30 minutes, followed by a final wash. Finally, TMB substrate solution was added and incubated for 30 minutes, during which time HRP acted upon the substrate to produce a blue color. Upon addition of stop solution (hydrochloric acid), the HRP enzymatic reaction was stopped and the solution turned a yellow color with maximum absorbance at 450 nm. Absorbance of microplate wells was read within 30 minutes of stopping the substrate reaction.

2-13   Determination of Reactive Oxidative Species

To determine the degree of ROS generated, a fluorometric assay, utilizing the unique intracellular oxidation of 2′,7′-dichlorofluorescin diacetate (DCF-DA), was used. Freshly isolated crypt cells were seeded into 96-well plates in triplicate. Cells were immediately treated with 5 µM DCF-DA and fluorescence was monitored over 45 minutes in the dark. Fluorescence was measured using a Synergy H4 Microplate

Reader (Biotek Instruments) set to 37°C. Measurements were made using a 485/20 nm excitation and a 528/20 nm emission filter pair and a gain sensitivity setting of 55%. Readings were made from the bottom every 30 seconds for a total of 45 minutes [377].

2-14   Real time polymerase chain reactions (qPCR)

A total of 2 µg of total RNA was converted into cDNA with an Applied Biosystems high-capacity cDNA Reverse Transcription Kit according to manufacturer's instructions. After reverse transcription cDNA was diluted 10 times with RNase-free water and 5 µL was used in PCR reactions using NEB Taq DNA polymerase with standard Taq buffer. Quantitative analysis of specific mRNA expression was performed using real-time PCR by subjecting the resulting cDNA to PCR amplification using the LightCycler 96 Real Time PCR System (Roche). The 25 µL reaction mix contained 0.1 µL of 10 µM forward primer and 0.1 µL of 10 µM reverse primer (40 nM final concentration of each primer), 12.5 µL of SYBR Green Universal Mastermix, 11.05 µL of nuclease-free water, and 100 ng of cDNA sample. Assay controls were incorporated onto the same plate, namely, no-template controls to test for the contamination of any assay reagents.

After sealing the plate with an optical adhesive cover, the thermocycling conditions were initiated at 95°C for 30 sec, followed by 45-65 PCR cycles of denaturation at 95°C for 10 sec, annealing at 55-60°C for 1 min, and an extension phase at 70°C for 30 sec. Melting curve (dissociation stage) was performed by the end of each cycle to ascertain the specificity of the primers and the purity of the final PCR product. The real time-PCR data were analyzed using the relative gene expression i.e. (ΔΔCT) method as described in Applied Biosystems User Bulletin No.2 and explained further by Livak and Schmittgen (2001) [378]. Briefly, the ΔCT values were calculated in every sample for each gene of interest as follows: CT gene of interest – CT reporter gene, with β-actin as the reporter gene. Calculation of relative changes in the expression level of one specific gene (ΔΔCT) was performed by subtraction of ΔCT of

control (vehicle treated animals at 6 or 24 h time points) from the ΔCT of the corresponding treatment groups. The values and ranges given in different figures were determined as follows: $2^{-\Delta(\Delta CT)}$ with $\Delta\Delta$CT + S.E. and $\Delta\Delta$CT − S.E., where S.E. is the standard error of the mean of the $\Delta(\Delta CT)$ value. For a list of primer sequences used, see Table 2.3. Where fold changes are indicated, all samples have first been normalized to their respective actin loading controls, and then fold changes calculated as compared to baseline wild-type animals.

Table 2.3: List of Primers used for Real-Time qPCR Experiments

Gene Name	Gene Symbol	Forward Primer Sequence	Reverse Primer Sequence	Product Size (bp)	Annealing Temperature (°C)
Beta actin	ACTB	GTG ACG TTG ACA TCC GTA AAG A	GCC GGA CTC ATC GTA CTC C	245	55
Mus musculus runt related transcription factor 2	RUNX2	CAG TC TTC ACA AAT CCT CC CCA	TCA TAC TGG GAT GAG GAA TGC G	168	58
Yes-associated protein 1	YAP1	TAC ATA AAC CAT AAG AAC AAG ACC ACA	GCT TCA CTG GAG CAC TCT GA	100	58
Tumor protein 73	TP73	TGC TCC GCA CCC TTA TAA CC	GAA CTC CAC AGG TGC TCG AA	170	58
TEA family domain member 1	TEAD1	AAG CTG AAG GTA ACA AGC ATG G	GCT GAC GTA GGC TCA AAC CC	260	58
Heme oxygenase 1	HO1	GTG ATG GAG CGT CCA CAGC	TGG TGG CCT CCT TCA GGG	67	60
DNA methyltransferase 1	DNMT1	AAA GTG TGA TCC CGA AGA TCA AC	TGG TAC TTC AGG TTA GGG TCG TCT A	79	58

94

2-15 Reverse transcription polymerase chain reactions (RT-PCR)

A total of 2 µg of total RNA was converted into cDNA with an Applied Biosystems high-capacity cDNA Reverse Transcription Kit according to manufacturer's instructions. After reverse transcription cDNA was diluted 10 times with RNase-free water and 5 µL was used in PCR reactions using NEB Taq DNA polymerase with standard Taq buffer. PCR parameters were initial denaturation 94°C for 2 min, followed by 35 cycles of denaturation at 94°C for 1 min, annealing for 1 min, and extensions at 68°C for 1 min (35 cycles), followed by a final extension 68°C for 10 min. PCR products were analyzed on a 2% agarose gel and visualized with ethidium bromide. For a list of primer sequences used, see Table 2.4. Where fold changes are indicated, all samples have first been normalized to their respective actin loading controls, and then fold changes calculated as compared to baseline wild-type animals.

Table 2.4: List of Primers used for Reverse Transcriptase RT-PCR Experiments

Gene Name	Gene Symbol	Forward Primer Sequence	Reverse Primer Sequence	Product Size (bp)	Annealing Temperature (°C)
Beta actin	ACTB	GTG ACG TTG ACA TCC GTA AAG A	GCC GGA CTC ATC GTA CTC C	245	55
Mus musculus transformation related protein 53	TP53	TCA GTT CAT TGG GAC CAT CCT G	AAA ATG TCT CCT GGC TCA GAG G	182	58
Ras association domain family member 1a	RASSF1A	ATG TCG GCG GAG CCA GAA CTC ATT GAA CTA	CAC GTT CGT ATC CCG CTC TAG TGC AGA GT	357	62 *Note, from van der Weyden et al.[282]

2-16   DNA methylation analysis by pyrosequencing

Pyrosequencing to determine methylation status was carried out using the Qiagen Pyromark Advanced kit according to the manufacturer's instructions. Briefly, genomic DNA isolated from mouse colonic tissue was bisulfite modified using the Qiagen Epitect Bisulfite Conversion kit, using the instructions for "Sodium Bisulfite Conversion of Unmethylated Cytosines in DNA from Low-Concentration Solutions" according to the manufacturer's instructions. The resulting bisulfite modified DNA was then used as a template to amplify the region of interest using a biotinylated primer set for the first exon of *Rassf1a* provided by Qiagen (cat # PM00416290). A small amount of DNA was run on an agarose gel to confirm product amplification, and the 15 µL of PCR product was used in the Pyromark Advanced system. Amplified product was loaded into the Pyromark machine along with the appropriate binding buffers, reagents (Pyromark Advanced Kit), and a sequencing primer, and the Pyromark Q24 was used to analyze the nucleotide sequence and compare it against the expected sequence of the region of interest.

Bisulfite modification converts cytosine nucleotide to uracil, however, methylated cytosine residues are protected from this effect. Following bisulfite cleanup and PCR amplification, any uracils will have been converted to thymine, while methylated cytosines will remain cytosine. The Pyromark system measure whether a cytosine or a thymine residue is present at each predicted CpG island and generate a percentage of methylation based on the product ratios. A positive control includes a synthetically methylated genomic mouse DNA sample and a negative control contains no template DNA.

2-17 Electrophorectic mobility shift assay (EMSA)

EMSA was carried out as previously described [374]. Briefly, duplex DNA specific for the NFκB binding site was end-labeled with [γ-32P] ATP by using T4 polynucleotide kinase, purified using a G-50 sephadex column (Roche) and allowed to associate with 4 μg of the nuclear extracts containing NFκB for 30 min at room temperature. The oligonucleotide was AAATGTGGGATTTTCCCATGA for crypt cell NFκB analysis (the NFκB binding site from the IL-6 promoter) and TCAGAGGGGACTTTCCGAGAGG for BMDM NFκB analysis (the NFκB binding site from the IL-8 promoter). DNA/protein complexes were then separated by non-denaturing gel electrophoresis, dried onto Whatman filter paper and autoradiographed. Nuclear extracts were prepared using NE-PER (ThermoFisher Scientific) as per manufacturer's instructions). Binding buffer was 100 mM Tris-HCL pH 6.5, 500 mM KCl, 1.2 mM EDTA, 12 mM DTT, 20% glycerol and 1 μg Salmon Sperm DNA. The purity of fractions was confirmed with anti-β-tubulin (cytosolic fraction) or anti-lamin B (nuclear fraction).

2-18 Collection and handling of human samples

We have collected over 400 blood samples and approximately 200 biopsy samples from pediatric and adult IBD and control patients attending regular clinic appointments at the University of Alberta. We have also collaborated with researchers in the Centre for Excellence in Gastrointestinal Inflammation and Immunity Research (CEGIIR) at the University of Alberta, the Alberta IBD Consortium, and the Alberta Health Services pathology bank to obtain additional patient biopsy samples as necessary. Samples were collected from patients with active disease as well as those in remission from areas of active inflammation as well as from areas showing no gross inflammation when available. For results presented in this thesis, samples presented are from patients with active disease from regions of gross inflammation. Samples are

from both ulcerative colitis and Crohn's disease patients and from colonic and ileal regions as indicated in results.

We also received blood and tumor biopsy samples from colorectal cancer patients from collaborations with the Cross Cancer Institute Tumor Bank. All biopsy and tumor samples were flash-frozen in liquid nitrogen and stored at -80°C. Samples were transferred to Z-fix fixative for 24-36 hours in order to fix the samples prior to being dehydrated and paraffin-embedded as described previously [376]. Biopsy samples were also mounted for IHC immunoblotting to assess the usefulness of novel IBD biomarkers identified in the mouse models.

2-19   Statistical Analyses

Statistical analyses were performed using one-way or two-way ANOVA with Tukey or Bonferroni post-hoc tests respectively, or Students t-test (two-tailed), as indicated using the GraphPad Prism 5 software. All statistics were non-parametric. Survival analysis was done using Kaplan-Meier curves and Mantel-Cox tests. Results are considered significant if the p-value is <0.05. All experiments were carried out at least three times with biological replicates. Error bars in all graphs represent the standard error. Statistics for individual experiments are indicated with the graph or figure legends. Sample size calculations are shown in Table 2.5.

Table 2.5: Sample Size Calculations for Mouse Models and Human Samples

Table 2.5.1: Sample size calculation for animal models (95% Confidence):
$n \geq 2[P.I.*SD/\text{clinical difference}]^2$ Where: $\alpha = 0.05$, $\beta = 80\%$, $1-\beta = 0.2$ Power Index (P.I.)= $1.96 + 0.84 = 2.80$ Clinical difference=DAI score of ≥ 4 $n \geq 2[(2.8*2.37)/4]^2$ $n \geq 5.5$, therefore a minimum of 6 animals are needed per group in order to achieve statistical significance with 95% confidence.
Table 2.5.2: Sample size calculation for human IBD patient samples (95% Confidence):
$n \geq [(N)(p)(1-p)]/[(N-1)(D)+(p)(1-p)]$ Where: $D = [\text{Confidence Interval}]^2/[z^2]$; $D = (0.05)^2/1.96^2$, $D = 0.00065$ N= Population of IBD patients at the University of Alberta Hospital p= Prior assumption of a positive result; $p = 0.50$ $n \geq [500*0.5*0.5]/[(499*0.00065)+(0.5*0.5)]$ $n \geq 217.7$, therefore a minimum of 218 IBD patient samples will need to be collected in order to achieve statistical significance with 95% confidence.

Chapter Three: The Tumor Suppressor Protein RASSF1A is Essential for Recovery in Acute Inflammation

Disclaimer: The majority of this chapter has been previously published elsewhere as "Gordon M, El-Kalla M, Zhao Y, Fiteih Y, Law J, Baksh S, et al. *The tumor suppressor gene, RASSF1A, is essential for protection against inflammation -induced injury.* PLOS One. (2013, Oct 16), 8(10): e75483" [3]. The sections presented here represent work contributed by M. Gordon. Additional experiments may be found in the published paper, as well as the published Master of Science theses of Mohamed El-Kalla [379] and Yuewen Zhao [380]. In particular, M. El-Kalla and Y. Zhao aided in the experiments and data analysis covered in section 3.1, 3.2.1, and 3.2.2. Y. Fiteih contributed to section 3.2.4 in carrying out experiments and data analysis. N. Volodko contributed to section 3.2.4 in carrying out experiments and data analysis. S. Baksh was the supervisory author of the manuscript and was responsible for all *in vitro* kinase assay experiments and additional biochemistry experiments present in the original published paper.

Abstract:

Ras association domain family protein 1A (RASSF1A) is a tumor suppressor gene silenced in cancer. Here we report that RASSF1A is a novel regulator of intestinal inflammation as $Rassf1a^{+/-}$, $Rassf1a^{-/-}$ and an intestinal epithelial cell specific knockout mouse ($Rassf1a^{IEC-KO}$) rapidly became sick following dextran sulphate sodium (DSS) administration, a chemical inducer of colitis. $Rassf1a$ knockout mice displayed clinical symptoms of inflammatory bowel disease including: increased intestinal permeability, enhanced cytokine/chemokine production, elevated nuclear factor of kappa light polypeptide gene enhancer in B-cells (NFκB) activity, elevated colonic cell death and epithelial cell injury. Furthermore, epithelial restitution/repair was inhibited in DSS-treated $Rassf1a^{-/-}$ mice with reduction of several makers of proliferation including Yes associated protein (YAP)-driven proliferation. Surprisingly, tyrosine phosphorylation of YAP was detected which coincided with increased nuclear p73 association, BAX-driven epithelial cell death and p53 accumulation resulting in enhanced apoptosis and poor survival of DSS-treated $Rassf1a$ knockout mice. We can inhibit these events and promote the survival of DSS-treated $Rassf1a$ knockout mice with intraperitoneal injection of the c-ABL and c-ABL related protein tyrosine kinase inhibitor, imatinib/gleevec. However, p53 accumulation was not inhibited by imatinib/gleevec in the $Rassf1a^{-/-}$ background which revealed the importance of p53-dependent cell death during intestinal inflammation. These observations suggest that tyrosine phosphorylation of YAP (to drive p73 association and up-regulation of pro-apoptotic genes such as BAX) and accumulation of p53 are consequences of inflammation-induced injury in DSS-treated $Rassf1a^{-/-}$ mice. Mechanistically, we can detect robust associations of RASSF1A with membrane proximal Toll-like receptor (TLR) components to suggest that RASSF1A may function to interfere and restrict TLR-driven activation of NFκB. Failure to restrict NFκB resulted in the inflammation-induced DNA damage driven tyrosine phosphorylation of YAP, subsequent p53 accumulation and loss of intestinal epithelial homeostasis.

3-1   Introduction

The Ras association domain family protein 1A (RASSF1A) is frequently lost in human cancers by promoter-specific methylation [1]. RASSF1A (but not RASSF5A/Nore1A) was previously shown to associate with tumor necrosis factor α receptor 1 (TNF-R1) to promote cell death [239]. Although RASSF5A lacks association with TNF-R1, $Rassf5a^{-/-}$ mice do have defective TNF-α responses suggesting that RASSF5A may influence TNF-α signaling and apoptosis through alternate pathways such as interactions with sterile-20 like pro-apoptotic kinases, MST1/2 (mammalian Hippo) [245]. $Rassf1a^{-/-}$ mice are viable and fertile, have normal cell cycle parameters and sensitivity to DNA-damaging agents and show no signs of gross genomic instability [293,304]. They do, however, develop tumors in response to chemical carcinogens and develop spontaneous tumors by 18 months of age. Several animals had B-cell lymphomas and others had tumors localized within the gastrointestinal tract suggesting an important role for RASSF1A in gastrointestinal physiology [293,304]. Recently, it was demonstrated that the $p53^{-/-}Rassf1a^{-/-}$ double knockout mice are viable, fertile and developmentally normal [381]. However, the loss of p53 (even in the heterozygous state) led to >60% of the animals developing tumors in the absence of $Rassf1a$ [381]. These tumors include several adenocarcinomas and sarcomas localized within the lungs. However, there was no evidence of colonic hyperplasia [381]. The $p53^{-/-}Rassf1a^{-/-}$ double knockout mice also revealed enhanced cytokinesis failure and chromosomal abnormalities leading to aneuploidy which suggests importance in mitotic regulation and tumor suppressor function.

It has been determined that 80% of sporadic colorectal cancer (CRC) tumors have somatic and germline mutations within the tumor suppressor gene, adenomatous polyposis coli (APC) [382]. In the absence of APC, β-catenin freely translocates to the nucleus where it signals an intracellular cascade resulting in the transcription of hundreds of genes [383-385]. The loss of RASSF1A in the context of the $APC^{min/+}$ mice

($Rassf1a^{-/-}APC^{min/+}$ mice) has been reported to result in increased β-catenin nuclear localization, intestinal adenomas and poorer survival than single knockout littermate controls [386]. These data would suggest the importance of the early loss of RASSF1A during premalignant formation of adenocarcinomas that may lead to increased malignant transformation and tumorigenesis. The loss of both APC and RASSF1A function may be key initiating events in the formation of CRC and these observations highlight the importance of RASSF1A in intestinal physiology [89,385].

It has been demonstrated that TNF-R1 is a unique death receptor that can activate a cell death pathway through RASSF1A, triggering BAX activation and mitochondrial-driven apoptosis [1,239,262,387]. In addition, TNF-R1 can also promote a pro-inflammatory response through nuclear factor kappa B (NFκB) pathways [12]. NFκB is an important mediator of inflammation and the pathogenesis of intestinal inflammation and inflammatory bowel disease (IBD) [75]. TLRs can also activate a potent NFκB response and defend against invading pathogens [388]. Of the RASSF family members, RASSF6 and 8 were demonstrated to modulate NFκB activity but a mechanism was not proposed [389,390]. Recently, Song et al. (2012) demonstrated that RASSF2 can associate with the IKK complex to inhibit NFκB [339,390,391] and several reports indicate that RASSF1C and 8 may influence the function of the WNT/β-catenin pathways, pathways important for the appearance of intestinal tumorigenesis [339,390].

It is currently unknown if RASSF1A can influence NFκB activation via TNF-R1 or TLR pathways. However, epigenetic analysis does reveal promoter specific methylation of RASSF1A resulting in loss of expression in ulcerative colitis (UC) patients [88], a form of IBD. Interestingly, IL-6 can drive epigenetic loss of RASSF1A via DNA methyltransferase 1 (DNMT1) up-regulation [392,393] suggesting that inflammation can drive expression loss of RASSF1A. In this study, we demonstrate an *in vivo* function for RASSF1A in restricting NFκB-dependent inflammation linked to the TLR pathway. Furthermore, we can demonstrate that NFκB-dependent inflammation can modulate

epithelial proliferation and the appearance of tyrosine phosphorylation of the Hippo pathway target, Yes-associated protein (YAP). We believe that tyrosine phosphorylated YAP can up-regulate pro-apoptotic genes to drive intestinal epithelial apoptosis. Restricting NFκB-dependent inflammation and tyrosine phosphorylation of YAP will maintain epithelial homeostasis, promote epithelial restitution and allow recovery from inflammation induced injury.

Previous findings in our lab showed decreased survival of *Rassf1a*$^{-/-}$ mice following exposure to DSS. Administration of DSS in the drinking water results in colitis in rodents, mimicking human symptoms. These symptoms include weight loss, diarrhea and rectal bleeding. Upon DSS treatment, *Rassf1a*$^{-/-}$ mice became sick within 5-9 days post-treatment with reduced activity, piloerection, a general moribund state/hunched posture, lack of grooming, severe rectal bleeding, and significantly reduced survival (Figure 3.1). Wild-type mice displayed only mild symptoms of DSS-induced intestinal injury and demonstrated full recovery from DSS exposure. *Rassf1a*$^{-/-}$ mice revealed >25% loss of body weight, increased disease symptoms, significantly shortened colon, and decreased crypt depth in contrast to wild-type mice. Histological sections stained with H&E revealed severe colonic disruption with mucosal/crypt damage (cryptitis and crypt abscesses) in *Rassf1a*$^{-/-}$ mice with evident cellular infiltrates composed of immune cells. DSS-treated wild type mice revealed minimal colonic morphology changes and significantly less cellular infiltrates [379]. Surprisingly, the *Rassf1a*$^{+/-}$ hemizygous mice also demonstrated similar symptoms to the *Rassf1a*$^{-/-}$ mice suggesting haploinsufficiency at the *Rassf1a* locus. Since DSS-treated *Rassf1a*$^{+/-}$ mice phenocopy the Rassf1a$^{-/-}$ mice data henceforth is primarily presented for the *Rassf1a*$^{-/-}$ mice.
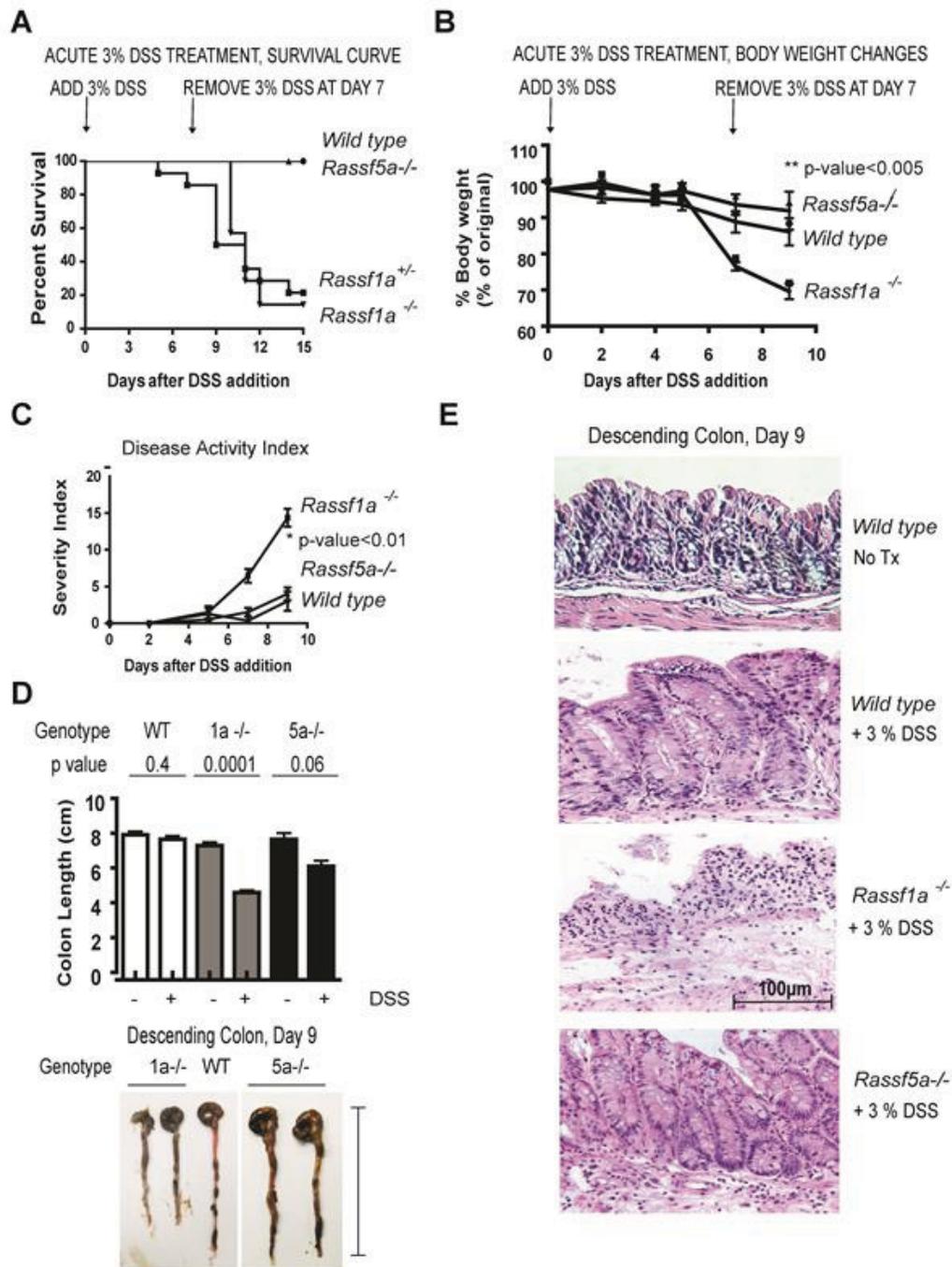
Figure 3.1: *Rassf1a−/−* **animals are sensitive to dextran sodium sulphate (DSS) treatment.** Mice were subjected to 3% DSS solution followed by day 7 replacement with regular water to allow for recovery. **(A)** A Kaplan-Meier curve monitoring % survival following DSS treatment. p-value<0.0001 (WT/*Rassf5a−/−* vs *Rassf1a−/−*) and 0.0023 (WT/*Rassf5a−/−* vs *Rassf1a+/−*); n=12–20. **(B)** Body weight changes following DSS treatment. p-value<0.005 (WT/*Rassf5a−/−* vs *Rassf1a−/−*); n=12–20. **(C)** Disease activity index (DAI) following DSS treatment. p-value<0.01 (WT/*Rassf5a−/−* vs *Rassf1a−/−*), n=12–20. **(D)** Colon length at day 9 of DSS treatment. The indicated p-values represent the difference between −/+DSS treatments within the genotypes; p-value [WT vs *Rassf1a−/−* (+DSS)] =0.0001; WT vs *Rassf5a−/−* (+DSS) =0.01; and *Rassf1a−/−* vs *Rassf5a−/−* (+DSS) <0.0005. A representative picture is shown in the bottom panel indicating how colon length was measured. **(E)** A longitudinal cross-section of the descending colon stained with H&E is shown for untreated and DSS-treated animals. All images 40X. All untreated colon sections samples were very similar to untreated colon sections from wild type mice.

106

Additional studies to specifically explore the role of RASSF1A in intestinal physiology, an intestinal epithelial cell specific knockout to RASSF1A, $Rassf1a^{IEC\text{-}KO}$, was generated by mating $Rassf1a\text{-}LoxP$ conditional mice [293] with the Villin-Cre transgenic mouse and the knockout allele detected by PCR. Villin is an intestinal-related cytoskeletal protein that is associated with brush border microvilli. RASSF1A knockout was confirmed by PCR utilizing genomic DNA from colonic sections as previously published [293]. Similar to the $Rassf1a^{-/-}$ mice, DSS-treated $Rassf1a^{IEC\text{-}KO}$ animals displayed <25% survival with significant loss of body weight, colon length, disrupted colonic crypts, decreased crypt depth, severe disease activity indices, and elevated histopathological scores. In addition, DSS-treated $Rassf1a^{IEC\text{-}KO}$ animals had elevated IL-6 and MCP-1, increased NFκB DNA binding activity in $Rassf1a^{IEC\text{-}KO}$ bone marrow cells and colon crypt cells, and significant increases in colonic tissue MPO and colonic tissue HA levels [380] (Figure 3.2). Taken together, these data strengthen the protective role of RASSF1A in restricting unwanted NFκB and following DSS-induced inflammation injury [3].
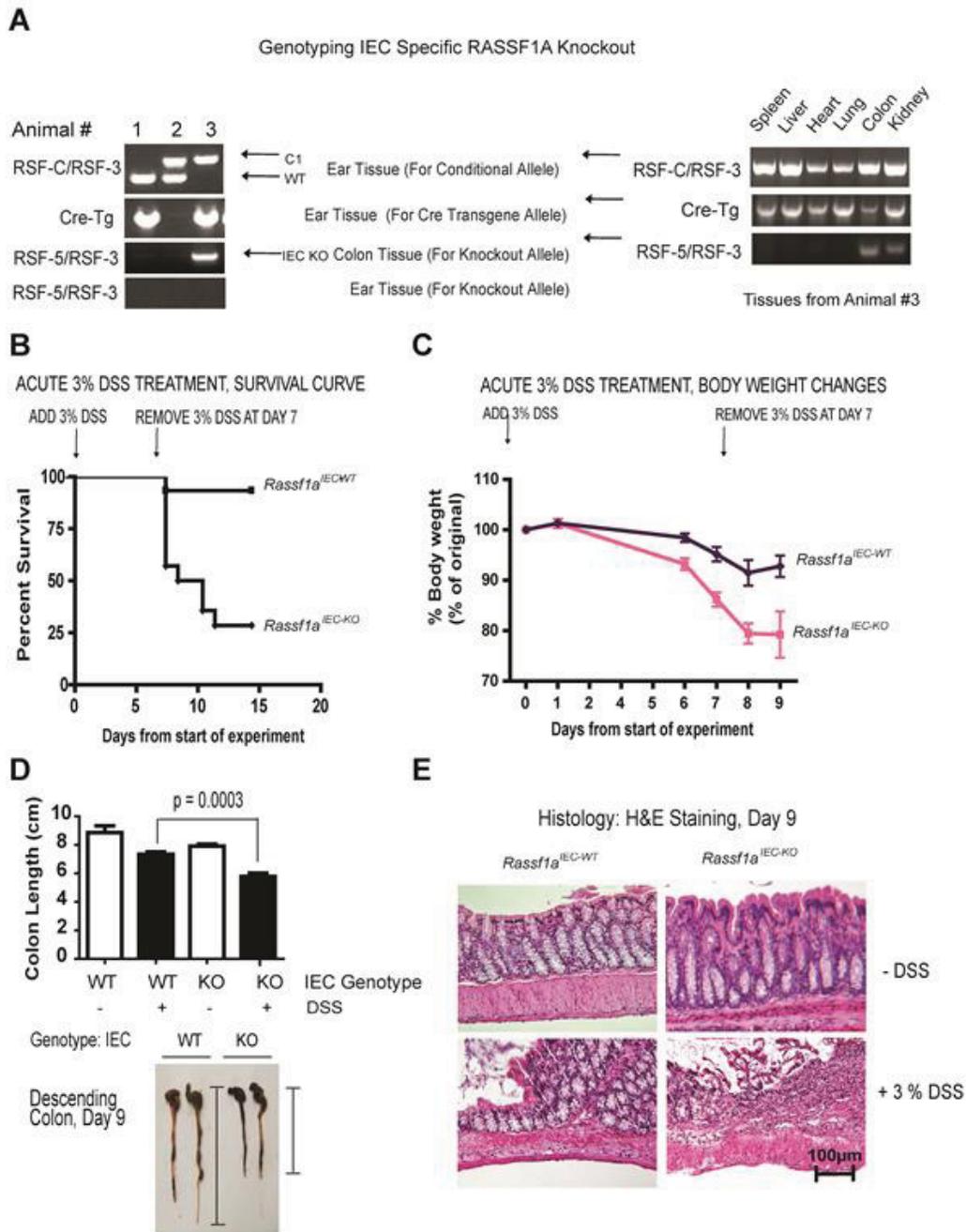
Figure 3.2: RASSF1A intestinal cell-specific knockout (*Rassf1a IEC-KO*) phenocopy *Rassf1a−/−* mice following DSS-induced inflammation. (**A**) PCR detection of the conditional LoxP-1A allele and knockout allele for 1A upon Cre transgene expression in *Rassf1a IEC-KO* animals. Left panel, As an example, animal #3 contained the IEC-specific knockout, as the conditional allele (c1) and the Cre transgene (Cre-Tg) were observed in the ear tissue and colon. C1=conditional allele; WT=wild-type allele. Right panel, genotyping in various mouse tissues. (**B**) Reduced survival of *Rassf1a IEC-KO* animals exposed to 3% DSS solution. p-value [*Rassf1a IEC-WT* vs *Rassf1a IEC-KO*] =0.001, n=12. (**C**) Decreased body weight change following DSS treatment. p-value=0.001 (*Rassf1a IEC-WT* vs *Rassf1a IEC-KO*), n=12. (**D**) Shortened colon length following DSS-treatment of *Rassf1a IEC-KO* vs *Rassf1a IEC-WT* mice on day 9. p-value (*Rassf1a IEC-WT* vs *Rassf1a IEC-KO*) =0.003, n=11. Bottom, Representation of how colon length was measured. (**E**) Longitudinal cross-section of the descending colon stained with H&E from untreated and DSS-treated *Rassf1a IEC-WT* and *Rassf1a IEC-KO* mice revealed severely disrupted colonic histology.

3-2 Results

3-2.1 DSS treated *Rassf1a*$^{-/-}$ mice have enhanced inflammation

Histological sections from DSS-treated *Rassf1a*$^{-/-}$ colons also revealed mild epithelial hyperplasia as reflected by increased inflammation scores in *Rassf1a*$^{-/-}$ treated mice (Figure 3.3 A). Using mouse colonoscopy, we observed significant DSS-induced injury by day 8 in *Rassf1a*$^{-/-}$ versus wild-type or *Rassf5a*$^{-/-}$ mice. Reduction of proper colonic striations and disappearance of a normal vascular pattern together with the presence of erythema was observed in the *Rassf1a*$^{-/-}$ mice indicating active inflammation (Figure 3.3 B). Together, these findings suggest that RASSF1A is important for protection against DSS-induced intestinal inflammation.

To determine the mechanism of DSS-induced injury in *Rassf1a*$^{-/-}$ mice, levels of inflammatory biomarkers were assessed. Serum levels of IL-6, IL-12 and MCP-1 (but not IL-1β, TNF-α, IFN-γ or IL-23) were elevated in *Rassf1a*$^{-/-}$ mice compared to wild-type or *Rassf5a*$^{-/-}$ mice (Figure 3.3 C–E). Following DSS treatment, NFκB specific activity in bone marrow cells from *Rassf1a*$^{-/-}$ animals was significantly higher than in wild-type or *Rassf5a*$^{-/-}$ bone marrow cells (Figure 3.3 F). The detected activity was specific for NFκB (Figure 3.3 F, lane 4) and lost in the presence of a cold competitor oligonucleotide or an NFκB mutant DNA binding oligonucleotide (Figure 3.3 F, lanes 4 and 5, respectively). We further characterized inflammation injury in *Rassf1a*$^{-/-}$ versus wild-type mice by measuring myeloperoxidase (MPO, a glycoprotein rapidly released by activated neutrophils which may also cause extraceullar tissue damage) and hyaluronic acid (HA) release. Following DSS-induced intestinal injury, HA synthase (HAS) up-regulates HA production in macrophages and lamina propria lymphocytes [394], targeting TLR2 and TLR4, and subsequently promoting TLR4/2-driven NFκB activity [395]. We observed a significant increase in both serum and colon tissue levels of MPO (Figure

3.4 D) and serum HA levels (Figure 3.4 E) in DSS-treated *Rassf1a*$^{-/-}$ mice (a 2-3 fold increase in both markers was observed). As MPO is a marker of activated neutrophils, which are typically only found in inflamed tissues, the significant elevation of MPO seen in *Rassf1a*$^{-/-}$ mice suggests extensive dysregulation of the inflammatory response in these mice. The presence of activated neutrophils in the circulating blood of these mice suggest a widespread immune activation in these mice extending beyond the local colonic tissue. This further suggests that RASSF1A may be important in restricting inflammatory signaling beyond just colonic epithelial cells. Elevated HA levels may indicate a sustained need to activate TLR4-driven protective responses to promote epithelial repair in the continued presence of inflammation-induced damage [395]. In contrast, elevation of MPO may be detrimental to the recovery from DSS-induced injury and may have significantly contributed to the decreased survival of *Rassf1a*$^{-/-}$ mice.
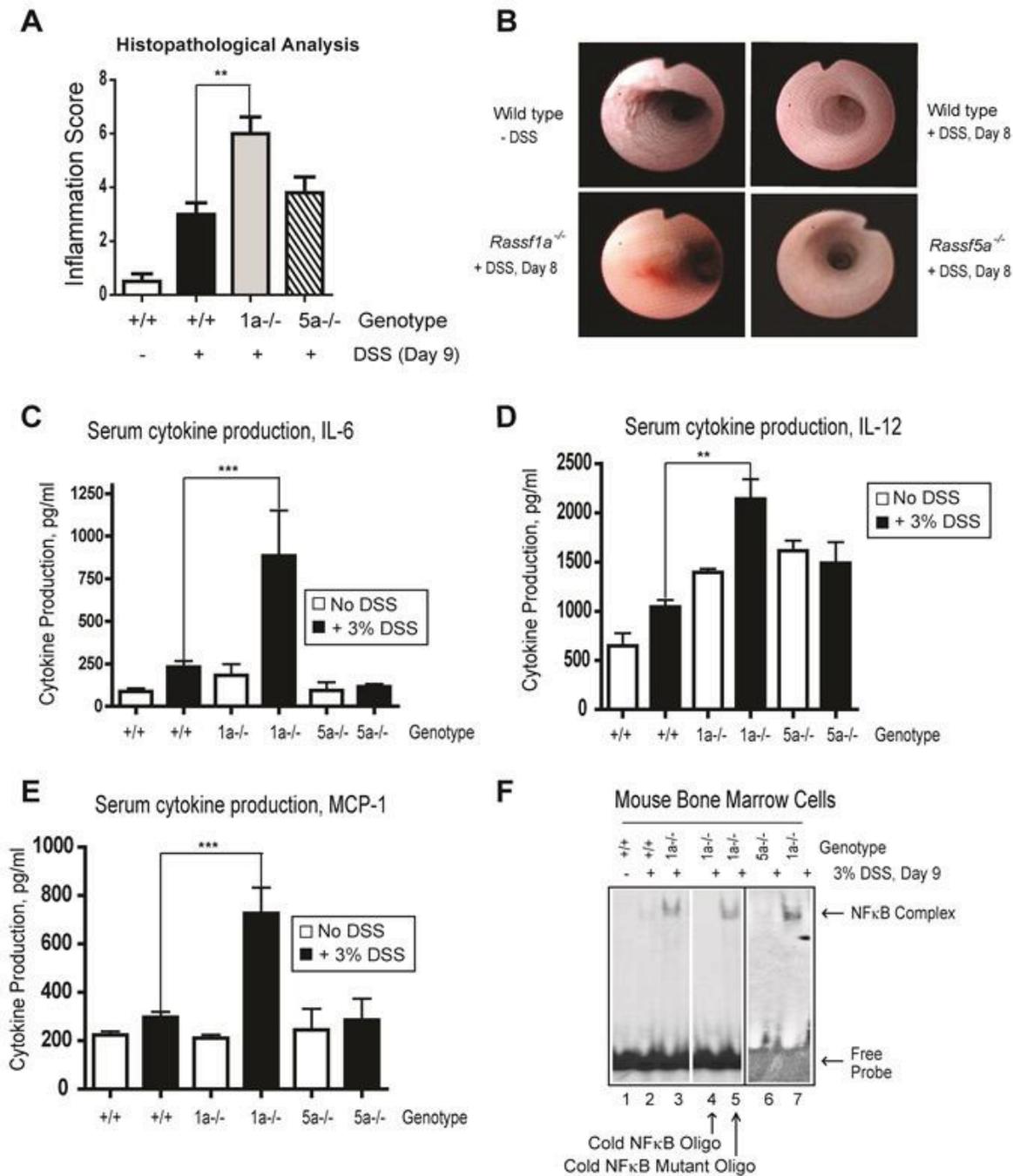
Figure 3.3: *Rassf1a−/−* animals have elevated inflammatory biomarkers following DSS treatment. (**A**) Inflammation scoring of colon sections stained with H&E. p-value of wild type (+DSS) vs *Rassf1a−/−* is <0.001 and wild type (+DSS) vs *Rassf5a−/−* is >0.05 (n=5–10). (**B**) Colonoscopy images of 3% DSS-treated animals. The *Rassf1a−/− mice* (+DSS) were euthanized on day 9 due to disease, whereas all others recovered from 3% DSS treatment. Untreated *Rassf1a−/−* or *Rassf5a−/−* mice had images similar to wild type untreated mice. (**C-E**) Blood serum levels of the indicated cytokines. The p-value of DSS treated wild type vs *Rassf1a−/−* =0.0001 for IL-6 and MCP-1; 0.005 for IL-12; n=10–14 per group. (**F**) NFκB DNA binding in nuclear extracts derived from bone marrow cells upon DSS treatment. Cold wild type or mutant NFκB oligonucleotide was added to determine the specificity of the observed band (lanes 4 and 5, respectively). Lanes 3 and 7 are the same treatment and genotype but BMDM was obtained from different animals. For (**A**) and (**F**), all untreated results for *Rassf1a−/−* and *Rassf5a−/−* were similar to wild type (untreated).
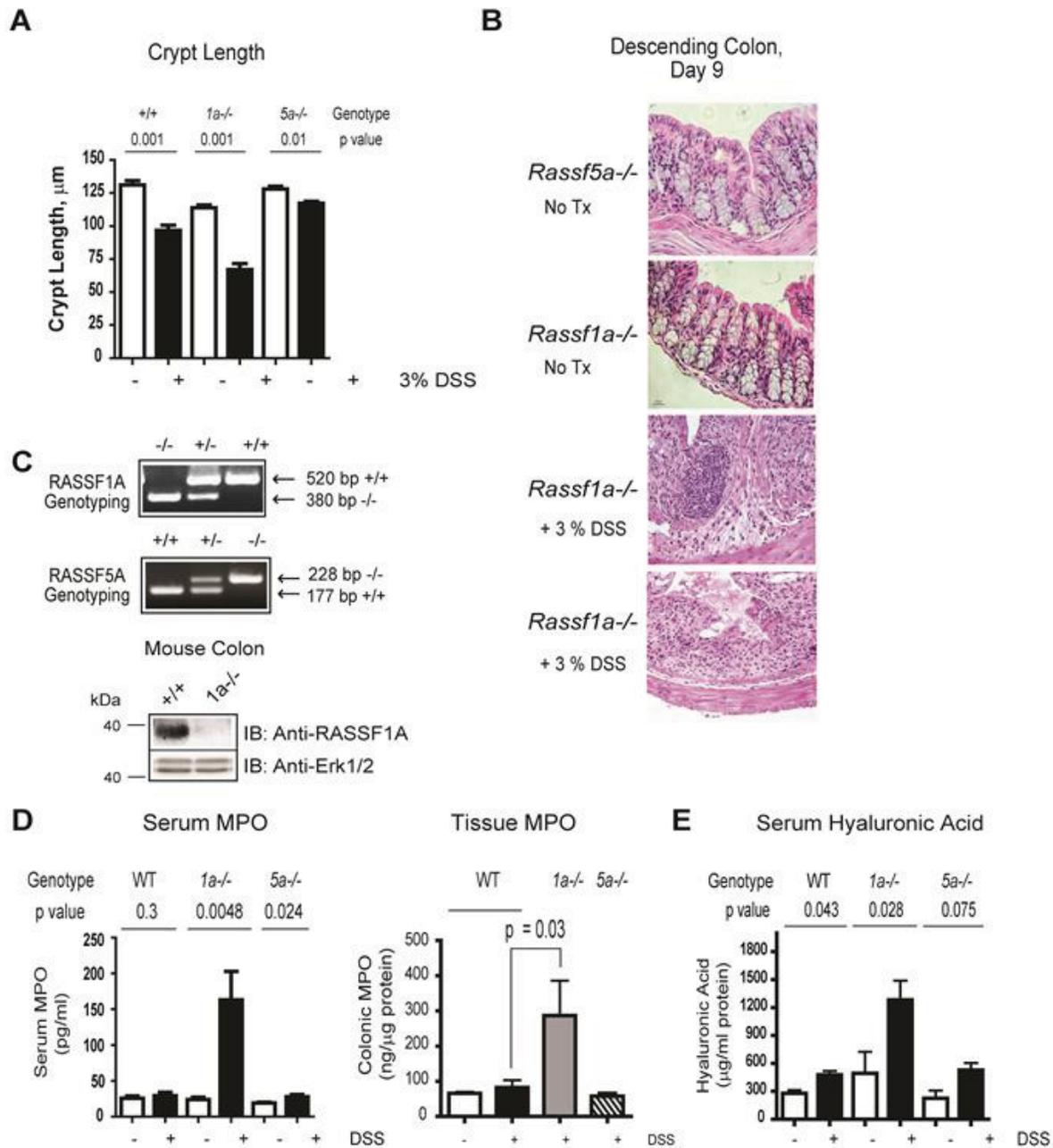
Figure 3.4: Genotyping and characterization of DSS-treated *Rassf1a−/−* mice. (**A**) Crypt length of the indicated genotypes and treatments. Data was obtained from several histological sections similar to previous figures. p-value for the difference in crypt depth between wild type (+DSS) vs *Rassf1a−/−* mice (+DSS) <0.0005 (n=14). (**B**) Histological representations of the colon from DSS-treated *Rassf1a−/−* mice at day 9. These sections revealed the presence of lymphoid aggregates (dense circle of cells) in several areas of DSS treated colonic sections from *Rassf1a−/−* mice. This would suggest active recruitment of immune cells to the inflamed area. (**C**) Genotyping of *Rassf1a−/−* and *Rassf5a−/−* animals. Immunoblot of a colon tissue preparation is shown in the bottom panel for RASSF1A and the loss of RASSF5A in the *Rassf5a−/−* mice has been published (231). (**D-E**) *Rassf1a−/−* animals show increased levels of serum or tissue myeloperoxidase (MPO) (**D**) and hyaluronic acid (HA, **E**). For serum MPO, p-values wild type (+DSS) vs *Rassf1a−/−* mice (+DSS) <0.0001; *Rassf1a−/−* (+DSS) vs *Rassf5a−/−* mice (+DSS) <0.05. Tissue MPO, p-value [wild type vs *Rassf5a−/−* (+DSS)] >0.05 and (**C-F**) wild type (+/+) vs *Rassf5a−/−* (treated) all <0.05 with n=4–6. For serum HA, p-values wild type (+DSS) vs *Rassf1a−/−* mice (+DSS) is <0.005; *Rassf1a−/−* (+DSS) vs *Rassf5a−/−* mice (+DSS) <0.01. n=10–15 for each biomarker.

3-2.2 Defective epithelial restitution in *Rassf1a*$^{-/-}$ mice following acute DSS-induced injury

The increased epithelial permeability and decreased survival of DSS-treated *Rassf1a*$^{-/-}$ mice could be explained by the damage caused by disruption of the epithelial barrier (and damaged paracellular space), elevated cell death (apoptosis) or defects in epithelial cell repair and lack of crypt cell proliferation [396]. Due to increased colonic permeability and mucosal/crypt damage in *Rassf1a*$^{-/-}$ and *Rassf1a*$^{IEC-KO}$ mice following DSS insult (Figure 3.1 D–E and Figure 3.2 D–E) we speculate that RASSF1A may influence pathways involved in epithelial restitution and/or cell repair to regain normal epithelial architecture. Proliferating cell nuclear antigen (PCNA) staining of tissue colon sections from *Rassf1a*$^{-/-}$ and *Rassf1a*$^{IEC-KO}$ mice treated with DSS confirmed reduced crypt cell proliferation versus wild-type or *Rassf5a*$^{-/-}$ (Figure 3.6 A). Because the DSS model of colitis is primarily a model of epithelial damage and repair, it will be interesting to confirm these findings in other models of colitis, although we expect similar findings due to the dramatic differences seen between *Rassf1a*$^{-/-}$ and *Rassf1a*$^{IEC-KO}$ mice compared to wild type mice.

We also observed significant PARP cleavage (a marker of late apoptosis) in colon lysates (Figure 3.5 C) and increased TUNEL-positive staining in colonic sections (a marker of condensed nuclei and indicative of apoptosis) (Figure 3.5 D) from DSS-treated *Rassf1a*$^{-/-}$ and *Rassf1a*$^{IEC-KO}$ mice. The substantial increase in apoptosis in DSS-treated *Rassf1a*$^{-/-}$ and *Rassf1a*$^{IEC-KO}$ mice is likely a significant contributing factor to the decreased survival observed for these mice in Figure 3.1 A and 3.2 B.
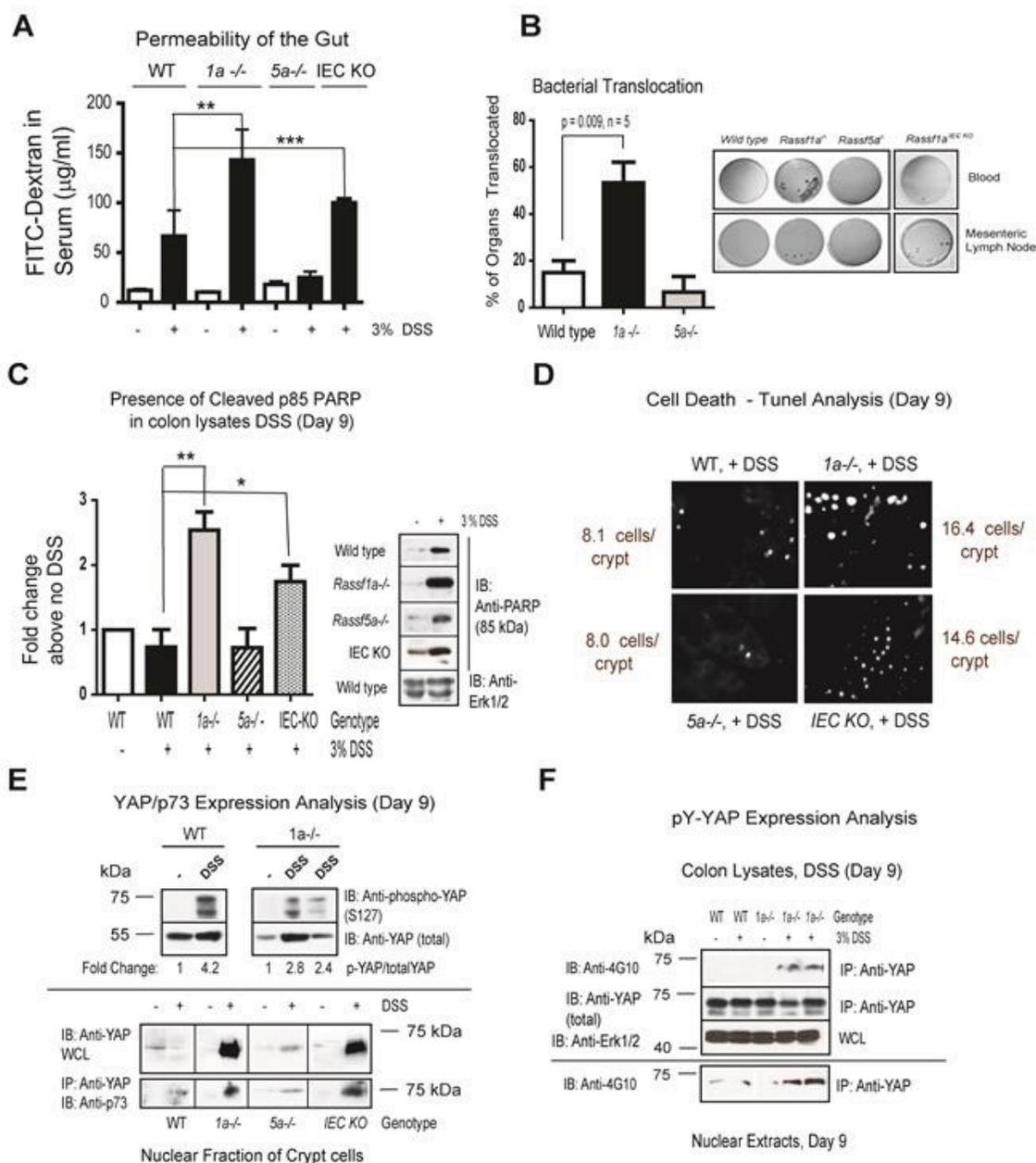
Figure 3.5: Loss of RASSF1A results in altered intestinal homeostasis. (**A**) Gut permeability of the indicated animals was determined by FITC-dextran fluorimetry on day 9 post-DSS addition. p-values (all + DSS): wild-type vs *Rassf1a−/−* <0.01; wild-type vs *Rassf5a−/−* >0.05; *Rassf1a−/−* vs *Rassf5a−/−* =0.005, wild-type vs *Rassf1a IEC-KO* =0.0001, n=6–10 per group. (**B**) Right panel, bacterial transloca-tion to blood and mesenteric lymph nodes as indicated (liver and spleen also revealed some translocation). Left panel, histogram plot of the percentage of these four areas colonized with bacteria. (**C**) Analysis for PARP cleavage was carried out as indicated on day 9 post-DSS treatment. "**" p-value<0.005 and "*" <0.03, n=5–7 for all genotypes and treatments. p-value wild-type (+DSS) vs *Rassf5a−/−* (+DSS) >0.05. (**D**) TUNEL positive staining (bright dots) was carried out as a late marker of cell death. The mean number of cells/crypt shown was counted 6 times. p-value wild-type (+DSS) vs *Rassf1a−/−* or *Rassf1a IEC-KO* (+DSS) =0.002 and 0.04 respectively. (**E**) Colon lysates (top panel) or nuclear fraction of isolated crypt cells (bottom panel) from the indicated genotypes were used to detect total or phosphoserine (S)127 YAP, total YAP and p73 in the nuclear fractions. All treatments and genotypes had similar levels of total p73 following total lysate analysis by immunoblotting (data not shown). (**F**) Detection of total or pY-YAP as indicated. Purity of nuclear and cytoplasmic fractions are shown in Figure 3.9. For (**C-D**) all untreated results for *Rassf1a−/−*, *Rassf5a−/−* and *Rassf1a IEC-KO* (untreated) were similar to wild type (untreated).
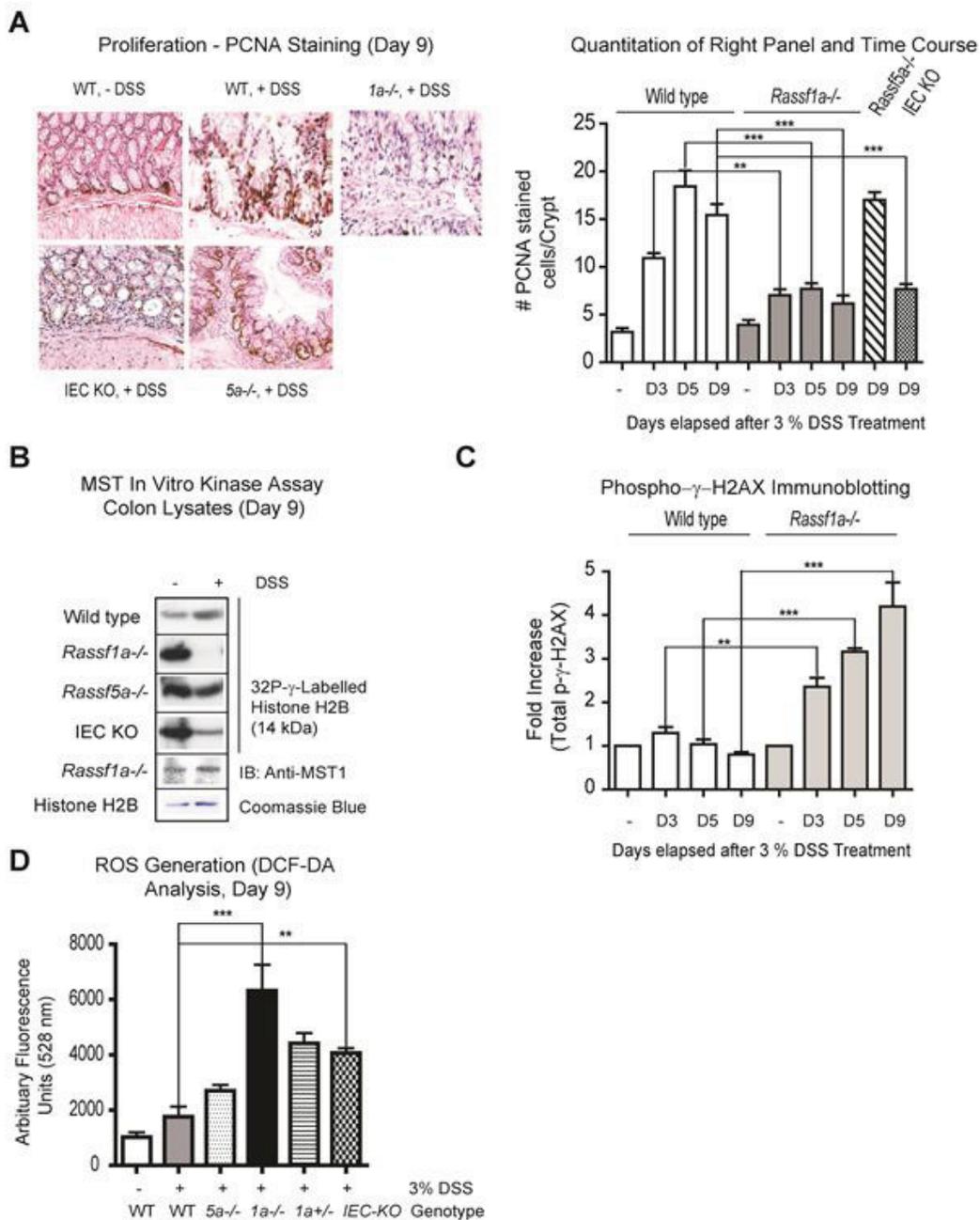
Figure 3.6: The loss of RASSF1A results in decreased crypt cell proliferation and increased cell death following DSS-induced inflammation injury. (**A**) Measurement of PCNA positive proliferation in colonic sections. Biotinylated PCNA staining was detected using diaminobenzidine (DAB) which appears as a brown precipitated over the H&E stained sections. "****" p-value=0.0001 and "***" =0.001, n=12–15 for all genotypes and treatments. p-value wild type (+DSS) vs *Rassf5a−/−* (+DSS) >0.05. Percent PCNA staining was calculated by counting three independent histological sections from each group. (**B**) MST1 in vitro kinase assay was carried out on colon lysates from the indicated genotypes using Histone H2B. MST1 expression is shown for the −/+ DSS-treated *Rassf1a−/−* mice. Similar results were obtained for the other genotypes and experiment was carried out twice with similar results. (**C**) Time course analysis of DNA damage utilizing expression of phospho-γ-H2AX. "****" p-value=0.0001 and "***" =0.001(**D**) Fluorometric analysis of production of ROS using intracellular oxidation of DCF-DA by freshly isolated colon crypt cells from the indicated genotypes. p-values wild-type (+/+, +DSS) vs *Rassf1a−/−* or *Rassf1a+/−* mice (+DSS) <0.0001; wild type (+DSS) vs *Rassf1a IEC-KO* mice <0.001; wild type (+DSS) vs *Rassf5a−/−* mice (+DSS) >0.05 (n=8 for all genotypes). For (**A** and **C**) all untreated results for *Rassf1a−/−*, *Rassf5a−/−*, *Rassf1a IEC-KO* were similar to wild type (untreated).

3-2.3 DSS treatment of *Rassf1a⁻ᐟ⁻* mice triggers tyrosine phosphorylation of Yes-Associated Protein (YAP) following acute inflammatory injury

RASSF1A can normally promote cell death via TNF-R1 and the loss of RASSF1A should result in decreased cell death. We, in fact, can detect enhanced cell death by PARP and TUNEL analysis (Figure 3.5 C–D). We thus explored alternative explanations for how the loss of RASSF1A may result in increased intestinal apoptosis. RASSF1A is a component of the Rassf/Salvador/Hippo pathway that can modulate cell death, organ size and cellular proliferation [250,353,354]. It is thought that in mammalian cells, RASSF1A can function to activate MST1/2, resulting in the activation of LATS and downstream serine phosphorylation events [358]. Activated LATS can lead to the inactivation (by cytoplasmic re-localization and retention) of the Yes-associated protein (YAP), a key diver of proliferation (known as Yorkie [Yki] in Drosophila) linked to the TEAD family of transcription factors [254] Removal of either *Yki* from intestinal stem cells in Drosophila [397] or YAP in *Yap⁻ᐟ⁻* mice [398] revealed poor survival and decreased epithelial cell proliferation in response to DSS treatment (characteristics similar to what we have observed). However, we are arguing for the important role of RASSF1A in restricting NFκB and downstream effects that hyperactivation of NFκB can cause. Although inflammation was not investigated in either of these studies, it does suggest an important role for both RASSF1A and YAP in modulating crypt cell proliferation and survival following DSS-induced inflammation injury.

In the absence of RASSF1A, there was a significant reduction in S127 phosphorylation of YAP (Figure 3.5 E, top panel) and enhanced nuclear presence of p73 associated YAP (Figure 3.5 E, bottom panel). Reduced S127-phosphorylated YAP and increased nuclear presence of YAP would be expected to result in increased YAP-driven transcription to drive proliferation of intestinal crypt cells in the canonical Hippo pathway. Enhanced proliferation can be observed in wild-type mice upon DSS treatment

but not in DSS-treated *Rassf1a*^{-/-} and *Rassf1a*[IEC-KO] mice (Figure 3.6 A). DSS-treated *Rassf1a*^{-/-} and *Rassf1a*[IEC-KO] mice clearly revealed enhanced nuclear levels of YAP but reduced crypt proliferation (as determined by PCNA staining in Figure 3.6 A). However, increased crypt apoptosis (as determined by elevated PARP cleavage and TUNEL staining) can be observed in line with reduced crypt proliferation (Figure 3.5 C–D). Furthermore, MST kinase activity was dramatically reduced in DSS-treated of *Rassf1a*^{-/-} and *Rassf1a*[IEC-KO] mice (Figure 3.6 B) in agreement with enhanced nuclear presence of YAP.

Further detailed analysis revealed increased tyrosine phosphorylation (pY) of YAP in DSS-treated *Rassf1a*^{-/-} mice in colon lysates/nuclear fractions (Figure 3.5 F) and in colonic sections (Figure 3.7 A). A clear difference in pY-YAP between DSS-treated wild type and *Rassf1a*^{-/-} mice was observed as early as day 5 post DSS addition that continued to increase towards Day 9 (Figure 3.7 A, right panel). Previous studies have suggested a functional role for pY-YAP/p73 complex to ultimately drive pro-apoptotic gene expression, especially BAX [399,400]. In support of these arguments, we detected enhanced nuclear presence of a pY-YAP/p73 complex (Figure 3.5 E, bottom panel), increased BAX expression by immunohistochemistry and immunoblotting (Figure 3.7 B) in intestinal crypt cells from DSS-treated *Rassf1a*^{-/-} and *Rassf1a*[IEC-KO] mice but not in samples from wild-type or *Rassf5a*^{-/-} treated mice. This suggests that a pY-YAP/p73 driven up-regulation of BAX may promote intestinal cell death leading to increased gut permeability, lack of effective epithelial repair and poor survival of DSS-treated *Rassf1a*^{-/-} and *Rassf1a*[IEC-KO] mice.

Previous studies have suggested a functional role for c-ABL-driven tyrosine 357 phosphorylation of YAP in response to DNA damage [364,401]. This resulted in the formation of a pY-YAP/p73 complex to drive pro-apoptotic gene expression, especially BAX [399,400]. We detected enhanced Y357 phosphorylation in Rassf1a knockout mice using a Y357 YAP antibody (Figure 3.5 F and Figure 3.7 A). In addition, we also

observed increased DNA damage as early as Day 3 (Figure 3.7 C and Figure 3.5 C), oxidative damage by Days 5-9 (Figure 3.7 D) as well as significant ROS production in colon samples from *in vivo* DSS-treated *Rassf1a* knockout mice (Figure 3.6 D). DNA and oxidative damage of colonic cells have been characterized as significant factors in the pathogenesis of IBD [402,403]. Similar to IBD patients, inflammation-induced injury in our *Rassf1a* knockout mice has associated DNA and oxidative damage. Since we can observe DNA damage as early as Day 3, we speculate that this may be driving the tyrosine phosphorylation of YAP observed by Days 3–5 (Figure 3.7 A). YAP tyrosine phosphorylation following DSS-induced inflammation injury will in turn drive colonic cell death (via p73 association and transcriptional activation of cell death genes) and poor survival of DSS-treated *Rassf1a* knockout animals.
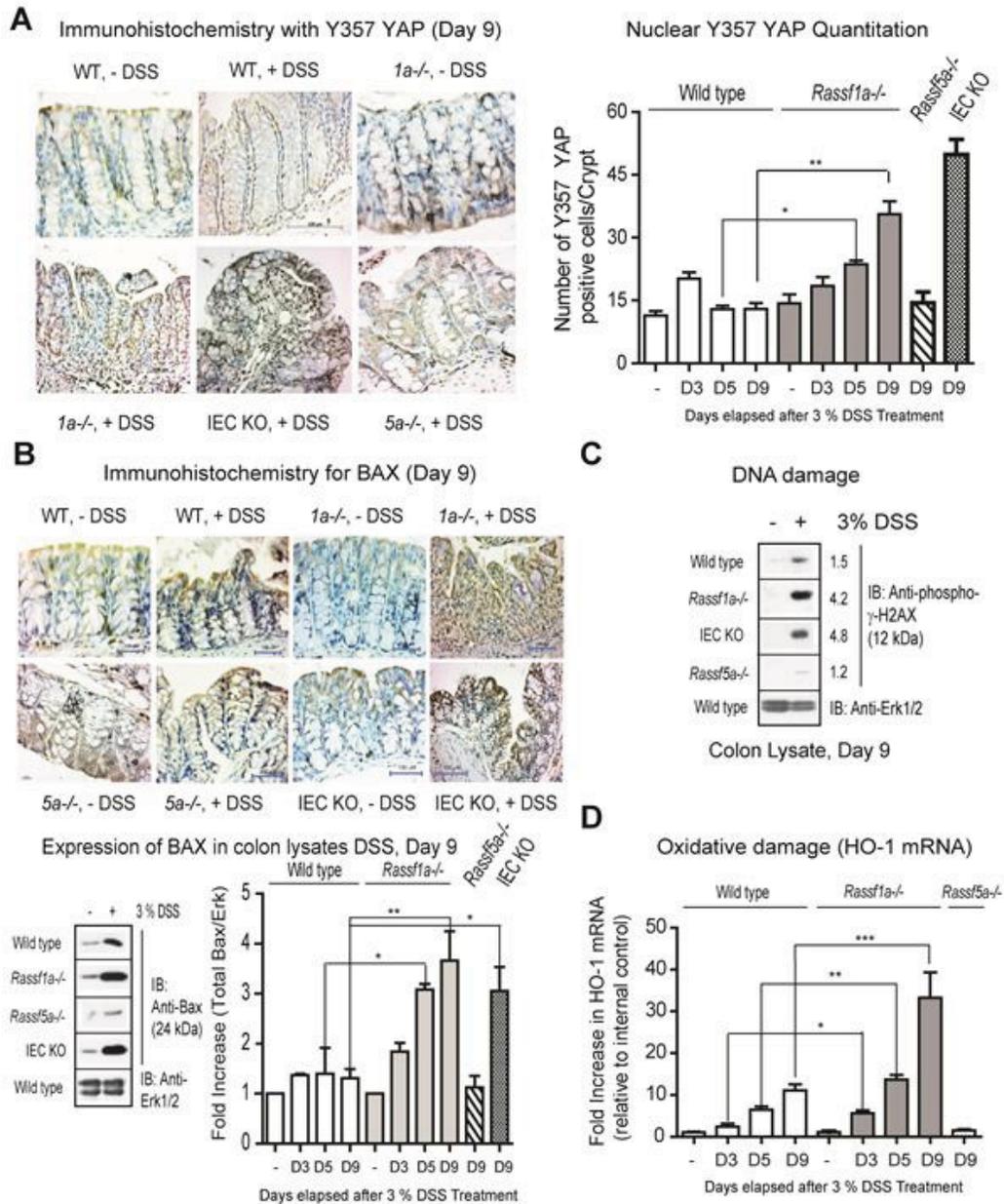
Figure 3.7: *Rassf1a−/−* **mice fail to recover following DSS treatment due to abnormal YAP signaling.** (**A**) Phosphotyrosine (pY)-YAP IHC with anti-Y357-YAP was carried out on colon sections as indicated. Left panel, IHC of colon sections using anti-Y357-YAP. Right panel, 1000 cells were scored for nuclear presence of YAP Y357. For graph, "**" p-value<0.01 and "*" <0.05, n=5–7 for all genotypes and treatments. p-value wild-type (+DSS) vs *Rassf5a−/−* (+ DSS) >0.05. (**B**) Top panel, analysis of BAX expression by IHC was carried out as indicated on colonic tissue sections on day 9 post-DSS treatment. Bottom panel, expression of BAX in colon lysates from day 9 DSS-treated animals as indicated (fold induction of the immunoblotting results are graphed in the right panel). For graph, "**" p-value<0.01 and "*" <0.05, n=5–7 for all genotypes and treatments. p-value wild-type (+DSS) vs *Rassf5a−/−* (+DSS) <0.05. Wild type ERK only shown as representation due to space; all samples normalized to individual ERK appropriately. (**C**) Analysis for the DNA damage marker, phospho-γ-H2AX, following in vivo DSS insult in colon lysates. Numbers represent fold change relative to phospho-γ-H2AX levels in untreated wild type animals. Wild type ERK only shown as representation due to space; all samples normalized to individual ERK appropriately. (**D**) Real time PCR analysis for an oxidative damage marker hemexogenase-1 (HO-1) utilizing colonic mRNA (n=4 for all and D designates the day that the tissues were harvested). p-value of wild type (+DSS) versus *Rassf5a−/−* is <0.05 (Day 3), <0.01 (Day 5) and <0.001 (Day 9) with n=4–6 per day per sample. The *Rassf1a IEC-KO* result was comparable to the result in the DSS treated *Rassf1a−/−* mice.

3-2.4 Imatinib mesylate/Gleevec can protect *Rassf1a*$^{+/-}$ mice but not *Rassf1a*$^{-/-}$ mice from DSS-induced inflammatory injury

Next, we wanted to inhibit the protein tyrosine kinase (PTK) for YAP in order to prevent a pY-YAP/p73 driven transcription of pro-apoptotic genes (such as BAX) and possibly aid in promoting the enhanced survival of DSS-treated *Rassf1a* knockout mice. As mentioned earlier, YAP has been shown to be tyrosine phosphorylated by c-ABL in response to DNA damage. Imatinib mesylate/gleevec (hereafter referred to as imatinib) was developed to specifically inhibit c-ABL (IC$_{50}$ of 25 nM) [404] and has been successful utilized to treat leukemia patients. However, it can also inhibit c-Kit and PDGF-R at 400 nM [404]. Imatinib treatment of our *Rassf1a*$^{+/-}$ mice (IP injections of 60 mg/kg body weight of imatinib on Days 3 and 6 of an acute 3% DSS treatment) resulted in >80% survival (Figure 3.8 A), low disease activity indices (Figure 3.9 A), low histopathological scoring of <2 (*Rassf1a*$^{+/-}$ mice normally have >6, Figure 3.8 B), reduced IL-6 (Figure 3.8 C), reduced cell death (Figure 3.8 D and Figure 3.9 B), reduced DNA and oxidative damage (Figure 3.9 C–D, purity of nuclear extracts is shown in 3.9 E), regain normal crypt architecture (Figure 3.8 E and Figure 3.11 A) and increased PCNA staining (increased proliferation, Figure 3.11 A).

Imatinib significantly reduced the appearance of pY-YAP as determined by immunohistochemical staining (Figure 3.8 E) and immunoblotting (Figure 3.11 B). Furthermore, there was increased c-ABL kinase activity towards FLAG-YAP in colon lysates from the *Rassf1a*$^{+/-}$ mice that was inhibited by imatinib (Figure 3.8 F). The increased kinase activity of c-ABL was not inhibited by a direct modulation by RASSF1A as exogenous addition of GST-RASSF1A did not interfere with the kinase activity of c-ABL as determined by our *in vitro* method (Figure 3.8 F, top panel, last two lanes on the right). Thus c-ABL activity may be indirectly modulated by RASSF1A and increased c-ABL activity is most likely a result of increased DNA damage during intestinal inflammation. Taken together, our data suggested that inhibition of the c-ABL class of

PTKs was effective in reversing the detrimental effects of a 3% DSS treatment in DSS-treated $Rassf1a^{+/-}$ mice.

In contrast to imatinib-treated $Rassf1a^{+/-}$ mice, imatinib-treated $Rassf1a^{-/-}$ mice did have different survival outcomes. We did notice that the clinical onset of disease was delayed 2-3 days when compared to DSS-treated $Rassf1a^{+/-}$ or $Rassf1a^{-/-}$ mice (Figure 3.8 A). Imatinib-treated $Rassf1a^{-/-}$ mice had comparable disease activity indices to imatinib-treated $Rassf1a^{+/-}$ mice until Day 8, but by Days 9-10, imatinib-treated $Rassf1a^{-/-}$ mice worsened with higher disease activity indices (Figure 3.9 A). Surprisingly, imatinib-treated $Rassf1a^{-/-}$ mice revealed reduced pY-YAP 357 (Figure 3.8 E and Figure 3.11 C), reduced inflammation scores and cytokine production (Figure 3.8 B-C) indicating that imatinib treatment was interfering with a key mechanism promoting early intestinal damage during the DSS treatment. However, the higher disease activity indices on Days 9-10 and poor survival of imatinib-treated $Rassf1a^{-/-}$ mice may be attributed to a robust degree of cell death (Figure 3.8 D and Figure 3.9 B), DNA damage (Figure 3.9 C, bottom panel), and c-ABL kinase activity following DSS-induced inflammation. c-ABL kinase activity was, again, not affected by the exogenous addition of GST-RASSF1A (Figure 3.8 F, bottom panel). Equal amounts of FLAG-YAP were utilized as revealed by Coomassie blue staining in Figure 3.11 D.
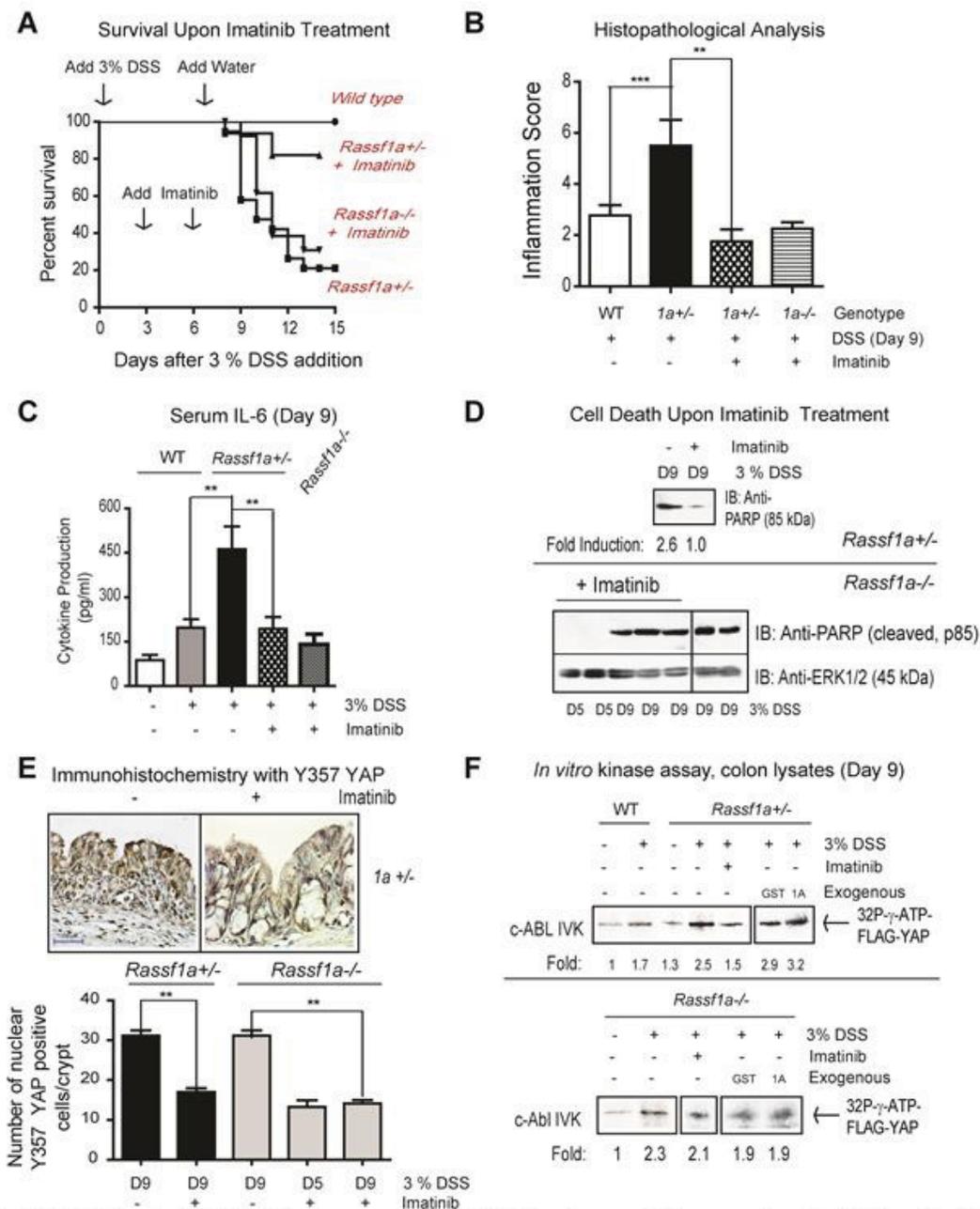
Figure 3.8: The PTK inhibitor, imatinib, inhibits the appearance of pY-YAP and promoted increased survival of *Rassf1a+/−* but not *Rassf1a−/−* mice animals following inflammation-induced injury. (A) *Rassf1a+/−* or *Rassf1a−/−* mice were intraperitoneally injected with the PTK inhibitor, imatinib at 50mg/kg body weight on days 3 and 6 following 3% DSS addition. p-value between survival of DSS-treated wild type and *Rassf1a+/−* was <0.0001 (n=17) and between DSS-treated *Rassf1a+/−* (+imatinib) versus DSS-treated *Rassf1a+/−* was <0.01 (n=17). No significance difference was observed between DSS-treated *Rassf1a+/−* and DSS-treated *Rassf1a−/−* (+imatinib) mice. Following DSS/gleevec treatment, (B) histological analysis of colonic sections, (C) serum IL-6, (D) cell death via PARP (late marker of apoptosis); (E) phospho-YAP by IHC, and (F) *In vitro* kinase activity was carried out for c-ABL using colon lysates from DSS-treated wild type and *Rassf1a+/−* (top panel) and *Rassf1a−/−* (bottom panel) mice with over-expressed FLAG-YAP as substrate. Fold changes are relative to wild type untreated. For (B) p-value between wild type versus *Rassf1a+/−* mice (+DSS) was 0.004, wild type versus *Rassf1a+/−* mice +DSS +gleevec was >0.1 and wild type versus *Rassf1a−/−* mice (+DSS +gleevec) was >0.4 (n=4–8). For (C), p-value between wild type versus *Rassf1a+/−* mice (+DSS) and *Rassf1a+/−* mice (+DSS +gleevec) versus *Rassf1a+/−* mice (+DSS) was 0.004 and wild type versus *Rassf1a+/−* mice (+DSS +gleevec) was >0.3 and wild type versus *Rassf1a−/−* mice (+DSS +gleevec) was >0.2 (n=4–8). For (E) p-values of *Rassf1a+/−* mice or *Rassf1a−/−* mice (+DSS −/+gleevec) was <0.001 (n=10).
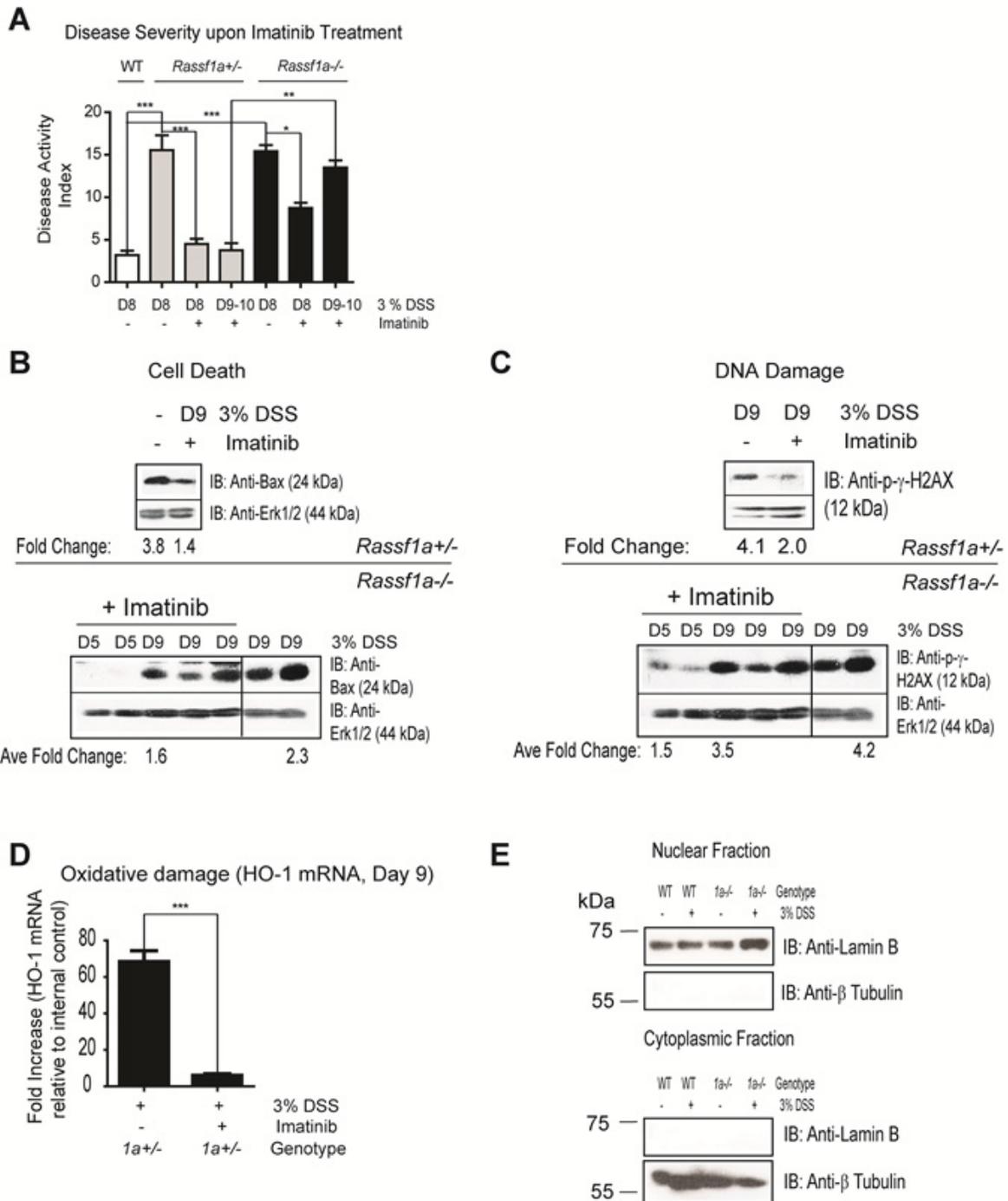
Figure 3.9: The PTK inhibitor, imatinib reverses the damaging effects of DSS treatment in *Rassf1a+/−* but not *Rassf1a−/−* knock-out mice. Imatinib was administered intraperitoneally at 50mg/kg body weight on Days 3 and 6 and (**A**) Disease activity index, (**B**) cell death using BAX immunoblotting (as an early marker of apoptosis) (in colon lysates), (**C**) the DNA damage marker phospho-γ-H2AX (in colon lysates) and (**D**) the oxidative damage marker, HO-1was carried out as indicated (source of sample was colonic mRNA). (**E**) Purity of our nuclear and cytoplasmic fractions was tested as indicated. Fold changes are compared to wild type untreated, following normalization to sample ERK. p-values "*" <0.02, "***" <0.001, "****" <0.0001

Further analysis of this discrepancy, revealed that the cleavage of c-ABL was more apparent in DSS-treated $Rassf1a^{-/-}$ mice (Figure 3.10 A) and highly elevated in imatinib treated $Rassf1a^{-/-}$ mice (Figure 3.10 B), especially the presence of the predominant 25 kDa cleaved (but active) fragment of c-ABL (Figure 3.10 A and B, marked with "*") [405,406]. Interestingly, DSS-treated wild type animals revealed almost undetectable levels of p53 whereas DSS-treated $Rassf1a^{+/-}$ or $Rassf1a^{-/-}$ mice (Figure 3.10 C) revealed highly elevated or accumulated levels of p53 (as early as Day 3 for the DSS-treated $Rassf1a^{-/-}$ mice).

The accumulation of p53 was more apparent by Day 9 and increased in imatinib-treated animals (Figure 3.10 C) whereby p53 levels not only accumulated but p53 appears to be modified to a slower migrating form around 75 kDa (Figure 3.10 C, lanes 9–12). Under DSS or imatinib treatment, p53 mRNA levels do not appear to be significantly different, eliminating transcriptional control (Figure 3.10 D). Evidence for p53 stabilization can be seen in Figure 3.11 E and does reveal that imatinib can interfere with p53 dependent ubiquitination and increased in the DSS and imatinib-treated $Rassf1a^{-/-}$ mice (Figure 3.11 D-E). Since c-ABL can be caspase cleaved and its resultant active fragment can phosphorylate the p53 inhibitor/E3 ligase, Mdm2 [407], we speculate that in the absence of RASSF1A, DSS-induced inflammation injury can result in accumulated p53 and significantly higher levels of cell death and poor recovery following DSS-induced inflammation injury.
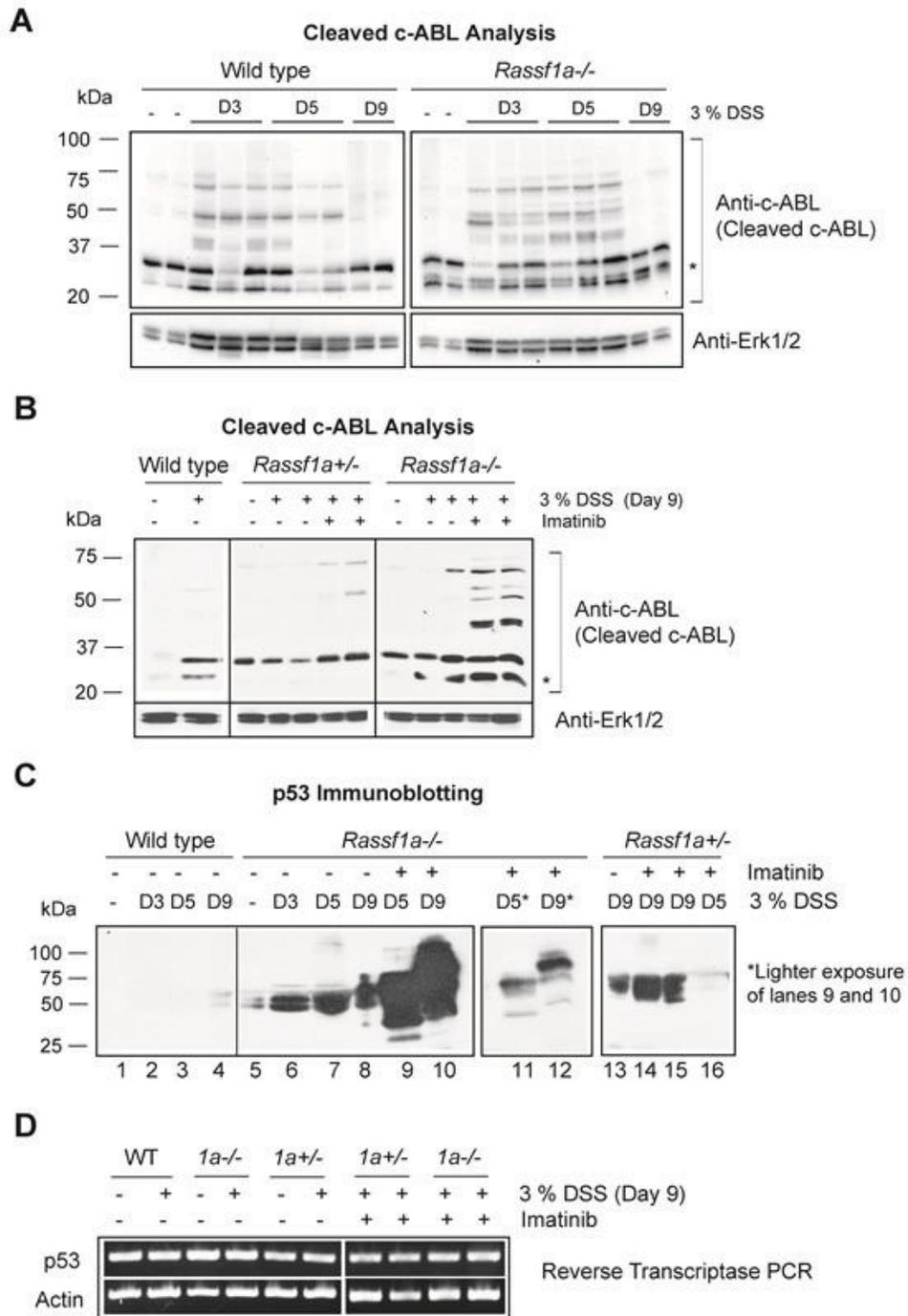
Figure 3.10: The loss of RASSF1A results in cleavage of c-ABL and accumulation of p53. (**A**) Expression of c-ABL following DSS treatment as indicated. Erk1/2 was used as loading control and D=days after DSS addition. (**B**) Imatinib treatment of *Rassf1a−/−* mice (but not *Rassf1a+/−* mice) results in increased cleavage of c-ABL and sustained p25 cleaved form of c-ABL (indicated by *). (**C**) c-ABL cleavage can result in phosphorylation of Mdm2 and stabilization of p53 to promote cell death. The loss of both alleles of *Rassf1a* results in increased expression of p53 and its modification. (**D**) Reverse transcriptase analysis of p53 expression revealed no transcriptional changes in p53 expression following neither DSS treatment nor with imatinib addition.
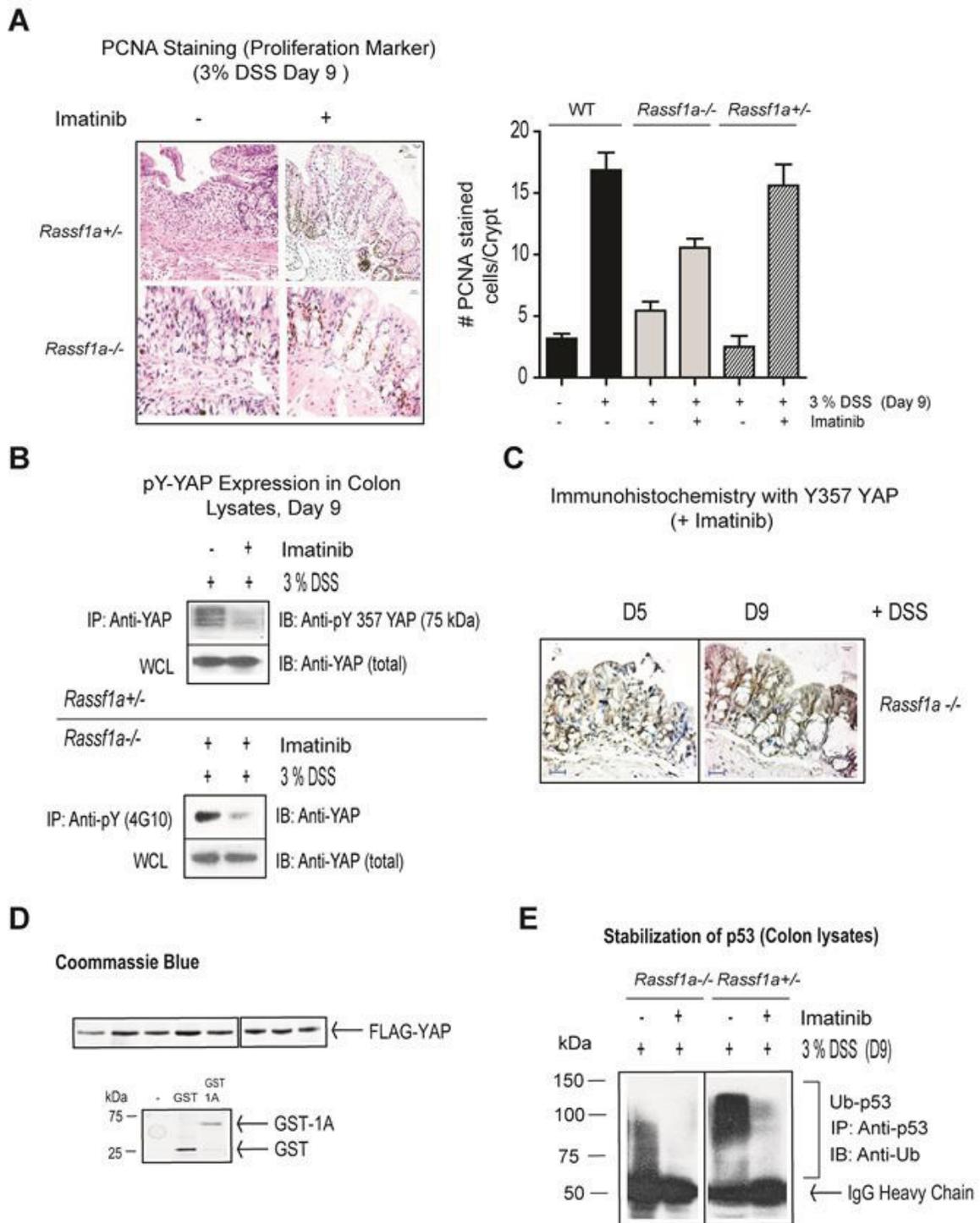
Figure 3.11: Further biomarkers of intestinal inflammation were analyzed. (**A**) PCNA staining with quantitation on the right panel, (**B**) Detection of pY-YAP was carried out as indicated, (**C**) pY-YAP immunohistochemistry carried out, (**D**) Expression of FLAG-YAP (top panel), GST and GST-1A (bottom panel) used in *in vitro* kinase assay in Figure 3.8. (**E**) Ubiquitination of p53 was carried out as indicated in colon lysate samples. All baseline (untreated) results not shown were significantly not different from wild type (untreated).

3-3 Discussion and Future Directions

An underlying hallmark of many inflammatory diseases is the enhanced activation of transcription factors, including NFκB and elevated production of NFκB - regulated cytokines. These responses are needed to promote innate immunity activation and stimulate the repair process. No single animal model can explain the pathogenesis of IBD suggesting that IBD has multifactorial etiologies [408,409]. The present study argues that RASSF1A is an important regulatory element to restrict NFκB activity. Unrestricted NFκB activity can significantly contribute to poor recovery following inflammation-induced injury and inhibit the ability to promote efficient epithelial repair and survival (Figure 3.12).

We have demonstrated that DSS-treated *Rassf1a*$^{-/-}$ and *Rassf1a*$^{IEC-KO}$ mice have elevated NFκB activity. Mechanistically RASSF1A appears to restrict complex formation of MyD88/TRAF6/IRAK and thus interfere with NFκB activation. RASSF1A forms robust associations upon LPS or DSS stimulation with the membrane proximal complexes MyD88/TLR4 and TRAF6/IRAK2 (see Gordon et al. full manuscript [3]) in order to restrict NFκB activity. Since both LPS and DSS can stimulate TLR4, we believe that RASSF1A functions through TLR4 to inhibit IKK and the cytoplasmic/nuclear shuttling of NFκB.

We also have *in vivo* evidence to demonstrate that YAP becomes tyrosine phosphorylated in response to DSS-induced inflammation injury most likely by the c-ABL class of PTKs. YAP was originally identified by its association with the YES Src tyrosine kinase [410] and has been demonstrated to be a transcription factor whose cytoplasmic/nuclear shuttling is controlled by post-translational phosphorylation events [411,412]. During DSS-induced inflammation injury in both *Rassf1a*$^{+/-}$ and *Rassf1a*$^{-/-}$ mice, we observed elevated level of nuclear tyrosine phosphorylated YAP, enhanced YAP/p73 associations (Figure 3.5 E) and elevated levels of BAX expression to promote apoptosis (Figures 3.5 and 3.7). Recently, van der Weyden et al. [259] demonstrated that

the combined loss of *Rassf1a* and *Runx2* promoted the formation of oncogenic YAP1/TEAD transcriptional complexes to promote tumorigenesis. We observed reduced S127 phosphorylated YAP (possibly indicating reduced YAP/TEAD transcriptional complexes) in DSS-treated *Rassf1a*$^{-/-}$ mice. We propose that our results demonstrate that the early loss of *Rassf1a* can lead to enhanced inflammation, a key pre-condition to cancer and inflammation driven activation of YAP/p73 complexes to promote cell death. YAP1/TEAD complexes may arise after prolonged chronic inflammation to promote proliferation in support of the findings of van der Weyden et al. [259]. It has been demonstrated that IL-6 can promote the activation of DNA methyltransferase 1 (DNMT1) [393,413] and DNMT1 can epigenetically silence RASSF1A [392,414] to provide a mechanism whereby inflammation may drive epigenetic silencing of RASSF1A and loss of the function of this tumor suppressor protein.

The c-ABL tyrosine kinase can phosphorylate YAP upon DNA damage, selectively promoting a YAP/p73 complex to drive the expression of pro-apoptotic genes [364]. Since we cannot observe inhibition of c-ABL kinase by exogenous addition of RASSF1A, we speculate that NFκB may transcriptionally up-regulate a PTK or that NFκB dependent-inflammation will promote DNA damage to drive the tyrosine phosphorylation of YAP via c-ABL or c-ABL-like kinases (Figure 3.12). Either mode of regulation would result in an abnormal tyrosine phosphorylation of YAP to yield increased epithelial apoptosis as well as p53 accumulation to further promote apoptosis. These events would result in poor survival following intestinal inflammation induced injury. Inhibiting this abnormal phosphorylation of YAP using the c-ABL class of PTK inhibitors (imatinib) reversed the damaging effects of DSS induced intestinal inflammation but only in a *Rassf1a*$^{+/-}$ background.

In a *Rassf1a*$^{-/-}$ background, imatinib partially reversed the effects of DSS-induced inflammation but did not allow the animal to recover due a robust accumulation of p53 towards Day 9 that may have resulted in more apoptosis and poor recovery.

Interestingly, in Day 9 imatinib-treated $Rassf1a^{-/-}$ mice, p53 was accumulated and modified (Figure 3.10 C, lane 9). We have not identified what this modification is (most likely one of many p53 phosphorylated residues) but we are currently exploring this and, if unique, may be an interesting biomarker for disease prognosis, whereby increased levels of pY-YAP may indicate more severe disease. Alternatively, the increased cleavage of c-ABL into a 20 kDa constitutively active form may be responsible for the failure of $Rassf1a^{-/-}$ mice to respond to imatinib treatment. Imatinib inhibits the PTK activity of c-ABL by binding to the ATP binding region located in hydrophobic pockets created by the N-terminal α helix of c-ABL. With the cleavage of c-ABL to only the catalytic subunit, it is possible that the loss of the α helix region reduces the ability of imatinib to bind and inhibit c-ABL. PTK inhibitors able to bind c-ABL directly at the catalytic region without hydrophobic interactions may show an improved effect.

It is known that caspase cleaved c-ABL can phosphorylate the p53 E3 ligase, Mdm2, to inhibit Mdm2-dependent degradation of p53 and allow it to accumulate [407]. Accumulated p53 can then associate with the anti-apoptotic inhibitor, Bcl-2 to promote cell death [415]. This may explain why imatinib-treated $Rassf1a^{-/-}$ mice are not protected from DSS-induced inflammation and have similar or enhanced cell death. Curiously, we cannot absolutely eliminate tyrosine phosphorylation of YAP using imatinib (Figure 3.11 B) nor most of the biomarkers of inflammation or cell death. This would suggest that other PTKs may also influence tyrosine phosphorylation of YAP upon inflammation induced injury in the absence of RASSF1A. YES, the other known PTK for YAP, has two NFκB binding sites within its promoter region (as documented by http://www.genecards.org/cgi-bin/carddisp.pl?gene=YES1) and could be up-regulated by NFκB activation due to the failure of RASSF1A to restrict NFκB activation (Figure 3.12). Preliminary results do reveal increased c-YES expression upon DSS-induced stimulation in $Rassf1a^{+/-}$ and $Rassf1a^{-/-}$ colon lysates (unpublished observations). We are currently exploring how NFκB may regulate YES expression, if YES kinase activity is elevated in DSS-treated $Rassf1a$ knockout mice and if the YES inhibitor, dasatinib, can promote the survival of DSS-treated $Rassf1a$ knockout mice.

Our results demonstrate that the loss of *Rassf1a* resulted in the loss of MST1 kinase activity (Figure 3.8 B) and the increased nuclear presence of tyrosine phosphorylation of YAP (Figure 3.5F and 7A). The studies by van der Weyden et al. [259], Ren et al. [397], Cai et al. [398], Zhou et al. [416] and Matallanas et al. [365] explored MST/RASSF1A dependent-regulation of YAP serine phosphorylation. However, during intestinal inflammation in our system, YAP transcriptional activities drive apoptosis in the absence of MST1/2 activity (see Figure 3.8 B). Recently, it was shown that YAP1 does not require MST1/2 to drive the proliferation of keratinocytes [417] in support of MST1/2 independent YAP functions. Furthermore, although Matallanas et al. [365] demonstrated that RASSF1A can promote a YAP/p73 association they did not determine YAP phosphorylation linked to S127 or Y357. We argue that intestinal inflammation is driving a RASSF1A indirect affect on YAP through elevated NFκB activity to transcriptionally up-regulate a PTK to tyrosine phosphorylate YAP or, alternatively, in promoting enhanced DNA damage to activate a YAP PTK. Either way, it is an MST1/2 independent effect.

As mentioned earlier, DSS-treated *Yap*$^{-/-}$ mice have decreased survival and proliferation and increased cell death upon DSS treatment that is very similar to our inflammation phenotype [398]. However, Cai et al. [398] did not explore tyrosine phosphorylation of YAP but did show reduced YAP phospho-S127 with increased time post-DSS addition [398]. We have evidence that increased c-ABL cleavage (most likely by caspases) and accumulated p53 may occur in parallel to p73/YAP driven cell death following DSS-induced inflammation injury (based on the results in Figure 3.10 C). This may explain why DSS-treated *Yap*$^{-/-}$ mice have elevated apoptosis and poor survival in the absence of YAP. It has been shown in chronic UC patients that p53 is up-regulated in crypt cells and neutralizing antibodies to TNF-α reduce the levels of p53 and IBD-related symptoms of UC patients [418] in support of the important role for p53 in intestinal epithelial cell death.

In addition to p53, PUMA (p53 up-regulated modulator of apoptosis) has been shown to be up-regulated in intestinal cells following DSS treatment in mice and in colonic biopsies from UC patients suggesting an important role for other pro-apoptotic proteins in the pathogenesis of colitis [419]. Preliminary microarray analyses on colonic RNA isolated from DSS-treated wild-type and *Rassf1a*$^{-/-}$ mice revealed up-regulation of several pro-apoptotic genes. These genes were increased 2-4 fold with p-values <0.02 and include the death associated protein 3 (DAP3, increased 2.82 fold), programmed cell death 10 (PDCD10, increased 2.17 fold), PRKC apoptosis WT1 regulator (PAWR, increased 3.16 fold) and death effector domain-containing (DEDD, increased 4.71 fold) (Table 3.1). It will be interesting to explore if any of these are transcriptionally regulated by YAP/p73 in response to intestinal inflammation.

Efficient epithelial proliferation/repair is an integral part of recovery following inflammation-induced injury [396]. Preliminary data suggest that we can observe altered β-catenin/E-cadherin adherens junctions on colon sections from DSS-treated *Rassf1a* knockout mice during the recovery phase following DSS addition (Day 9,unpublished observations). Altered β-catenin/E-cadherin associations together with elevation of tyrosine phosphorylated YAP will result in abnormal formation of epithelial junctions and the appearance of a "leaky gut". Interestingly, YAP is over-expressed in CRC patients and RASSF1A is epigenetically silenced in CRC patients [89]. The loss of RASSF1A may, therefore, affect other aspects of epithelial restitution with YAP activity an integral part of this process. Failure to efficiently reseal and re-establish epithelial cell homeostasis will lead to an unnecessary inflammatory response, poor recovery and an early phase of colitis-associated carcinogenesis [420,421].

An important element for recovery from inflammation-induced damage is efficient repair. During the pathogenesis of IBD, it has been documented that DNA damage [422], oxidative damage [423,424] and abnormal ROS levels [424] are elevated in a similar manner

to what we have observed for DSS-treated *Rassf1a* knockout mice. Reactive oxygen species (ROS) are generated by inflammatory cells, neutrophils and macrophages and surround the inflamed mucosa [424]. High levels of ROS can lead to changes in colonic membrane permeability, decreased mucosal barrier of intestinal epithelial cells and to increased DNA and oxidative damage. Both DNA and oxidative damage can lead to c-ABL activation to drive the formation of tyrosine phosphorylated YAP and a YAP/p73-dependent transcriptional program. Inhibitors of ROS generation or DNA damage may be interesting angles to pursue in the future.

In addition to c-ABL and YES as potential PTKs for YAP, preliminary microarray analyses on colonic RNA isolated from DSS-treated wild-type and *Rassf1a*$^{-/-}$ mice revealed a 7.5 fold increase in TNK2 (a tyrosine kinase, non receptor type 2 also known as ACK1) and a 2.3 fold increase in c-Mer proto-oncogene tyrosine kinase (MERTK) (see Table 4.1 next chapter). MERTK has several potential NFκB binding sites (as documented by http://www.genecards.org/cgi-bin/carddisp.pl?gene=MERTK) and can modulate the autophosphorylation of TNK2. MERTK can also regulate cytokine production and clearance of apoptotic cells [425]. Very little is known about TNK2 other than its association with cdc42 in order to maintain it in a GTP bound form [426] and TNK2-dependent tyrosine phosphorylation of the androgen and epidermal growth factor receptor [427]. These observations provide interesting candidates to pursue that may function to drive the tyrosine phosphorylation of YAP and a YAP/p73 transcriptional program. Inhibiting the devastating effect of tyrosine phosphorylated YAP/p73-driven activation of pro-apoptotic genes and epithelial cell damage in the absence of RASSF1A may aid in designing future treatment schemes for patients with chronic inflammation. In fact, there has been one report to document the beneficial effects of protein tyrosine kinase inhibitors in treating IBD [428].

Our study provides a mechanistic understanding of DSS-induced inflammation injury in the absence of RASSF1A. Biomarker analyses for the *Rassf1a*$^{+/-}$ and

Rassf1a$^{-/-}$ mice revealed similar outcomes suggesting similar mechanisms of disease pathogenesis (except for responsiveness to imatinib). As can be observed in Figure 3.1 A, we did notice a slight delay in the appearance of clinical symptoms in the *Rassf1a*$^{+/-}$ mice, especially in the appearance of rectal bleeding. However, both *Rassf1a*$^{+/-}$ and *Rassf1a*$^{-/-}$ mice had similar survival rates at the end of the experiment and the delay at the beginning of the experiment was not statistically significant. We are currently exploring biomarker analyses between Day 0 and Day 8 to explore molecular differences between *Rassf1a*$^{+/-}$ and *Rassf1a*$^{-/-}$ mice. Interestingly, it has recently been demonstrated that p53 functions to recruit DAXX and DNMT1 to CpG methylation sites on RASSF1A and epigenetically silence RASSF1A [272]. p53 is accumulated in DSS-treated animals, in IBD patients, and can also silence RASSF1A by direct regulation of epigenetic silencing by DNA methylation of its promoter. Furthermore, RASSF1A epigenetic silencing can be detected in ulcerative colitis patients [88] and upon IL-6 production [392]. We, therefore, speculate that chronic inflammation will result in the loss of epigenetic loss of RASSF1A and RASSF1A may be an early change in the pathogenesis of ulcerative colitis. The *Rassf1a*$^{+/-}$, *Rassf1a*$^{-/-}$ and *Rassf1a*$^{IEC-KO}$ mice may be useful models for understanding IBD and other inflammatory disorders.
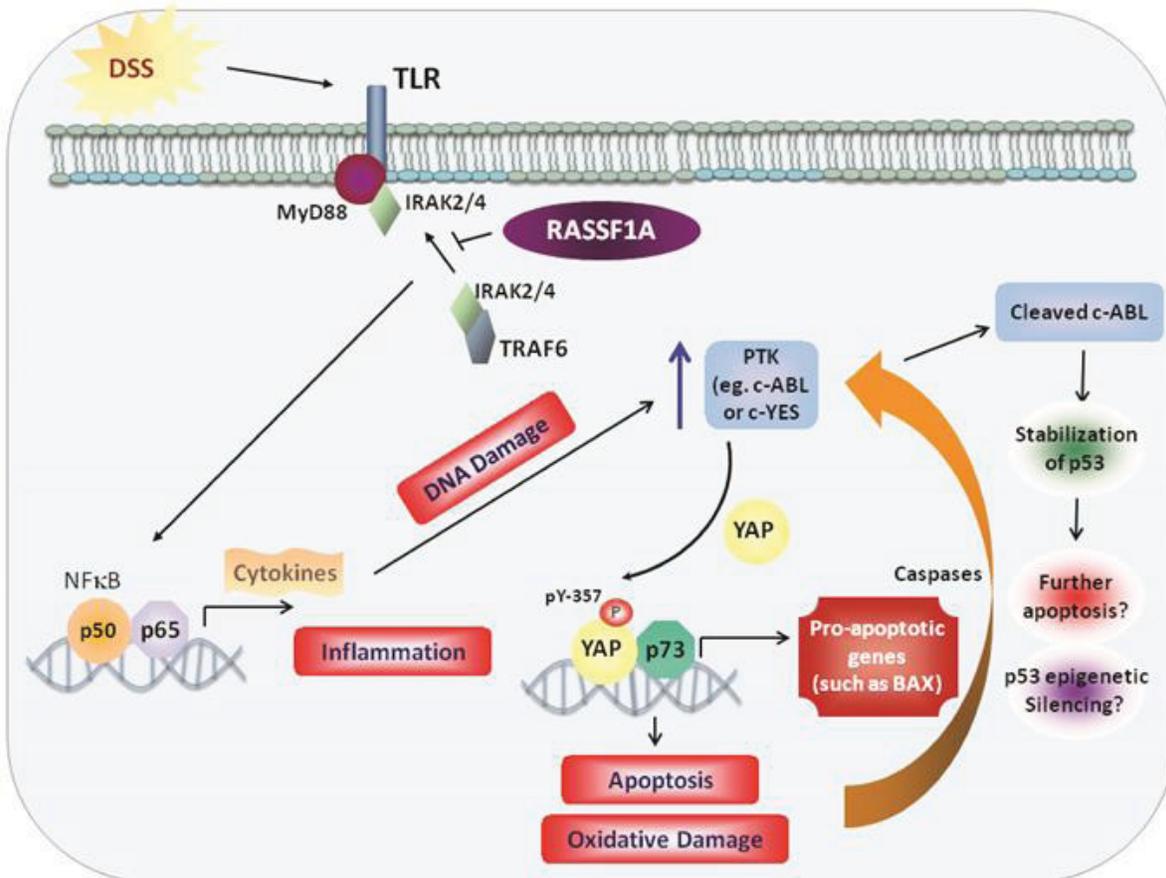
Figure 3.12: Model for RASSF1A regulation of NFκB and YAP. RASSF1A restricts NFκB activity by interfering with the ability of membrane proximal TLR/MyD88/TRAF6/IRAK2/4 to promote downstream signaling to NFκB. This results in the interference of NFκB-dependent gene transcription and the activation of inflammatory pathways. Through regulating NFκB activity (and early increases in DNA damage), RASSF1A indirectly regulates the activity (and possibly the expression) of a PTK to tyrosine phosphorylation YAP (possibly through c-ABL or c-YES). Increased PTK activity (in the absence of RASSF1A) would drive tyrosine phosphorylation of YAP and increased pY-YAP/p73 transcriptional up-regulation of pro-apoptotic genes such as BAX. Increased levels of BAX (and other p73/pY YAP targets) results in apoptosis, intestinal inflammation, oxidative (and DNA damage) and colonic injury. Sustained levels of apoptosis will result in the pro-apoptotic cleavage of c-ABL to stabilize p53. Accumulated p53 can further promote cell death and further colonic injury and poor recovery following inflammation insults.

134

Table 3.1: *Rassf1a-/-* mice show increased levels of apoptotic markers and NFκB transcriptional targets.
Microarray analyses of colonic RNA isolated from DSS-treated wild type and *Rassf1a-/-* mice revealed up-regulation of several pro-apoptotic genes in the colon of DSS-treated *Rassf1a-/-* mice.

Protein Symbol	Protein Name	Fold change	p-value	Primary Function from GeneCards [556]	NFκB binding status
DAP3	Death associated protein 3	2.82 up	0.004	Involved in mediating interferon-gamma-induced cell death	Interacts with NFκB
PDCD10	Programmed cell death 10	2.17 up	0.008	Promotes cell proliferation. Modulates apoptotic pathways.	N/A
PAWR	PRKC apoptosis WT1 regulator	3.16 up	0.001	Induces apoptosis in certain cancer cells by activation of the Fas pro-death pathway and co-parallel inhibition of NF-κ-B transcriptional activity.	NFκB binding site
DEDD	Death effector domain-containing	4.71 up	0.009	Regulates degradation of intermediate filaments during apoptosis.	NFκB binding site
DEDD2	Death effector domain-containing 2	2.02 up	0.003	May play a critical role in death receptor-induced apoptosis and may target CASP8 and CASP10 to the nucleus. May regulate degradation of intermediate filaments during apoptosis.	NFκB binding site
AIFM2	Apoptosis-inducing factor, mitochondrion-associated, 2	3.70 up	0.017	Oxidoreductase, which may play a role in mediating a p53/TP53 dependent apoptosis response. Probable oxidoreductase that acts as a caspase-independent mitochondrial effector of apoptotic cell death.	NFκB binding site

Chapter Four: Loss of RASSF1A Causes Accelerated and Aggravated Inflammation Driven Neoplasia during Chronic Inflammation

4-1 Introduction

Inflammatory Bowel Diseases (IBD) includes Crohn's disease (CD) and ulcerative colitis (UC), affecting both pediatric and adult patients. IBD is characterized by an intense inflammation of the GI tract resulting in severe symptoms including weight loss, abdominal pain, rectal bleeding, and diarrhea [24-26]. About 1/3 of all cancer cases are preceded by chronic inflammation, including chronic IBD leading to colorectal or colon cancer [7,16,17,19]. Although the predisposition to cancer has been well documented, the exact mechanism involved is unknown.

Currently, the causes of IBD are unknown, but research suggests that IBD is caused by a combination of genetic predisposition, environmental influences (e.g. climate, diet, pathogens), intestinal microbial disruptions, and immunologic dysfunction [33,35,37,49]. Molecularly, inflammation is characterized by hyperactivation of several transcription factors such as nuclear factor kappa B (NFκB), and elevated production of pro-inflammatory cytokines and chemokines upon activation of surface receptors [5-8]. NFκB signaling pathways regulate immunity and inflammation, and dysregulated and constitutive NFκB signaling has been implicated in several cancers [9,11,20,159]. Together, these changes may allow the creation of a neoplastic microenvironment, however, the exact molecular mechanisms whereby chronic inflammation may lead to neoplasia is unknown.

Because we have previously documented a role for RASSF1A in restricting inflammation, cell death, and DNA damage in an acute model of inflammation [3], this study aimed to further characterize how RASSF1A may affect molecular mechanisms

that link inflammation and cancer. RASSF1A loss has previously been shown to be highly associated with colorectal cancer development [89,347,429-431], and may also be lost in some UC patients [88].To this end, we utilized an established model of inflammation driven carcinogenesis, whereby mice are subjected to several inflammatory episodes using the colonic irritant dextran sodium sulfate (DSS) in order to mimic a chronic inflammatory state. Mice are injected with a single dose of azoxymethane (AOM, a pro-carcinogen) prior to these inflammatory episodes as AOM exposure has been shown to decrease the time to tumor appearance using the DSS chronic model [146,156-158].

Preliminary pilot studies demonstrated that *Rassf1a$^{-/-}$* mice have reduced survival in this model compared to wild type mice (similar to the acute inflammatory model, see Appendix A2) and increased susceptibility to inflammation related dysplasia, specifically the development of intramucosal carcinomas. Therefore, for these studies our protocol was modified slightly in order for the *Rassf1a$^{-/-}$* mice to survive the experiment to completion by using an initial dose of 8 mg/kg of AOM (modifications to [157]) followed by 2% DSS for cycles of 5 days, followed by 7 days recovery over three cycles.

In our previous study, we identified that loss of RASSF1A resulted in increased levels of pro-inflammatory cytokines, increased histological evidence of ulceration and cell injury, increased levels of oxidative and DNA damage, and increased levels of tyrosine phosphorylation of Yes-associated protein (YAP), driving unrestricted pro-apoptotic programming [3]. YAP has also been strongly associated with colon cancers [351,353,416,432,433] primarily through its ability to bind pro-proliferative transcription factors when found in the nucleus. Because mice lacking RASSF1A appeared to be unable to properly respond to DNA damage and also show significant up-regulation in total YAP levels as well as increased and aberrant tyrosine phosphorylation of YAP, we propose that loss of RASSF1A may promote inflammation driven tumorigenesis and provide a key link between chronic inflammation and cancer development. Sustained inflammation may create a pro-inflammatory tumor microenvironment and may also

promote dysregulation of wound healing mechanisms, and increased levels of DNA damage will likely promote increased mutations in *Rassf1a*$^{-/-}$ mice.

4-2   Results

4-2.1   *Rassf1a*^{-/-} mice show increased susceptibility to inflammation induced carcinogenesis

The use of a single exposure to a pro-carcinogen, AOM, in combination with cycled exposure to the chemical irritant DSS is an established mode for studying inflammation driven carcinogenesis. DSS is a chemical irritant of the colonic mucosa resulting in epithelial barrier damage, microbial invasion, and NFκB activation. Administration of DSS in the drinking water results in colitis in rodents, mimicking human symptoms of UC. Under chronic inflammation conditions, approximately 70% of *Rassf1a*^{-/-} mice survived, compared to 80% of wild type mice, a difference of 10%, however, this number was not statistically significant (Figure 4.1 A). Of note, nearly all of these deaths were in the male population, suggesting males are more susceptible to succumbing to DSS-induced colitis, which is consistent with previous reports [147,149,434].

Similar to our acute model, *Rassf1a*^{-/-} mice showed more body weight loss as well as significantly increased clinical symptoms (DAI Index) (Figure 4.1 B and C left panels). Interestingly, it was noted that there were significant male/female weight change differences within each group, males showed significantly more body weight loss than females, and *Rassf1a*^{-/-} males showing significantly more body weight loss than wild type males. In females, a significant difference in body weight loss was seen, however no clear pattern has emerged- at times *Rassf1a*^{-/-} females show increased, at times decreased body weight changes compared to wild type (Figure 4.1 B right panel).

In terms of disease activity, again *Rassf1a*^{-/-} males showed a significantly increased level of clinical symptoms compared to both *Rassf1a*^{-/-} females as well as to wild type males, and while *Rassf1a*^{-/-} females showed less severe disease activity than

Rassf1a⁻/⁻ males, they still showed significantly increased symptoms compared to wild type females (Figure 4.1 C right panel). We did not observe comparable male/female differences in our acute studies, however, this is likely due to the fact that the differences seen in our chronic model became more apparent at a later timepoint past the first inflammatory cycle. We speculate that differences in metabolic functioning and hormonal influences likely contribute to the observed differences between males and females in our chronic model, and that these influences explain why sex-related differences in disease outcomes appear more noticeable over a longer period of time. Increased susceptibility of males to DSS induced colitis has been previously reported and our results further emphasize the need to further illuminate what factors drive sex-based differences in the inflammatory response.
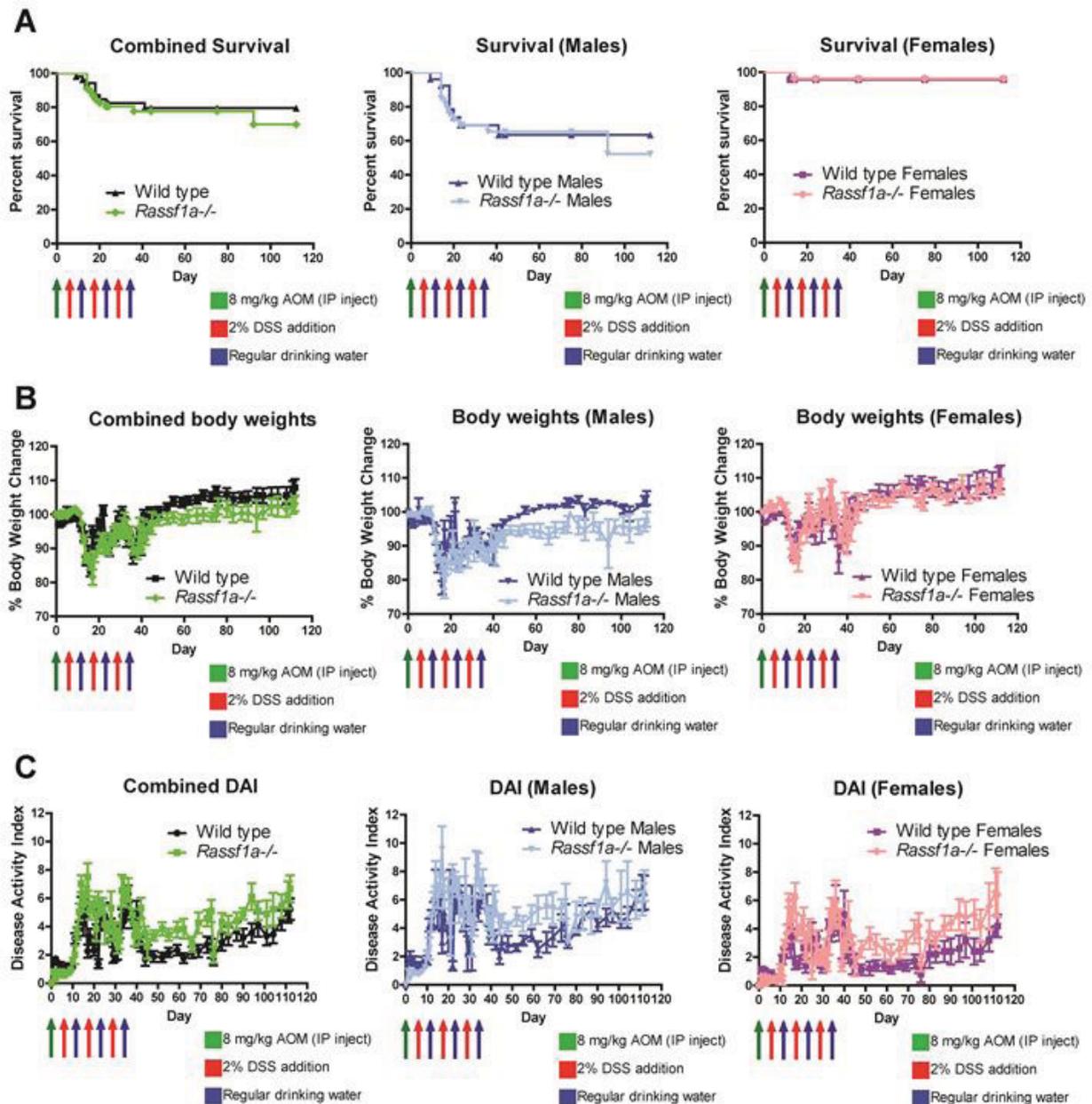
Figure 4.1. *Rassf1a-/-* mice show increased susceptibility to inflammation induced carcinogenesis. (**A**) *Rassf1a-/-* mice show over-all decreased survival compared to WT mice, and males are more susceptible in both genotypes. p-value= not significant for WT vs *Rassf1a-/-* overall, <0.02 for WT and <0.01 for *Rassf1a-/-* males versus females. (**B**) *Rassf1a-/-* mice show increased percentage body weight loss compared to WT, and males show overall increased body weight loss compared to females. p-value<0.001 at Day 17, <0.01 at Day 20, <0.05 at Day 75 for combined body weight comparisons, p-value<0.001 at Day 17, <0.01 at Day 20, <0.05 at Days 22 and 80 for WT males vs *Rassf1a-/-* males, p-value<0.05 at Days 18, 27, 29, 30, and 66, <0.01 at Days 20, 23, 28, <0.001 ay Days 22 and 24 for *Rassf1a-/-* males versus females. (**C**) Male/female disease activity differences and *Rassf1a-/-* mice show increased percentage body weight loss compared to WT. p-value<0.001 at Days 17, 20, and 22, <0.05 at Day 18, for combined body weight comparisons, <0.001 at Day 17, <0.01 at Days 20 and 22 for WT males vs *Rassf1a-/-* males, <0.05 at Days 12, 16, 24, <0.001 at Day 14, <0.0001 at Days 18, 21, and 23 for WT males versus females, <0.01 at Days 18, 28, 30, <0.001 at Days 22, 23, and 25, <0.05 at Day 29 for *Rassf1a-/-* males vs females, and <0.001 at Day 17 for WT females versus *Rassf1a-/-* females. n=28-32 for males and n=24 for females for all graphs

4-2.2 *Rassf1a⁻ᐟ⁻* mice show sustained histological levels of inflammation, early onset inflammation induced dysplasia, and increased histological dysplasia

In order to determine at what point neoplastic changes might be occurring, mice were harvested at several time points throughout the experiment; after each inflammatory cycle (Days 14, 24, and 44), one month after the final inflammatory stimulus (Day 75), and at the experiment end (Day 112). Colonic sections were collected from the distal, middle, and proximal areas of the colon, and scored for histological evidence of inflammation and/or neoplastic changes. Histological evidence of colonic inflammation throughout the entire colon was seen in both wild type and *Rassf1a⁻ᐟ⁻* mice, however, similar to the acute model, *Rassf1a⁻ᐟ⁻* mice appear to show sustained and increased colonic inflammation compared to wild type mice. At Day 75, one month after the final inflammatory stimulus, wild type mice show reduced histological signs of inflammation, while *Rassf1a⁻ᐟ⁻* mice continue to show significantly increased signs of inflammation until the final time point (Figure 4.2 A). While male mice tended to show slightly higher inflammation scores compared to females, this was not statistically significantly different.

Rassf1a⁻ᐟ⁻ mice also demonstrated evidence of intramucosal dysplasia as early as Day 44 (immediately after the last inflammatory stimulus cycle), at which time wild type mice show only occasional moderate dysplasia. As early as Day 44 and continuing to Day 112, *Rassf1a⁻ᐟ⁻* mice show significantly increased dysplasia scores compared to wild type mice, with evidence of invasive carcinoma as early as Day 75, while wild type mice show only adenomatous dysplasia and intramucosal carcinoma even at Day 112 (Figure 4.2 B). Female mice tended to show mildly higher but non-significant dysplasia scores compared to males. Taken together, this evidence suggests that mice lacking *Rassf1a* appear to be susceptible to earlier onset inflammation driven colorectal carcinoma, and mice lacking *Rassf1a* are also more susceptible to higher grade

neoplastic changes than wild type mice. Because *Rassf1a*$^{-/-}$ mice show sustained histological inflammation, this suggests the chronic inflammation is likely contributing to the tumor microenvironment and the accumulation of tumorigenic mutations, and that lack of RASSF1A promotes the early creation of a tumor friendly microenvironment in response to unrestricted inflammation.
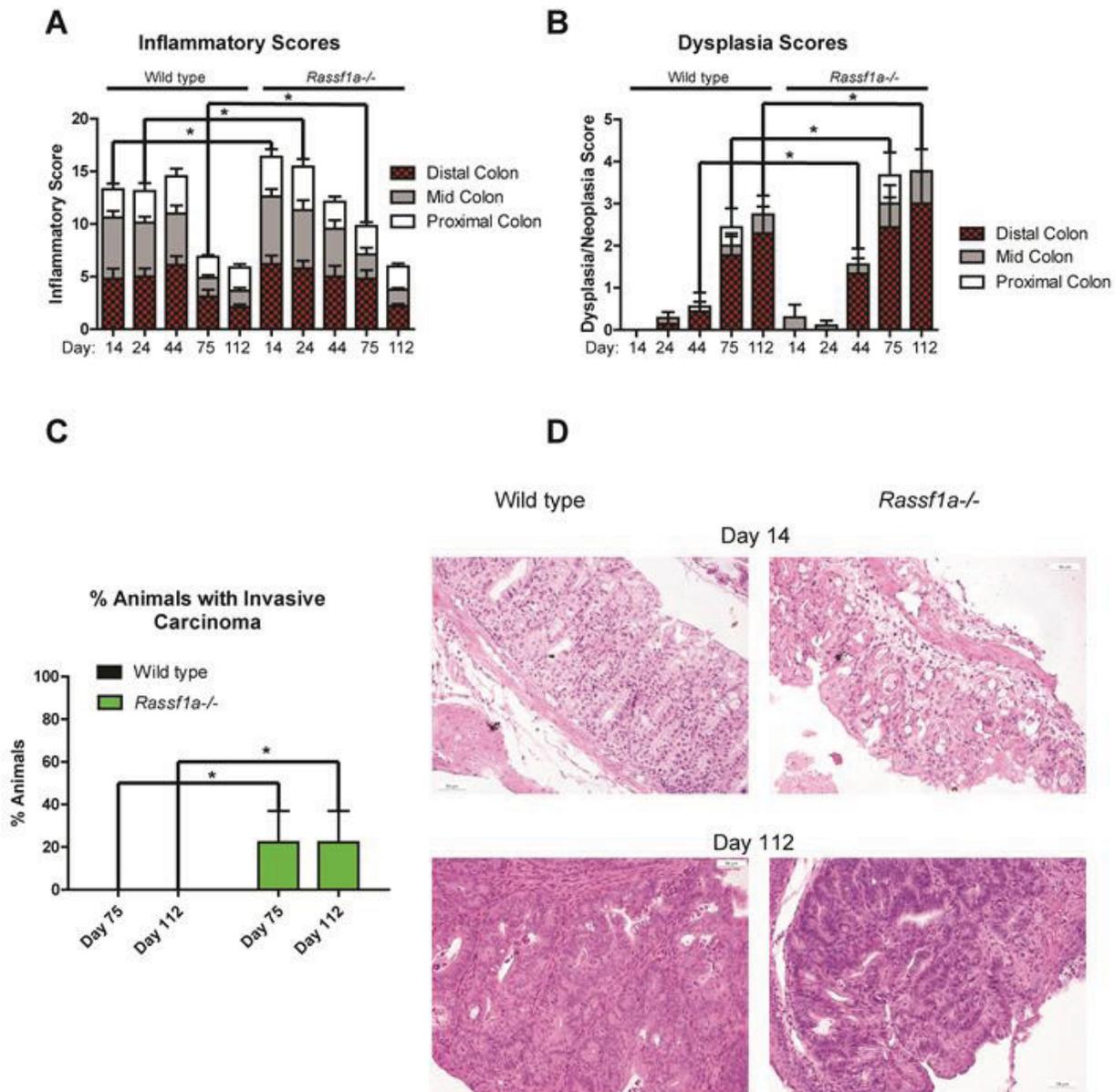
Figure 4.2. *Rassf1a-/-* **mice show sustained histological levels of inflammation, early onset inflammation induced dysplasia, and increased histological dysplasia** (**A**) *Rassf1a-/-* mice show sustained colonic inflammation following inflammation induced carcinogenesis. p-value <0.05 at Day 14, <0.02 at Day 24, >0.05 at Day 44, <0.01 at Day 75, and >0.05 at Day 112 for *Rassf1a-/-* vs WT. (**B**) *Rassf1a-/-* mice show early onset inflammation induced colonic dysplasia and higher grade neoplasia compared to WT mice. p-value<0.04 at Day 44, <0.02 at Day 75, and <0.03 at Day 112 for *Rassf1a-/-* vs WT, all other time points show no significance. (**C**) *Rassf1a-/-* mice are more prone to develop invasive carcinoma than WT mice. p-value<0.04 at Days 75 and 112 for *Rassf1a-/-* vs WT mice. (**D**) Representative distal colonic sections showing inflammatory changes (Day 14) and dysplastic changes (Day 112) in *Rassf1a-/-* and WT mice. Note the severe ulceration and loss of tissue architecture in *Rassf1a-/-* mice compared to WT at Day 14, and the appearance of disorganized gland-like appearance of dysplastic regions in both genotypes. *Rassf1a-/-* mice also show tumor invasion into the surrounding mucosa, and enlarged nuclei as well as condensed chromatin typical of high grade dysplasia. n=7-10 at each time point for each group at each time point (**A-D**). No significant differences between sexes was seen for histological features.

144

4-2.3 *Rassf1a*^{-/-} mice show dysregulated inflammatory biomarkers during inflammation induced carcinogenesis

In order to further determine the mechanism of DSS-induced injury and inflammation driven carcinogenesis in *Rassf1a*$^{-/-}$ mice, we assessed serum levels of several inflammatory biomarkers known to be associated with IBD and/or CRC pathogenesis. In keeping with our previous observations from the acute model and in line with the histological inflammation scoring (see Figure 3.1), pro-inflammatory cytokine and chemokine levels were elevated and sustained in *Rassf1a*$^{-/-}$ mice compared to wild type mice, however, no significant differences between sexes were observed.

Elevated and sustained levels of pro-inflammatory serum IL-6, IL-12, CXCL1, and MCP-1 are observed in *Rassf1a*$^{-/-}$ mice compared to wild type mice following initial inflammatory stimulus and throughout the experiment (Figure 4.3 A-D). IL-6, already significantly higher in *Rassf1a*$^{-/-}$ mice than wild type mice at baseline, shows a rapid induction in *Rassf1a*$^{-/-}$ mice at Day 14 (following initial inflammatory stimulus), followed by a tapering return to baseline levels, which remain significantly higher than in the wild type mice (Figure 4.3 A). Active IL-12, also at high baseline levels in *Rassf1a*$^{-/-}$ mice compared to wild type, showed sustained elevated levels of IL-12 compared to wild type mice (an apparent downward trend in *Rassf1a*$^{-/-}$ is not statistically significant) until the end of the experiment, further supporting an impaired restriction of pro-inflammatory signaling in *Rassf1a*$^{-/-}$ mice (Figure 4.3 B). CXCL1 (aka KC/GRO) levels are significantly elevated compared to wild type only at Days 14 and 44, following the first and third inflammatory stimuli (Figure 4.3 C).

MCP-1, a chemokine which targets monocytes and dendritic cells to sites of inflammation, was also significantly elevated compared to wild type mice at Day 14

following initial inflammatory insult, and remained significantly elevated until Day 75, at which point aggressive carcinoma has appeared in most *Rassf1a*$^{-/-}$ mice (Figure 4.3 D). Elevated MCP-1 levels in IBD patients have previously been shown to correlate with enhanced disease severity and MCP-1 expression has also been associated with increased incidence of a cancer phenotype [74-79]. In a similar manner, *Rassf1a*$^{-/-}$ show decreased levels of the anti-inflammatory cytokine IL-10, further suggesting an impairment of *Rassf1a*$^{-/-}$ mice in their ability to shut-down inflammatory signaling (Figure 4.3 E).

Interestingly, serum TGF-β appears to significantly decrease in both *Rassf1a*$^{-/-}$ and wild type mice following the initial inflammatory stimulus, and remains at relatively low levels until the end of the experiment. *Rassf1a*$^{-/-}$ mice show a significant increase in TGF-β levels at Day 24, after the second inflammatory stimulus, while showing significantly decreased levels compared to wild type at Day 75 (Figure 4.3 F). Both wild type and *Rassf1a*$^{-/-}$ mice TGF-β levels return to near the higher baseline levels by the end of the experiment. Finally, when we examined the activation status of NFκB transcription factor complexes in nuclear extracts derived from bone marrow cells from our mice, we see that following DSS treatment and throughout our experiment, NFκB specific activity in bone marrow cells from *Rassf1a*$^{-/-}$ animals was significantly higher than in wild-type bone marrow cells, similar to what we have previously characterized in our acute study (Figure 4.3 G). Taken together, these results emphasize the importance of RASSF1A in regulating and restricting the NFκB response and in restricting pro-inflammatory signaling.
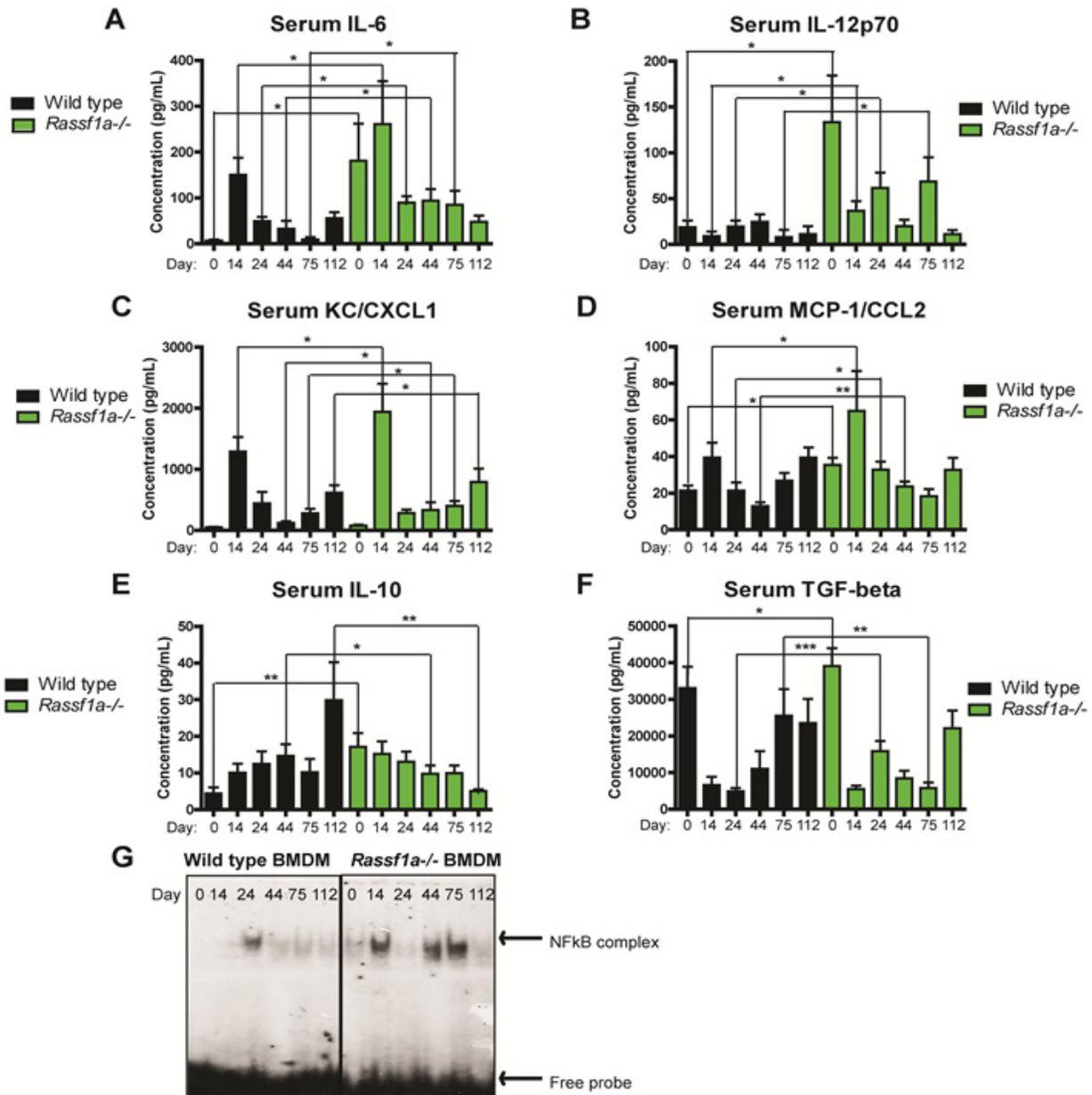
Figure 4.3. *Rassf1a-/-* mice show dysregulated inflammatory biomarkers during inflammation induced carcinogenesis.
(**A**) *Rassf1a-/-* mice show increased and sustained serum levels of IL-6 following inflammation induced carcinogenesis. p-value<0.02 at Day 0, <0.03 at Day 14, <0.04 at Day 24, <0.02 at Day 44, <0.01 at Day 75, and >0.05 at Day 112 for *Rassf1a-/-* vs WT. (**B**) *Rassf1a-/-* mice show increased and sustained serum levels of active IL-12 following inflammation induced carcinogenesis. p-value<0.02 at Day 0, <0.03 at Day 14, <0.04 at Day 24, >0.05 at Day 44, <0.01 at Day 75, and >0.05 at Day 112 for *Rassf1a-/-* vs WT. (**C**) *Rassf1a-/-* mice show increased serum levels of KC/CXCL1 following inflammation induced carcinogenesis. p-value>0.05 at Days 0 and 24, <0.04 at Days 14, 44, and 112,and <0.05 at Day 75 for *Rassf1a-/-* vs WT. (**D**) *Rassf1a-/-* mice show increased serum levels of MCP-1 following inflammation induced carcinogenesis. p-value<0.02 at Day 0, <0.03 at Days 14 and 24, <0.008 at Day 44, >0.05 at Days 75 and 112 for *Rassf1a-/-* vs WT. (**E**) *Rassf1a-/-* mice show decreasing levels of anti-inflammatory IL-10 following inflammation induced carcinogenesis. p-value<0.003 at Day 0, >0.05 at Days 14, 24, and 75, <0.01 at Day 44, and <0.001 at Day 112 for *Rassf1a-/-* vs WT. (**F**) TGF-b levels initially decrease after inflammatory stimulus and increase after neoplasia. p-value<0.04 at Day 0, >0.05 at Days 14, 44, and 112, <0.0006 at Day 24, and <0.001 at Day 75 for *Rassf1a-/-* versus WT. For all graphs shown (**A-F**), n=7-10 for each time point. (**G**) NFκB DNA binding in nuclear extracts derived from bone marrow cells upon DSS treatment. *Rassf1a-/-* mice show increased and sustained binding of NFκB throughout the experiment. No significant male/female differences were seen for data presented in this figure.

147

4-2.4 Wild type mice show loss of *Rassf1a* mRNA expression following chronic inflammatory stimulus

When compiling the dysplasia scores for the wild type mice, it was noted that although *Rassf1a*^{-/-} mice did show overall increased earlier onset and increased severity of colonic dysplasia, wild type mice appear to be nearing similar levels of dysplasia near the end of the experiment. One possible explanation for this observation could be the loss of RASSF1A protein expression and function in these animals. All wild type mice were confirmed to have (and all knockout *Rassf1a*^{-/-} mice were confirmed to lack) the *Rassf1a* gene present using genotyping PCR as previously described (Figure 3.4 C, [3,293]). Previous studies have suggested that sustained inflammation can induce hypermethylation of genes typically associated with cell death and classed as tumor suppressor such as APC and p53 [413,435-437]. Using RT-PCR, we examined the expression of *Rassf1a* mRNA in colonic samples from wild type mice over the course of our chronic inflammation driven carcinogenesis experiment.

As early as following one cycle of 2% DSS administration for 5 days, wild-type mice showed significant loss of colonic *Rassf1a* mRNA expression compared to untreated mice (Figure 4.4 A). Loss of *Rassf1a* expression may be somewhat transient, as faint expression is regained at Day 44 (10 days recovery after three cycles of 2% DSS) (Figure 4.4 A bottom panel), however loss appears to be complete at the final two time points of the experiment. *Rassf1a* loss in wild type mice may explain why wild type mice appear more similar to the *Rassf1a*^{-/-} knockout mice as the experiment progresses over time, and demonstrates the importance of the RASSF1A protein in normal colonic function.

In order to study whether the loss of *Rassf1a* mRNA was due to hypermethylation, as is frequently seen in human colon cancers, the methylation status

of 6 CpG loci in the first exon of *Rassf1a* was examined using pyrosequencing. Of the 6 examined CpG loci, only the second CpG site showed any significant increase in methylation levels compared to baseline, with an approximately 5% increase in CpG methylation at this locus by the end of the experiment (Figure 4.4 C). In concordance with the RT-PCR mRNA results, methylation changes appear to be slightly transient, with an overall increase in methylation at CpG site 2 but a slight decrease at Day 44. However, while there are significant changes at CpG site 2, there were no global changes in methylation observed over the 6 examined CpG sites, with most of the other sites showing either little change or an overall decrease in the levels of methylation (Figure 4.4 B). Similarly, real-time qPCR analysis of DNMT1 expression levels showed no significant changes in wild type animals over the course of the experiment, although there is a slight increase in expression at the final time point (Figure 4.4 E). Taken together, these results indicate that while *Rassf1a* methylation may contribute in part to inflammation driven loss of *Rassf1a* expression in mice, other ways of suppression, such as microRNA mRNA inhibition may be at play and will need to be explored.
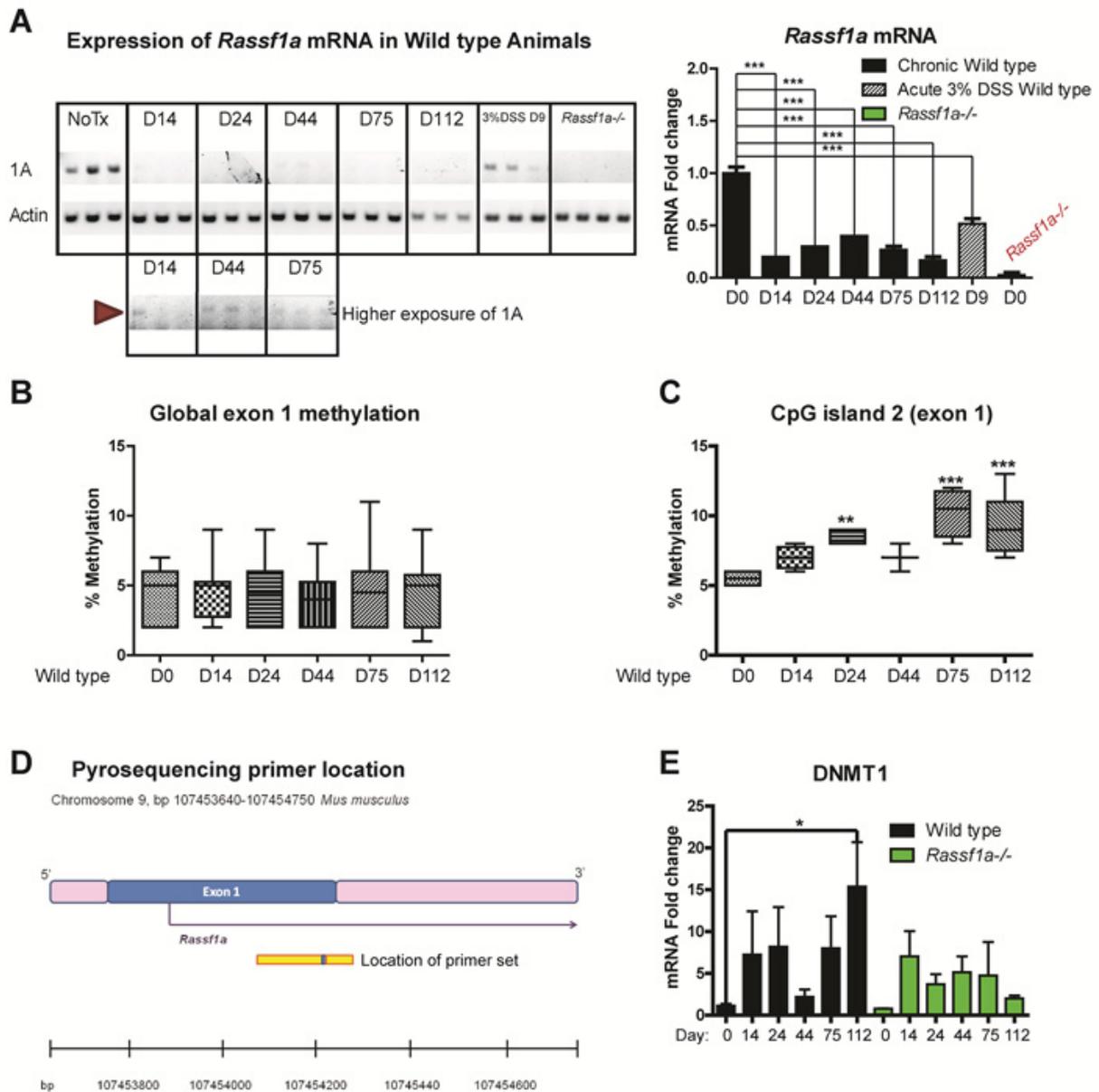
Figure 4.4. Wild type mice show loss of *Rassf1a* mRNA expression following chronic inflammatory stimulus. (A) RT-PCR analysis of *Rassf1a* mRNA expression utilizing colonic mRNA from wild type mice. Wild type mice show significant but transient loss of *Rassf1a* mRNA following inflammatory stimuli with near complete loss toward the end of the experiment. Lower panel shows higher exposure of time points with faint expression. Right panel is quantitation of *Rassf1a* mRNA expression fold change compared to untreated wild type animals. All groups had p-value<0.0001 compared to wild type. n=4 for each time point. **(B)** Wild type mice do not show global methylation changes in exon 1 of *Rassf1a*. Six CpG islands in exon 1 were examined for methylation changes using pyrosequencing analysis of colonic DNA. p-value>0.05 n=4 for each time point **(C)** Wild type mice show some transient methylation changes at CpG island 2 of exon 1 of *Rassf1a*. "**" p-value<0.001, "***" p-value<0.0001 For **B** and **C**, %methylation indicates the average percentage of the CpG site methylated across samples. **(D)** Schematic depicting location of primer set used for pyrosequencing analysis in B and C. Adapted from Qiagen.com. Yellow bars represent primers, mapping to the antisense strand of *Rassf1a*. The yellow bar represents the location of the primer set used. **(E)** DNMT colonic mRNA expression analysis using q-PCR. "*"p-value<0.02 between wild type Days 0 and 112, no other changes were significant. n=4-8. No significant male/female differences were seen for any data presented in this figure.

4-2.5 *Rassf1a⁻ᐟ⁻* show dysregulated apoptotic and proliferative signaling during inflammation induced carcinogenesis

As *Rassf1a⁻ᐟ⁻* mice show increased and early onset neoplasia, it is not surprising that *Rassf1a⁻ᐟ⁻* mice also show increased susceptibility to DNA damage, as evidenced by the appearance of phosphorylated histone 2A (γH2A.X), a marker of DNA double-strand breaks (Figure 4.5 A) [438,439]. Not only are γH2A.X levels increased in *Rassf1a⁻ᐟ⁻* mice upon inflammatory insult, but they appear to remain elevated after removal of inflammatory stimuli and into the appearance of neoplastic tumorigenesis (Days 44 and 75). The dramatic increase and prolonged levels of DNA damage in *Rassf1a⁻ᐟ⁻* mice suggest an impaired DNA damage response in these mice and highlight the role of RASSF1A in DNA damage control which has been previously described [89,240,326,366].

Oxidative damage has been previously shown to contribute to DNA damage and drive oncogenic mutations [82,440-442], and therefore it is not surprising that *Rassf1a⁻ᐟ⁻* mice show increased susceptibility to oxidative damage compared to wild type animals. Similar to what was seen in our acute experiments, *Rassf1a⁻ᐟ⁻* mice showed a dramatic increase in the levels of heme oxygenase-1 (HO-1) mRNA expression following an initial inflammatory stimulus (Figure 4.5 B). HO-1 expression is induced in response to oxidative stress and correlated with increased levels of ROS [443-445]. Wild type mice show a moderate response to oxidative stress, with a slight increase upon initial inflammatory stimulus (Day 14), and a resurgence upon tumorigenesis (Days 75 and 112) while *Rassf1a⁻ᐟ⁻* mice show a substantial response upon initial inflammatory stimulus, which is relatively sustained until tumorigenesis, with a second increase once neoplastic changes are established (Day 112) (Figure 4.5 B). Similar to IBD patients, inflammation induced injury in our *Rassf1a* knockout mice has associated DNA and oxidative damage.

In order to determine whether loss of RASSF1A dysregulated proliferative signaling, we also examined crypt cell proliferation by staining colonic sections for proliferating nuclear cell antigen (PCNA). As seen in our acute model, *Rassf1a*$^{-/-}$ mice show reduced PCNA staining indicating reduced proliferative ability post inflammatory stimulus, compared to wild type animals, suggesting a wound healing defect (Figure 4.5 C). Intriguingly, while *Rassf1a*$^{-/-}$ mice continue to show reduced nuclear PCNA staining, suggesting reduced proliferative ability during inflammatory stages, they show a rapid increase in proliferation at Day 75, when tumorigenesis is in full swing. At Day 75, when *Rassf1a*$^{-/-}$ mice show initial signs of invasive carcinoma (Figure 4.2) they show the highest levels of crypt cell proliferation. Taken together, these results imply that RASSF1A may play a crucial in eliciting a normal wound-healing response, and that loss of RASSF1A contributes to reduced epithelial restitution in the short term, while also contributing to unrestricted and inappropriate epithelial cell growth in the context of sustained inflammation.

Dysregulation of apoptotic signaling is thought to be one of the major drivers of cancer development [286]. The ability of our immune system to properly identify and destroy cells containing DNA mutations or high levels of cellular damage prevents the accumulation of potentially oncogenic cells. To this end, we analyzed how RASSF1A influences apoptotic signaling in a chronic inflammatory context. In accordance with our acute model and with the appearance of high levels of DNA and oxidative damage, *Rassf1a*$^{-/-}$ mice also show increased levels of the late apoptosis marker PARP (Figure 4.5 D). Interestingly, the increased levels of cleaved PARP are sustained throughout our entire chronic model, suggesting that despite tumorigenesis and increased tumor grade, *Rassf1a*$^{-/-}$ mice still display dysregulated apoptotic signaling and increased cell death. BAX, a marker of mitochondrial directed apoptosis, shows a similar pattern to that of PARP, as does p53, a transcription factor responsible for driving pro-apoptotic signals (Figure 4.6 A and B). Wild type mice show an induction of BAX at Day 44 and 75, which is when tumorigenesis begins, suggesting that wild type mice are attempting to increase apoptotic signals as a counter to the proliferation of cancerous cells as a normal

defense against the development of tumors, while *Rassf1a*$^{-/-}$ mice show a relative decrease in BAX at these time points (although BAX levels are still elevated overall compared to wild type mice). *Rassf1a*$^{-/-}$ mice also show overall higher levels of p53, with particular accumulation at Days 75 and 112, at the appearance of invasive carcinoma, while wild type p53 levels remain relatively stable (Figure 4.6 A and B).

TUNEL, a marker of DNA nicks and nuclear condensation caused by late-stage apoptosis, shows a slightly different pattern (Figure 4.6 C). While *Rassf1a*$^{-/-}$ mice show an initial increase in TUNEL staining (and other apoptotic markers) at Day 14 following initial inflammatory stimulus, they then show a decrease in TUNEL levels until later time points, when invasive carcinoma is established. Wild type mice show an overall increase in TUNEL staining until the very end of the experiment, with a peak at Days 44 and 75 in a similar pattern to that seen in BAX expression. This again suggests that wild type mice are mounting an increased apoptotic response in order to counteract proliferative signals. Interestingly, histological examination of TUNEL localization in later stages of the experiment reveal interesting expression pattern differences. In the acute phase, both *Rassf1a*$^{-/-}$ and wild type mice show increased TUNEL staining in areas of ulceration, with higher levels in *Rassf1a*$^{-/-}$ mice primarily due to the increased frequency of ulcerative lesions and increased cellular damage. In later phases in wild type mice, TUNEL staining can be seen equally distributed through dysplastic tissue as well as the surrounding tissue and stroma. *Rassf1a*$^{-/-}$ mice, however, show little TUNEL staining in dysplastic regions while the surrounding tissue and stroma show significantly higher levels (Figure 4.6). This suggests that the dysregulation of apoptotic signaling seen in the acute phase in *Rassf1a*$^{-/-}$ mice continues into tumorigenesis, and suggests an important role for stromal contributions to neoplastic development.
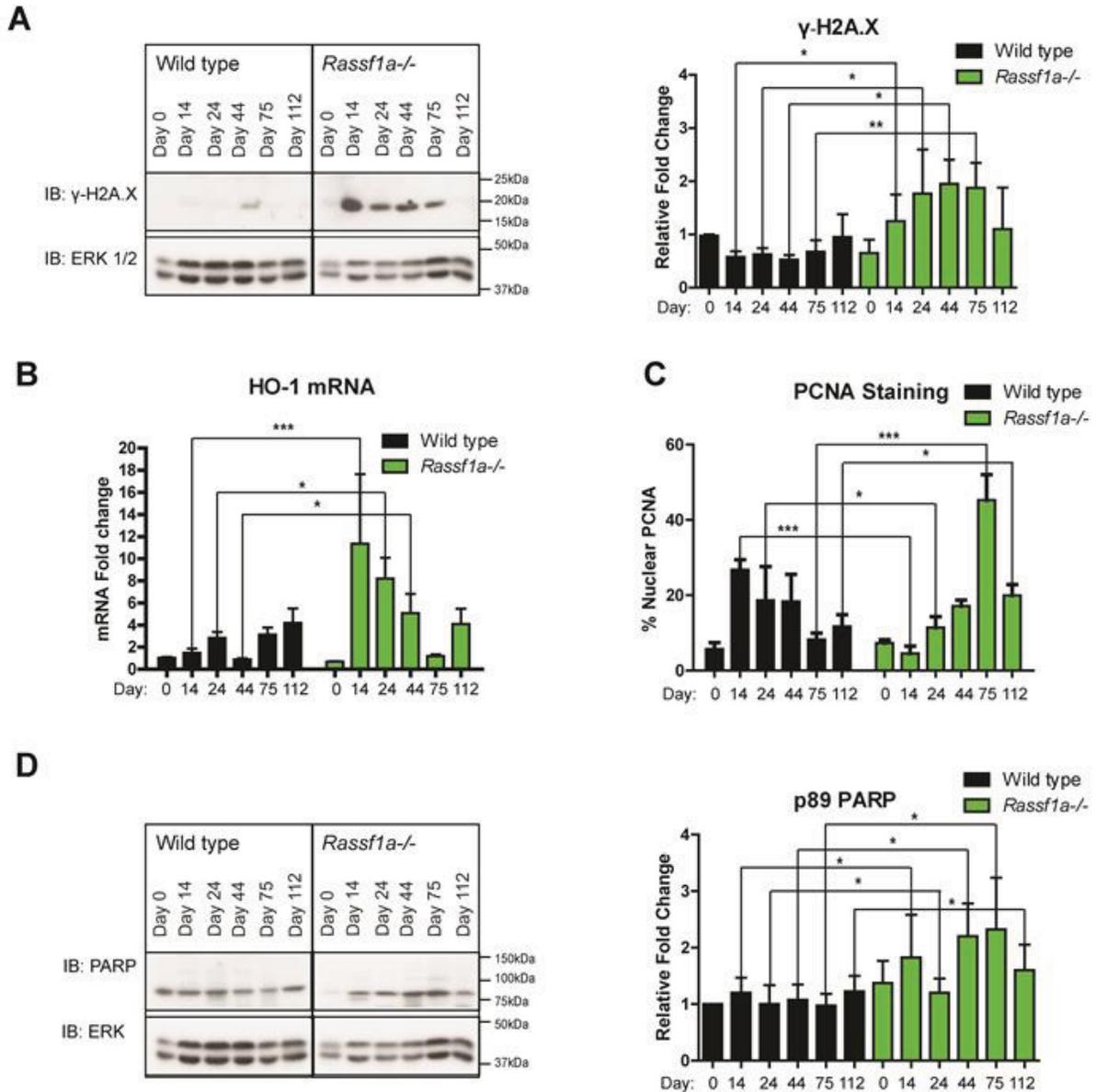
Figure 4.5 *Rassf1a-/-* **mice show increased cellular damage and dysregulated proliferative signaling during inflammation induced carcinogenesis.** (**A**) Analysis for the DNA damage marker, phospho-γ-H2AX, in colon lysates (experiment repeated four times with similar results) shows increased evidence of DNA damage in *Rassf1a-/-* mice. Right panel shows quantitation of left. p-value>0.05 at Day 0, <0.01 at Day 14, <0.05 at Days 24 and 112, and <0.02 at Days 44 and 75 for *Rassf1a-/-* vs WT. (**B**) q-PCR analysis for the oxidative damage marker HO-1 utilizing colonic mRNA shows increased oxidative damage in Rassf1a-/- mice. p-value<0.0001 at Day 14 and <0.05 at Days 24 and 44 for *Rassf1a-/-* vs WT. n=6-8 for each time point. (**C**) Measurement of PCNA positive proliferation in colonic sections. Percent PCNA staining was calculated by counting 4 groups of 1000 cells in 3-4 independent histological sections from each genotype and time point. p-value>0.05 at Days 0 and 44, <0.0001 at Days 14 and 75, <0.01 at Day 24, and <0.03 at Day 112 for *Rassf1a-/-* vs WT. (**D**) Analysis for PARP cleavage (p89 PARP) by immunoblot in colon lysates shows increased PARP cleavage in *Rassf1a-/-* mice (experiment repeated four times with similar results). Right panel shows quantitation of left. p-value>0.05 at Day 0, <0.04 at Days 14, 44, and 112, <0.01 at Day 24, and <0.02 at Day 75 for *Rassf1a-/-* vs WT. No significant male/female differences were seen for any data presented in this figure. All fold changes are compared to untreated wild type mice.

154
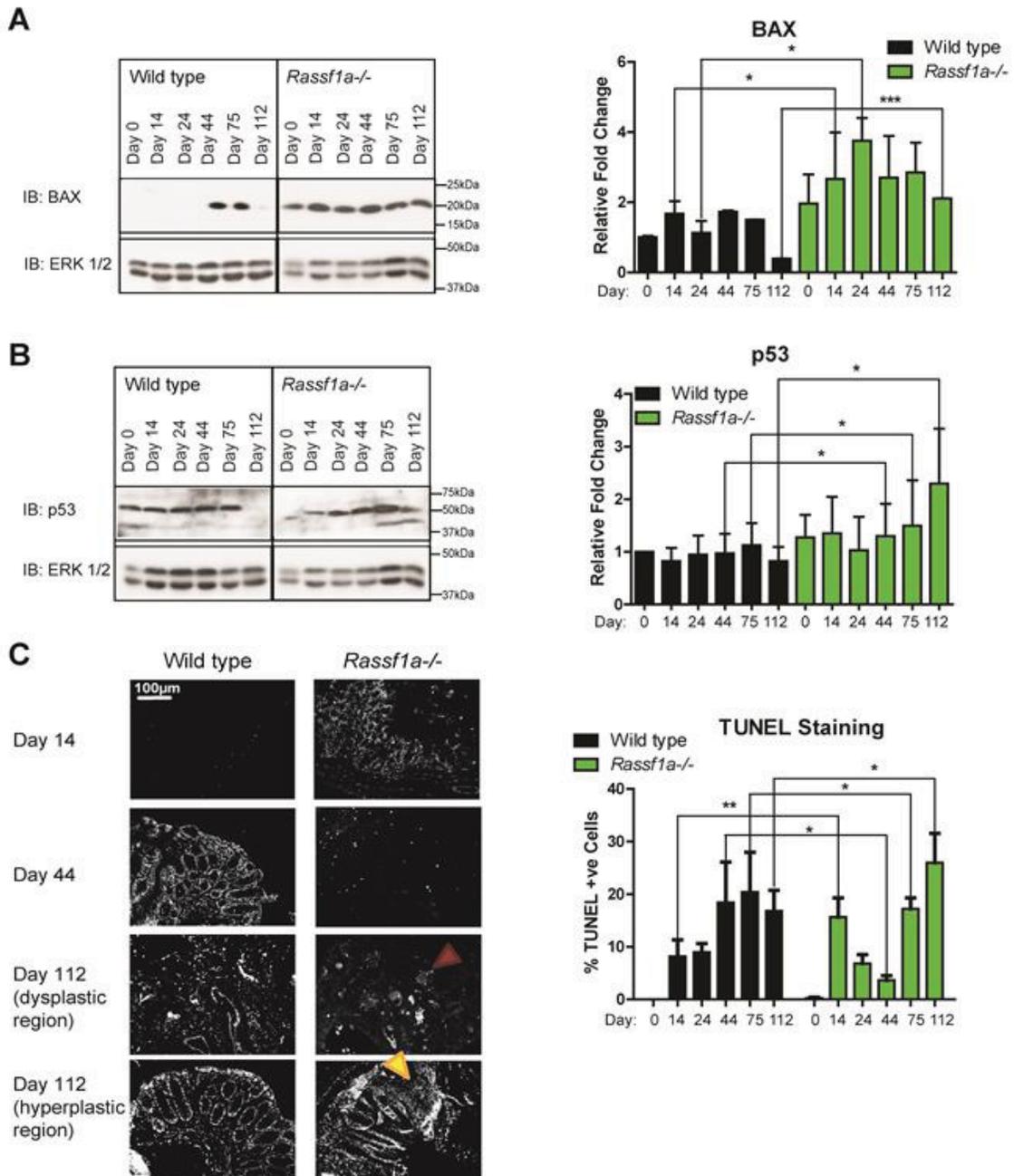
Figure 4.6 *Rassf1a-/-* mice show dysregulated apoptotic signaling during inflammation induced carcinogenesis. (**A**) Analysis for BAX expression by immunoblot in colon lysates (experiment repeated four times with similar results). Right panel shows quantitation of left. p-value>0.05 at Days 0, 44, and 75, <0.02 at Days 14 and 24, and <0.0001 at Day 112 for *Rassf1a-/-* vs WT. (**B**) Analysis for p53 expression by immunoblot in colon lysates (experiment repeated four times with similar results). Right panel shows quantitation of left. p-value>0.05 at Days 0, 14, and 24, <0.04 at Day 44, <0.01 at Day 75, and <0.03 at Day 112 or *Rassf1a-/-* vs WT. (**C**) TUNEL positive staining (bright dots) was carried out as a late marker of cell death (left panel, representative sections). Percent TUNEL staining was calculated by counting 4 groups of 1000 cells in 3-4 independent histological sections from each genotype and time point. Right panel is quantitation of left. p-value>0.05 at Days 0 and 24, <0.006 at Day 14, and <0.02 at Days 44, 75, and 112 for *Rassf1a-/-* vs WT. Note the localization of TUNEL staining in *Rassf1a-/-* mice is restricted to necrotic pockets in dysplastic tissue (red arrow) and increased in stromal regions in hyperplastic regions (yellow arrow) compared to a more even distribution in WT mice. No significant male/female differences were seen for any data presented in this figure.

155

4-2.6 *Rassf1a^-/-* mice show dysregulated YAP signaling during inflammation induced carcinogenesis

In our acute study, we established that in response to DSS exposure and activation of pro-inflammatory signaling mice show increased cell death and DNA damage, as well as tyrosine phosphorylation of Yes-associated protein (YAP) by the activated tyrosine kinase ABL, promoting YAP association with p73 and transcription of apoptotic molecules such as BAX. In the absence of RASSF1A this process becomes unrestricted and uncontrolled levels of cell death contribute to the development of severe inflammatory disease and failure to recover [3]. We therefore wished to examine the dynamics of YAP signaling in our chronic model, particularly as dysregulation of the Hippo pathway and YAP signaling has been implicated in cancer development, and recent studies have shown a growing connection between RASSF family signaling and Hippo signaling [351,353,354,411].

As described in our acute study, increased level of caspase activation has been shown to cleave the ABL tyrosine kinase into catalytically active subunits, the smallest of which is a 20 kDa fragment consisting solely of the catalytic subunit [405,406]. Similar to our acute model, we see an increase in the appearance of cleaved ABL upon DSS stimulation and *Rassf1a^-/-* mice showed increased levels of cleaved (active) ABL products compared to wild type animals (Figure 4.7 A and B). Interestingly, *Rassf1a^-/-* mice continued to accumulate higher levels of cleaved ABL throughout our experiment, both during the inflammatory phase as well as throughout tumorigenesis. Taken with the increased levels of DNA damage seen in these mice (Figure 4.5), this suggests that unrestricted inflammation in mice lacking Rassf1a causes increased c-ABL activation, and likely unrestricted downstream phosphorylation of YAP.

In addition to dysregulated levels of ABL kinase in *Rassf1a*$^{-/-}$ mice, we also observed a not unexpected accumulation of YAP. Both wild type and *Rassf1a*$^{-/-}$ mice show an increase in YAP levels following initial DSS insult (Day 14). Of note is that another up-regulation of YAP levels occurs in all animals again at Day 44 at the time of tumor initiation, and elevated levels of YAP persist past this point in *Rassf1a*$^{-/-}$ mice (Figure 4.7 A). Serine 127 YAP phosphorylation increases in both sets of animals at Day 14, although at a lower level in *Rassf1a*$^{-/-}$ animals than in wild types, as described previously (Figure 4.7 A). As S127 phosphorylation restricts YAP to the cytoplasm, this increase likely indicates an attempt to shut down YAP signaling, particularly as total YAP levels are concurrently raising. *Rassf1a*$^{-/-}$ mice, but not wild type mice, also show an increase in pS127-YAP levels starting at Day 44.

Despite increased levels of pS127-YAP phosphorylation, we observed a significant increase in nuclear localized pY357-YAP in *Rassf1a*$^{-/-}$ mice using immunohistologically stained tissue sections (Figure 4.7 B and C). Wild type mice show an increase of pY357-YAP levels following inflammatory events as described previously, but appear to be capable of shutting down this signaling cascade after DSS insults are removed. *Rassf1a*$^{-/-}$ mice, however, continue to show elevated levels of nuclear pY357-YAP throughout the experiment, further confirming that these mice appear to be deficient in their ability to restrict pY357-YAP signaling. Interestingly, total levels of pY357-YAP were increased in *Rassf1a*$^{-/-}$ mice in addition to the nuclear localization, with a noticeable cytoplasmic population in addition to the nuclear population at later time points (Figure 4.7 B). As serine 127 phosphorylation is also increased at these times, it appears that some of the tyrosine phosphorylated YAP may be sequestered in the cytoplasm, suggesting that the overall increase in pY-YAP levels allows the nuclear accumulation of YAP and continued YAP-directed transcription.

We next looked at the mRNA expression status of the key binding partners of YAP. Wild type mice showed varying levels of YAP mRNA expression throughout the

experiment, with an approximately two-fold increase near the end of the experiment. In contrast with this, YAP mRNA levels in *Rassf1a*^{-/-} mice remained mostly constant, with an elevation in total YAP mRNA occurring only at the end of the experiment (Figure 4.8 A). As Western blotting revealed an increase in total levels of YAP in *Rassf1a*^{-/-} compared to wild type mice, this suggests that loss of RASSF1A may stabilize YAP protein levels in an inflammatory setting. In the case of YAP binding partners, we can see an excellent switch between the expression of pro-proliferative partners and pro-apoptotic partners (Figure 4.8 B-D). After initial inflammatory stimulation (Day 14), transcription of TEAD1 is reduced while transcription of p73 is increased, in both wild type and *Rassf1a*^{-/-} animals. Throughout the duration of the rest of the experiment, wild type animals appear to show a continued reciprocal relationship between the up-regulation of TEAD1 mRNA and the down-regulation of p73, or vice versa. As may have been predicted in a cancer model, at the end of the experiment when most of the wild type animals show intramucosal carcinoma, p73 levels are decreasing and TEAD1 levels are significantly up.

Rassf1a^{-/-} mice show a disproportionately high level of p73 transcription throughout the experiment, which likely contributes to the continued elevation of apoptotic markers throughout (Figures 4.5 and 4.6). In a similar manner, wild type mice also show up-regulation of RUNX2 at time points when p73 expression is being down-regulated. It is interesting that in wild type animals both TEAD1 and RUNX2 show their most prominent up-regulation at Day 112. Immunoprecipitation experiments will need to be used to confirm binding of p73, RUNX, and TEAD to YAP and to determine relative binding frequencies across tumor pathogenesis.

Of note is that *Rassf1a*^{-/-} mice appear to show complete dysregulation of normal expression patterns of all three examined transcription factors (Figure 4.8). Although there appear to be some relative shifts showing opposite increases and decreases between apoptotic and proliferative transcription factors, all three proteins have

abnormally high mRNA expression throughout most of the experiment, compared to both baseline and wild type. Both p73 and RUNX2 show an abnormally low expression at Day 75, for an unknown reason. These abnormal expression patterns suggest that loss of RASSF1A may completely dysregulate all YAP directed transcription. Of particular interest is the fact that despite *Rassf1a*^{-/-} mice showing up to several hundred times increased p73 mRNA expression, the protein levels show only a maximally two-fold increase at Day 14. Due to the overall dysregulation and up-regulation of all three examined YAP binding partners, future immunoprecipitation experiments are crucial to completely understanding how RASSF1A may regulate YAP transcriptional programs.
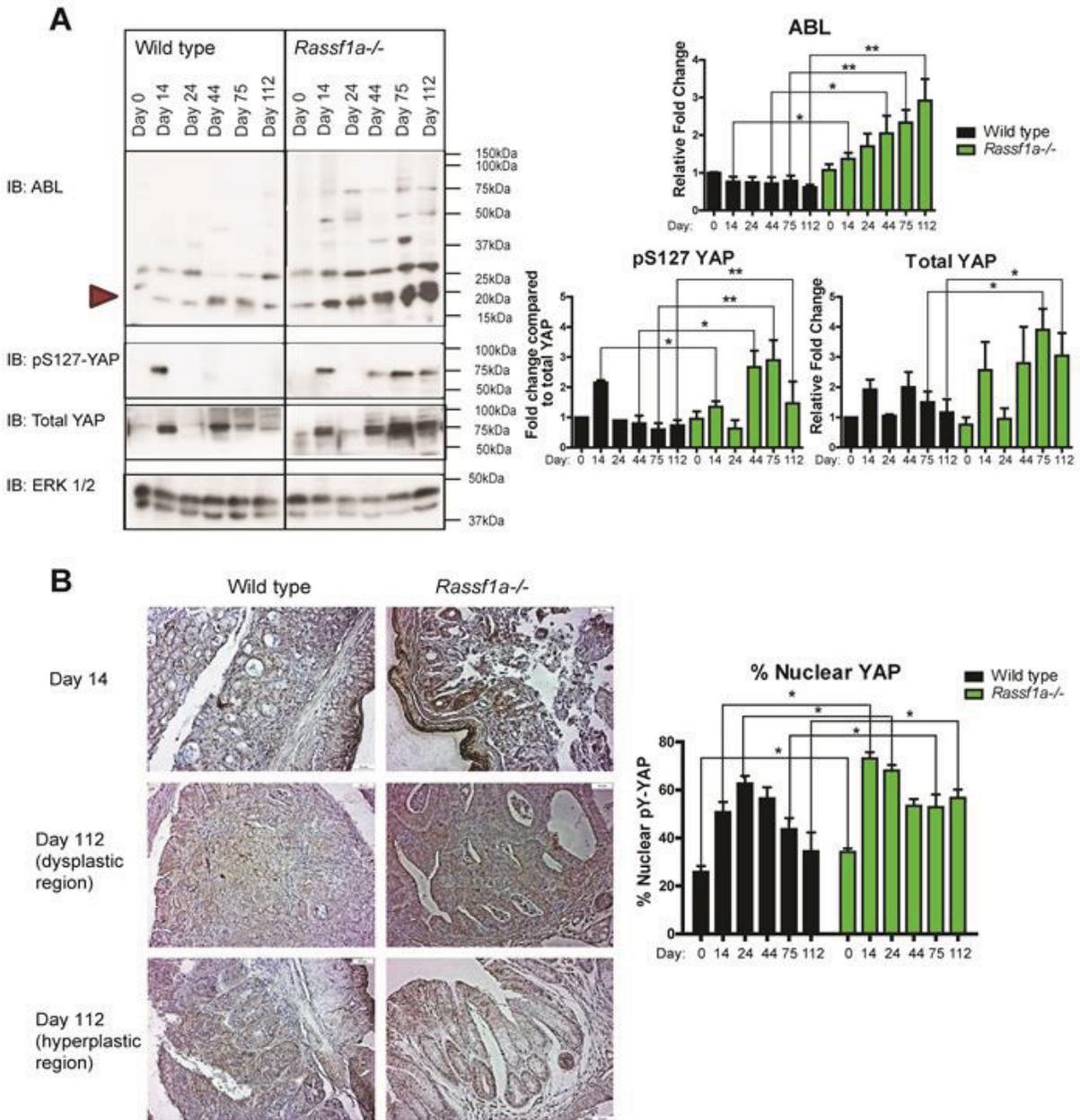
Figure 4.7 Loss of RASSF1A results in cleavage of c-Abl and accumulation of tyrosine phosphorylated YAP. (**A**) Analysis for ABL, pS127-YAP, and total YAP expression by immunoblot in colon lysates (experiment repeated four times with similar results). Right panel shows quantitations of left. For **ABL**: p-value>0.05 at Days 0 and 24, <0.02 at Days 14 and 44, <0.001 at Days 75 and 112 for *Rassf1a-/-* vs WT. For **pS127-YAP**: p-value>0.05 at Days 0 and 24, <0.008 at Day 14, <0.02 at Day 44, <0.03 ay Day 75, and <0.01 at Day 112 for *Rassf1a-/-* vs WT. For **total YAP**: p-value>0.05 at Days 0, 14, 24, and 44, <0.04 at Day 75, and <0.03 at Day 112 for *Rassf1a-/-* vs WT. (**B**) IHC with an antibody specific to pY357-YAP was carried out on mouse colonic sections as indicated. Brown stain (DAB) indicates pY-YAP, blue hematoxylin counterstain. All images 20X. *Rassf1a-/-* mice show increased levels of pY-YAP in colonic epithelial cells, as well increased nuclear localization upon acute DSS insult. Neoplastic sections (Day 112) appear to show increased total levels of pY-YAP with cytoplasmic and nuclear staining. *Rassf1a-/-* mice show dramatically increased total and nuclear levels of pY-YAP upon DSS treatment compared to wild type animals. Percent nuclear pY-YAP staining was calculated by counting 4 groups of 1000 cells in 3-4 independent histological sections from each genotype and time point. Right panel is quantitation of left. p-value<0.06 at Day 0, <0.02 at Days 14 and 75, <0.03 at Days 24 and 44, and <0.01 at Day 112 for *Rassf1a-/-* vs WT. No significant male/female differences were seen for any data presented in this figure.

160
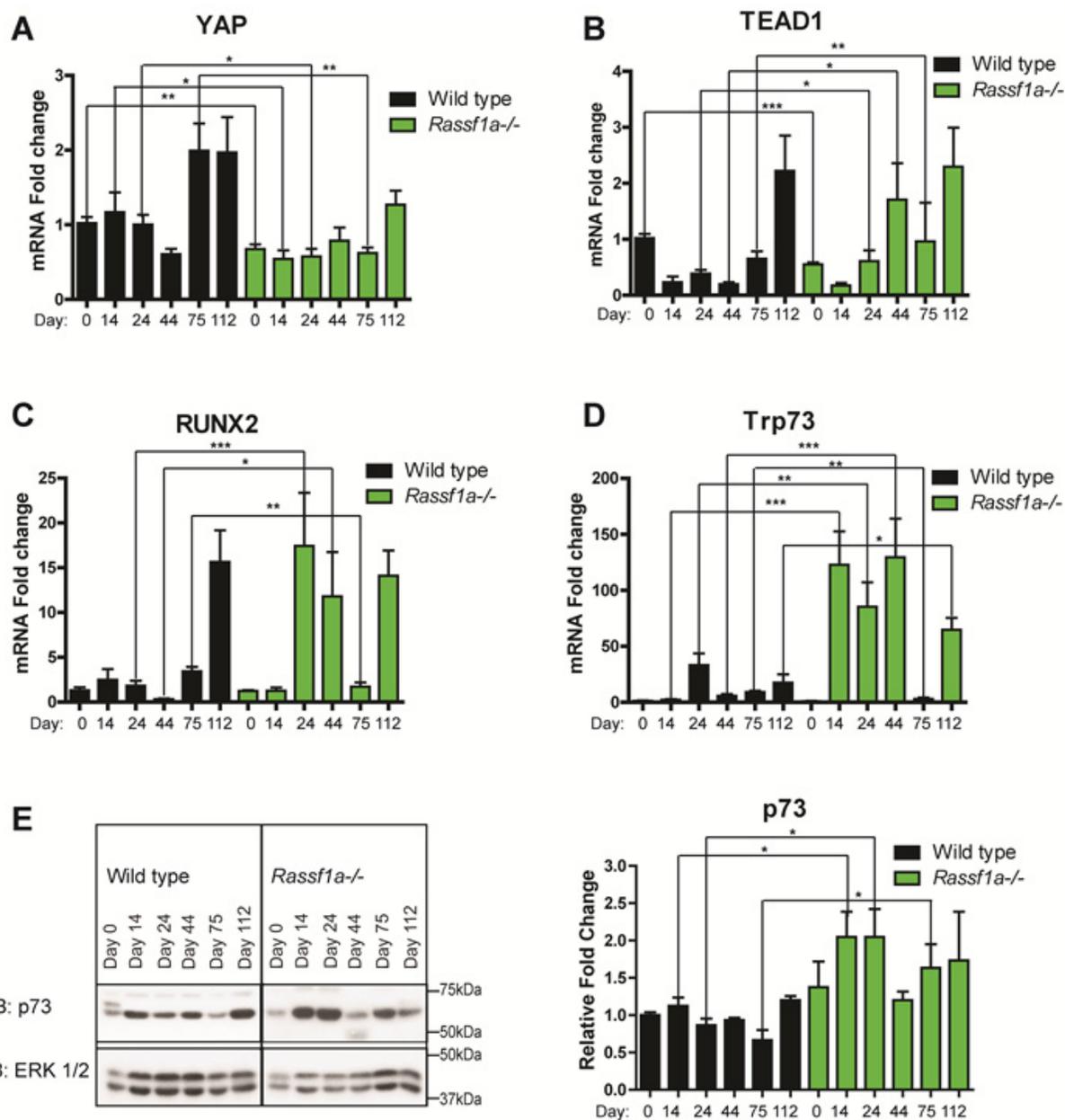
Figure 4.8 *Rassf1a-/-* mice show dysregulated YAP co-transcriptional binding partner switching during inflammation induced carcinogenesis. (**A**) YAP colonic mRNA expression analysis using q-PCR. p-value<0.004 at Days 0 and 14, <0.02 at Day 24, >0.05 at Days 44 and 112, and <0.001 at Day 75 for *Rassf1a-/-* vs WT. (**B**) TEAD1 colonic mRNA expression analysis using q-PCR. p-value<0.0001 at Day 0, >0.05 at Days 14 and 112, <0.05 at Day 24, <0.01 at Day 44, and <0.006 at Day 75 for *Rassf1a-/-* vs WT. (**C**) RUNX2 colonic mRNA expression analysis using q-PCR. p-value>0.05 at Days 0, 14, and 112, <0.0006 at Day 24, <0.01 at Day 44, and <0.006 at Day 75 for *Rassf1a-/-* vs WT. (**D**) Trp73 colonic mRNA expression analysis using q-PCR. p-value>0.05 at Day 0, <0.0001 at Days 14 and 44, <0.004 at Day 24, <0.005 at Day 75, and <0.01 at Day 112 for *Rassf1a-/-* vs WT. n=4-8 for **A-D** (**E**) Analysis for Trp73 expression by immunoblot in colon lysates (experiment repeated four times with similar results). Right panel shows quantitations of left. p-value>0.05 at Days 0, 44, 75, and 112, and <0.04 at Days 14 and 24, for *Rassf1a-/-* vs WT. No significant male/female differences were seen for any data presented in this figure.

4-3 Discussion and Future Directions

Under chronic inflammation conditions, approximately 70% of *Rassf1a*$^{-/-}$ mice survived, compared to 80% of wild type mice (Figure 4.1 A). Of note, nearly all of these deaths were in the male population, suggesting males are more susceptible to succumbing to DSS-induced colitis, which is consistent with previous reports [147,149,434]. Similar to what we have previously described in our acute model, *Rassf1a*$^{-/-}$ mice showed more body weight loss as well as significantly increased clinical symptoms (DAI Index) (Figure 4.1 B and C left panels). Interestingly, it was noted that there were significant male/female weight change differences within each group, males showed significantly more body weight loss than females, and *Rassf1a*$^{-/-}$ males showing significantly more body weight loss than wild type males. In terms of disease activity, again *Rassf1a*$^{-/-}$ males showed a significantly increased level of clinical symptoms compared to both *Rassf1a*$^{-/-}$ females as well as to wild type males, and while *Rassf1a*$^{-/-}$ females showed less severe disease activity than *Rassf1a*$^{-/-}$ males, they still showed significantly increased symptoms compared to wild type females (Figure 4.1 C right panel). Taken together, these findings confirm our previous observations that *Rassf1a*$^{-/-}$ mice are highly susceptible to DSS-induced colitis.

As *Rassf1a*$^{-/-}$ mice continued to show a higher DAI index, indicating disease symptom severity, throughout our experiment, this confirms our previous findings that *Rassf1a*$^{-/-}$ appear to be deficient in their ability to restrict inflammatory responses compared to wild type animals. In accordance with this conclusion, *Rassf1a*$^{-/-}$ mice appear to show sustained histological evidence of colonic inflammation compared to wild type mice throughout our chronic model. At Day 75, one month after the final inflammatory stimulus, wild type mice show reduced histological signs of inflammation, while *Rassf1a*$^{-/-}$ mice continue to show significantly increased signs of inflammation until the end of the experiment (Figure 4.2 A).

Rassf1a^{-/-} mice demonstrated evidence of intramucosal dysplasia as early as Day 44 (immediately after the last inflammatory stimulus cycle), at which time wild type mice show only occasional moderate dysplasia. As early as Day 44 and continuing to Day 112, *Rassf1a*^{-/-} mice show significantly increased dysplasia scores compared to wild type, with evidence of invasive carcinoma by Day 75, while wild type mice show only adenomatous dysplasia and intramucosal carcinoma, with none of the wild type mice examined showing evidence of tumor progression to an invasive state (Figure 4.2 B). In keeping with the observation that mice lacking RASSF1A are susceptible to a more severe degree of neoplastic development, several *Rassf1a*^{-/-} mice developed anal prolapses due to bowel thickening and tumor burden, while anal prolapses were not observed in our wild type mice. Because *Rassf1a*^{-/-} mice show sustained histological inflammation, this suggests the chronic inflammation is likely contributing to the tumor microenvironment and the accumulation of tumorigenic mutations. Future studies to examine whether loss of RASSF1A contributes an increase in metastases from the colon will be intriguing; the most common location for primary colon tumor metastasis is to the liver, therefore future studies will include an examination of liver samples isolated from our AOM/DSS treated *Rassf1a*^{-/-} mice for histological evidence of metastatic colon cancer.

Also in keeping with observations from our acute model and histological evidence, we have seen evidence that loss of RASSF1A results in hyperactivation of NFκB and dysregulation of inflammatory cytokines and chemokines. Bone marrow cells collected from mice throughout our experiment show significantly increased levels of NFκB activation and binding to NFκB oligos (Figure 4.3 F). Pro-inflammatory cytokine and chemokine levels were elevated and sustained in *Rassf1a*^{-/-} mice compared to wild type mice. Elevated and sustained levels of pro-inflammatory serum IL-6, IL-12, CXCL1, and MCP-1 are observed in *Rassf1a*^{-/-} mice compared to wild type mice following initial inflammatory stimulus and throughout the experiment (Figure 4.3 A-D). IL-6, already significantly higher in *Rassf1a*^{-/-} mice than wild type mice at baseline, shows a rapid induction in *Rassf1a*^{-/-} mice at Day 14 (following initial inflammatory stimulus), followed

163

by a tapering return to baseline levels, which continue to remain significantly higher than in the wild type mice (Figure 4.3 A). Active IL-12, also at high baseline levels in *Rassf1a*$^{-/-}$ mice compared to wild type, showed sustained elevated levels of IL-12 compared to wild type mice until the end of the experiment, further supporting an impaired restriction of pro-inflammatory signaling in *Rassf1a*$^{-/-}$ mice (Figure 4.3 B).

CXCL1 (aka KC/GRO) is a neutrophil attracting chemokine that has complex roles in promoting inflammatory responses and angiogenesis. Significantly increased CXCL1 levels have been implicated in both IBD as well as CRC, both in inflamed and neoplastic tissues [5,6]. CXCL1 levels in *Rassf1a*$^{-/-}$ mice are significantly elevated compared to wild type only at Days 14 and 44, following the first and third inflammatory stimuli (Figure 4.3 C), suggesting that CXCL1 likely plays a more important role in the inflammatory response than in tumorigenesis in this model. MCP-1, a chemokine which targets monocytes and dendritic cells to sites of inflammation, was significantly elevated compared to wild type mice at Day 14 following initial inflammatory insult, and remained significantly elevated until Day 75, at which point aggressive carcinoma has appeared in most *Rassf1a*$^{-/-}$ mice (Figure 4.3 D). Elevated MCP-1 levels in IBD patients have previously been shown to correlate with enhanced disease severity and MCP-1 expression has also been associated with increased incidence of a cancer phenotype [446-449]. In a similar manner, *Rassf1a*$^{-/-}$ show decreased levels of the anti-inflammatory cytokine IL-10, further suggesting an impairment of *Rassf1a*$^{-/-}$ mice in their ability to shut-down inflammatory signaling (Figure 4.3 E).

Interestingly, serum TGF-β appears be significantly decreased in both *Rassf1a*$^{-/-}$ and wild type mice following the initial inflammatory stimulus, and remains at relatively low levels until the end of the experiment. *Rassf1a*$^{-/-}$ mice show a significant increase in TGF-β levels at Day 24, after the second inflammatory stimulus, while showing significantly decreased levels compared to wild type at Day 75 (Figure 4.3 F). Both wild type and *Rassf1a*$^{-/-}$ mice TGF-β levels return to baseline levels by the end of the

experiment. TGF-β is a complex signaling protein, regulating cell growth and differentiation, inflammation and tissue homeostasis, and angiogenesis. How TGF-β affects signaling pathways is highly dependent on the cell environment [450-453]. IL-6 has been shown to decrease the apoptotic signaling ability of TGF-β [454,455], and it is possible that the high levels of IL-6 in *Rassf1a*^{-/-} mice contribute to the decreased levels of TGF-β until the end of the experiment. TGF-β has also been implicated in epithelial to mesenchymal transition (EMT) in cooperation with β-catenin/WNT signaling in the colon [70,451,456,457], warranting further examination into β-catenin transcriptional activation, as well as an examination of possible evidence of EMT which may be contributing to neoplastic development.

Although *Rassf1a*^{-/-} mice show overall increased earlier onset and increased severity of colonic dysplasia, wild type mice appear to be nearing similar levels of dysplasia near the end of the experiment. Likewise, the differences between body weight loss and disease activity (DAI) also appear to close in on each other near the end of the experiment. One possible explanation for this observance could be the loss of RASSF1A protein expression and function in these animals. Previous studies have suggested that sustained inflammation can induce hypermethylation of genes typically associated with cell death and classed as tumor suppressor such as APC and p53 [435-437]. Particularly, elevated levels of IL-6 have been implicated in initiating and sustaining hypermethylation of several genes by up-regulating DNMT1 activity [392,393,435]. At least one study has shown approximately 26% of ulcerative colitis patients exhibiting promoter hypermethylation at the RASSF1A locus [88] and we have seen similar levels in preliminary studies, enforcing the idea that inflammatory processes may initiate the loss of RASSF1A at an early time point.

Using RT-PCR, we examined the expression of *Rassf1a* mRNA in wild type mice over the course of our chronic inflammation driven carcinogenesis experiment. As early as following one cycle of 2% DSS for 5 days, wild-type mice showed significant loss of

Rassf1a mRNA expression compared to untreated mice. Loss of *Rassf1a* expression may be somewhat transient, as faint expression is regained at Day 44 (10 days recovery after three cycles of 2% DSS), however loss appears to be complete at the final two time points of the experiment (Figure 4.4 A). *Rassf1a* loss in wild type mice may explain why wild type mice appear to behave in a manner more similar to the *Rassf1a*$^{-/-}$ knockout mice as the experiment progresses over time, and demonstrates the importance of the RASSF1A protein in normal colonic function.

In order to study whether the loss of *Rassf1a* mRNA was due to hypermethylation, as is frequently seen in human colon cancers, the methylation status of 6 CpG loci in the first exon of *Rassf1a* was examined using bisulfite converson and pyrosequencing analysis. Of the 6 examined CpG loci, only the second CpG site showed any significant increase in methylation levels compared to baseline, with an approximately 5% increase in CpG methylation at this locus by the end of the experiment (Figure 4.4 C). In concordance with the RT-PCR mRNA results, methylation changes appear to be slightly transient, with an overall increase in methylation at CpG site 2 but a slight decrease at Day 44. However, while there are significant changes at CpG site 2, there were no global changes in methylation observed over the 6 examined CpG sites, with most of the other sites showing either little change or an overall decrease in the levels of methylation (Figure 4.4 B). A preliminary analysis examining 14 CpG islands in the promoter region of *Rassf1a* in our wild type mice shows a slight global increase at the *Rassf1a* promoter from about 2.5% at Day 0 to about 5% at Days 14, 44, and 112, suggesting that promoter methylation patterns may be more revealing than those seen in exon 1 (unpublished observations).

Real-time qPCR analysis of DNMT1 expression levels also showed no significant changes in wild type animals over the course of the experiment, although there is a slight increase in expression at the final time point (Figure 4.4 E). It is possible that other DNA methyltransferases are responsible for methylating the *Rassf1a* locus and

166

decreasing *Rassf1a* mRNA expression, or that DNMT activity occurs at a time point not captured in our model. Because of the low levels of methylation detected by pyrosequencing analysis, however, while *Rassf1a* methylation may contribute in part to inflammation driven loss of *Rassf1a* expression in mice, other methods of suppression, such as microRNA inhibition may be at play and will need to be explored. Indeed, RASSF1A has been shown to be down-regulated in response to miR602 microRNA expression [274,458], and at least one study has shown a two -fold increase in miR602 in response to inflammatory stimulus [459]. Further investigation of the role of microRNAs on RASSF1A regulation, particularly in an inflammatory setting, are needed.

As *Rassf1a*^{-/-} mice show increased and early onset neoplasia, it is not surprising that *Rassf1a*^{-/-} mice also show increased susceptibility to DNA damage, as evidenced by the appearance of phosphorylated histone 2A (γH2A.X), a marker of DNA double-strand breaks (Figure 4.5) [438,439]. Phosphorylation of H2A.X by ATM and ATM-Rad3-related (ATR) kinases occurs in a 1:1 ratio to double-strand breaks and serves to recruit DNA repair proteins such as Breast cancer 1, early onset (BRCA1) and Nibrin (NBS1). Increased DNA damage in *Rassf1a*^{-/-} mice may be a result of prolonged inflammation, and may contribute to the creation of a tumor microenvironment [460,461]. Once double-strand breaks have been repaired, H2A.X is de-phosphorylated by PP2A, making the presence of γH2A.X (the phosphorylated form of H2A.X) an excellent marker of DNA damage [439,462]. Not only are γH2A.X levels increased in *Rassf1a*^{-/-} mice upon inflammatory insult, but appear to remain elevated after removal of inflammatory stimuli and into the appearance of neoplastic tumorigenesis (Days 44 and 75).

The dramatic increase and prolonged levels of DNA damage in *Rassf1a*^{-/-} mice suggest impaired DNA damage response in these mice and highlight the role of RASSF1A in DNA damage control. Previous studies have identified a role for RASSF1A in DNA damage repair, and RASSF1A has been shown to be crucial in ATM directed DNA damage repair [240,328,463]. It is probable that *Rassf1a*^{-/-} mice are more susceptible

to initial DNA damage in an inflammatory setting, and that the additional loss of the ability of ATM to phosphorylate RASSF1A and induce cell cycle arrest and DNA repair causes accumulation of DNA damage in mice lacking RASSF1A. Thus, RASSF1A plays an important role in modulating the appearance of as well as the extent of DNA damage caused by inflammatory stimuli.

Oxidative damage has been previously shown to contribute to DNA damage and drive oncogenic mutations [82,440-442], and therefore it is not surprising that *Rassf1a*^{-/-} mice show increased susceptibility to oxidative damage compared to wild type animals (Figure 4.5 C). Similar to what was seen in our acute experiments, *Rassf1a*^{-/-} mice showed a dramatic increase in the levels of heme oxygenase-1 (HO-1) mRNA expression following an initial inflammatory stimulus (Figure 4.5 C, Day 14). HO-1 expression is induced in response to oxidative stress and correlated with increased levels of ROS [443-445]. HO-1 acts by scavenging oxidants created by the degradation of heme [464]. Wild type mice show a moderate response to oxidative stress, with a slight increase upon initial inflammatory stimulus (Day 14), and a resurgence upon tumorigenesis (Days 75 and 112) while *Rassf1a*^{-/-} mice show a substantial response upon initial inflammatory stimulus, which is relatively sustained until tumorigenesis, and a second increase once neoplastic changes are established (Day 112) (Figure 4.5 C). These results suggest that *Rassf1a*^{-/-} mice are defective in their ability to respond to oxidative stress, and that sustained oxidative damage may be contributing to the sustained DNA damage seen in these animals.

As seen in our acute model, *Rassf1a*^{-/-} mice show reduced proliferative ability post inflammatory stimulus, compared to wild type animals, suggesting a wound healing defect (Figure 4.5 D). Intriguingly, while *Rassf1a*^{-/-} mice continue to show less nuclear PCNA staining, suggesting reduced proliferative ability during inflammatory stages, they show a rapid increase in proliferation at Day 75, when tumorigenesis is fully underway. At Day 75, when *Rassf1a*^{-/-} mice show initial signs of invasive carcinoma (Figure 4.2)

they also show the highest levels of proliferative ability. As γH2A.X levels reach maximum accumulation during the inflammatory stage, it is likely that DNA mutations accumulated at this point may drive the increase in proliferative signaling and tumorigenesis.

In accordance with our acute model and with the appearance of high levels of DNA and oxidative damage, *Rassf1a*^{-/-} mice show increased levels of the apoptotic marker PARP (Figure 4.5 E and F). Interestingly, the increased levels of cleaved PARP are sustained throughout our entire chronic model, suggesting that despite tumorigenesis and increased tumor grade, *Rassf1a*^{-/-} mice still display dysregulated apoptotic signaling and increased cell death. BAX, a marker of mitochondrial directed apoptosis, shows a similar pattern to that of PARP, as does p53, a transcription factor responsible for driving pro-apoptotic signals (Figure 4.6). Wild type mice show an induction of BAX at Day 44 and 75, which is when tumorigenesis begins, suggesting that wild type mice are attempting to increase apoptotic signals as a counter to the proliferation of cancerous cells as a normal defense against the development of tumors (Figure 4.6 C and D). This may help to explain why wild type mice do not show significant tumor development until a later time point than *Rassf1a*^{-/-} mice.

Rassf1a^{-/-} mice show overall higher levels of p53, with particular accumulation at Days 75 and 112, at the appearance of invasive carcinoma (Figure 4.6 E and F). Normally, p53 forms homo-tetramer complexes in order to properly bind DNA and execute its transcriptional activity to promote apoptosis [465,466]. However, some mutations in p53 can disrupt the proper formation of these tetramers and create p53 aggregates, abrogating its ability to properly bind DNA and creating a loss-of-function phenotype despite increased total levels of protein [467-469]. In this case, increased levels of p53 may be used as a cancer biomarker and contribute to tumorigenesis [467,469]. Indeed, a recent study has shown that mice lacking both RASSF1A and p53 show higher levels of tumorigenesis [381]. It is possible that despite higher levels of p53

169

accumulation in *Rassf1a^-/-* mice that the excessive DNA and oxidative damage from the inflammatory phase may have caused a loss-of-function mutation, therefore it will be interesting to further investigate the sequence of p53 in our mice to see if mutations are arising in this model. Alternatively, p53 has also been shown to be activated in response to pro-inflammatory stimuli and oxidative damage, and may cross-talk with NFκB signaling [470-473]. Therefore, it may be that the loss of RASSF1A in our mice has created an additional feedback loop whereby dysregulated NFκB signaling may disrupt normal p53 signaling. The relationship between RASSF1A and p53 and how they may interact will be a promising starting point for future research, and likely represents a molecular link between inflammatory processes, apoptotic signaling, and progression to a cancer state.

TUNEL, a marker of DNA nicks and nuclear condensation caused by late-stage apoptosis, shows a slightly different pattern (Figure 4.6 A and B). While *Rassf1a^-/-* mice show an initial increase in TUNEL staining (and other apoptotic markers) at Day 14 following initial inflammatory stimulus, they then show a decrease in TUNEL levels until later time points, when invasive carcinoma is established. Wild type mice show an overall increase in TUNEL signaling until the very end of the experiment, with a peak at Days 44 and 75 in a similar pattern to that seen in BAX expression. This again suggests that wild type mice are mounting an increased apoptotic response in order to counteract proliferative signals. Interestingly, histological examination of TUNEL localization in later stages of the experiment reveal interesting expression pattern differences between genotypes. In the acute phase, both *Rassf1a^-/-* and wild type mice show increased TUNEL staining in areas of ulceration, with higher levels in *Rassf1a^-/-* mice primarily due to the increased frequency of ulcerative lesions and increased cellular damage. In later phases in wild type mice, TUNEL staining can be seen equally distributed through dysplastic tissue as well as the surrounding tissue and stroma. *Rassf1a^-/-* mice, however, show little TUNEL staining in dysplastic regions while the surrounding tissue and stroma show significantly higher levels (Figure 4.6 B). This suggests that the dysregulation of apoptotic signaling seen in the acute phase in *Rassf1a^-/-* mice

continues into tumorigenesis, and suggests an important role for stromal contributions to neoplastic development.

Recent research has begun to suggest that tissue irritation caused by chronic inflammation and associated cell death can stimulate stromal macrophages to release pro-proliferative signals that can cause inappropriate growth in the surrounding tissues [83,474]. Prolonged epithelial damage may also elicit a stromal wound-healing response which may inappropriately promote enhanced epithelial cell propagation [475]. Once a tumor has begun to rapidly grow and invade the surrounding area, cancer cells often secrete matrix metalloproteinases (MMPs) to degrade the surrounding mucosa and allow further invasion. The degradation of stromal mucosa paradoxically results in the further release of pro-growth factors, feeding back into further tumor development [476-478]. Because *Rassf1a*$^{-/-}$ mice are more susceptible to invasive carcinoma at a relatively early stage compared to wild type mice, it is likely that the increased apoptosis in ulcerated and stromal regions and the resultant release of pro-growth factors is a major driver of tumor growth in these mice.

In our acute study, we established that in response to DSS exposure and activation of pro-inflammatory signaling mice show increased cell death and DNA damage, as well as tyrosine phosphorylation of Yes-associated protein (YAP) by the activated tyrosine kinase ABL, promoting YAP association with p73 and transcription of apoptotic molecules such as BAX [3]. In the absence of RASSF1A this process becomes unrestricted and uncontrolled levels of cell death contribute to the development of severe inflammatory disease and failure to recover [3]. YAP is a complex signaling molecule that is most commonly associated with its ability to transcriptionally activate proliferation via Hippo signaling; therefore its role in promoting cell death was somewhat surprising. In reality, however, YAP acts as a co-transcriptional binding partner to a variety of transcription factors to form stable transcriptional complexes, and which protein YAP is bound to dramatically influences its transcriptional activity. The three

primary proteins that YAP tends to form transcriptional complexes with are TEAD, RUNX, and p73. YAP association and activation with TEAD proteins primarily drives pro-proliferative growth signaling, association with RUNX proteins primarily drives the differentiation of mesenchymal stem cells but can also drive proliferation, and association with p73 drives pro-apoptotic signaling [411,479,480]. YAP that has been phosphorylated at serine127 by LATS proteins binds to 14-3-3 complexes to become sequestered in the cytoplasm, thereby restricting transcriptional activity.

While we do not have a complete understanding of how YAP binding partner switching is controlled, previous research has indicated that inhibition of S127 phosphorylation of YAP allows YAP to translocate to the nucleus, where it primarily binds TEAD factors to induce proliferation. Phosphorylation of YAP by ABL or YES kinases at tyrosine 357 and serine phosphorylation at S381 by LATS has been shown to allow YAP to associate with p73. While it is commonly accepted that YAP primarily binds TEAD proteins, the mechanism regulating a switch from TEAD to RUNX directed transcription remains poorly understood, and it is unclear whether YAP-TEAD and YAP-RUNX complexes exist in discrete cellular circumstances or whether they may exist simultaneously. Activated RUNX promotes transcription of the E3 ubiquitin ligase Itch, which ubiquitinates p73 and targets it for destruction. Tyrosine phosphorylation of YAP at Y357 disrupts the YAP-RUNX complex, resulting in the reduction of Itch ligases and allowing the accumulation of p73 and the creation of YAP-p73 complexes [399,481].

As described in our acute study, increased levels of caspase activation have been shown to cleave the ABL tyrosine kinase into catalytically active subunits, the smallest of which is a 20 kDa fragment consisting solely of the catalytic subunit [405,406]. ABL kinase activity is primarily regulated by internal folding interactions caused by an interaction between its SH3 domain and internal linker sequence, which internalizes the kinase domain and causes functional inactivation. Caspase cleavage of ABL disrupts this interaction, therefore caspase cleaved fragments containing the kinase domain are

constitutively active [405,406]. Similar to our acute model, we see an increase in the appearance of cleaved ABL upon DSS stimulation and *Rassf1a*^{-/-} mice showed increased levels of cleaved ABL products compared to wild type animals (Figure 4.7 A and B). Interestingly, *Rassf1a*^{-/-} mice continued to accumulate higher levels of cleaved ABL throughout our experiment, both during the inflammatory phase as well as throughout tumorigenesis. This is likely due to the sustained high levels of DNA damage seen in these mice (Figure 4.5 A)

In addition to dysregulated levels of ABL kinase in *Rassf1a*^{-/-} mice, we also observed a not unexpected accumulation of YAP (Figure 4.7 A). Both wild type and *Rassf1a*^{-/-} mice show an increase in YAP levels following initial DSS insult (Day 14), which likely represents a response to initial DNA damage and initiation of the YAP/p73 apoptotic signaling described earlier. Of note is that another up-regulation of YAP levels occurs in all animals again at Day 44 at the time of tumor initiation, and elevated levels of YAP persist past this point in *Rassf1a*^{-/-} mice (Figure 4.7 A). Serine 127 YAP phosphorylation increases in both sets of animals at Day 14, although at a lower level in *Rassf1a*^{-/-} animals than in wild types as described previously (Figure 4.7 A). As S127 phosphorylation restricts YAP to the cytoplasm, this increase likely indicates an attempt to shut down YAP signaling, particularly as total YAP levels are concurrently rising. *Rassf1a*^{-/-} mice, but not wild type mice, also show an increase in pS127-YAP levels starting at Day 44, possibly as an attempt to restrict YAP directed proliferation as tumors progress.

Despite increased levels of pS127-YAP phosphorylation, we observed a significant increase in nuclear localized pY357-YAP in *Rassf1a*^{-/-} mice using immunohistologically stained tissue sections (Figure 4.7 C and D). Wild type mice show an increase of pY357-YAP levels following inflammatory events as described previously [3], but appear to be capable of shutting down this signaling cascade after DSS insults are removed. *Rassf1a*^{-/-} mice continue to show elevated levels of nuclear pY357-YAP

throughout the experiment, further confirming that these mice appear to be deficient in their ability to restrict pY357-YAP signaling. Interestingly, total levels of pY357-YAP were increased in *Rassf1a$^{-/-}$* mice in addition to the nuclear localization, with a noticeable cytoplasmic population in addition to the nuclear population at later time points (Figure 4.7 C). As serine 127 phosphorylation is also increased at these times, it appears that some of the tyrosine phosphorylated YAP may be sequestered in the cytoplasm, suggesting that the overall increase in pY-YAP levels allows the nuclear accumulation.

YAP is regulated by a series of phosphorylation events, with additional putative serine and threonine sites identified. However, the functions of these sites are not clearly understood, and it is likely that multiple phosphorylation events and an as yet unknown phosphorylation hierarchy more finely dictate YAP function (M. Sudol, work in progress). Indeed, at least two studies have found that phosphorylation at additional sites in addition to S127 can disrupt YAP cytoplasmic sequestering by 14-3-3 [482,483]. A further investigation of the YAP phosphorylation hierarchy is warranted and will likely reveal important novel regulations of YAP function. Additionally, it will be interesting to examine whether other PTKs are capable of tyrosine phosphorylating YAP and contributing to the increased nuclear localization of pY-YAP that we see in our model. YAP has previously been shown to be tyrosine phosphorylated by YES in addition to ABL, and we have identified 9 other PTKs that are significantly (p-value <0.05) up-regulated in the absence of RASSF1A at least two fold from a microarray screen comparing mRNA from colonic tissue in wild type and *Rassf1a$^{-/-}$* mice from our acute studies (Table 4.1).

Because YAP phosphorylation, while important, clearly needs further study, we also looked at the mRNA expression status of the key binding partners of YAP. Wild type mice showed varying levels of YAP mRNA expression throughout the experiment, with an approximately two-fold increase near the end of the experiment. In contrast with

this, YAP mRNA levels in *Rassf1a*^{-/-} mice remained mostly constant, with an elevation in total YAP mRNA occurring only at the end of the experiment (Figure 4.8 A). As Western blotting revealed an increase in total levels of YAP in *Rassf1a*^{-/-} mice compared to wild type mice, this suggests that loss of RASSF1A may stabilize YAP protein levels in an inflammatory setting. YAP is typically subjected to ubiquitin independent degradation and degraded at a high rate in the absence of post-translation modifications [432,484,485]. YAP protein stabilization in the absence of RASSF1A may be due to the increased activity of ABL tyrosine phosphorylating YAP and allowing it to bind p73. Previous reports have shown that proteins normally regulated by ubiquitin independent degradation may escape this by binding to a "nanny" protein, such as NQO1. p73 is capable of binding to NQO1, and YAP-p73 binding may serve to protect YAP degradation as well [432,484-486].

In the case of YAP binding partners, we can see an excellent switch between pro-proliferative partners and pro-apoptotic partners (Figure 4.8 B-D). Both RUNX and TEAD proteins have been shown to be up-regulated in colon cancers [480,487-489]. After initial inflammatory stimulation (Day 14), transcription of TEAD1 is reduced while transcription of p73 is increased, in both wild type and *Rassf1a*^{-/-} animals. Throughout the duration of the rest of the experiment, wild type animals appear to show a continued reciprocal relationship between the up-regulation of TEAD1 mRNA and the down-regulation of p73, or vise versa. As may have been predicted in a cancer model, at the end of the experiment when most of the wild type animals show intramucosal carcinoma, p73 levels are decreasing and TEAD1 levels are significantly up.

Rassf1a^{-/-} mice show a disproportionately high level of p73 transcription throughout the experiment, which likely contributes to the continued elevation of apoptotic markers throughout (Figures 4.5 and 4.6). In a similar manner, wild type mice also show up-regulation of RUNX2 at time points when p73 expression is being down-regulated. It is interesting that in wild type animals both TEAD1 and RUNX2 show their

most prominent up-regulation at Day 112. RUNX2 has recently been shown to be capable of binding with other co-transcriptional elements, such as p53 and potentially estrogen receptor β, in order to promote proliferation [490]. RUNX2 is capable of binding to DNA bound p53 in order to repress p53 regulated pro-apoptotic signaling, and nuclear localization of RUNX2 has been shown to be pro-proliferative in colon cells [259,489-491]. It is therefore possible that TEAD and RUNX proteins may be being simultaneously induced and competing with each other to bind YAP and drive proliferation or TEAD may be binding YAP to drive proliferation while RUNX effects pro-proliferative signaling through another mechanism. Immunoprecipitation experiments will need to be used to confirm binding of p73, RUNX, and TEAD to YAP and to determine relative binding frequencies across tumor pathogenesis.

Of note is that *Rassf1a*^{-/-} mice appear to show complete dysregulation of normal expression patterns of all three examined transcription factors (Figure 4.8). Although there appear to be some relative shifts showing opposite increases and decreases between apoptotic and proliferative transcription factors, all three proteins have abnormally high mRNA expression throughout most of the experiment, compared to both baseline and wild type. Both p73 and RUNX2 show an abnormally low expression at Day 75, for an unknown reason. These abnormal expression patterns suggest that loss of RASSF1A may completely dysregulate all YAP directed transcription. Of particular interest is the fact that despite *Rassf1a*^{-/-} mice showing up to several hundred times increased p73 mRNA expression, the protein levels show only a maximally two-fold increase at Day 14. It is possible that additional unknown microRNA mechanisms are regulating the destruction of extraneous p73 transcripts, and that this programming may be enhanced in the absence of RASSF1A. Further elucidation of how RASSF1A may mediate microRNA functions would be an interesting future study. Due to the overall dysregulation and up-regulation of all three examined YAP binding partners, future immunoprecipitation experiments and examination of transcriptional targets are crucial to completely understanding how RASSF1A may regulate YAP transcriptional programs.

Overall, we have shown an important role for RASSF1A in maintaining normal intestinal function and restricting inflammation induced injury. We have shown a mechanistic understanding of several ways in which RASSF1A restricts the inflammatory response and in doing so also restricts the accumulation of DNA damage. Loss of RASSF1A not only aggravates symptoms of inflammatory disease, but also results in increased oxidative damage and accumulation of DNA damage leading to excessive cell death. We propose that this in turn creates further inflammation and creates a feedback loop in the absence of RASSF1A which likely leads to rapid accumulation of mutations and general genomic instability. Therefore, loss of RASSF1A results in appearance of inflammation-related colon cancer at an earlier time than normal, and also results in a rapid progression to a higher grade carcinoma.

We have shown evidence that general dysregulation of apoptotic and proliferative signaling occurs in the absence of RASSF1A, likely due in large part to a general up-regulation of the co-transcriptional activator YAP. In early inflammatory stages YAP appears to drive pro-apoptotic functions, however, preliminary evidence suggests that as DNA damage accrues, YAP may switch from a pro-apoptotic to a pro-proliferative signaling program. Additionally, while loss of RASSF1A results in general up-regulation of apoptosis even while tissues become dysplastic, we have shown that this apoptotic signaling may be primarily in the tissue mesenchyme, and that continued stromal apoptosis may be driving epithelial proliferation.

Finally, we have begun to examine other cancer signaling pathways, such as the WNT pathway, which may also be regulated by RASSF1A, although the context specific mechanisms remain unknown at this point (see Appendix A4). Previous reports have indicated that mice lacking *Rassf1a* show overall genomic instability [291,293,386,492]. Future studies examining whether loss of RASSF1A contributes to the accumulation of common mutations found in colon cancer, such as mutations in p53, K-ras, and APC,

will give further insight into whether the restrictive function of RASSF1A in inflammation contributes to the overall ability to maintain genomic stability.

Table 4.1: Candidate Tyrosine Kinases for pY-YAP

Table 4.1.1: PTKs known to tyrosine phosphorylate YAP

Protein Symbol	Protein Name	Primary Function(s) (from GeneCards) [556]	Selected Reference Citing Interaction
YES1	Yamaguchi sarcoma viral oncogene homolog 1	Non-receptor protein tyrosine kinase that is involved in the regulation of cell growth and survival, apoptosis, cell-cell adhesion, cytoskeleton remodeling, and differentiation.	Tamm et al. [401]
ABL1	Abelson tyrosine-protein kinase 1	Non-receptor tyrosine-protein kinase that plays a role in many key processes linked to cell growth and survival, DNA damage response and apoptosis.	Levy et al. [364].

Table 4.1.2: PTKs Identified from Genome Wide Microarray Screen comparing DSS treated *Rassf1a-/- mice* to WT mice (acute treatment)

Protein Symbol	Protein Name	Fold Change	p-value	Primary Function(s) (from GeneCards)
TNK2	Tyrosine kinase, non-receptor, 2	7.39 up	0.02083	Non-receptor tyrosine and serine/threonine-protein kinase that is implicated in cell spreading and migration, cell survival, cell growth and proliferation.
TIE1	Tyrosine kinase with immunoglobulin-like and EGF-like domains 1	4.55 up	0.01894	Transmembrane tyrosine-protein kinase that may modulate TEK/TIE2 activity and contribute to the regulation of angiogenesis
JAK3	Janus kinase 3	4.19 up	0.00201	A member of the Janus kinase family of tyrosine kinases involved in cytokine receptor-mediated intracellular signal transduction.
MAP2K3	Mitogen-activated protein kinase kinase 3	4.12 up	0.01587	Dual specificity kinase. Is activated by cytokines and environmental stress in vivo. Catalyzes the concomitant phosphorylation of a threonine and a tyrosine residue in the MAP kinase p38
STYK1	Serine/threonine/tyrosine kinase 1	3.07 up	0.00658	Probable tyrosine protein-kinase, which has strong transforming capabilities on a variety of cell lines. When overexpressed, it can also induce tumor cell invasion as well as metastasis in distant organs.
DSTYK	Dual serine/threonine and tyrosine protein kinase	2.97 up	0.02018	May induce both caspase-dependent apoptosis and caspase-independent cell death
APPL1	Adaptor protein, phosphotyrosine interaction, PH domain and leucine zipper containing 1	2.76 up	0.00587	Required for the regulation of cell proliferation in response to extracellular signals from an early endosomal compartment.
MERTK	c-mer proto-oncogene tyrosine kinase	2.33 up	0.03044	Receptor tyrosine kinase that transduces signals from the extracellular matrix into the cytoplasm
FLT3	FMS-like tyrosine kinase 3	2.17 up	0.03024	Encodes a class III receptor tyrosine kinase that regulates hematopoiesis.

Chapter Five: Translational Application of Tyrosine Phosphorylated YAP as a Human Biomarker in IBD and CRC

5-1 Introduction

Animal model systems and *in vitro* models provide necessary and useful platforms for our understanding of the biochemical and molecular mechanisms underlying many cellular functions and how dysfunction of these may lead to disease. However, while model systems enhance our understanding of complex signaling pathways, we would ultimately like to confirm the relevance of our findings in humans, and find useful ways to translate our expanded knowledge by improving disease diagnosis or prognosis by developing new biomarker assays and targeted therapeutics. *In vitro* studies are often performed using over- or under-expression models that may not be physiologically likely to occur in physiological systems, and conflicting *in vitro* studies highlight that experimental technique and user error may greatly bias some studies. As species specific differences in gene expression, immunologic response, and general physiologies may also cause findings in an animal model system to be untrue in humans, it is important to validate findings in a human system whenever possible. Once experimental results have been validated in a human model, we are better positioned to apply the findings of basic research into new diagnostic and therapeutic techniques.

By design, a good diagnostic test is both sensitive and specific [493,494]. Specificity refers to the ability of a diagnostic test to give accurate positive results: a highly specific test will have no false positives outside of the desired parameters. Sensitivity refers to the ability of a test to identify accurately all possible individuals affected: a highly sensitive test will have no false negatives [493,494]. For example, a test developed specifically and sensitively for prostate cancer should give no false positives and should also not identify other cancer types as positive results, and should also not give any

false negatives. For ideal use in medical fields, a test should be as sensitive and specific as possible.

In our acute model of IBD, mice showed between approximately 60-70% nuclear localization of pY357-YAP, and our chronic model showed up to 60-80% nuclear localization throughout inflammation and continued into carcinogenesis. As we have seen evidence of up-regulation of tyrosine phosphorylated YAP in our mouse model in mice showing symptoms of colitis, we wished to further test our findings in human IBD patients in order to validate our findings and assess their usefulness as a potential diagnostic indicator of IBD.

5-2 Results

5-2.1 Colonic biopsies from inflammatory bowel disease patients, tubular adenoma patients, and colon cancer patients show increased levels of the nuclear tyrosine phosphorylated YAP biomarker

We have begun piloting the use of tyrosine phosphorylated YAP (pY357-YAP) as a biomarker on mouse and human colonic sections as a pilot, with promising results. Biopsy samples of inflamed regions were collected from patients identified at the University of Alberta Hospital as having IBD. Nuclear pY357-YAP appears to be significantly increased in colonic biopsy samples from ulcerative colitis (UC) and Crohn's disease (CD) patients compared to normal control samples (Figure 5.1). IBD patients show consistently high levels of nuclear pY357-YAP (approximately 55-65%), while tissue sections from normal healthy individuals showed less than 20% of cells positive for nuclear pY-YAP. Interestingly, biopsies from CD patients with small bowel inflammation show even higher levels of nuclear YAP proportions, with approximately 70-80% of cells staining positive for pY357-YAP. As CD patients are more prone to small bowel cancer than the general population [77,81], it will be interesting to examine the pY357-YAP status in small bowel cancer samples in addition to CRC in future studies.

In order to determine whether aberrant nuclear localization of pY357-YAP persisted into dysplasia, we also obtained biopsy samples from several patients exhibiting tubular adenoma (early stage dysplasia) as well as tumor samples from patients diagnosed with colon carcinomas. Patients with colonic dysplasia showed between 70-90% positive staining, similar to the results we have seen in our mouse model. Also similar to our mouse model, dysplasia patients also show overall levels of

pY357-YAP, with increased cytoplasmic staining as well as nuclear staining, although the significance of this is as yet unknown.

A

Normal Control

Ulcerative colitis

Crohn's disease

Tubular adenoma/polyps

Colorectal cancer tumor

% Nuclear pY-YAP
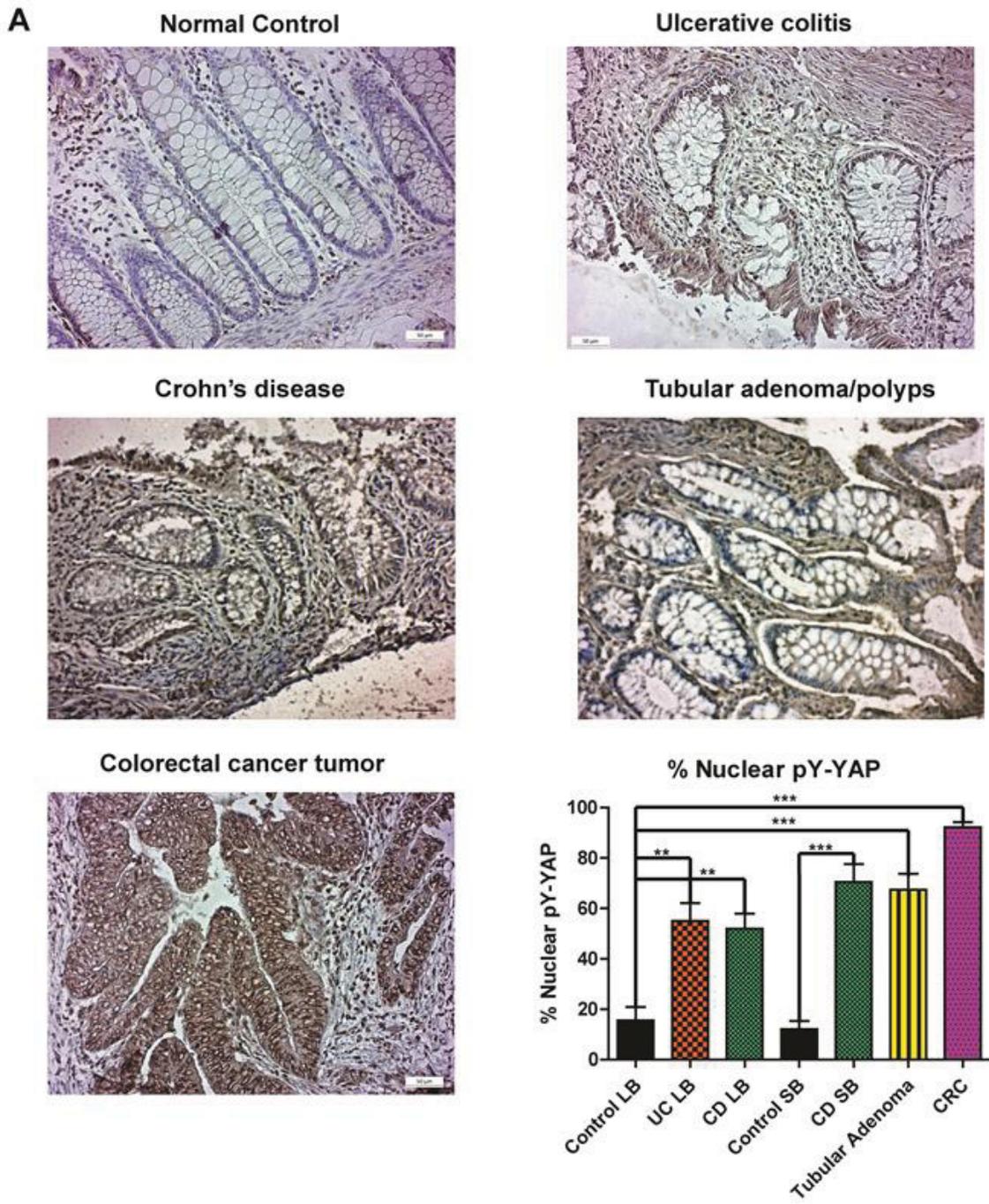
Figure 5.1. Colonic biopsies from IBD patients and CRC patients show elevated levels of the pY357-YAP biomarker. (A) Represen-
tative sections from colonic biopsies from normal, ulcerative colitis (UC), and Crohn's disease (CD) patients. IBD patients appear to show
increased total and nuclear levels of pY357-YAP compared to healthy controls. Brown stain(DAB) indicates pY-YAP. All images 20X. Cells
were scored for the number of nuclear pY-YAP positive cells per crypt from the pY-YAP IHC. p-value<0.003 for UC vs large bowel control,
p-value<0.002 for large bowel CD vs large bowel control, p-value<0.0003 for small bowel CD vs small bowel control, p-value<0.0004 for
tubular adenoma vs large bowel control, and p-value<0.0001 for CRC vs large bowel control. No significant difference between UC and
CD patients (p-value=0.7468). Percent nuclear pY-YAP staining was calculated by counting 4 groups of 1000 cells from 5-10 independent
patient histological sections from each group. LB=large bowel, SB=small bowel

5-3   Discussion and Future Directions

In concurrence with our observations in mice, we have shown that IBD and colon cancer patients show consistently elevated levels of pY357-YAP. As we have seen in our mouse studies that elevated levels of pY357-YAP are consistent with increased levels of pro-apoptotic signals and cell death, it is likely that dysregulated apoptotic signaling and excessive cell death is contributing to the disease pathogenesis in IBD patients. Our mouse model illustrated that pY357-YAP directed apoptosis is further dysregulated and unrestricted in mice lacking RASSF1A, therefore it may be useful to couple *RASSF1A* status with pY357-YAP immunostaining in human subjects. Our current study focused on obtaining biopsies from regions showing gross macroscopic inflammation, and further studies should be undertaken to determine whether adjacent tissue shows a similar up-regulation in pY357-YAP status in order to better determine the test specificity. Additionally, future studies should also examine biopsies of patients in symptomatic and macroscopic remission in order to determine whether tyrosine phosphorylation of YAP is transiently associated with active inflammation or whether levels remain high in IBD patients throughout remission.

The finding that colon cancer patients also exhibit extremely high levels of pY357-YAP compared to normal patients (approximately 75% higher) suggests a specific molecular link, highlighting the importance of YAP signaling in both diseases. Indeed, high levels of total nuclear YAP have previously been identified in colon cancers [353,416,487], and while it has been thought that nuclear YAP represented oncogenic YAP that directed proliferative signaling, future studies will need to examine the phosphorylation status of YAP in order to better understand its role in human colon cancers. As CD patients with small bowel disease are more prone to small bowel cancer than the general population [77,81] and also showed higher levels of pY357-YAP compared to CD patients with colonic disease, it will be interesting to examine the pY357-YAP status in small bowel cancer samples in addition to CRC in future studies.

As we have seen up-regulation of pY357-YAP in response to dysregulated inflammatory signaling, future studies will also have to determine whether the pY357-YAP biomarker is up-regulated only in IBD, or whether other inflammatory diseases are also similarly affected. We are currently looking to examine the pY357-YAP status in primary sclerosing cholangitis (PSC) and cholangiocarcinoma patients. Results from PSC patient will be of particular interest, as 5-25% of UC patients develop PSC at some point after developing UC, and patients with UC-PSC are at 4 fold increased risk of developing colon cancers compared to UC patients [495-497]. Because the percentage of positive pY-YAP staining increases from IBD to tubular adenoma to carcinoma, if future studies show a similar increased in pY-YAP staining in PSC and cholangiocarcinoma patients as we have described in IBD and CRC patients, the pY-YAP biomarker may indicate a tendency toward inflammation-induced cancer development. Likewise, if new biopsies can be obtained from the same patients already examined to see how their pY-YAP status has changed since our last collection, we may have a better idea of the stability of the pY-YAP biomarker and how useful this may be in diagnosis/prognosis. Additionally, results from PSC/cholangiocarcinoma patients may help us understand whether RASSF1A plays direct roles in restricting both inflammatory and carcinogenic signaling, or whether RASSF1A's role in restricting carcinogenesis are more tightly linked to its role in restricting inflammatory signaling.

As we have observed an increase in tyrosine phosphorylated YAP as being associated with excessive cell death and increased disease severity, pY357-YAP may also provide a novel target for future therapeutics. If the kinase(s) contributing to YAP phosphorylation can be fully confirmed, tyrosine kinase inhibitors may provide a new useful therapeutic strategy for patients showing high levels of pY357-YAP. At least one report has suggested that imatinib, a tyrosine kinase inhibitor targeted against ABL, with lower inhibition against other Src kinases, may have contributed to the resolution of IBD symptoms in one patient following failure to respond to other medications [428]. Imatinib is also used in the treatment of some CRC cases, with varying success, suggesting that

in some instances use of a PTK inhibitor during inflammatory disease may reduce the likelihood of IBD progressing to CRC.

We have begun piloting the use of tyrosine kinase inhibitors in our mouse models with varying success. Imatinib showed some ablation of symptoms in *Rassf1a*$^{+/-}$ but not *Rassf1a*$^{-/-}$ mice, suggesting that patient genetic profiling might be necessary in order to tailor future therapeutics [3]. Additionally, while imatinib lowered the presence of nuclear pY357-YAP, it did not completely reverse its appearance, suggesting that other tyrosine kinases may also be contributing to YAP phosphorylation. Tyrosine kinase inhibitors are also tricky to use as therapies, due to the large number of processes governed by a relatively few tyrosine kinases. It is therefore likely that combination therapeutics will likely prove to have the greatest effect. Because of the potential for tyrosine kinase inhibitors to interfere with other cellular signaling pathways, we would recommend that if tyrosine kinase inhibitors were considered as a future therapeutic option for IBD patients that presence of high levels of pY357-YAP be confirmed histologically. Use of pY357-YAP immunostaining may therefore be useful as both a disease biomarker as well as indicative of potential therapy choice.

Chapter Six: Final Summary

We have characterized an important role for the tumor-suppressor protein RASSF1A in regulating intestinal inflammation and in regulating the progression from an inflammatory state to a state of inflammation-driven colon cancer. As we have identified that RASSF1A is important for restricting pro-inflammatory signaling, it appears that loss of RASSF1A creates a feedback loop: increased inflammatory signaling leads to increased DNA damage and increased oxidative damage, increased oxidative damage likely contributes to further DNA damage, and increased DNA damage causes increased tyrosine phosphorylation of YAP, which in turn leads to increased levels of cell death, and finally appears to initiate a further inflammatory response. As this dysregulated feedback loop progress, DNA damage accumulates, likely leading to mutagenesis and genomic instability (Figure 6.1). Therefore, loss of RASSF1A results in appearance of inflammation-related colon cancer at an earlier time than normal, and also results in a rapid progression to a higher grade carcinoma.

We have shown evidence that general dysregulation of apoptotic and proliferative signaling occurs in the absence of RASSF1A, likely due in large part to a general up-regulation of the co-transcriptional activator YAP. In early inflammatory stages YAP appears to drive pro-apoptotic functions, however, preliminary evidence suggests that as DNA damage accrues, YAP may switch from a pro-apoptotic to a pro-proliferative signaling program. Additionally, while loss of RASSF1A results in general up-regulation of apoptosis even while tissues become dysplastic, we have shown that this apoptotic signaling may be primarily in the tissue mesenchyme, and that continued stromal apoptosis may be driving epithelial proliferation. We have also shown that other cancer signaling pathways, such as the WNT pathway, may also be regulated by RASSF1A, although the context specific mechanisms remain unknown at this point.

Finally, we have shown that our research has a potential translational application in the usage of pY357-YAP as a biomarker of IBD and colon cancers. Patient samples show significant increases in pY357-YAP levels in IBD and CRC patients, but not in normal control samples. This also validates that molecular changes seen in our acute inflammation and chronic inflammation-driven carcinogenesis models likely hold true in human IBD and CRC. Our identification of dysregulated pY357-YAP, particularly in the absence of RASSF1A, as a key molecular link between inflammation and cancer make it a useful biomarker for IBD and also suggests that tyrosine kinase inhibitor therapies may be a useful novel therapeutic in IBD patients, and may possibly reduce the incidences of IBD related CRC, although further studies in our mouse models are needed.
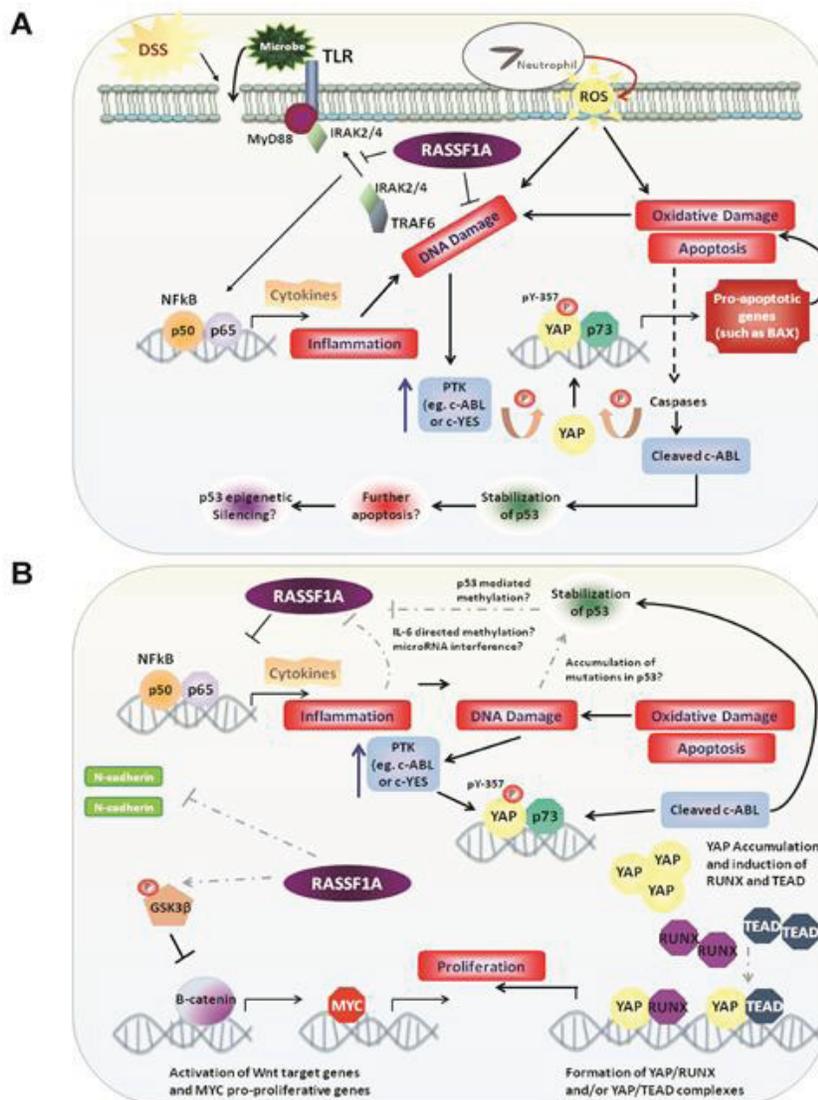
Figure 6.1 Summary model of RASSF1A influences on inflammation and cancer signaling. (A) RASSF1A restricts NFκB activity by interfering with the ability of membrane proximal TLR/MyD88/TRAF6/IRAK2/4 to promote downstream signaling to NFκB. This results in the interference of NFκB-dependent gene transcription and the activation of inflammatory pathways. Through regulating NFκB activity and early increases in DNA damage, RASSF1A indirectly regulates the activity (and possibly the expression) of a PTK to tyrosine phosphorylation YAP (possibly through c-ABL or c-YES). Increased PTK activity (in the absence of *Rassf1a*) drives tyrosine phosphorylation of YAP and increased pY-YAP/p73 transcriptional up-regulation of pro-apoptotic genes such as BAX. Sustained levels of apoptosis will result in the pro-apoptotic cleavage of constitutively active c-ABL to stabilize p53. Accumulated p53 can further promote cell death and further colonic injury and poor recovery following inflammation insults. In the absence of *Rassf1a*, increased levels of inflammation, oxidative damage, and apoptosis likely create a feedback loop which increases DNA damage levels and therefore results in increased PTK activity and increased levels of pY-YAP, further continuing the unrestricted cycle. **(B)** Prolonged and/or unrestricted inflammation leads to increased levels of oxidative and DNA damage, particularily in the absence of *Rassf1a*. This in turn leads to increased levels of pY-YAP and YAP accumulation, accumulation of RUNX and TEAD proteins, and likely the formation of pro-proliferative YAP/RUNX and/or YAP/TEAD complexes. Increased levels of proliferation in response to unrestricted inflammatory activation likely contributes to inflammation driven carcinogenesis. Additionally, chronic inflammation directs the down-regulation of Rassf1a mRNA expression, resulting in loss of RASSF1A protein. Although the exact mechanism for this down-regulation is as yet unknown, it is likely through either epigenetic methylation (possibly directed by increased levels of either IL-6 or p53), or possibly by microRNA interference (such as miR602). Finally, we have preliminary evidence that RASSF1A may indirectly influence the restriction of WNT pathway elements to further restrict inflammation directed pro-proliferative signaling, and that RASSF1A may also indirectly influence adherins junction proteins, with RASSF1A appearing to restrict excessive N-cadherin expression post inflammatory stimulus. Grey dashed arrows represent indirect or unknown mechanims for **A** and **B**.

190

References:

(1) Gordon M, and Baksh S. RASSF1A: Not a prototypical Ras effector. Small GTPases 2011;2(3):148-157.

(2) Gordon M, Mohamed El-Kalla, Baksh S. RASSF1 Polymorphisms in Cancer. Molecular Biology International 2012.

(3) Gordon M, El-Kalla M, Zhao Y, Fiteih Y, Law J, Volodko N, et al. The Tumor Suppressor Gene, RASSF1A, Is Essential for Protection against Inflammation -Induced Injury. PLoS One 2013 10/16;8(10):e75483-e75483.

(4) Dorland's Medical Dictionary. 2007; Available at: http://medical-dictionary.thefreedictionary.com/inflammation. Accessed June, 2014.

(5) Germano G, Allavena P, Mantovani A. Cytokines as a key component of cancer-related inflammation. Cytokine 2008 09;43(3):374-379.

(6) Lazennec G, Richmond A. Chemokines and chemokine receptors: new insights into cancer-related inflammation. Trends Mol Med 2010 03;16(3):133-144.

(7) Mantovani A. Molecular Pathways Linking Inflammation and Cancer. Curr Mol Med 2010 06;10(4):369-373.

(8) Mantovani A, Garlanda C, Allavena P. Molecular pathways and targets in cancer-related inflammation. Ann Med 2010 04;42(3):161-170.

(9) Wang S, Liu Z, Wang L, Zhang X. NF-kappaB signaling pathway, inflammation and colorectal cancer. Cell Mol Immunol 2009 10;6(5):327-334.

(10) Dolcet X, Llobet D, Pallares J, Matias-Guiu X. NF-kB in development and progression of human cancer. Virchows Arch 2005 05;446(5):475-482.

(11) Hoesel B, Schmid JA. The complexity of NF-κB signaling in inflammation and cancer. Molecular Cancer 2013 09;12(1):1-15.

(12) Wajant H, Scheurich P. TNFR1-induced activation of the classical NF-κB pathway. FEBS Journal 2011 04;278(6):862-876.

(13) Magalhaes JG, Lee J, Geddes K, Rubino S, Philpott DJ, Girardin SE. Essential role of Rip2 in the modulation of innate and adaptive immunity triggered by Nod1 and Nod2 ligands. Eur J Immunol 2011 05;41(5):1445-1455.

(14) O'Neill LAJ, Golenbock D, Bowie AG. The history of Toll-like receptors--redefining innate immunity. Nature Reviews Immunology 2013(6):453.

(15) Mantovani A, Allavena P, Sica A, Balkwill F. Cancer-related inflammation. Nature 2008 07/24;454(7203):436.

(16) Kayton ML. Cancer and pediatric inflammatory bowel disease. Semin Pediatr Surg 2007 08;16(3):205-213.

(17) Harpaz N, Polydorides AD. Colorectal dysplasia in chronic inflammatory bowel disease: pathology, clinical implications, and pathogenesis. Arch Pathol Lab Med 2010 06;134(6):876-895.

(18) Hurley JJ, Turner J, Berrill J, Swift G, Dolwani S, Green J. Surveillance for colorectal cancer in patients with inflammatory bowel disease. Br J Hosp Med (Lond) 2010 10;71(10):562-567.

(19) Brackmann S, Andersen SN, AamodtT G, Langmark F, Clausen OPF, Aadland E, et al. Relationship between clinical parameters and the colitis-colorectal cancer interval in a cohort of patients with colorectal cancer in inflammatory bowel disease. Scand J Gastroenterol 2009 01;44(1):46-55.

(20) Azer SA, Sturm A, Dignass AU. Overview of molecular pathways in inflammatory bowel disease associated with colorectal cancer development. Eur J Gastroenterol Hepatol 2008;25; 14(3; 3):271; 348-281; 353.

(21) Colotta F, Allavena P, Sica A, Garlanda C, Mantovani A. Cancer-related inflammation, the seventh hallmark of cancer: links to genetic instability. Carcinogenesis 2009 07;30(7):1073-1081.

(22) Rook GAW, Dalgleish A. Infection, immunoregulation, and cancer. Immunol Rev 2011 03;240(1):141-159.

(23) Sica A, Allavena P, Mantovani A. Cancer related inflammation: the macrophage connection. Cancer Lett 2008 08/28;267(2):204-215.

(24) Marcus SB, Strople JA, Neighbors K, Weissberg-Benchell J, Nelson SP, Limbers C, et al. Fatigue and Health-Related Quality of Life in Pediatric Inflammatory Bowel Disease. Clinical Gastroenterology and Hepatology 2009 05;7(5):554-561.

(25) Haapamäki J, Roine RP, Sintonen H, Turunen U, Färkkilä M,A., Arkkila PET. Health-related quality of life in inflammatory bowel disease measured with the generic 15D instrument. Qual Life Res 2010 08;19(6):919-928.

(26) Crohn's and Colitis Foundation of Canada. The burden of inflammatory bowel disease (IBD) in Canada [electronic resource] : final report and recommendations /

approved by the Board of Directors of the Crohn's and Colitis Foundation of Canada. : Toronto, Ont. : Crohn's and Colitis Foundation of Canada, 2008 (Saint-Lazare, Quebec : Gibson Library Connections, 2009); 2008.

(27) Fedorak RN, Wong K, Bridges R. Canadian Digestive Health Foundation Public Impact Series. Inflammatory bowel disease in Canada: Incidence, prevalence, and direct and indirect economic impact. Can J Gastroenterol 2010;24(11):651-655.

(28) Sauer CG, Kugathasan S. Pediatric Inflammatory Bowel Disease: Highlighting Pediatric Differences in IBD. Gastroenterol Clin North Am 2009 12;38(4):611-628.

(29) Greenstein A, J., Janowitz H, D., Sachar D, B. The extra-intestinal complications of Crohn's disease and ulcerative colitis: a study of 700 patients. Medicine 1976 09;55(5):401-412.

(30) Gyde SN, Prior P, Macartney JC, Thompson H, Waterhouse JA, Allan RN, et al. Malignancy in Crohn's disease. Gut 2001 12;21; 49(12; 6):1024; 777-782.

(31) Louis E, Collard A, Oger AF, Degroote E, El Yafi F, Belaiche J. Behaviour of Crohn's disease according to the Vienna classification: changing pattern over the course of the disease. Gut 2001;49(6):777-782.

(32) Hanauer SB. Inflammatory bowel disease: Epidemiology, pathogenesis, and therapeutic opportunities. Inflamm Bowel Dis 2006;12:S3-S9.

(33) Morrison G, Headon B, Gibson P. Update in inflammatory bowel disease. Aust Fam Physician 2009 12;38(12):956-961.

(34) Sartor RB. Mechanisms of disease: pathogenesis of Crohn's disease and ulcerative colitis. Nat Clin Pract Gastroenterol Hepatol 2006 07;3(7):390-407.

(35) Shih DQ, Targan SR. Insights into IBD Pathogenesis. Curr Gastroenterol Rep 2009 12;11(6):473-480.

(36) Xavier RJ, Podolsky DK, Cosnes J, Gower-Rousseau C, Seksik P, Cortot A, et al. Unravelling the pathogenesis of inflammatory bowel disease. Nature 2011;140; 17(7152; 6; 7):427; 1785; 1564-U118; 1572.

(37) Braus NA, Elliott DE. Advances in the pathogenesis and treatment of IBD. Clinical Immunology 2009 07;132(1):1-9.

(38) Satsangi J, Silverberg MS, Vermeire S, Colombel J-. The Montreal classification of inflammatory bowel disease: controversies, consensus, and implications. Gut 2006(6):749.

(39) Vermeire S, Van Assche G, Rutgeerts P. Classification of inflammatory bowel disease: the old and the new. Curr Opin Gastroenterol 2012 07;28(4):321-326.

(40) Veloso FT, Carvalho J, Magro F. Immune-related systemic manifestations of inflammatory bowel disease. A prospective study of 792 patients. J Clin Gastroenterol 1996 07;23(1):29-34.

(41) Hildebrand H, Karlberg J, Kristiansson B. Longitudinal growth in children and adolescents with inflammatory bowel disease. J Pediatr Gastroenterol Nutr 1994 02;18(2):165-173.

(42) Pfefferkorn M, Burke G, Griffiths A, Markowitz J, Rosh J, Mack D, et al. Growth abnormalities persist in newly diagnosed children with crohn disease despite current treatment paradigms. J Pediatr Gastroenterol Nutr 2009 02;48(2):168-174.

(43) Thrash B, Patel M, Shah KR, Boland CR, Menter A. Cutaneous manifestations of gastrointestinal disease: Part II. J Am Acad Dermatol 2013 02;68(2):211.e1-211.e33.

(44) Danese S, Semeraro S, Papa A, Roberto I, Scaldaferri F, Fedeli G, et al. Extraintestinal manifestations in inflammatory bowel disease. World Journal of Gastroenterology 2005;11(46):7227-7236.

(45) Bernstein CN, Wajda A, Svenson LW, MacKenzie A, Koehoorn M, Jackson M, et al. The Epidemiology of Inflammatory Bowel Disease in Canada: A Population-Based Study. Am J Gastroenterol 2006 07;101(7):1559-1568.

(46) Loftus,Edward V.,,Jr. Clinical epidemiology of inflammatory bowel disease: Incidence, prevalence, and environmental influences. Gastroenterology 2004 05;126(6):1504-1517.

(47) Peyrin-Biroulet L. What is the patient's perspective: How important are patient-reported outcomes, quality of life and disability? Dig Dis 2010;28(3):463-471.

(48) Ardizzone S, Cassinotti A, Manes G, Porro GB. Immunomodulators for all patients with inflammatory bowel disease? Therap Adv Gastroenterol 2010 01;3(1):31-42.

(49) Engel MA, Neurath MF. New pathophysiological insights and modern treatment of IBD. J Gastroenterol 2010 06;45(6):571-583.

(50) Guidi L, Marzo M, Felice C, Mocci G, Sparano L, Pugliese D, et al. New biological agents for the treatment of the "high risk" IBD patients. Eur Rev Med Pharmacol Sci 2010;14(4):342-346.

(51) Nell S, Suerbaum S, Josenhans C. The impact of the microbiota on the pathogenesis of IBD: lessons from mouse infection models. Nat Rev Immunol 2010;8(8):564-577.

(52) Khor B, Gardet A, Xavier RJ. Genetics and pathogenesis of inflammatory bowel disease. Nature 2011 06/16;474(7351):307-317.

(53) Childers RE, Eluri S, Vazquez C, Weise RM, Bayless TM, Hutfless S. Family history of inflammatory bowel disease among patients with ulcerative colitis: A systematic review and meta-analysis. J Crohns Colitis 2014 06/26.

(54) Jostins L, Ripke S, Weersma RK, Duerr RH, McGovern DP, Hui KY, et al. Host-microbe interactions have shaped the genetic architecture of inflammatory bowel disease. Nature 2012 11/01;491(7422):119-124.

(55) Molodecky NA, Panaccione R, Ghosh S, Barkema HW, Kaplan GG. Challenges Associated with Identifying the Environmental Determinants of the Inflammatory Bowel Diseases. Inflamm Bowel Dis 2011;17(8):1792-1799.

(56) Molodecky NA, Kaplan GG. Environmental risk factors for inflammatory bowel disease. Gastroenterol Hepatol (N Y) 2010 05;6(5):339-346.

(57) Molodecky NA, Soon IS, Rabi DM, Ghali WA, Ferris M, Chernoff G, et al. Increasing Incidence and Prevalence of the Inflammatory Bowel Diseases With Time, Based on Systematic Review. Gastroenterology 2012;142(1):46-54.

(58) Hviid A, Svanström H, Frisch M. Antibiotic use and inflammatory bowel diseases in childhood. Gut 2011 01;60(1):49-54.

(59) Khalili H, Higuchi LM, Ananthakrishnan AN, Richter JM, Feskanich D, Fuchs CS, et al. Oral contraceptives, reproductive factors and risk of inflammatory bowel disease. Gut 2013(8):1153.

(60) Kaplan G. Air pollution and the inflammatory bowel diseases. Inflamm Bowel Dis 2011 05;17(5):1146-1148.

(61) Kish L. Airborne particulate matter and a western style diet as potential environmental factors in the pathogenesis of inflammatory bowel disease [electronic resource]. : 2012; 2012.

(62) Karlinger K, Györke T, Makö E, Mester A, Tarján Z. The epidemiology and the pathogenesis of inflammatory bowel disease. Eur J Radiol 2000 09;35(3):154-167.

(63) Round JL, Mazmanion SK. The gut microbiota shapes intestinal immune responses during health and disease. Nature Reviews Immunology 2009(5):313.

(64) Sekirov I, Russell SL, Antunes L, Finlay BB. Gut Microbiota in Health and Disease. Physiol Rev 2010;90(3):859-904.

(65) Comito D, Romano C. Dysbiosis in the Pathogenesis of Pediatric Inflammatory Bowel Diseases. INT J INFLAM 2012:1-7.

(66) Morgan XC, Tickle TL, Sokol H, Gevers D, Devaney KL, Ward DV, et al. Dysfunction of the intestinal microbiome in inflammatory bowel disease and treatment. Genome Biology (Online Edition) 2012.

(67) Rigottier-Gois L. Dysbiosis in inflammatory bowel diseases: the oxygen hypothesis. ISME Journal: Multidisciplinary Journal of Microbial Ecology 2013 07;7(7):1256-1261.

(68) Wu N, Yang X, Zhang R, Li J, Xiao X, Hu Y, et al. Dysbiosis Signature of Fecal Microbiota in Colorectal Cancer Patients. Microb Ecol 2013(2):462.

(69) Scheiman JM, Sturm A, Dignass AU. NSAIDs, gastrointestinal injury, and cytoprotection. Gastroenterol Clin North Am 2008 06;25; 14(2; 3):279; 348-298; 353.

(70) Sturm A, Dignass AU. Epithelial restitution and wound healing in inflammatory bowel disease. World J Gastroenterol 2008 01/21;14(3):348-353.

(71) Schulzke JD, Ploeger S, Amasheh M, Fromm A, Zeissig S, Troeger H, et al. Epithelial Tight Junctions in Intestinal Inflammation. Ann N Y Acad Sci 2008 05/15;1165; 25; 14(3; 3):294; 271; 348-300; 281; 353.

(72) Bradford EM, Turner ES, Turner JR, Salim SY, Soderholm JD. Understanding the Epithelial Barrier in Inflammatory Bowel Disease. Inflamm Bowel Dis 2011 01;17(1):75; 362-381.

(73) Salim SY, Soderholm JD. Importance of Disrupted Intestinal Barrier in Inflammatory Bowel Diseases. Inflamm Bowel Dis 2011;17(1):362-381.

(74) MacDonald TT, Bell I, Monteleone G. Cytokine Regulation of Gut Inflammation in IBD. Inflammatory Bowel Disease Monitor 2010 04;10(4):111-116.

(75) Atreya I, Atreya R, Neurath MF. NF-kappaB in inflammatory bowel disease. J Intern Med 2008 06;263(6):591-596.

(76) Fleming M, Ravula S, Tatishchev S, F., Wang H, L. Colorectal carcinoma: Pathologic aspects. J Gastrointest Oncol 2012 09;3(3):153-173.

(77) Mattar MC, Lough D, Pishvaian MJ, Charabaty A. Current management of inflammatory bowel disease and colorectal cancer. Gastrointest Cancer Res 2011 03;4(2):53-61.

(78) Canadian Cancer Society. Canadian Cancer Statistics 2013. 2013; Available at: http://www.cancer.ca/~/media/cancer.ca/CW/cancer%20information/cancer%20101/Can

adian%20cancer%20statistics/canadian-cancer-statistics-2013-EN.pdf. Accessed May, 2013.

(79) Miniño A,M. Death in the United States, 2011. NCHS Data Brief 2013 03(115):1-8.

(80) Statistics Canada. Available at: http://www.cancer.ca/Canada-wide/About%20cancer/~/media/CCS/Canada%20wide/Files%20List/English%20files%20heading/PDF%20-%20Policy%20-%20Canadian%20Cancer%20Statistics%20-%20English/Canadian%20Cancer%20Statistics%202011%20-%20English.ashx, June 2011.

(81) Triantafillidis JK, Nasioulas G, Kosmidis PA. Colorectal cancer and inflammatory bowel disease: epidemiology, risk factors, mechanisms of carcinogenesis and prevention strategies. Anticancer Res 2009 07;29(7):2727-2737.

(82) Priolli DG, Canelloi TP, Lopes CO, Valdívia J,C.M., Martinez NP, Açari D,P., et al. Oxidative DNA damage and ß-catenin expression in colorectal cancer evolution. Int J Colorectal Dis 2013 05;28(5):713-722.

(83) Rakoff-Nahoum S. Why Cancer and Inflammation? Yale J Biol Med 2007 20140406;79:3-4.

(84) Vogelstein B, Kinzler KW. Cancer genes and the pathways they control. Nat Med 2004(8):789.

(85) Bozic I, Antal T, Ohtsuki H, Carter H, Kim D, Chen S, et al. Accumulation of driver and passenger mutations during tumor progression. Proc Natl Acad Sci U S A 2010(43):18545.

(86) Molodecky NA, Kareemi H, Parab R, Barkema HW, Quan H, Myers RP, et al. Incidence of Primary Sclerosing Cholangitis: a Systematic Review and Meta-Analysis. Hepatology 2011;53(5):1590-1599.

(87) Ishihara S, Aziz MM, Yuki T, Kazumori H, Kinoshita Y. Inflammatory bowel disease: review from the aspect of genetics. J Gastroenterol 2009 11;44(11):1097-1108.

(88) Wahab A, El-mezayen H, Sharad H, Rahman SA. Promoter hypermethylation of RASSF1A, MGMT, and HIC-1 genes in benign and malignant colorectal tumors. Tumor Biol 2011;32(5):845-852.

(89) Fernandes MS, Carneiro F, Oliveira C, Seruca R. Colorectal cancer and RASSF family--a special emphasis on RASSF1A. Int J Cancer 2013 01/15;132(2):251-258.

(90) van Engeland M, Roemen GMJM, Brink M, Pachen MMM, Weijenberg MP, de Bruïne A,P., et al. K-ras mutations and RASSF1A promoter methylation in colorectal cancer. Oncogene 2002 05/23;21(23):3792-3795.

(91) Cao D, Chen Y, Tang Y, Peng X, Dong H, Li L, et al. Loss of RASSF1A expression in colorectal cancer and its association with K-ras status. Biomed Res Int 2013;2013:976765-976765.

(92) Gibbons DL, Spencer J. Mouse and human intestinal immunity: same ballpark, different players; different rules, same score. Mucosal Immunology (1933-0219) 2011 03;4(2):148-157.

(93) Mestas J, Hughes CCW. Of mice and not men: differences between mouse and human immunology. J Immunol 2004 03/01;172(5):2731-2738.

(94) Doeing DC, Borowicz JL, Crockett ET. Gender dimorphism in differential peripheral blood leukocyte counts in mice using cardiac, tail, foot, and saphenous vein puncture methods. BMC Clinical Pathology 2003 01;3:3-6.

(95) Ganz T, Ouellette AJ, Selsted ME, Risso A. Defensins: antimicrobial peptides of innate immunity. J Leukoc Biol 2000 09;3; 10; 68(9; 11; 6):710; 1280; 785-720; 1289; 792.

(96) Ouellette AJ, Selsted ME, Risso A. Paneth cell defensins: Endogenous peptide components of intestinal host defense. J Leukoc Biol 2000;10; 68(11; 6):1280; 785-1289; 792.

(97) Risso A. Leukocyte antimicrobial peptides: multifunctional effector molecules of innate immunity. J Leukoc Biol 2000;68(6):785-792.

(98) Heinz S, Haehnel V, Karaghiosoff M, Schwarzfischer L, Müller M, Krause SW, et al. Species-specific regulation of Toll-like receptor 3 genes in men and mice. J Biol Chem 2003 06/13;278(24):21502-21509.

(99) Rehli M. Research update: Of mice and men: species variations of Toll-like receptor expression. Trends Immunol 2002;23:375-378.

(100) Trevani AS, Chorny A, Salamone G, Vermeulen M, Gamberale R, Schettini J, et al. Bacterial DNA activates human neutrophils by a CpG-independent pathway. Eur J Immunol 2003;33(11):3164-3174.

(101) Barnaba V, Watts C, de Boer M, Lane P, Lanzavecchia A, Denton MD, et al. Professional presentation of antigen by activated human T cells. Eur J Immunol 1999 01;24; 190; 29(1; 4; 5):71; 555; 1543-75; 566; 1550.

(102) Choo JK, Seebach JD, Nickeleit V, Shimizu A, Lei H, Sachs DH, et al. Species differences in the expression of major histocompatibility complex class II antigens on coronary artery endothelium: implications for cell-mediated xenoreactivity. Transplantation 1997 11/15;64(9):1315-1322.

(103) Crocker PR, Jefferies WA, Clark SJ, Chung LP, Gordon S. Species heterogeneity in macrophage expression of the CD4 antigen. J Exp Med 1987 08/01;166(2):613-618.

(104) Denton MD, Geehan CS, Alexander SI, Sayegh MH, Briscoe DM, Taams LS, et al. Endothelial cells modify the costimulatory capacity of transmigrating leukocytes and promote CD28-mediated CD4(+) T cell alloactivation. J Exp Med 1999;190; 29(4; 5):555; 1543-566; 1550.

(105) Colucci F, Di Santo J,P., Leibson PJ. Natural killer cell activation in mice and men: different triggers for similar weapons? Nat Immunol 2002 09;3(9):807-813.

(106) Pober JS, Kluger MS, Schechner JS, Murphy L, Mazanet MM, Taylor AC, et al. Human endothelial cell presentation of antigen and the homing of memory/effector T cells to skin. Cell Immunol 2001;941; 194; 167(2; 8):12; 150; 4378-25; 161; 4385.

(107) Murphy L, Mazanet MM, Taylor AC, Mestas J, Hughes C, Mestas J, et al. Single-cell analysis of costimulation by B cells, endothelial cells, and fibroblasts demonstrates heterogeneity in responses of CD4(+) memory T cells. Cell Immunol 2001;194; 167(2; 8):150; 4378-161; 4385.

(108) Farrar JD, Smith JD, Murphy TL, Leung S, Stark GR, Murphy KM. Selective loss of type I interferon-induced STAT4 activation caused by a minisatellite insertion in mouse Stat2. Nat Immunol 2000 07;1(1):65.

(109) Pearce EJ, Sher A. Functional dichotomy in the CD4+ T cell response to Schistosoma mansoni. Exp Parasitol 1991 07;73(1):110-116.

(110) Pan J, Xia L, McEver RP. Comparison of promoters for the murine and human P-selectin genes suggests species-specific and conserved mechanisms for transcriptional regulation in endothelial cells. J Biol Chem 1998 04/17;273(16):10058-10067.

(111) Zlotnik A, Yoshie O. Chemokines: A new classification system and their role in immunity. Immunity 2000;12(2):121-127.

(112) Sollid LM, Johansen F. Animal Models of Inflammatory Bowel Disease at the Dawn of the New Genetics Era. PLoS Medicine 2008 09;5(9):e198.

(113) Jones-Hall Y, Grisham MB. Immunopathological characterization of selected mouse models of inflammatory bowel disease: Comparison to human disease. Pathophysiology 2014 05/27.

(114) Rennick DM, Fort MM, Davidson NJ. Studies with IL-10-/- mice: an overview. J Leukoc Biol 1997 04;61(4):389-396.

(115) Bhan AK, Mizoguchi E, Smith RN, Mizoguchi A. Spontaneous chronic colitis in TCR alpha-mutant mice; an experimental model of human ulcerative colitis. Int Rev Immunol 2000;19(1):123-138.

(116) Ehrhardt RO, Ludviksson B. Induction of colitis in IL2-deficient-mice: the role of thymic and peripheral dysregulation in the generation of autoreactive T cells. Res Immunol 1997 10/19;148(8-9):582-588.

(117) Barnett M, Fraser A. Animal Models of Colitis: Lessons Learned, and Their Relevance to the Clinic. In: O'Connor M, editor. Ulcerative Colitis - Treatments, Special Populations and the Future. Available online at http://www.intechopen.com/books/ulcerative-colitistreatments-special-populations-and-the-future/animal-models-of-colitis-lessons-learned-and-their-relevanceto-the-clinic: INTECH Open Access Publisher, 2011-11-02; 2011.

(118) Mizoguchi A, Mizoguchi E. Animal models of IBD: linkage to human disease. Curr Opin Pharmacol 2010 10;10(5):578-587.

(119) Boismenu R, Chen Y. Insights from mouse models of colitis. J Leukoc Biol 2000 03;67(3):267-278.

(120) Kühn R, Löhler J, Rennick D, Rajewsky K, Müller W. Interleukin-10-deficient mice develop chronic enterocolitis. Cell 1993 10/22;75(2):263-274.

(121) Davidson NJ, Fort MM, Müller W, Leach MW, Rennick DM. Chronic colitis in IL-10-/- mice: insufficient counter regulation of a Th1 response. Int Rev Immunol 2000;19(1):91-121.

(122) Leach MW, Davidson NJ, Fort MM, Powrie F, Rennick DM. The role of IL-10 in inflammatory bowel disease: "Of mice and men". Toxicol Pathol 1999;27(1):123-133.

(123) Berg DJ, Davidson N, Kühn R, Müller W, Menon S, Holland G, et al. Enterocolitis and colon cancer in interleukin-10-deficient mice are associated with aberrant cytokine production and CD4(+) TH1-like responses. J Clin Invest 1996 08/15;98(4):1010-1020.

(124) Rennick D, Davidson N, Berg D. Interleukin-10 gene knock-out mice: a model of chronic inflammation. Clin Immunol Immunopathol 1995 09;76(3):S174-S178.

(125) Glocker E, Kotlarz D, Boztug K, Gertz EM, Schaffer AA, Noyan F, et al. Inflammatory bowel disease and mutations affecting the interleukin-10 receptor. N Engl J Med 2011;19; 140(21; 1; 6):2033; 115; 1704-123; U21.

(126) Moran CJ, Walters TD, Guo CH, Kugathasan S, Klein C, Turner D, et al. IL-10R Polymorphisms Are Associated with Very-early-onset Ulcerative Colitis. Inflamm Bowel Dis 2011;19; 140(1; 6):115; 1704-123; U21.

(127) Cho JH, Brant SR. Recent Insights Into the Genetics of Inflammatory Bowel Disease. Gastroenterology 2011;140(6):1704-U21.

(128) Fedorak RN, Gangl A, Elson CO, Rutgeerts P, Schreiber S, Wild G, et al. Recombinant human interleukin 10 in the treatment of patients with mild to moderately active Crohn's disease. Gastroenterology 2003;119; 3(6; 5):1473; 725-1482; 731.

(129) Marlow GJ, van Gent D, Ferguson LR. Why interleukin-10 supplementation does not work in Crohn's disease patients. World J Gastroenterol 2013 07/07;19(25):3931-3941.

(130) Braat H, Peppelenbosch MP, Hommes DW. Interleukin-10-based therapy for inflammatory bowel disease. Expert Opinion on Biological Therapy 2003;3(5):725-731.

(131) Sydora BC, Tavernini MM, Wessler A, Jewell LD, Fedorak RN. Lack of interleukin-10 leads to intestinal inflammation, independent of the time at which luminal microbial colonization occurs. Inflamm Bowel Dis 2003;9(2):87-97.

(132) Duchmann R, Kaiser I, Hermann E, Mayet W, Ewe K, Meyer ZB. Tolerance exists towards resident intestinal flora but is broken in active inflammatory bowel disease (IBD). Clinical & Experimental Immunology 1995 12;102(3):448-455.

(133) Sartor RB. Genetics and Environmental Interactions Shape the Intestinal Microbiome to Promote Inflammatory Bowel Disease Versus Mucosal Homeostasis. Gastroenterology 2010;139(6):1816-1819.

(134) Campbell JH, Foster CM, Vishnivetskaya T, Campbell AG, Yang ZK, Wymore A, et al. Host genetic and environmental effects on mouse intestinal microbiota. ISME Journal: Multidisciplinary Journal of Microbial Ecology 2012 11;6(11):2033-2044.

(135) Grisham MB, Volkmer C, Tso P, Yamada T. Metabolism of trinitrobenzene sulfonic acid by the rat colon produces reactive oxygen species. Gastroenterology 1991 08;101(2):540-547.

(136) Yamada Y, Marshall S, Specian RD, Grisham MB. A comparative analysis of two models of colitis in rats. Gastroenterology 1992 05;102(5):1524-1534.

(137) Wirtz S, Neufert C, Weigmann B, Neurath MF. Chemically induced mouse models of intestinal inflammation. Nature Protocols 2007(3):541.

(138) te Velde A,A., Verstege MI, Hommes DW. Critical appraisal of the current practice in murine TNBS-induced colitis. Inflamm Bowel Dis 2006 10;12(10):995-999.

(139) Fichtner-Feigl S, Fuss IJ, Preiss JC, Strober W, Kitani A. Treatment of murine Th1- and Th2-mediated inflammatory bowel disease with NF-kappa B decoy oligonucleotides. J Clin Invest 2005 11;115(11):3057-3071.

(140) Lawrance IC, Wu F, Leite AZA, Willis J, West GA, Fiocchi C, et al. A murine model of chronic inflammation-induced intestinal fibrosis down-regulated by antisense NF-kappa B. Gastroenterology 2003 12;125(6):1750-1761.

(141) Mazmanian SK, Round JL, Kasper DL. A microbial symbiosis factor prevents intestinal inflammatory disease. Nature 2008 05/29;453(7195):620-625.

(142) Scheiffele F, Fuss IJ. Induction of TNBS colitis in mice. Curr Protoc Immunol 2002 08;Chapter 15:15.19-15.19.

(143) Johansson MEV, Gustafsson JK, Sjöberg KE, Petersson J, Holm L, Sjövall H, et al. Bacteria Penetrate the Inner Mucus Layer before Inflammation in the Dextran Sulfate Colitis Model. PLoS ONE 2010 08;5(8):1-9.

(144) Iwaya H, Maeta K, Hara H, Ishizuka S. Mucosal permeability is an intrinsic factor in susceptibility to dextran sulfate sodium-induced colitis in rats. Exp Biol Med (Maywood) 2012 04;237(4):451-460.

(145) Okayasu I, Hatakeyama S, Yamada M, Ohkusa T, Inagaki Y, Nakaya R. A novel method in the induction of reliable experimental acute and chronic ulcerative colitis in mice. Gastroenterology 1990 03;98(3):694-702.

(146) Okayasu I, Yamada M, Mikami T, Yoshida T, Kanno J, Ohkusa T. Dysplasia and carcinoma development in a repeated dextran sulfate sodium-induced colitis model. Journal of Gastroenterology & Hepatology 2002 10;17(10):1078-1083.

(147) Perše M, Cerar A, Alferez DG, Ryan AJ, Goodlad RA, Wright NA, et al. Dextran Sodium Sulphate Colitis Mouse Model: Traps and Tricks. Journal of Biomedicine and Biotechnology 2010;37(4):767-772.

(148) Solomon L, Mansor S, Mallon P, Donnelly E, Hoper M, Loughrey M, et al. The dextran sulphate sodium (DSS) model of colitis: an overview. Comparative Clinical Pathology 2010(3):235.

(149) Mähler M, Bristol IJ, Leiter EH, Workman AE, Birkenmeier EH, Elson CO, et al. Differential susceptibility of inbred mouse strains to dextran sulfate sodium-induced colitis. Am J Physiol 1998 03;274(3):G544-G551.

(150) Melgar S, Karlsson A, Michaëlsson E. Acute colitis induced by dextran sulfate sodium progresses to chronicity in C57BL/6 but not in BALB/c mice: correlation between symptoms and inflammation. Am J Physiol Gastrointest Liver Physiol 2005 06;288(6):G1328-G1338.

(151) Kitajima S, Takuma S, Morimoto M. Changes in Colonic Mucosal Permeability in Mouse Colitis Induced with Dextran Sulfate Sodium. Experimental Animals 1999;48(3):137-143.

(152) Hirono I, Kuhara K, Yamaji T, Hosaka S, Golberg L. Carcinogenicity of dextran sulfate sodium in relation to its molecular weight. Cancer Lett 1983 02;18(1):29-34.

(153) Gaudio E, Taddei G, Vetuschi A, Sferra R, Frieri G, Ricciardi G, et al. Dextran sulfate sodium (DSS) colitis in rats - Clinical, structural, and ultrastructural aspects. Dig Dis Sci 2000;44; 21(7; 4):1458; 757-1475; 768.

(154) Cooper HS, Murthy S, Kido K, Yoshitake H, Flanigan A. Dysplasia and cancer in the dextran sulfate sodium mouse colitis model. Relevance to colitis-associated neoplasia in the human: a study of histopathology, B-catenin and p53 expression and the role of inflammation. Carcinogenesis 2000;21(4):757-768.

(155) Dieleman, Palmen, Akol, Bloemena, PEÑA, Meuwissen, et al. Chronic experimental colitis induced by dextran sulphate sodium (DSS) is characterized by Th1 and Th2 cytokines. Clinical & Experimental Immunology 1998 12;114(3):385-391.

(156) De Robertis M, Massi E, Poeta ML, Carotti S, Morini S, Cecchetelli L, et al. The AOM/DSS murine model for the study of colon carcinogenesis: From pathways to diagnosis and therapy studies. J Carcinog 2011 03/24;10:9-9.

(157) Tanaka T, Kohno H, Suzuki R, Yamada Y, Sugie S, Mori H. A novel inflammation-related mouse colon carcinogenesis model induced by azoxymethane and dextran sodium sulfate. Cancer Sci 2003 11;94(11):965-973.

(158) Okayasu I, Ohkusa T, Kajiura K, Kanno J, Sakamoto S. Promotion of colorectal neoplasia in experimental murine ulcerative colitis. Gut 1996;39(1):87-92.

(159) Greten FR, Karin M. The IKK/NF-kappa B activation pathway - a target for prevention and treatment of cancer. Cancer Lett 2004;206(2):193-199.

(160) Ichikawa-Tomikawa N, Sugimoto K, Satohisa S, Nishiura K, Chiba H. Possible Involvement of Tight Junctions, Extracellular Matrix and Nuclear Receptors in Epithelial Differentiation. J Biomed Biotechnol 2011:1-10.

(161) Poritz LS, Garver KI, Green C, Fitzpatrick L, Ruggiero F, Koltun WA. Loss of the tight junction protein ZO-1 in dextran sulfate sodium induced colitis. J Surg Res 2007 06/01;140(1):12-19.

(162) Araki Y, Mukaisyo K, Sugihara H, Fujiyama Y, Hattori T. Increased apoptosis and decreased proliferation of colonic epithelium in dextran sulfate sodium-induced colitis in mice. Oncol Rep 2010 10;24(4):869-874.

(163) Laroui H, Ingersoll SA, Hong CL, Baker MT, Ayyadurai S, Charania MA, et al. Dextran Sodium Sulfate (DSS) Induces Colitis in Mice by Forming Nano-Lipocomplexes with Medium-Chain- Length Fatty Acids in the Colon. PLoS ONE 2012 03;7(3):1-12.

(164) Alex P, Zachos NC, Nguyen T, Gonzales L, Chen TE, Conklin LS, et al. Distinct Cytokine Patterns Identified from Multiplex Profiles of Murine DSS and TNBS-induced Colitis. Inflamm Bowel Dis 2009;15(3):341-352.

(165) Dieleman LA, Ridwan BU, Tennyson GS, Beagley KW, Bucy RP, Elson CO, et al. Dextran sulfate sodium-induced colitis occurs in severe combined immunodeficient mice. Gastroenterology 1994 12;107; 15; 137(6; 3; 11):1643; 454; 2572S-1652; 462; 2575S.

(166) Krieglstein CF, Cerwinka WH, Sprague AG, Laroux FS, Grisham MB, Koteliansky VE, et al. Collagen-binding integrin alpha1beta1 regulates intestinal inflammation in experimental colitis. J Clin Invest 2002 12;110(12):1773-1782.

(167) Axelsson LG, Landström E, Goldschmidt TJ, Grönberg A, Bylund-Fellenius A. Dextran sulfate sodium (DSS) induced experimental colitis in immunodeficient mice: effects in CD4(+) -cell depleted, athymic and NK-cell depleted SCID mice. Inflamm Res 1996 04;45(4):181-191.

(168) Kanwar B, Gao DW, Hwang AB, Grenert JP, Williams SP, Franc B, et al. In vivo imaging of mucosal CD4+ T cells using single photon emission computed tomography in a murine model of colitis. J Immunol Methods 2008 01/01;329(1-2):21-30.

(169) Morgan ME, Zheng B, Koelink PJ, van dK, Haazen L, van Roest M, et al. New Perspective on Dextran Sodium Sulfate Colitis: Antigen-Specific T Cell Development during Intestinal Inflammation. PLOS ONE 2013;8(7).

(170) van Dop W,A., Marengo S, te Velde A,A., Ciraolo E, Franco I, ten Kate F,J., et al. The absence of functional PI3Kgamma prevents leukocyte recruitment and ameliorates DSS-induced colitis in mice. Immunol Lett 2010 06/15;131(1):33-39.

(171) Femia AP, Caderni G. Rodent models of colon carcinogenesis for the study of chemopreventive activity of natural products. Planta Med 2008(13):1602.

(172) Sohn OS, Ishizaki H, Yang CS, Fiala ES, Megaraj V, Ding XX, et al. Metabolism of azoxymethane, methylazoxymethanol and N-nitrosodimethylamine by cytochrome P450IIE1. Carcinogenesis 2009 01;12; 27; 30(1; 4; 2):127; 656; 183-131; 662; 196.

(173) Takahashi M, Wakabayashi K. Gene mutations and altered gene expression in azoxymethane-induced colon carcinogenesis in rodents. Cancer Sci 2004 06;95(6):475-480.

(174) Rosenberg DW, Giardina C, Tanaka T. Mouse models for the study of colon carcinogenesis. Carcinogenesis 2009;30(2):183-196.

(175) Megaraj V, Ding XX, Fang C, Kovalchuk N, Zhu Y, Zhang QY, et al. Role of Hepatic and Intestinal P450 Enzymes in the Metabolic Activation of the Colon

Carcinogen Azoxymethane in Mice. Chem Res Toxicol 2009;27; 30(4; 2):656; 183-662; 196.

(176) Corpet DE, Pierre F. How good are rodent models of carcinogenesis in predicting efficacy in humans? A systematic review and meta-analysis of colon chemoprevention in rats, mice and men. Eur J Cancer 2005(13):1911.

(177) Kobaek-Larsen M, Thorup I, Diederichsen A, Fenger C, Hoitinga MR. Review of colorectal cancer and its metastases in rodent models: comparative aspects with those in humans. Comp Med 2000 02;50(1):16-26.

(178) Vivona AA, Shpitz B, Medline A, Bruce WR, Hay K, Ward MA, et al. K-ras mutations in aberrant crypt foci, adenomas and adenocarcinomas during azoxymethane-induced colon carcinogenesis. Carcinogenesis 1993 09;14(9):1777-1781.

(179) Boivin GP, Washington K, Yang K, Ward JM, Pretlow TP, Russell R, et al. Pathology of mouse models of intestinal cancer: Consensus report and recommendations. Gastroenterology 2004;124; 206(3; 2):762; 193-777; 199.

(180) Borinstein SC, Conerly M, Dzieciatkowski S, Biswas S, Washington MK, Trobridge P, et al. Aberrant DNA methylation occurs in colon neoplasms arising in the azoxymethane colon cancer model. Mol Carcinog 2010 01;49(1):94-103.

(181) Feinberg AP, Vogelstein B. Hypomethylation distinguishes genes of some human cancers from their normal counterparts. Nature 1983 01/06;301(5895):89.

(182) Feinberg AP, Ohlsson R, Henikoff S. The epigenetic progenitor origin of human cancer. Nature Reviews Genetics 2006 01;7(1):21-33.

(183) Gaudet F, Hodgson JG, Eden A, Jackson-Grusby L, Dausman J, Gray JW, et al. Induction of Tumors in Mice by Genomic Hypomethylation. Science 2003(5618):489.

(184) Gkouskou KK, Deligianni C, Tsatsanis C, Eliopoulos AG, Buchler G, Wos-Oxley M, et al. The gut microbiota in mouse models of inflammatory bowel disease. Inflamm Bowel Dis 2012;4; 18(5):943-954.

(185) Buchler G, Wos-Oxley M, Smoczek A, Zschemisch NH, Neumann D, Pieper DH, et al. Strain-specific colitis susceptibility in IL10-deficient mice depends on complex gut microbiota-host interactions. Inflamm Bowel Dis 2012;18(5):943-954.

(186) Lawley TD, Clare S, Walker AW, Stares MD, Connor TR, Raisen C, et al. Targeted Restoration of the Intestinal Microbiota with a Simple, Defined Bacteriotherapy Resolves Relapsing Clostridium difficile Disease in Mice. PLoS Pathogens 2012 10;8(10):1-14.

(187) Madsen K, Cornish A, Soper P, McKaigney C, Jijon H, Yachimec C, et al. Probiotic bacteria enhance murine and human intestinal epithelial barrier function. Gastroenterology 2001 09;121(3):580-591.

(188) Nishimura T, Andoh A, Hashimoto T, Kobori A, Tsujikawa T, Fujiyama Y. Cellobiose Prevents the Development of Dextran Sulfate Sodium (DSS)-Induced Experimental Colitis. Journal of Clinical Biochemistry and Nutrition 2010;46(2):105-110.

(189) Santos A, San Mauro M, Marquina Diaz D, Langen M, Dieleman LA. Prebiotics and their long-term influence on the microbial populations of the mouse bowel. Food Microbiol 2009;15(3):454-462.

(190) Schultz M, Veltkamp C, Dieleman LA, Grenther WB, Wyrick PB, Tonkonogy SL, et al. Lactobacillus plantarum 299V in the treatment and prevention of spontaneous colitis in interleukin-10-deficient mice. Inflamm Bowel Dis 2002 03;8(2):71-80.

(191) Sheil B, Shanahan F, O'Mahony L. Probiotic effects on inflammatory bowel disease. J Nutr 2007(3).

(192) Langen M, Dieleman LA. Prebiotics in Chronic Intestinal Inflammation. Inflamm Bowel Dis 2009;15(3):454-462.

(193) Irving PM, Gibson PR. Infections and IBD. Nature Clinical Practice Gastroenterology and Hepatology 2008(1):18.

(194) Rodemann JF, Dubberke ER, Reske KA, Seo DH, Stone CD, Rolhion N, et al. Incidence of Clostridium difficile Infection in Inflammatory Bowel Disease. Inflamm Bowel Dis 2007;13(3; 10):339; 1277-1283.

(195) Rolhion N, Darfeuille-Michaud A. Adherent-invasive Escherichia coli in inflammatory bowel disease. Inflamm Bowel Dis 2007;13(10):1277-1283.

(196) Eckmann L. Animal models of inflammatory bowel disease - Lessons from enteric infections. Inflammatory Bowel Disease: Genetics, Barrier Function, Immunologic Mechanisms, and Microbial Pathways 2006;1072:28-38.

(197) Wine E, Shen-Tu G, Gareau MG, Goldberg HA, Licht C, Ngan B, et al. Osteopontin mediates Citrobacter rodentium-induced colonic epithelial cell hyperplasia and attaching-effacing lesions. Am J Pathol 2010 09;177; 139(3; 6):1320; 1816-1332; 1819.

(198) Borenshtein D, McBee ME, Schauer DB. Utility of the Citrobacter rodentium infection model in laboratory mice. Curr Opin Gastroenterol 2008;24(1):32-37.

(199) Stecher B, Hapfelmeier S, Müller C, Kremer M, Stallmach T, Hardt W. Flagella and chemotaxis are required for efficient induction of Salmonella enterica serovar

Typhimurium colitis in streptomycin-pretreated mice. Infect Immun 2004 07;72(7):4138-4150.

(200) Gradel KO, Nielsen HL, SchA[cedilla]nheyder HC, Ejlertsen T, Kristensen B, Nielsen H. Increased Short- and Long-Term Risk of Inflammatory Bowel Disease After Salmonella or Campylobacter Gastroenteritis. Gastroenterology 2009(2):495.

(201) Coombes BK, Coburn BA, Potter AA, Gomis S, Mirakhur K, Li Y, et al. Analysis of the contribution of Salmonella pathogenicity islands 1 and 2 to enteric disease progression using a novel bovine ileal loop model and a murine model of infectious enterocolitis. Infect Immun 2005 11;73(11):7161-7169.

(202) Que JU, Hentges DJ, Barthel M, Hapfelmeier S, Quintanilla-Martinez L, Kremer M, et al. Effect of streptomycin administration on colonization resistance to Salmonella typhimurium in mice. Infect Immun 2005 04;48; 71; 73(1; 5; 6):169; 2839; 3228-174; 2858; 3241.

(203) Barthel M, Hapfelmeier S, Quintanilla-Martinez L, Kremer M, Rohde M, Hogardt M, et al. Pretreatment of mice with streptomycin provides a Salmonella enterica serovar typhimurium colitis model that allows analysis of both pathogen and host. Infect Immun 2005;71; 73(5; 6):2839; 3228-2858; 3241.

(204) Stecher B, Macpherson AJ, Hapfelmeier S, Kremer M, Stallmach T, Hardt WD. Comparison of Salmonella enterica serovar Typhimurium colitis in germfree mice and mice pretreated with streptomycin. Infect Immun 2005;73(6):3228-3241.

(205) Higgins LM, Frankel G, Douce G, Dougan G, MacDonald TT. Citrobacter rodentium infection in mice elicits a mucosal Th1 cytokine response and lesions similar to those in murine inflammatory bowel disease. Infect Immun 1999 06;67(6):3031-3039.

(206) Wang Y, Xiang G, Kourouma F, Umar S. Citrobacter rodentium-induced NF-kappaB activation in hyperproliferating colonic epithelia: role of p65 (Ser536) phosphorylation. Br J Pharmacol 2006 07;148(6):814-824.

(207) Deng W, Vallance BA, Li Y, Puente JL, Finlay BB. Citrobacter rodentium translocated intimin receptor (Tir) is an essential virulence factor needed for actin condensation, intestinal colonization and colonic hyperplasia in mice. Mol Microbiol 2003 04;48(1):95-115.

(208) Barthold SW, Coleman GL, Bhatt PN, Osbaldiston GW, Jonas AM. The etiology of transmissible murine colonic hyperplasia. Lab Anim Sci 1976 12;26(6):889-894.

(209) Bhinder G, Sham HP, Chan JM, Morampudi V, Jacobson K, Vallance BA. The Citrobacter rodentium mouse model: studying pathogen and host contributions to infectious colitis. J Vis Exp 2013 02/19(72):e50222-e50222.

(210) Barthold S.W., Osbaldiston G.W., Jonas A.M. Dietary, bacterial, and host genetic interactions in the pathogenesis of transmissible murine colonic hyperplasia. Lab Anim Sci 1977.

(211) Borenshtein D, Nambiar PR, Groff EB, Fox JG, Schauer DB, Vallance BA, et al. Development of fatal colitis in FVB mice infected with Citrobacter rodentium. Infect Immun 2003 07;75; 71(7; 6):3271; 3443-3281; 3453.

(212) Vallance BA, Deng WY, Jacobson K, Finlay BB. Host susceptibility to the attaching and effacing bacterial pathogen Citrobacter rodentium. Infect Immun 2003;71(6):3443-3453.

(213) Khan MA, Ma CX, Knodler LA, Valdez Y, Rosenberger CM, Deng WY, et al. Toll-like receptor 4 contributes to colitis development but not to host defense during Citrobacter rodentium infection in mice. Infect Immun 2007;74; 179(5; 1):2522; 566-2536; 577.

(214) Lebeis SL, Bommarius B, Parkos CA, Sherman MA, Kalman D. TLR signaling mediated by MyD88 is required for a protective innate immune response by Neutrophils to Citrobacter rodentium. Journal of Immunology 2007;179(1):566-577.

(215) Ma C, Wickham ME, Guttman JA, Deng W, Walker J, Madsen KL, et al. Citrobacter rodentium infection causes both mitochondrial dysfunction and intestinal epithelial barrier disruption in vivo: role of mitochondrial associated protein (Map). Cell Microbiol 2006 10;8(10):1669-1686.

(216) Guttman JA, Li Y, Wickham ME, Deng W, Vogl AW, Finlay BB, et al. Attaching and effacing pathogen-induced tight junction disruption in vivo. Cell Microbiol 2006 04;8; 74(4; 11):634; 6075-645; 6084.

(217) Guttman JA, Samji FN, Li YL, Vogl AW, Finlay BB. Evidence that tight junctions are disrupted due to intimate bacterial contact and not inflammation during attaching and effacing pathogen infection in vivo. Infect Immun 2006;74(11):6075-6084.

(218) Maaser C, Housley MP, Vallance BA, Finlay BB, Varki N, Kagnoff MF, et al. Clearance of Citrobacter rodentium requires B cells but not secretory IgA or IgM antibodies. Gastroenterology 2002;122(4):A44-A44.

(219) Simmons CP, Clare S, Ghaem-Maghami M, Uren TK, Rankin J, Huett A, et al. Central role for B lymphocytes and CD4+ T cells in immunity to infection by the attaching and effacing pathogen Citrobacter rodentium. Infect Immun 2002 09;71; 70(9; 4):5077; 2070-5086; 2081.

(220) Vallance BA, Deng WY, Knodler LA, Finlay BB. Mice lacking T and B lymphocytes develop transient colitis and crypt hyperplasia yet suffer impaired bacterial clearance during Citrobacter rodentium infection. Infect Immun 2002;70(4):2070-2081.

(221) Warne PH, Viciana PR, Downward J, Buday L, Downward J. Direct interaction of Ras and the amino-terminal region of Raf-1 in vitro. Nature 1993;1786(6435; 2):352; 178-187.

(222) Buday L, Downward J, Grossmann KS, Rosario M, Birchmeier C, Birchmeier W. Many faces of Ras activation. Advances in Cancer Research 2010;1786; 106(2):178; 53-187; 89.

(223) Tidyman WE, Rauen KA. The RASopathies: developmental syndromes of Ras/MAPK pathway dysregulation. Curr Opin Genet Dev 2009(3):230.

(224) Bentires-Alj M, Kontaridis MI, Neel BG, Grossmann KS, Rosario M, Birchmeier C, et al. Stops along the RAS pathway in human genetic disease. Nat Med 2010 03;12; 106(3):283; 53-285; 89.

(225) Grossmann KS, Rosario M, Birchmeier C, Birchmeier W. The Tyrosine Phosphatase Shp2 in Development and Cancer. Advances in Cancer Research 2010;106:53-89.

(226) Chin L, Tam A, Pomerantz J, Wong M, Holash J, Bardeesy N, et al. Essential role for oncogenic Ras in tumour maintenance. Nature 1999 07/29;400(6743):468.

(227) Downward J. Ras signalling and apoptosis. Curr Opin Genet Dev 1998 02;8(1):49-54.

(228) Cox AD, Der CJ. The dark side of Ras: regulation of apoptosis. Oncogene 2003 12/08;22(56):8999-9006.

(229) Terada K, Kaziro Y, Satoh T. Analysis of Ras-dependent signals that prevent caspase-3 activation and apoptosis induced by cytokine deprivation in hematopoietic cells. Biochem Biophys Res Commun 2000 01/07;267(1):449-455.

(230) Tsuneoka M, Mekada E. Ras/MEK signaling suppresses Myc-dependent apoptosis in cells transformed by c-myc and activated ras. Oncogene 2000 01/06;19(1):115.

(231) Gómez J, Martínez C, Fernández B, García A, Rebollo A. Ras activation leads to cell proliferation or apoptotic cell death upon interleukin-2 stimulation or lymphokine deprivation, respectively. Eur J Immunol 1997 07;27(7):1610-1618.

(232) Latinis KM, Carr LL, Peterson EJ, Norian LA, Eliason SL, Koretzky GA. Regulation of CD95 (Fas) ligand expression by TCR-mediated signaling events. J Immunol 1997 05/15;158(10):4602-4611.

(233) Sherwood V, Recino A, Jeffries A, Ward A, Chalmers AD, Fujita H, et al. The N-terminal RASSF family: a new group of Ras-association-domain-containing proteins,

with emerging links to cancer formation. Biochem J 2005 12/23;425; 280(2; 6):303; 5022-311; 5031.

(234) Richter AM, Pfeifer GP, Dammann RH, Pfeifer GP, Dammann R, Tommasi S, et al. The RASSF proteins in cancer; from epigenetic silencing to functional characterization. Biochim Biophys Acta 2009;1796; 20; 20(2; 8; 27):114; R344; 3563-128; R345; 3567.

(235) Fujita H, Fukuhara S, Sakurai A, Yamagishi A, Kamioka Y, Nakaoka Y, et al. Local activation of Rap1 contributes to directional vascular endothelial cell migration accompanied by extension of microtubules on which RAPL, a Rap1-associating molecule, localizes. J Biol Chem 2004;280; 24; 28; 19(6; 11; 14; 23):5022; 4943; 4520; 2020-5031; 4954; 4535; 2025.

(236) Ortiz-Vega S, Khokhlatchev A, Nedwidek M, Zhang X, Dammann R, Pfeifer GP, et al. The putative tumor suppressor RASSF1A homodimerizes and heterodimerizes with the Ras-GTP binding protein Nore1. Oncogene 2002 02/21;21; 24; 28; 19(9; 11; 14; 23):1381; 4943; 4520; 2020-1390; 4954; 4535; 2025.

(237) Rodriguez-Viciana P, Sabatier C, McCormick F, Foley CJ, Freedman H, Choo SL, et al. Signaling specificity by Ras family GTPases is determined by the full spectrum of effectors they regulate. Mol Cell Biol 2004;24; 28; 19(11; 14; 23):4943; 4520; 2020-4954; 4535; 2025.

(238) Derks S, Postma C, Moerkerk PTM, van dB, Carvalho B, Hermsen MAJA, et al. Promoter methylation precedes chromosomal alterations in colorectal cancer development. Cellular Oncology 2006 09;28(5):247-257.

(239) Foley CJ, Freedman H, Choo SL, Onyskiw C, Fu NY, Yu VC, et al. Dynamics of RASSF1A/MOAP-1 association with death receptors. Mol Cell Biol 2009;28; 19(14; 23):4520; 2020-4535; 2025.

(240) Hamilton G, Yee KS, Scrace S, O'Neill E. ATM regulates a RASSF1A-dependent DNA damage response. Curr Biol 2009 12/15;19(23):2020-2025.

(241) Avruch J, Xavier R, Bardeesy N, Zhang X, Praskova M, Zhou D, et al. Rassf family of tumor suppressor polypeptides. J Biol Chem 2009 04/24;284(17):11001-11005.

(242) Harjes E, Harjes S, Wohlgemuth S, Muller KH, Krieger E, Herrmann C, et al. GTP-Ras disrupts the intramolecular complex of C1 and RA domains of Nore1. Structure 2006;14; 27; 278; 285(5; 14; 24; 45):881; 1995; 21938; 35029-888; 2005; 21943; 35038.

(243) Stieglitz B, Bee C, Schwarz D, Yildiz O, Moshnikova A, Khokhlatchev A, et al. Novel type of Ras effector interaction established between tumour suppressor NORE1A

and Ras switch II. EMBO J 2008;27; 278; 285(14; 24; 45):1995; 21938; 35029-2005; 21943; 35038.

(244) Vos MD, Martinez A, Ellis CA, Vallecorsa T, Clark GJ, Park J, et al. The pro-apoptotic Ras effector Nore1 may serve as a Ras-regulated tumor suppressor in the lung. J Biol Chem 2003;278; 285(24; 45):21938; 35029-21943; 35038.

(245) Park J, Kang SI, Lee SY, Zhang XF, Kim MS, Beers LF, et al. Tumor Suppressor Ras Association Domain Family 5 (RASSF5/NORE1) Mediates Death Receptor Ligand-induced Apoptosis. J Biol Chem 2010;285(45):35029-35038.

(246) Pan D. The hippo signaling pathway in development and cancer. Dev Cell 2010 10/19;19(4):491-505.

(247) Delpire E. The mammalian family of sterile 20p-like protein kinases. Pflugers Arch 2009 09;458(5):953-967.

(248) Praskova M, Khoklatchev A, Ortiz-Vega S, Avruch J. Regulation of the MST1 kinase by autophosphorylation, by the growth inhibitory proteins, RASSF1 and NORE1, and by Ras. Biochem J 2004 07/15;381:453-462.

(249) Ura S, Nishina H, Gotoh Y, Katada T. Activation of the c-Jun N-terminal kinase pathway by MST1 is essential and sufficient for the induction of chromatin condensation during apoptosis. Mol Cell Biol 2007 08;27(15):5514-5522.

(250) Halder G, Johnson RL. Hippo signaling: growth control and beyond. Development 2011 01;138(1):9-22.

(251) Aoyama Y, Avruch J, Zhang X. Nore1 inhibits tumor cell growth independent of Ras or the MST1/2 kinases. Oncogene 2004 04/22;23(19):3426-3433.

(252) Oh HJ, Lee K, Song SJ, Jin MS, Song MS, Lee JH, et al. Role of the tumor suppressor RASSF1A in Mst1-mediated apoptosis. Cancer Res 2006 03/01;66(5):2562-2569.

(253) Ikeda M, Hirabayashi S, Fujiwara N, Mori H, Kawata A, Iida J, et al. Ras-association domain family protein 6 induces apoptosis via both caspase-dependent and caspase-independent pathways. Exp Cell Res 2007 04/15;313(7):1484-1495.

(254) Avruch J, Zhou D, Fitamant J, Bardeesy N. Mst1/2 signalling to Yap: gatekeeper for liver size and tumour development. Br J Cancer 2011 01/04;104(1):24-32.

(255) Del Re D,P., Matsuda T, Zhai P, Gao S, Clark GJ, Van DW, et al. Proapoptotic Rassf1A/Mst1 signaling in cardiac fibroblasts is protective against pressure overload in mice. J Clin Invest 2010 10;120(10):3555-3567.

(256) Densham RM, O'Neill E, Munro J, König I, Anderson K, Kolch W, et al. MST kinases monitor actin cytoskeletal integrity and signal via c-Jun N-terminal kinase stress-activated kinase to regulate p21Waf1/Cip1 stability. Mol Cell Biol 2009 12;29(24):6380-6390.

(257) Kim D, Shu S, Coppola MD, Kaneko S, Yuan Z, Cheng JQ, et al. Regulation of proapoptotic mammalian ste20-like kinase MST2 by the IGF1-Akt pathway. PLoS One 2005 03/09;5; 29; 18(3; 23; 6):e9616; 6309; 637-e9616; 6320; 650.

(258) Oh S, Lee D, Kim T, Kim TS, Oh HJ, Hwang CY, et al. Crucial Role for Mst1 and Mst2 Kinases in Early Embryonic Development of the Mouse. Mol Cell Biol 2005;29; 18(23; 6):6309; 637-6320; 650.

(259) van der Weyden L, Papaspyropoulos A, Poulogiannis G, Rust AG, Rashid M, Adams DJ, et al. Loss of RASSF1A synergizes with deregulated RUNX2 signaling in tumorigenesis. Cancer Res 2012 08/01;72(15):3817-3827.

(260) Baksh S, Tommasi S, Fenton S, Yu VC, Martins LM, Pfeifer GP, et al. The tumor suppressor RASSF1A and MAP-1 link death receptor signaling to bax conformational change and cell death. Mol Cell 2005;18(6):637-650.

(261) Ghazaleh HA, Chow RS, Choo SL, Pham D, Olesen JD, Wong RX, et al. 14-3-3 mediated regulation of the tumor suppressor protein, RASSF1A. Apoptosis 2010 02;15(2):117-127.

(262) Vos MD, Dallol A, Eckfeld K, Allen NPC, Donninger H, Hesson LB, et al. The RASSF1A tumor suppressor activates Bax via MOAP-1. J Biol Chem 2006 02/24;281(8):4557-4563.

(263) Jung H, Jung JS, Whang YM, Kim YH. RASSF1A Suppresses Cell Migration through Inactivation of HDAC6 and Increase of Acetylated a-Tubulin. Cancer Res Treat 2013 06;45(2):134-144.

(264) Oceandy D, Pickard A, Prehar S, Zi M, Mohamed TMA, Stanley PJ, et al. Tumor suppressor Ras-association domain family 1 isoform A is a novel regulator of cardiac hypertrophy. Circulation 2009 08/18;120(7):607-616.

(265) Rosenquist M. 14-3-3 Proteins in Apoptosis. Braz J Med Biol Res 2003 04;36(4):403-408.

(266) Molzan M, Schumacher B, Ottmann C, Baljuls A, Polzien L, Weyand M, et al. Impaired binding of 14-3-3 to C-RAF in Noonan syndrome suggests new approaches in diseases with increased Ras signaling. Mol Cell Biol 2010 10;30(19):4698-4711.

(267) Rushworth LK, Hindley AD, O'Neill E, Kolch W. Regulation and role of Raf-1/B-Raf heterodimerization. Mol Cell Biol 2006 03;26(6):2262-2272.

(268) Wu D, Pan W. GSK3: a multifaceted kinase in Wnt signaling. Trends Biochem Sci 2010 03;35(3):161-168.

(269) Verma SK, Ganesan TS, Parker PJ. The tumour suppressor RASSF1A is a novel substrate of PKC. FEBS Lett 2008 06/25;582(15):2270-2276.

(270) Rong R, Jiang LY, Sheikh MS, Huang Y. Mitotic kinase Aurora-A phosphorylates RASSF1A and modulates RASSF1A-mediated microtubule interaction and M-phase cell cycle regulation. Oncogene 2007 12/06;26(55):7700-7708.

(271) Tian Y, Hou Y, Zhou X, Cheng H, Zhou R. Tumor suppressor RASSF1A promoter: p53 binding and methylation. PLoS One 2011 02/25;6(2):e17017-e17017.

(272) Zhang HL, He J, Li JS, Tian D, Gu LB, Zhou MX. Methylation of RASSF1A gene promoter is regulated by p53 and DAXX. FASEB Journal 2013;27(1):232-242.

(273) Li Q, Zhu F, Chen P. miR-7 and miR-218 epigenetically control tumor suppressor genes RASSF1A and Claudin-6 by targeting HoxB3 in breast cancer. Biochem Biophys Res Commun 2012(1):28.

(274) Yang L, Ma Z, Wang D, Zhao W, Chen L, Wang G. MicroRNA-602 regulating tumor suppressive gene RASSF1A is overexpressed in hepatitis B virus-infected liver and hepatocellular carcinoma. Cancer Biol Ther 2010 05/15;9(10):803-808.

(275) Dammann R, Schagdarsurengin U, Seidel C, Strunnikova M, Rastetter M, Baler K, et al. The tumor suppressor RASSF1A in human carcinogenesis: an update. Histol Histopathol 2005;20(2):645-663.

(276) Dallol A, Agathanggelou A, Fenton SL, Ahmed-Choudhury J, Hesson L, Vos MD, et al. RASSF1A interacts with microtubule-associated proteins and modulates microtubule dynamics. Cancer Res 2004 06/15;64(12):4112-4116.

(277) El-Kalla M, Onyskiw C, Baksh S. Functional importance of RASSF1A microtubule localization and polymorphisms. Oncogene 2010 10/21;29(42):5729-5740.

(278) Shivakumar L, Minna J, Sakamaki T, Pestell R, White MA. The RASSF1A tumor suppressor blocks cell cycle progression and inhibits cyclin D1 accumulation. Mol Cell Biol 2002 06;22(12):4309-4318.

(279) Dallol A, Cooper WN, Al-Mulla F, Agathanggelou A, Maher ER, Latif F. Depletion of the Ras association domain family 1, isoform A-associated novel microtubule-associated protein, C19ORF5/MAP1S, causes mitotic abnormalities. Cancer Res 2007 01/15;67(2):492-500.

(280) Liu L, Xie R, Yang C, McKeehan WL. Dual function microtubule- and mitochondria-associated proteins mediate mitotic cell death. Cell Oncol 2009;31(5):393-405.

(281) Liu L, Vo A, Liu G, McKeehan WL. Putative tumor suppressor RASSF1 interactive protein and cell death inducer C19ORF5 is a DNA binding protein. Biochem Biophys Res Commun 2005 07/08;332(3):670-676.

(282) Xie R, Nguyen S, McKeehan K, Wang F, McKeehan WL, Liu L. Microtubule-associated protein 1S (MAP1S) bridges autophagic components with microtubules and mitochondria to affect autophagosomal biogenesis and degradation. J Biol Chem 2011 03/25;286(12):10367-10377.

(283) Leading causes of death in Canada [electronic resource]. : Ottawa : Statistics Canada, 2008-; 2004.

(284) Wang F, Tan W, Guo D, Zhu X, Qian K, He S. Altered Expression of Signaling Genes in Jurkat Cells upon FTY720 Induced Apoptosis. International Journal of Molecular Sciences 2010 09;11(9):3087-3105.

(285) Hanahan D, Weinberg RA. Review: The Hallmarks of Cancer. Cell 2000;100:57-70.

(286) Hanahan D, Weinberg RA. Review: Hallmarks of Cancer: The Next Generation. Cell 2011;144:646-674.

(287) van der Weyden L, Adams DJ. The Ras-association domain family (RASSF) members and their role in human tumourigenesis. BBA - Reviews on Cancer 2007 09;1776(1):58-85.

(288) Donninger H, Vos MD, Clark GJ. The RASSF1A tumor suppressor. J Cell Sci 2007 09/15;120:3163-3172.

(289) Pelosi G, Fumagalli C, Trubia M, Sonzogni A, Rekhtman N, Maisonneuve P, et al. Dual role of RASSF1 as a tumor suppressor and an oncogene in neuroendocrine tumors of the lung. Anticancer Res 2010 10;30(10):4269-4281.

(290) Kitagawa D, Kajiho H, Negishi T, Ura S, Watanabe T, Wada T, et al. Release of RASSF1C from the nucleus by Daxx degradation links DNA damage and SAPK/JNK activation. EMBO J 2006;25(14):3286-3297.

(291) Vos MD, Martinez A, Elam C, Dallol A, Taylor BJ, Latif F, et al. A role for the RASSF1A tumor suppressor in the regulation of tubulin polymerization and genomic stability. Cancer Res 2004 06/15;64(12):4244-4250.

(292) Rong R, Jin W, Zhang J, Sheikh MS, Huang Y. Tumor suppressor RASSF1A is a microtubule-binding protein that stabilizes microtubules and induces G2/M arrest. Oncogene 2004 10/28;23(50):8216-8230.

(293) van der Weyden L, Tachibana KK, Gonzalez MA, Adams DJ, Ng BL, Petty R, et al. The RASSF1A isoform of RASSF1 promotes microtubule stability and suppresses tumorigenesis. Mol Cell Biol 2005 09;25(18):8356-8367.

(294) Kashuba VI, Pavlova TV, Grigorieva EV, Kutsenko A, Yenamandra SP, Li J, et al. High Mutability of the Tumor Suppressor Genes RASSF1 and RBSP3 (CTDSPL) in Cancer. PLoS ONE 2009 05;4(5):1-12.

(295) Schagdarsurengin U, Seidel C, Ulbrich EJ, Kölbl H, Dittmer J, Dammann R. A polymorphism at codon 133 of the tumor suppressor RASSF1A is associated with tumorous alteration of the breast. Int J Oncol 2005 07;27(1):185-191.

(296) Gao BN, Xie XJ, Huang CX, Shames DS, Chen T, Lewis CM, et al. RASSF1A polymorphism A133S is associated with early onset breast cancer in BRCA1/2 mutation carriers. Cancer Res 2008;68(1):22-25.

(297) Kanzaki H, Hanafusa H, Yamamoto H, Yasuda Y, Imai K, Yano M, et al. Single nucleotide polymorphism at codon 133 of the RASSF1 gene is preferentially associated with human lung adenocarcinoma risk. Cancer Lett 2005;238; 6; 19; 65(1; 22; 1; 1):128; 2788; 24; 92-134; 2794; 30; 98.

(298) Bergqvist J, Latif A, Roberts SA, Hadfield KD, Lalloo F, Howell A, et al. RASSF1A polymorphism in familial breast cancer. Fam Cancer 2010 09;9(3):263-265.

(299) Min SS, Jin SC, Su JS, Tae HY, Lee H, Dae-Sik Lim. The Centrosomal Protein RAS Association Domain Family Protein 1A (RASSF1A)-binding Protein 1 Regulates Mitotic Progression by Recruiting RASSF1A to Spindle Poles. J Biol Chem 2005 02/04;280(5):3920-3927.

(300) Liu L, Tommasi S, Lee D, Dammann R, Pfeifer GP. Control of microtubule stability by the RASSF1A tumor suppressor. Oncogene 2003 11/06;22(50):8125-8136.

(301) Moshnikova A, Frye J, Shay JW, Minna JD, Khokhlatchev AV, Cuschieri L, et al. The growth and tumor suppressor NORE1A is a cytoskeletal protein that suppresses growth by inhibition of the ERK pathway. J Biol Chem 2005 03/24;281; 6; 19; 65(12; 22; 1; 1):8143; 2788; 24; 92-8152; 2794; 30; 98.

(302) Cuschieri L, Nguyen T, Vogel J, Raynaud-Messina B, Merdes A, Tommasi S, et al. Control at the cell center - The role of spindle poles in cytoskeletal organization and cell cycle regulation. Curr Opin Cell Biol 2005;6; 19; 65(22; 1; 1):2788; 24; 92-2794; 30; 98.

(303) Raynaud-Messina B, Merdes A, Tommasi S, Dammann R, Zhang ZQ, Wang Y, et al. Gamma-Tubulin Complexes and Microtubule Organization. Curr Opin Cell Biol 2005;19; 65(1; 1):24; 92-30; 98.

(304) Tommasi S, Dammann R, Zhang ZQ, Wang Y, Liu LM, Tsark WM, et al. Tumor susceptibility of Rassf1a knockout mice. Cancer Res 2005;65(1):92-98.

(305) Liu L, Vo A, McKeehan WL. Specificity of the methylation-suppressed A isoform of candidate tumor suppressor RASSF1 for microtubule hyperstabilization is determined by cell death inducer C19ORF5. Cancer Res 2005 03/01;65(5):1830-1838.

(306) Man C, Rosa J, Lee LTO, Lee VHY, Chow BKC, Lo KW, et al. Latent membrane protein 1 suppresses RASSF1A expression, disrupts microtubule structures and induces chromosomal aberrations in human epithelial cells. Oncogene 2007 05/10;26(21):3069-3080.

(307) Mondello C, Scovassi AI. Apoptosis: a way to maintain healthy individuals. Subcell Biochem 2010;50:307-323.

(308) Van Herreweghe F, Festjens N, Declercq W, Vandenabeele P, Pennarun B, Meijer A, et al. Tumor necrosis factor-mediated cell death: to break or to burst, that's the question. Cell Signal 2004;1805; 16(2; 2):123; 139-140; 144.

(309) Pennarun B, Meijer A, de Vries E, Kleibeuker JH, Kruyt F, de Jong S, et al. Playing the DISC: Turning on TRAIL death receptor-mediated apoptosis in cancer. Cell Signal 2004;1805; 16; 54; 173(2; 2; 1; 5):123; 139; 109; 2976-140; 144; 116; 2984.

(310) Thorburn A, Fischer JR, Ohnmacht U, Rieger N, Zemaitis M, Stoffregen C, et al. Death receptor-induced cell killing. Cell Signal 2004;16; 54; 173(2; 1; 5):139; 109; 2976-144; 116; 2984.

(311) Yu J, Ni M, Xu J, Zhang H, Gao B, Gu J, et al. Methylation profiling of twenty promoter-CpG islands of genes which may contribute to hepatocellular carcinogenesis. BMC Cancer 2002 01;2:29-14.

(312) Schagdarsurengin U, Wilkens L, Steinemann D, Flemming P, Kreipe HH, Pfeifer GP, et al. Frequent epigenetic inactivation of the RASSF1A gene in hepatocellular carcinoma. Oncogene 2003 03/27;22(12):1866.

(313) Jing F, Yuping W, Yong C, Jie L, Jun L, Xuanbing T, et al. CpG island methylator phenotype of multigene in serum of sporadic breast carcinoma. Tumour Biol 2004 08;31; 54; 173(4; 1; 5):321; 109; 2976-331; 116; 2984.

(314) Fischer JR, Ohnmacht U, Rieger N, Zemaitis M, Stoffregen C, Kostrzewa M, et al. Promoter methylation of RASSF1A, RAR beta and DAPK predict poor prognosis of

patients with malignant mesothelioma. Lung Cancer 2004;54; 173(1; 5):109; 2976-116; 2984.

(315) Kang TB, Ben-Moshe T, Varfolomeev EE, Pewzner-Jung Y, Yogev N, Jurewicz A, et al. Caspase-8 serves both apoptotic and nonapoptotic roles. Journal of Immunology 2004;173(5):2976-2984.

(316) Bialik S, Kimchi A. The death-associated protein kinases: structure, function, and beyond. Annu Rev Biochem 2006;75:189-210.

(317) Gozuacik D, Kimchi A. DAPk protein family and cancer. Autophagy 2006 04/20;2(2):74-79.

(318) Mor I, Carlessi R, Ast T, Feinstein E, Kimchi A, Bialik S, et al. Death-associated protein kinase increases glycolytic rate through binding and activation of pyruvate kinase. Oncogene 2008;7(6; 6):683; 1089-1098.

(319) Bialik S, Berissi H, Kimchi A, Song SJ, Kim SJ, Song MS, et al. A high throughput proteomics screen identifies novel substrates of death-associated protein kinase. Cancer Res 2009;7; 69; 27(6; 22; 12):1089; 8540; 680-1098; 8544; 688.

(320) Song SJ, Kim SJ, Song MS, Lim DS, Demon D, Van Damme P, et al. Aurora B-Mediated Phosphorylation of RASSF1A Maintains Proper Cytokinesis by Recruiting Syntaxin16 to the Midzone and Midbody. Cancer Res 2009;69; 27(22; 12):8540; 680-8544; 688.

(321) Demon D, Van Damme P, Vanden Berghe T, Vandekerckhove J, Declercq W, Gevaert K, et al. Caspase substrates: easily caught in deep waters? Trends Biotechnol 2009;27(12):680-688.

(322) Riedl SJ, Shi Y. Molecular mechanisms of caspase regulation during apoptosis. Nature Reviews Molecular Cell Biology 2004 11;5(11):897-907.

(323) Donninger H, Allen N, Henson A, Pogue J, Williams A, Gordon L, et al. Salvador protein is a tumor suppressor effector of RASSF1A with hippo pathway-independent functions. J Biol Chem 2011 05/27;286(21):18483-18491.

(324) Yi M, Yang J, Chen X, Li J, Li X, Wang L, et al. RASSF1A suppresses melanoma development by modulating apoptosis and cell-cycle progression. J Cell Physiol 2011 09;226(9):2360-2369.

(325) Min SS, Su JS, Ayad NG, Jin SC, Joo HL, Hyun KH, et al. The tumour suppressor RASSF1A regulates mitosis by inhibiting the APC-Cdc20 complex. Nat Cell Biol 2004 02;6(2):129-137.

(326) Whitehurst AW, Ram R, Shivakumar L, Gao B, Minna JD, White MA. The RASSF1A tumor suppressor restrains anaphase-promoting complex/cyclosome activity during the G1/S phase transition to promote cell cycle progression in human epithelial cells. Mol Cell Biol 2008 05;28(10):3190-3197.

(327) Liu L, Baier K, Dammann R, Pfeifer GP, Chow C, Wong N, et al. The tumor suppressor RASSF1A does not interact with Cdc20, an activator of the anaphase-promoting complex. Cell Cycle 2007 07/01;6; 31; 64; 286(13; 15; 1; 9):1663; 1975; 102; 6971-1665; 1987; 107; 6978.

(328) Chow C, Wong N, Pagano M, Lun S, Nakayama KI, Nakayama K, et al. Regulation of APC/C-Cdc20 activity by RASSF1A-APC/C-Cdc20 circuitry. Oncogene 2012;31; 64; 286(15; 1; 9):1975; 102; 6971-1987; 107; 6978.

(329) Mochizuki T, Furuta S, Mitsushita J, Shang WH, Ito M, Yokoo Y, et al. Inhibition of NADPH oxidase 4 activates apoptosis via the AKT/apoptosis signal-regulating kinase 1 pathway in pancreatic cancer PANC-1 cells. Oncogene 2006 06/22;25; 30; 25(26; 10; 14):3699; 4269; 3286-3707; 4281; 3297.

(330) Fenton SL, Dallol A, Agathanggelou A, Hesson L, Ahmed-Choudhury J, Baksh S, et al. Identification of the E1A-regulated transcription factor p120(E4F) as an interacting partner of the RASSF1A candidate tumor suppressor gene. Cancer Res 2004;64; 286(1; 9):102; 6971-107; 6978.

(331) Jiang LY, Rong R, Sheikh MS, Huang Y. Cullin-4A.DNA Damage-binding Protein 1 E3 Ligase Complex Targets Tumor Suppressor RASSF1A for Degradation during Mitosis. J Biol Chem 2011;286(9):6971-6978.

(332) Dreijerink K, Braga E, Kuzmin I, Geil L, Duh F, Angeloni D, et al. The Candidate Tumor Suppressor Gene, RASSF1A, from Human Chromosome 3p21.3 is Involved in Kidney Tumorigenesis. Proc Natl Acad Sci U S A 2006;274; 441; 23; 291(13; 53; 35; 6):7504; 37538; 227; 5941; L1185-37543; 236; 5949; L1190.

(333) Kim ST, Lim DS, Canman CE, Kastan MB, Zhou X, Li TT, et al. Substrate specificities and identification of putative substrates of ATM kinase family members. J Biol Chem 2011;274; 441; 23; 291; 67; 11(53; 35; 6; 3):37538; 227; 5941; L1185; 1054-37543; 236; 5949; L1190; 1061.

(334) Dammann R, Li C, Yoon J, Chin PL, Bates S, Pfeifer GP. Epigenetic inactivation of a RAS association domain family protein from the lung tumour suppressor locus 3p21.3. Nat Genet 2000 07;25(3):315.

(335) Zhou X, Li TT, Feng X, Hsiang E, Xiong Y, Guan KL, et al. Targeted polyubiquitylation of RASSF1C by the Mule and SCF beta-TrCP ligases in response to DNA damage. Biochem J 2011;441; 23; 291; 67; 11(35; 6; 3):227; 5941; L1185; 1054-236; 5949; L1190; 1061.

(336) Li JF, Wang FL, Protopopov A, Malyukova A, Kashuba V, Minna JD, et al. Inactivation of RASSF1C during in vivo tumor growth identifies it as a tumor suppressor gene. Oncogene 2011;23; 291; 67; 11(35; 6; 3):5941; L1185; 1054-5949; L1190; 1061.

(337) Amaar YG, Minera MG, Hatran LK, Strong DD, Mohan S, Reeves ME, et al. Ras association domain family 1C protein stimulates human lung cancer cell proliferation. Cancer Res 2011;291; 67; 11(6; 3):L1185; 1054-L1190; 1061.

(338) Reeves ME, Baldwin SW, Baldwin ML, Chen S, Moretz JM, Aragon RJ, et al. Ras-association domain family 1C protein promotes breast cancer cell migration and attenuates apoptosis. BMC Cancer 2011 01;10; 67; 11(3):562; 1054-575; 1061.

(339) Estrabaud E, Lassot I, Blot G, Le Rouzic E, Tanchou V, Quemeneur E, et al. RASSF1C, an isoform of the tumor suppressor RASSF1A, promotes the accumulation of beta-catenin by interacting with betaTrCP. Cancer Res 2007 02/01;67(3):1054-1061.

(340) Malpeli G, Amato E, Dandrea M, Fumagalli C, Debattisti V, Boninsegna L, et al. Methylation-associated down-regulation of RASSF1A and up-regulation of RASSF1C in pancreatic endocrine tumors. BMC Cancer 2011;11.

(341) Knudson AG, J. Mutation and cancer: statistical study of retinoblastoma. Proc Natl Acad Sci U S A 1971 04;68(4):820-823.

(342) Volodko N, Gordon M, Salla M, Ghazaleh HA, Baksh S. RASSF tumor suppressor gene family: Biological functions and regulation. FEBS Lett 2014(16):2671.

(343) Agathanggelou A, Honorio S, Macartney DP, Martinez A, Dallol A, Rader J, et al. Methylation associated inactivation of RASSF1A from region 3p21.3 in lung, breast and ovarian tumours. Oncogene 2001 03/22;20(12):1509.

(344) An B, Kondo Y, Okamoto Y, Shinjo K, Kanemitsu Y, Komori K, et al. Characteristic methylation profile in CpG island methylator phenotype-negative distal colorectal cancers. Int J Cancer 2010 11/01;127(9):2095-2105.

(345) Ahlquist T, Bottillo I, Danielsen SA, Meling GI, Rognum TO, Lind GE, et al. RAS signaling in colorectal carcinomas through alteration of RAS, RAF, NF1, and/or RASSF1A. Neoplasia 2008 07;10(7):680.

(346) Oliveira C, Velho S, Domingo E, Preto A, Hofstra RMW, Hamelin R, et al. Concomitant RASSF1A hypermethylation and KRAS/BRAF mutations occur preferentially in MSI sporadic colorectal cancer. Oncogene 2005 11/17;24(51):7630-7634.

(347) Sakamoto N, Terai T, Ajioka Y, Abe S, Kobayasi O, Hirai S, et al. Frequent hypermethylation of RASSF1A in early flat-type colorectal tumors. Oncogene 2004 11/25;23(55):8900-8907.

(348) Wagner KJ, Cooper WN, Grundy RG, Caldwell G, Jones C, Wadey RB, et al. Frequent RASSF1A tumour suppressor gene promoter methylation in Wilms' tumour and colorectal cancer. Oncogene 2002 10/17;21(47):7277-7282.

(349) Wang YC, Yu ZH, Liu C, Xu LZ, Yu W, Lu J, et al. Detection of RASSF1A promoter hypermethylation in serum from gastric and colorectal adenocarcinoma patients. World Journal of Gastroenterology 2008 05/21;14(19):3074.

(350) Zhao B, Li L, Guan KL. Hippo signaling at a glance. J Cell Sci 2010;123(23):4001-4006.

(351) Zhao B, Li L, Lei QY, Guan KL. The Hippo-YAP pathway in organ size control and tumorigenesis: an updated version. Genes Dev 2010;24(9):862-874.

(352) Lamar JM, Stern P, Liu H, Schindler JW, Jiang ZG, Hynes RO, et al. The Hippo pathway target, YAP, promotes metastasis through its TEAD-interaction domain. Proc Natl Acad Sci U S A 2010;109; 123(37; 23):E2441; 4001-E2450; 4006.

(353) Avruch J, Zhou DW, Bardeesy N. YAP oncogene overexpression supercharges colon cancer proliferation. Cell Cycle 2012;11(6):1090-1096.

(354) Fausti F, Agostino SD, Sacconi A, Strano S, Blandino G. Hippo and rassf1a Pathways: A Growing Affair. Molecular Biology International 2012;2012:2090-2182.

(355) Guo C, Tommasi S, Liu L, Yee J, Dammann R, Pfeifer GP. RASSF1A is part of a complex similar to the Drosophila Hippo/Salvador/Lats tumor-suppressor network. Curr Biol 2007 04/17;17(8):700-705.

(356) Zhao B, Wei X, Li W, Udan RS, Yang Q, Kim J, et al. Inactivation of YAP oncoprotein by the Hippo pathway is involved in cell contact inhibition and tissue growth control. Genes Dev 2007;21(21):2747-2761.

(357) Zhao B, Lei Q, Guan K. The Hippo-YAP pathway: new connections between regulation of organ size and cancer. Curr Opin Cell Biol 2008 12;20(6):638-646.

(358) Guo C, Zhang XY, Pfeifer GP. The Tumor Suppressor RASSF1A Prevents Dephosphorylation of the Mammalian STE20-like Kinases MST1 and MST2. J Biol Chem 2011;286(8):6253-6261.

(359) Dittfeld C, Richter AM, Steinmann K, Klagge-Ulonska A, Dammann RH. The SARAH Domain of RASSF1A and Its Tumor Suppressor Function. Molecular Biology International 2012 01:1-10.

(360) Konsavage,Wesley M.,,Jr, Yochum GS. Intersection of Hippo/YAP and Wnt/ß-catenin signaling pathways. Acta Biochim Biophys Sin (Shanghai) 2013 02;45(2):71-79.

(361) Konsavage,Wesley M.,,Jr, Kyler SL, Rennoll SA, Jin G, Yochum GS. Wnt/ß-catenin signaling regulates Yes-associated protein (YAP) gene expression in colorectal carcinoma cells. J Biol Chem 2012 04/06;287(15):11730-11739.

(362) Imajo M, Miyatake K, Iimura A, Miyamoto A, Nishida E. A molecular mechanism that links Hippo signalling to the inhibition of Wnt/ß-catenin signalling. EMBO J 2012 03/07;31(5):1109-1122.

(363) Rosenbluh J, Nijhawan D, Cox AG, Li X, Neal JT, Schafer EJ, et al. ß-Catenin-driven cancers require a YAP1 transcriptional complex for survival and tumorigenesis. Cell 2012 12/21;151(7):1457-1473.

(364) Levy D, Adamovich Y, Reuven N, Shaul Y. Yap1 phosphorylation by c-Abl is a critical step in selective activation of proapoptotic genes in response to DNA damage. Mol Cell 2008 02/15;29(3):350-361.

(365) Matallanas D, Romano D, Yee K, Meissl K, Kucerova L, Piazzolla D, et al. RASSF1A elicits apoptosis through an MST2 pathway directing proapoptotic transcription by the p73 tumor suppressor protein. Mol Cell 2007 09/21;27(6):962-975.

(366) Park SH, Jung JK, Jin SC, Lee SR, Gi YL, Hyung JK, et al. RASSF1A suppresses the activated K-Ras-induced oxidative DNA damage. Biochem Biophys Res Commun ;408:149-153.

(367) De Jager PL, Franchimont D, Waliszewska A, Bitton A, Cohen A, Langelier D, et al. The role of the Toll receptor pathway in susceptibility to inflammatory bowel diseases. Genes & Immunity 2007 07;8(5):387-397.

(368) Araki A, Kanai T, Ishikura T, Makita S, Uraushihara K, Iiyama R, et al. MyD88-deficient mice develop severe intestinal inflammation in dextran sodium sulfate colitis. J Gastroenterol 2005 01;40(1):16-23.

(369) Fukata M, Chen A, Vamadevan AS, Cohen J, Breglio K, Krishnareddy S, et al. Toll-like receptor-4 promotes the development of colitis-associated colorectal tumors. Gastroenterology 2007 12;133(6):1869-1881.

(370) Parasuraman S, Raveendran R, Kesavan R. Blood sample collection in small laboratory animals. J Pharmacol Pharmacother 2010 07;1(2):87-93.

(371) Xiao H, Gulen MF, Qin JZ, Yao JH, Bulek K, Kish D, et al. The Toll-interleukin-1 receptor member SIGIRR regulates colonic epithelial homeostasis, inflammation, and tumorigenesis. Immunity 2007;26; 276(4; 22):461; 19276-475; 19285.

(372) Booth C, Patel S, Bennion GR, Potten CS. The isolation and culture of adult mouse colonic epithelium. Epithelial Cell Biol 1995;4(2):76-86.

(373) Hoffman AG, Kuksis A. Improved isolation of villus and crypt cells from rat small intestinal mucosa. Can J Physiol Pharmacol 1979 08;57(8):832-842.

(374) Baksh S, Widlund HR, Frazer-Abel A, Du J, Fosmire S, Fisher DE, et al. NFATc2-mediated repression of cyclin-dependent kinase 4 expression. Mol Cell 2001 11;10; 26; 276(5; 4; 22):1071; 461; 19276-1081; 475; 19285.

(375) Meira LB, Bugni JM, Green SL, Lee C, Pang B, Borenshtein D, et al. DNA damage induced by chronic inflammation contributes to colon carcinogenesis in mice. J Clin Invest 2008 07;118(7):2516-2525.

(376) Steinhardt AA, Gayyed MF, Klein AP, Dong JX, Maitra A, Pan D, et al. Expression of Yes-associated protein in common solid tumors. Hum Pathol 2008;39(11):1582-1589.

(377) Wang H, Joseph JA. Quantifying cellular oxidative stress by dichlorofluorescein assay using microplate reader. Free Radic Biol Med 1999.

(378) Livak KJ, Schmittgen TD, Steinhardt AA, Gayyed MF, Klein AP, Dong JX, et al. Analysis of relative gene expression data using real-time quantitative PCR and the 2(T)(-Delta Delta C) method. Methods 2008;25; 39(4; 11):402; 1582-408; 1589.

(379) El-Kalla M. Biological role of the tumor suppressor protein, RASSF1A in inflammation and cancer [electronic resource]. : 2010; 2010.

(380) Zhao Y. Role of RASSF1A in intestinal inflammation [electronic resource]. : 2011; 2011.

(381) Tommasi S, Besaratinia A, Wilczynski SP, Pfeifer GP. Loss of Rassf1a enhances p53-mediated tumor predisposition and accelerates progression to aneuploidy. Oncogene 2011 02/10;30(6):690-700.

(382) Al-Sohaily S, Biankin A, Leong R, Kohonen-Corish M, Warusavitarne J, Stamos JL, et al. Molecular pathways in colorectal cancer. J Gastroenterol Hepatol 2012;5; 31(9; 1; 12):1423; 2714-2736.

(383) Stamos JL, Weis WI, Valenta T, Hausmann G, Basler K. The beta-Catenin Destruction Complex. EMBO J 2012;5; 31(1; 12):2714-2736.

(384) Valenta T, Hausmann G, Basler K. The many faces and functions of beta-catenin. EMBO J 2012;31(12):2714-2736.

(385) March HN, Rust AG, Wright NA, Hoeve Jt, de Ridder J, Eldridge M, et al. Insertional mutagenesis identifies multiple networks of cooperating genes driving intestinal tumorigenesis. Nat Genet 2011(12):1202.

(386) van der Weyden L, Arends MJ, Dovey OM, Harrison HL, Lefebvre G, Conte N, et al. Loss of Rassf1a cooperates with Apc^{Min} to accelerate intestinal tumourigenesis. Oncogene 2008 07/24;27(32):4503-4508.

(387) Law J, Yu VC, Baksh S. Modulator of Apoptosis 1: A Highly Regulated RASSF1A-Interacting BH3-Like Protein. Molecular Biology International 2012 01:1-10.

(388) Rakoff-Nahoum S, Medzhitov R. Toll-like receptors and cancer. Nature Reviews Cancer 2009(1):57.

(389) Allen NPC, Donninger H, Vos MD, Eckfeld K, Hesson L, Gordon L, et al. RASSF6 is a novel member of the RASSF family of tumor suppressors. Oncogene 2007 09/13;26(42):6203-6211.

(390) Lock FE, Underhill-Day N, Dunwell T, Matallanas D, Cooper W, Hesson L, et al. The RASSF8 candidate tumor suppressor inhibits cell growth and regulates the Wnt and NF-kappaB signaling pathways. Oncogene 2012 07/29;29; 31(30; 5):4307; 1147-4316; 1159.

(391) Song H, Kim H, Lee K, Lee DH, Kim TS, Song JY, et al. Ablation of Rassf2 induces bone defects and subsequent haematopoietic anomalies in mice. EMBO J 2012;31(5):1147-1159.

(392) Braconi C, Huang N, Patel T. MicroRNA-dependent regulation of DNA methyltransferase-1 and tumor suppressor gene expression by interleukin-6 in human malignant cholangiocytes. Hepatology 2010 03;51(3):881-890.

(393) Foran E, Garrity-Park M, Mureau C, Newell J, Smyrk TC, Limburg PJ, et al. Upregulation of DNA methyltransferase-mediated gene silencing, anchorage-independent growth, and migration of colon cancer cells by interleukin-6. Mol Cancer Res 2010 04;8(4):471-481.

(394) Stenson WF. Hyaluronic acid and intestinal inflammation. Curr Opin Gastroenterol 2010 03;26(2):85-87.

(395) Zheng L, Riehl TE, Stenson WF. Basic—Alimentary Tract: Regulation of Colonic Epithelial Repair in Mice by Toll-Like Receptors and Hyaluronic Acid. Gastroenterology 2009;137(6):2041-2051.

(396) Crosby LM, Waters CM. Epithelial repair mechanisms in the lung. Am J Physiol 2010(6):715.

(397) Ren F, Wang B, Yue T, Yun E, Ip YT, Jiang J, et al. Hippo signaling regulates Drosophila intestine stem cell proliferation through multiple pathways. Proc Natl Acad Sci U S A 2010;24(49; 21):21064; 2383-2388.

(398) Cai J, Zhang NL, Zheng YG, de Wilde R, Maitra A, Pan DJ, et al. The Hippo signaling pathway restricts the oncogenic potential of an intestinal regeneration program. Genes Dev 2011;24; 16(21; 8):2383; 808-2388; 821.

(399) Levy D, Adamovich Y, Reuven N, Shaul Y, Zhang H, Wu SN, et al. The Yes-associated protein 1 stabilizes p73 by preventing Itch-mediated ubiquitination of p73. Apoptosis 2011 04;14; 16(4; 8):743; 808-751; 821.

(400) Zhang H, Wu SN, Xing D. YAP accelerates A beta(25-35)-induced apoptosis through upregulation of Bax expression by interaction with p73. Apoptosis 2011;16(8):808-821.

(401) Tamm C, Böwer N, Annerén C. Regulation of mouse embryonic stem cell self-renewal by a Yes-YAP-TEAD2 signaling pathway downstream of LIF. 2011; .

(402) Colgan SP, Taylor CT. Hypoxia: an alarm signal during intestinal inflammation. Nature Reviews Gastroenterology & Hepatology 2010(5):281.

(403) Almenier HA, Al Menshawy H,H., Maher MM, Al Gamal S. Oxidative stress and inflammatory bowel disease. Front Biosci (Elite Ed) 2012 01/01;4:1335-1344.

(404) Deininger M, Buchdunger E, Druker BJ. The development of imatinib as a therapeutic agent for chronic myeloid leukemia. Blood 2005 04/01;105(7):2640-2653.

(405) Barilà D, Rufini A, Condò I, Ventura N, Dorey K, Superti-Furga G, et al. Caspase-dependent cleavage of c-Abl contributes to apoptosis. Mol Cell Biol 2003 04;23(8):2790-2799.

(406) Machuy N, Rajalingam K, Rudel T, Goldberg Z, Vogt Sionov R, Berger M, et al. Requirement of caspase-mediated cleavage of c-Abl during stress-induced apoptosis. EMBO J 2002 03;11; 21(3; 14):290; 3715-300; 3727.

(407) Goldberg Z, Vogt Sionov R, Berger M, Zwang Y, Perets R, Van Etten R, et al. Tyrosine phosphorylation of Mdm2 by c-Abl: implications for p53 regulation. EMBO J 2009;21; 141; 8(14; 5; 1):3715; 1566; 49-3727; U88; 57.

(408) Saleh M, Trinchieri G, van Limbergen J, Philpott D, Griffiths AM. Innate immune mechanisms of colitis and colitis-associated colorectal cancer. Gastroenterology 2011;141(1; 5):9; 1566-U88.

(409) van Limbergen J, Philpott D, Griffiths AM, Bertini E, Oka T, Sudol M, et al. Genetic Profiling in Inflammatory Bowel Disease: From Association to Bedside. Gastroenterology 2009;141; 8(5; 1):1566; 49-U88; 57.

(410) Sudol M, Bork P, Einbond A, Kastury K, Druck T, Negrini M, et al. Characterization of the mammalian YAP (Yes-associated protein) gene and its role in

defining a novel protein module, the WW domain. J Biol Chem 2009 06/16;270; 8(24; 1):14733; 49-14741; 57.

(411) Bertini E, Oka T, Sudol M, Strano S, Blandino G. YAP At the crossroad between transformation and tumor suppression. Cell Cycle 2009;8(1):49-57.

(412) Basu S, Totty NF, Irwin MS, Sudol M, Downward J. Akt phosphorylates the Yes-associated protein, YAP, to induce interaction with 14-3-3 and attenuation of p73-mediated apoptosis. Mol Cell 2003 01;11(1):11-23.

(413) Hodge DR, Cho E, Copeland TD, Guszczynski T, Yang E, Seth AK, et al. IL-6 enhances the nuclear translocation of DNA cytosine-5-methyltransferase 1 (DNMT1) via phosphorylation of the nuclear localization sequence by the AKT kinase. Cancer Genomics Proteomics 2007 11/20;4(6):387-398.

(414) Liao X, Siu MK, Chan KY, Wong ES, Ngan HY, Chan QK, et al. Hypermethylation of RAS effector related genes and DNA methyltransferase 1 expression in endometrial carcinogenesis. Int J Cancer 2006 07/15;123; 26(2; 12):296; 4421-302; 4434.

(415) Deng XM, Gao FQ, Flagg T, Anderson J, May WS, Schlegelmilch K, et al. Bcl2's flexible loop domain regulates p53 binding and survival. Mol Cell Biol 2003;26; 144; 52(12; 5; 9):4421; 782; 1297-4434; 795; 1303.

(416) Zhou D, Zhang Y, Wu H, Barry E, Yin Y, Lawrence E, et al. Mst1 and Mst2 protein kinases restrain intestinal stem cell proliferation and colonic tumorigenesis by inhibition of Yes-associated protein (Yap) overabundance. Proc Natl Acad Sci U S A 2011(49):19463.

(417) Schlegelmilch K, Mohseni M, Kirak O, Pruszak J, Rodriguez JR, Zhou DW, et al. Yap1 Acts Downstream of alpha-Catenin to Control Epidermal Proliferation. Cell 2003;144; 52(5; 9):782; 1297-795; 1303.

(418) Goretsky T, Dirisina R, Sinh P, Mittal N, Managlia E, Williams DB, et al. p53 mediates TNF-induced epithelial cell apoptosis in IBD. Am J Pathol 2012 10;181(4):1306-1315.

(419) Dirisina R, Katzman RB, Goretsky T, Managlia E, Mittal N, Williams DB, et al. p53 and PUMA independently regulate apoptosis of intestinal epithelial cells in patients and mice with colitis. Gastroenterology 2011 09;141(3):1036-1045.

(420) Kjellev S. The trefoil factor family – small peptides with multiple functionalities. Cellular & Molecular Life Sciences 2009 04/15;66(8):1350-1369.

(421) Loncar MB, Al-azzeh E, Sommer P, Marinovic M, Schmehl K, Kruschewski M, et al. Tumour necrosis factor alpha and nuclear factor kappa B inhibit transcription of human TFF3 encoding a gastrointestinal healing peptide. Gut 2003;52(9):1297-1303.

(422) Scrace SF, O'Neill E. RASSF Signalling and DNA Damage: Monitoring the Integrity of the Genome? Molecular Biology International 2012 01:1-11.

(423) Biasi F, Poli G, Oteiza PI, Leonarduzzi G. Inflammatory bowel disease: mechanisms, redox considerations, and therapeutic targets. Antioxidants & Redox Signaling 2013(14):1711.

(424) Roessner A, Kuester D, Malfertheiner P, Schneider-Stock R. Oxidative stress in ulcerative colitis-associated carcinogenesis. Pathology - Research & Practice 2008 07/25;204(7):511-524.

(425) Anwar A, Keating AK, Joung D, Sather S, Kim GK, Sawczyn KK, et al. Mer tyrosine kinase (MerTK) promotes macrophage survival following exposure to oxidative stress. J Leukoc Biol 2012 07;86; 445(1):73; 255-79; 264.

(426) Lin Q, Wang J, Childress C, Yang WN, Zhang HL, He J, et al. The activation mechanism of ACK1 (activated Cdc42-associated tyrosine kinase 1). Biochem J 2013;445; 27(1):255; 232-264; 242.

(427) Mahajan NP, Liu Y, Majumder S, Warren MR, Parker CE, Mohler JL, et al. Activated Cdc42-Associated Kinase Ack1 Promotes Prostate Cancer Progression via Androgen Receptor Tyrosine Phosphorylation. Proc Natl Acad Sci U S A 2007(20):8438.

(428) Magro F, Costa C. Long-standing remission of Crohn's disease under imatinib therapy in a patient with Crohn's disease. Inflamm Bowel Dis 2006;12(11):1087-1089.

(429) Miranda E, Destro A, Malesci A, Balladore E, Bianchi P, Baryshnikova E, et al. Genetic and epigenetic changes in primary metastatic and nonmetastatic colorectal cancer. Br J Cancer 2006 10/23;95(8):1101-1107.

(430) Gonzalo V, Lozano JJ, Muñoz J, Balaguer F, Pellisé M, de Miguel CR, et al. Aberrant Gene Promoter Methylation Associated with Sporadic Multiple Colorectal Cancer. PLoS ONE 2010 01;5(1):1-8.

(431) Dong SM, Lee EJ, Jeon ES, Park CK, Kim KM. Progressive methylation during the serrated neoplasia pathway of the colorectum. Modern Pathology 2005;18(2):170-178.

(432) Oren M, Aylon Y. The hippo signaling pathway and cancer [electronic resource] / Moshe Oren, Yael Aylon, editors. : New York, NY : Springer, c2013; 2013.

(433) Wang L, Shi S, Guo Z, Zhang X, Han S, Yang A, et al. Overexpression of YAP and TAZ Is an Independent Predictor of Prognosis in Colorectal Cancer and Related to the Proliferation and Metastasis of Colon Cancer Cells. PLoS ONE 2013 06;8(6):1-12.

(434) Ding S, Walton KLW, Blue RE, MacNaughton K, Magness ST, Lund PK, et al. Mucosal Healing and Fibrosis after Acute or Chronic Inflammation in Wild Type FVB-N Mice and C57BL6 Procollagen a1(I)-Promoter-GFP Reporter Mice. PLoS ONE 2012 08;7(8):1-16.

(435) Hodge DR, Peng B, Cherry JC, Hurt EM, Fox SD, Kelley JA, et al. Interleukin 6 supports the maintenance of p53 tumor suppressor gene promoter methylation. Cancer Res 2003 06/01;65; 63(11; 22):4673; 7641-4682; 7645.

(436) Kulis M, Esteller M. DNA methylation and cancer. Adv Genet 2010;70:27-56.

(437) Muller HM, Widschwendter A, Fiegl H, Ivarsson L, Goebel G, Perkmann E, et al. DNA methylation in serum of breast cancer patients: An independent prognostic marker. Cancer Res 2003;63(22):7641-7645.

(438) Rogakou EP, Nieves-Neira W, Boon C, Pommier Y, Bonner WM. Initiation of DNA fragmentation during apoptosis induces phosphorylation of H2AX histone at serine 139. J Biol Chem 2000 03/31;275(13):9390-9395.

(439) Sharma A, Singh K, Almasan A. Histone H2AX phosphorylation: a marker for DNA damage. Methods Mol Biol 2012;920:613-626.

(440) Brierley DJ, Martin SA. Oxidative stress and the DNA mismatch repair pathway. Antioxid Redox Signal 2013 06/20;18(18):2420-2428.

(441) Sosa V, Moliné T, Somoza R, Paciucci R, Kondoh H, LLeonart ME, et al. Oxidative stress and cancer: an overview. Ageing Res Rev 2013 01;12; 12(1; 12):376; 931-390; 947.

(442) Gorrini C, Harris IS, Mak TW. Modulation of oxidative stress as an anticancer strategy. Nature Reviews Drug Discovery 2013;12(12):931-947.

(443) Choi AM, Alam J. Heme oxygenase-1: function, regulation, and implication of a novel stress-inducible protein in oxidant-induced lung injury. Am J Respir Cell Mol Biol 1996 07;15(1):9-19.

(444) Datla SR, Dusting GJ, Mori TA, Taylor CJ, Croft KD, Jiang F. Induction of Heme Oxygenase-1 In Vivo Suppresses NADPH Oxidase--Derived Oxidative Stress. Hypertension (0194911X) 2007 10;50(4):636-642.

(445) Le WD, Xie WJ, Appel SH. Protective role of heme oxygenase-1 in oxidative stress-induced neuronal injury. J Neurosci Res 1999 06/15;56(6):652-658.

(446) Reinecker HC, Loh EY, Ringler DJ, Mehta A, Rombeau JL, MacDermott RP, et al. Monocyte-chemoattractant protein 1 gene expression in intestinal epithelial cells and

inflammatory bowel disease mucosa. Gastroenterology 1996 01;108; 59(1; 6):40; 804-50; 812.

(447) Grimm MC, Elsbury S, Pavli P, Doe WF, McClellan JL, Davis JM, et al. Enhanced expression and production of monocyte chemoattractant protein-1 in inflammatory bowel disease mucosa. J Leukoc Biol 2005;59; 303; 25(6; 10; 5):804; G1087; 3581-812; G1095; 3584.

(448) McClellan JL, Davis JM, Steiner JL, Enos RT, Jung SH, Carson JA, et al. Linking tumor-associated macrophages, inflammation, and intestinal tumorigenesis: role of MCP-1. Anticancer Res 2005;303; 25(10; 5):G1087; 3581-G1095; 3584.

(449) Baier PK, Eggstein S, Wolff-Vorbeck G, Baumgartner U, Hopt UT. Chemokines in human colorectal carcinoma. Anticancer Res 2005;25(5):3581-3584.

(450) Kubiczkova L, Sedlarikova L, Hajek R, Sevcikova S. TGF-ß -- an excellent servant but a bad master. Journal of Translational Medicine 2012 01;10(1):183-206.

(451) Massagué J. TGFß signalling in context. Nat Rev Mol Cell Biol 2012 10;13(10):616-630.

(452) Guan F, Schaffer L, Handa K, Hakomori S. Functional role of gangliotetraosylceramide in epithelial-to-mesenchymal transition process induced by hypoxia and by TGF-{beta}. FASEB J 2010 12;24(12):4889-4903.

(453) Ikushima H, Miyazono K. TGFbeta signalling: a complex web in cancer progression. Nat Rev Cancer 2010 06;10(6):415-424.

(454) Zhang XL, Topley N, Ito T, Phillips A. Interleukin-6 regulation of transforming growth factor (TGF)-beta receptor compartmentalization and turnover enhances TGF-beta1 signaling. J Biol Chem 2005 04/01;280(13):12239-12245.

(455) Chen RH, Chang MC, Su YH, Tsai YT, Kuo ML. Interleukin-6 inhibits transforming growth factor-beta-induced apoptosis through the phosphatidylinositol 3-kinase/Akt and signal transducers and activators of transcription 3 pathways. J Biol Chem 1999 08/13;274(33):23013-23019.

(456) Talbot LJ, Bhattacharya SD, Kuo PC. Epithelial-mesenchymal transition, the tumor microenvironment, and metastatic behavior of epithelial malignancies. Int J Biochem Mol Biol 2012;3(2):117-136.

(457) Attisano L, Wrana JL. Signal integration in TGF-β, WNT, and Hippo pathways. F1000Prime Rep 2013 06/03;5:17-17.

(458) Arzumanyan A, Reis HMGPV, Feitelson MA. Pathogenic mechanisms in HBV- and HCV-associated hepatocellular carcinoma. Nature Reviews Cancer 2013 02;13(2):123-135.

(459) Ma J, Liu J, Wang Z, Gu X, Fan Y, Zhang W, et al. NF-kappaB-dependent MicroRNA-425 upregulation promotes gastric cancer cell growth by targeting PTEN upon IL-1ß induction. Molecular Cancer 2014 03;13(1):1-22.

(460) Kondoh M, Ohga N, Akiyama K, Hida Y, Maishi N, Towfik AM, et al. Hypoxia-induced reactive oxygen species cause chromosomal abnormalities in endothelial cells in the tumor microenvironment. PLoS One 2013 11/15;8(11):e80349-e80349.

(461) Gilbert LA. DNA-damage-mediated remodeling of normal and tumor microenvironments modulates cell survival. Massachusetts Institute of Technology 2012 20141003;2012.

(462) Kuo LJ, Yang LX. gamma-H2AX - A novel biomarker for DNA double-strand breaks. In Vivo 2008;22(3):305-309.

(463) Matallanas D, Romano D, Yee K, Meissl K, Kucerova L, Piazzolla D, et al. RASSF1A elicits apoptosis through an MST2 pathway directing proapoptotic transcription by the p73 tumor suppressor protein. Mol Cell 2011 09/21;27; 144(6; 5):962; 782-975; 795.

(464) Bansal S, Biswas G, Avadhani NG. Mitochondria-targeted heme oxygenase-1 induces oxidative stress and mitochondrial dysfunction in macrophages, kidney fibroblasts and in chronic alcohol hepatotoxicity. Redox Biol 2013 07/23;2:273-283.

(465) Kitayner M, Rozenberg H, Kessler N, Rabinovich D, Shaulov L, Haran TE, et al. Structural Basis of DNA Recognition by p53 Tetramers. Mol Cell 2006(6):741.

(466) McLure KG, Lee PW. How p53 binds DNA as a tetramer. EMBO J 1998 06/15;17(12):3342-3350.

(467) Chan WM, Siu WY, Lau A, Poon R, Bom A, Rangel LP, et al. How many mutant p53 molecules are needed to inactivate a tetramer? Mol Cell Biol 2012;24; 287(8; 33):3536; 28152-3551; 28162.

(468) Bom A, Rangel LP, Costa D, de Oliveira G, Sanches D, Braga CA, et al. Mutant p53 Aggregates into Prion-like Amyloid Oligomers and Fibrils Implications for Cancer. J Biol Chem 2012;287(33):28152-28162.

(469) Xu J, Reumers J, Couceiro JR, De Smet F, Gallardo R, Rudyak S, et al. Gain of function of mutant p53 by coaggregation with multiple tumor suppressors. Nat Chem Biol 2011 05;7(5):285-295.

(470) Gambino V, De Michele G, Venezia O, Migliaccio P, Dall'Olio V, Bernard L, et al. Oxidative stress activates a specific p53 transcriptional response that regulates cellular senescence and aging. Aging Cell 2013 06;12(3):435-445.

(471) Gudkov AV, Gurova KV, Komarova EA. Inflammation and p53: A Tale of Two Stresses. Genes Cancer 2011 04;2(4):503-516.

(472) Lowe JM, Menendez D, Bushel PR, Shatz M, Kirk EL, Troester MA, et al. p53 and NF-κB coregulate proinflammatory gene responses in human macrophages. Cancer Res 2014 04/15;74(8):2182-2192.

(473) Portwine C. P53--the Link between Inflammation and Cancer? Pediatr Res 2000 05;47(5):573-573.

(474) Matsumoto S, Hara T, Mitsuyama K, Yamamoto M, Tsuruta O, Sata M, et al. Essential Roles of IL-6 Trans-Signaling in Colonic Epithelial Cells, Induced by the IL-6/Soluble-IL-6 Receptor Derived from Lamina Propria Macrophages, on the Development of Colitis-Associated Premalignant Cancer in a Murine Model. Journal of Immunology 2010;184(3):1543-1551.

(475) Troester MA, Lee MH, Carter M, Fan C, Cowan DW, Perez ER, et al. Activation of Host Wound Responses in Breast Cancer Microenvironment. Clinical Cancer Research 2009;15(22):7020-7028.

(476) Gialeli C, Theocharis AD, Karamanos NK. Roles of matrix metalloproteinases in cancer progression and their pharmacological targeting. FEBS Journal 2011 01;278(1):16-27.

(477) Kessenbrock K, Plaks V, Werb Z. Matrix Metalloproteinases: Regulators of the Tumor Microenvironment. Cell 2010;141(1):52-67.

(478) Said AH, Raufman J, Xie G. The Role of Matrix Metalloproteinases in Colorectal Cancer. Cancers 2014 03;6(1):366-375.

(479) Strano S, Fausti F, Di Agostino S, Sudol M, Blandino G, Bernardi R, et al. PML surfs into HIPPO tumor suppressor pathway. Frontiers in Oncology 2013 03;3:1-10.

(480) Ito Y. Oncogenic potential of the RUNX gene family: 'Overview'. Oncogene 2004 05/24;23(24):4198-4208.

(481) Levy D, Reuven N, Shaul Y. A regulatory circuit controlling itch-mediated p73 degradation by Runx. J Biol Chem 2008;283(41):27462-27468.

(482) Oh H, Irvine KD, Lee KK, Yonehara S. In vivo analysis of Yorkie phosphorylation sites. Oncogene 2012 04/30;28; 287(17; 12):1916; 9568-1927; 9578.

(483) Lee KK, Yonehara S. Identification of Mechanism That Couples Multisite Phosphorylation of Yes-associated Protein (YAP) with Transcriptional Coactivation and Regulation of Apoptosis. J Biol Chem 2012;287(12):9568-9578.

(484) Asher G, Tsvetkov P, Kahana C, Shaul Y. A mechanism of ubiquitin-independent proteasomal degradation of the tumor suppressors p53 and p73. Genes Dev 2005 02/01;19(3):316-321.

(485) Tsvetkov P, Myers N, Moscovitz O, Sharon M, Prilusky J, Shaul Y. Thermo-resistant intrinsically disordered proteins are efficient 20S proteasome substrates. Molecular Biosystems 2012;8(1):368-373.

(486) Tsvetkov P, Reuven N, Shaul Y. The nanny model for IDPs. Nature Chemical Biology 2009 11;5(11):778-781.

(487) Liang K, Zhou G, Zhang Q, Li J, Zhang C, Pobbati AV, et al. Expression of hippo pathway in colorectal cancer. Cancer Biology & Therapy 2013;14(3; 5):390-398.

(488) Pobbati AV, Hong WJ. Emerging roles of TEAD transcription factors and its coactivators in cancers. Cancer Biology & Therapy 2013;14(5):390-398.

(489) Pratap J, Lian JB, Javed A, Barnes GL, van Wijnen A, Stein JL, et al. Regulatory roles of Runx2 in metastatic tumor and cancer cell interactions with bone. Cancer Metastasis Rev 2006;25(4):589-600.

(490) Chuang LS, Ito K, Ito Y. RUNX family: Regulation and diversification of roles through interacting proteins. International Journal of Cancer 2013;132(6):1260.

(491) Ozaki T, Nakagawara A, Nagase H. RUNX Family Participates in the Regulation of p53-Dependent DNA Damage Response. International Journal of Genomics 2013(6):1260.

(492) Pefani D, Latusek R, Pires I, Grawenda AM, Yee KS, Hamilton G, et al. RASSF1A-LATS1 signalling stabilizes replication forks by restricting CDK2-mediated phosphorylation of BRCA2. Nat Cell Biol 2014 10;16(10):962-971.

(493) Enoe C, Georgiadis MP, Johnson WO. Estimation of sensitivity and specificity of diagnostic tests and disease prevalence when the true disease state is unknown. Prev Vet Med 2000;45(1-2):61-81.

(494) Pewsner D, Battaglia M, Minder C, Marx A, Bucher HC, Egger M. Ruling a diagnosis in or out with "SpPIn" and "SnNOut": a note of caution. BMJ 2004 07/24;329(7459):209-213.

(495) Ibrahim SH, Lindor KD. Current Management of Primary Sclerosing Cholangitis in Pediatric Patients. Pediatric Drugs 2011 04;13(2):87-95.

(496) Jing HN, Richard BG, Andrew JW, Catherine Ann MS. Original article—liver, pancreas, and biliary tract: Inflammatory Bowel Disease Is Associated With Poor Outcomes of Patients With Primary Sclerosing Cholangitis. Clinical Gastroenterology and Hepatology 2011;9:1092-1097.

(497) Toy E, Balasubramanian S, Selmi C, Li C, Bowlus CL. The prevalence, incidence and natural history of primary sclerosing cholangitis in an ethnically diverse population. BMC Gastroenterol 2011 07/18;11:83-83.

(498) Arnette C, Efimova N, Zhu X, Clark GJ, Kaverina I. Microtubule segment stabilization by RASSF1A is required for proper microtubule dynamics and Golgi integrity. Mol Biol Cell 2014 03;25(6):800-810.

(499) Korah R, Healy JM, Kunstman JW, Fonseca AL, Ameri AH, Prasad ML, et al. Epigenetic silencing of RASSF1A deregulates cytoskeleton and promotes malignant behavior of adrenocortical carcinoma. Molecular Cancer 2013 09;12(1):1-13.

(500) Kang J, Zhou Y, Weis TL, Liu H, Ulaszek J, Satgurunathan N, et al. Osteopontin regulates actin cytoskeleton and contributes to cell proliferation in primary erythroblasts. J Biol Chem 2008 03/14;283(11):6997-7006.

(501) Klampfer L. Cytokines, inflammation and colon cancer. Curr Cancer Drug Targets 2011 May;11(4):451-464.

(502) Apte RN, Dotan S, Elkabets M, White MR, Reich E, Carmi Y, et al. The involvement of IL-1 in tumorigenesis, tumor invasiveness, metastasis and tumor-host interactions. Cancer Metastasis Rev 2006;25(3):387-408.

(503) Matsuo Y, Sawai H, Ma J, Xu D, Ochi N, Yasuda A, et al. IL-1a secreted by colon cancer cells enhances angiogenesis: The relationship between IL-1a release and tumor cells' potential for liver metastasis. J Surg Oncol 2009 05;99(6):361.

(504) Gutman M, Fidler IJ. Biology of human colon cancer metastasis. World J Surg 1995 03/19;19(2):226-234.

(505) Patanaphan V, Salazar OM. Colorectal cancer: metastatic patterns and prognosis. South Med J 1993 01;86(1):38-41.

(506) Neurath MF, Apte RN, Dotan S, Elkabets M, White MR, Reich E, et al. Cytokines in inflammatory bowel disease. Cancer Metastasis Rev 2006;25(5; 3):329; 387-408.

(507) Kountouras J, Zavos C, Chatzopoulos D, Yarkoni S, Sagiv Y, Kaminitz A, et al. Therapy for colorectal cancer. N Engl J Med 2009 04/28;352; 58(17; 12):1820; 1705-1821; 1706.

(508) Yarkoni S, Sagiv Y, Kaminitz A, Askenasy N. Interleukin 2 targeted therapy in inflammatory bowel disease. Gut 2009;58(12):1705-1706.

(509) West GA, Matsuura T, Levine AD, Klein JS, Fiocchi C, Ruckert Y, et al. Interleukin 4 in inflammatory bowel disease and mucosal immune reactivity. Gastroenterology 1996;110; 2(6; 4):1683; 244-1695; 252.

(510) Ruckert Y, Schindler U, Heinig T, Nikolaus S, Raedler A, Schreiber S. IL-4 signaling mechanisms in inflammatory bowel disease mononuclear phagocytes. Inflamm Bowel Dis 1996;2(4):244-252.

(511) Fujino S, Andoh A, Bamba S, Ogawa A, Hata K, Araki Y, et al. Increased expression of interleukin 17 in inflammatory bowel disease. (Inflammatory Bowel Disease). Gut 2003(1):65.

(512) Wu D, Wu P, Huang Q, Liu Y, Ye J, Huang J. Interleukin-17: a promoter in colorectal cancer progression. Clin Dev Immunol 2013;2013:436307-436307.

(513) Nunes T, de Souza HS. Inflammasome in Intestinal Inflammation and Cancer. Mediators Inflamm 2013 01:1-8.

(514) Fan-Ching Lin, Young HA. The talented interferon-gamma. Advances in Bioscience and Biotechnology 2013(07):6.

(515) Leso V, Leggio L, Armuzzi A, Gasbarrini G, Gasbarrini A, Addolorato G. Role of the tumor necrosis factor antagonists in the treatment of inflammatory bowel disease: an update. Eur J Gastroenterol Hepatol 2010 07;22(7):779-786.

(516) Stobaugh DJ, Deepak P, Ehrenpreis ED. Risk of Solid Cancers With Tumor Necrosis Factor Alpha Inhibitor Therapy Among Inflammatory Bowel Disease Patients: An Analysis of the Food and Drug Administration Adverse Event Reporting System. Gastroenterology 2013;144(5):S416-S416.

(517) Liu ML, Guo SC, Stiles JK, Ostvik AE, Granlund AV, Bugge M, et al. The emerging role of CXCL10 in cancer (Review). Inflamm Bowel Dis 2013;2; 19(4; 2):583; 265-589; 274.

(518) Ostvik AE, Granlund AV, Bugge M, Nilsen NJ, Torp SH, Waldum HL, et al. Enhanced Expression of CXCL10 in Inflammatory Bowel Disease: Potential Role of Mucosal Toll-like Receptor 3 Stimulation. Inflamm Bowel Dis 2013;19(2):265-274.

(519) Mir A, Minguez M, Tatay J, Pascual I, Peña A, Sanchiz V, et al. Elevated serum eotaxin levels in patients with inflammatory bowel disease. Am J Gastroenterol 2002 06;97(6):1452.

(520) Woodruff SA, Masterson JC, Fillon S, Robinson ZD, Furuta GT. Role of Eosinophils in Inflammatory Bowel and Gastrointestinal Diseases. J Pediatr Gastroenterol Nutr 2011;52(6):650-661.

(521) Barahona-Garrido J, Yamamoto-Furusho J. New treatment options in the management of IBD - focus on colony stimulating factors. Biologics 2008 09;2(3):501-504.

(522) Egea L, Hirata Y, Kagnoff MF. GM-CSF: a role in immune and inflammatory reactions in the intestine. Expert Rev Gastroenterol Hepatol 2010 12;4(6):723-731.

(523) Ellis LM, Takahashi Y, Liu W, Shaheen RM, Bendardaf R, Buhmeida A, et al. Vascular endothelial growth factor in human colon cancer: biology and therapeutic implications. Oncologist 2009;5 Suppl 1; 28; 136(6; 2):11; 3865; 585-15; 3870; 595.

(524) Bendardaf R, Buhmeida A, Hilska M, Laato M, Syrjanen S, Syrjanen K, et al. VEGF-1 Expression in Colorectal Cancer is Associated with Disease Localization, Stage, and Long-term Disease-specific Survival. Anticancer Res 2009;28; 136(6; 2):3865; 585-3870; 595.

(525) Scaldaferri F, Vetrano S, Sans M, Arena V, Straface G, Stigliano E, et al. VEGF-A Links Angiogenesis and Inflammation in Inflammatory Bowel Disease Pathogenesis. Gastroenterology 2009;136(2):585-595.

(526) Tansey W,P. Mammalian MYC Proteins and Cancer. New Journal of Science 2014 01/01;2014(1).

(527) Zhang S, Li Y, Wu Y, Shi K, Bing L, Hao J. Wnt/ß-catenin signaling pathway upregulates c-Myc expression to promote cell proliferation of P19 teratocarcinoma cells. Anat Rec (Hoboken) 2012 12;295(12):2104-2113.

(528) Cowling VH, D'Cruz C, Chodosh LA, Cole MD. c-Myc transforms human mammary epithelial cells through repression of the Wnt inhibitors DKK1 and SFRP1. Mol Cell Biol 2007;27(14):5135-5146.

(529) You Z, Saims D, Chen S, Zhang Z, Guttridge DC, Guan K, et al. Wnt signaling promotes oncogenic transformation by inhibiting c-Myc-induced apoptosis. J Cell Biol 2007 04/29;157; 20; 27(3; 11; 14):429; 1394; 5135-440; 1404; 5146.

(530) Willert K, Jones KA, Cowling VH, D'Cruz C, Chodosh LA, Cole MD. Wnt signaling: is the party in the nucleus? Genes Dev 2007;20; 27(11; 14):1394; 5135-1404; 5146.

(531) Kam Y, Quaranta V. Cadherin-Bound ß-Catenin Feeds into the Wnt Pathway upon Adherens Junctions Dissociation: Evidence for an Intersection betweenß -Catenin Pools. PLoS ONE 2009 02;4(2):1-13.

(532) Yap AS, Brieher WM, Gumbiner BM. Molecular and functional analysis of cadherin-based adherens junctions. Annu Rev Cell Dev Biol 1997;13:119-146.

(533) Rai H, Ahmed J. N-Cadherin: A Marker Of Epithelial To Mesenchymal Transition In Tumor Progression. Internet J Oncol 2014;10(1):1-1.

(534) Tsanou E, Peschos D, Batistatou A, Charalabopoulos A, Charalabopoulos K. The E-Cadherin Adhesion Molecule and Colorectal Cancer. A Global Literature Approach. Anticancer Res 2008;28(6):3815-3826.

(535) Zhuo H, Jiang K, Dong L, Zhu Y, Lu L, Lu Y, et al. Overexpression of N-cadherin is correlated with metastasis and worse survival in colorectal cancer patients. Chinese Science Bulletin 2013(28-29):3529.

(536) El-Bahrawy M, Poulsom SR, Rowan AJ, Tomlinson IT, Alison MR. Characterization of the E-cadherin/catenin complex in colorectal carcinoma cell lines. Int J Exp Pathol 2004 04;85(2):65-74.

(537) El-Bahrawy M, Poulsom R, Jeffery R, Talbot I, Alison MR. The expression of E-cadherin and catenins in sporadic colorectal carcinoma. Hum Pathol 2001 11;32(11):1216-1224.

(538) Tucker E, Buda A, Janghra B, Cpoad J, Moorghan M, Havler M, et al. Abnormalities of the cadherin-catenin complex in chemically-induced colo-rectal carcinogenesis. Proc Nutr Soc 2003 02;62(1):229-236.

(539) Kong D, Li Y, Wang Z, Sarkar FH. Cancer Stem Cells and Epithelial-to-Mesenchymal Transition (EMT)-Phenotypic Cells: Are They Cousins or Twins? Cancers 2011 03;3(1):716-729.

(540) Kalluri R, Weinberg RA. The basics of epithelial-mesenchymal transition. J Clin Invest 2009 06;119(6):1420-1428.

(541) Aktas B, Tewes M, Fehm T, Hauch S, Kimmig R, Kasimir-Bauer S. Stem cell and epithelial-mesenchymal transition markers are frequently overexpressed in circulating tumor cells of metastatic breast cancer patients. Breast Cancer Res 2009;11(4):R46-R46.

(542) Straub BK, Rickelt S, Zimbelmann R, Grund C, Kuhn C, Iken M, et al. E-N-cadherin heterodimers define novel adherens junctions connecting endoderm-derived cells. J Cell Biol 2011(5):873.

(543) Hidalgo IJ, Raub TJ, Borchardt RT, Zucco F, Batto AF, Bises G, et al. Characterization of the human colon carcinoma cell line (Caco-2) as a model system for intestinal epithelial permeability. Gastroenterology 2005 03;96; 33; 21(3; 6; 1):736; 603; 1-749; 618; 26.

(544) Zucco F, Batto AF, Bises G, Chambaz J, Chiusolo A, Consalvo R, et al. An inter-laboratory study to evaluate the effects of medium composition on the differentiation and barrier function of Caco-2 cell lines. Cell Biol Toxicol 2005;33; 21(6; 1):603; 1-618; 26.

(545) Sambuy Y, Angelis I, Ranaldi G, Scarino ML, Stammati A, Zucco F. The Caco-2 cell line as a model of the intestinal barrier: influence of cell and culture-related factors on Caco-2 cell functional characteristics. Cell Biol Toxicol 2005;21(1):1-26.

(546) Calon A, Espinet E, Palomo-Ponce S, Tauriello DVF, Iglesias M, Céspedes MV, et al. Dependency of colorectal cancer on a TGF-ß-driven program in stromal cells for metastasis initiation. Cancer Cell 2012 11/13;22(5):571-584.

(547) Franses JW, Baker AB, Chitalia VC, Edelman ER. Stromal endothelial cells directly influence cancer progression. Sci Transl Med 2011 01/19;3(66):66ra5-66ra5.

(548) Quail DF, Joyce JA. Microenvironmental regulation of tumor progression and metastasis. Nat Med 2013(11):1423.

(549) Rosivatz E, Becker I, Bamba M, Schott C, Diebold J, Mayr D, et al. Neoexpression of N-cadherin in E-cadherin positive colon cancers. Internation Journal of Cancer 2004;111(5):711-719.

(550) Seglen PO, Gordon PB. 3-Methyladenine: Specific Inhibitor of Autophagic/Lysosomal Protein Degradation in Isolated Rat Hepatocytes. Proc Natl Acad Sci U S A 1982(6):1889.

(551) Vos MD, Ellis CA, Bell A, Birrer MJ, Clark GJ. Ras uses the novel tumor suppressor RASSF1 as an effector to mediate apoptosis. J Biol Chem 2000 11/17;275(46):35669-35672.

(552) Eckfeld K, Hesson L, Vos MD, Bieche I, Latif F, Clark GJ. RASSF4/AD037 is a potential ras effector/tumor suppressor of the RASSF family. Cancer Res 2004 12/01;64(23):8688-8693.

(553) Burbee DG, Forgacs E, Zöchbauer-Müller S, Shivakumar L, Fong K, Gao B, et al. Epigenetic inactivation of RASSF1A in lung and breast cancers and malignant phenotype suppression. J Natl Cancer Inst 2001 05/02;93; 68(9; 1):691; 22-699; 25.

(554) Lusher ME, Lindsey JC, Latif F, Pearson ADJ, Ellison DW, Clifford SC. Biallelic epigenetic inactivation of the RASSF1A tumor suppressor gene in medulloblastoma development. Cancer Res 2002 10/15;62(20):5906-5911.

(555) Pan Z, Kashuba VI, Liu X, Shao J, Zhang R, Jiang J, et al. High frequency somatic mutations in RASSF1A in nasopharyngeal carcinoma. Cancer Biol Ther 2005 10;4; 238(10; 1):1116; 128-1122; 134.

(556) Weizmann Institute of Science. GeneCards Database. Available at: http://www.genecards.org/. Accessed October, 2014.

Appendix

A1. *Rassf1a*^{-/-} mice are resistant to *Citrobacter rodentium* colonization

DSS induced models of colitis in rodents are well established, easy to use, and the severity of disease is highly controllable. However, chemical models of colitis are best to model colitis resulting from tissue irritation and injury rather than spontaneous colitis occurring due to genetic predisposition or in response to bacterial stimuli [113,147]. In order to further characterize how RASSF1A regulates intestinal inflammation, we employed the *Citrobacter rodentium* model of infectious colitis using our *Rassf1a*^{-/-} mice [198,209,212].

Interestingly, we were unable to successfully colonize our *Rassf1a*^{-/-} mice with *C. rodentium*. Mice were infected with *Citrobacter rodentium* via oral gavage and monitored for the presence of *C. rodentium* by rectal swabbing throughout the experiment. None of the mice showed prior evidence of *C. rodentium* infection at the time of inoculation. While we were able to culture *C. rodentium* from rectal swabs and colon lysates from wild type mice 7 days after inoculation (implying successfully infection) *Rassf1a*^{-/-} mice never showed evidence of *C. rodentium* infection (Figure A1 A). In addition to not being able to confirm infection in *Rassf1a*^{-/-} mice, we also observed a lack of body weight loss and disease symptoms compared to wild type mice (Figure A1 B and C). *C. rodentium* in mice typically results in body weight loss, diarrhea, possible rectal bleeding, crypt hyperplasia, and immune cell infiltration [209]. While we did not see significant immune cell infiltration (unpublished data), both wild type and *Rassf1a*^{-/-} mice did show evidence of crypt hyperplasia following *C. rodentium* infection (Figure A1 D). We did note that *Rassf1a*^{-/-} mice appeared to have higher levels of Gram negative bacteria able to be cultured on MacConkey plates, as well as a more diverse population compared to wild type mice (unpublished data). It is therefore possible that *Rassf1a*^{-/-} mice may have altered microbiota compared to wild type mice, despite being

housed in the same facility, and that this may have contributed to the abnormal response of *Rassf1a$^{-/-}$* mice to *C. rodentium* infection.

Discussion:

Citrobacter rodentium infection in mice involves adhesion to the host epithelial surface through the creation of attaching and effacing (A/E) lesions [196,197,205,207]. The creation of attaching and effacing lesions involves destruction of the surface microvilli, insertion of the bacterial Tir protein into the host epithelial cell, and subsequent cytoskeletal rearrangements [197,205,207]. RASSF1A has previously been shown to be important in regulating microtubule and cytoskeleton stabilization [277,293,498,499]. Because loss of RASSF1A has been shown to cause cytoskeletal defects, it is possible that *Rassf1a$^{-/-}$* mice are resistant to *C. rodentium* infection due to an inability of the bacteria to properly form attaching and effacing lesions in these mice. In fact, osteopontin, which has also been shown to regulate cytoskeleton dynamics, has previously been shown to be required for the creation of A/E lesions and successful *C. rodentium* infection [197,500], and it is possible that RASSF1A acts in a similar manner.

Alternatively, the enriched population of Gram negative bacteria in *Rassf1a$^{-/-}$* mice compared to wild type mice may have created a competitive microbial environment which does not favor *C. rodentium* colonization. Further evaluation of colonic section from *C. rodentium* inoculated *Rassf1a$^{-/-}$* for the presence of A/E lesions and pedestal formation will give further insight into whether loss of RASSF1A is protective against *C. rodentium* adhesion. In order to eliminate the possible confounding factor of microbial competition, it would be beneficial to co-culture *ex vivo Rassf1a$^{-/-}$* crypt cells or mouse embryonic fibroblasts (MEFs) with *C. rodentium* to determine whether *C. rodentium* is capable of infecting cells lacking RASSF1A *in vitro*.

In order to study the potential influences of the microbiota in *Rassf1a*$^{-/-}$ mice *in vivo*, in may also be useful to pre-treat *Rassf1a*$^{-/-}$ mice with antibiotics in order to clear the GI tract of competitive bacteria prior to *C. rodentium* inoculation. Because *C. rodentium* infection in mice is thought to be similar to pathogenic *E. coli* infection in humans, further insight into how RASSF1A may regulate bacterial infections may help in understanding *E. coli* infections in humans, and how genetic influences may predispose or protect to certain bacterial infections.
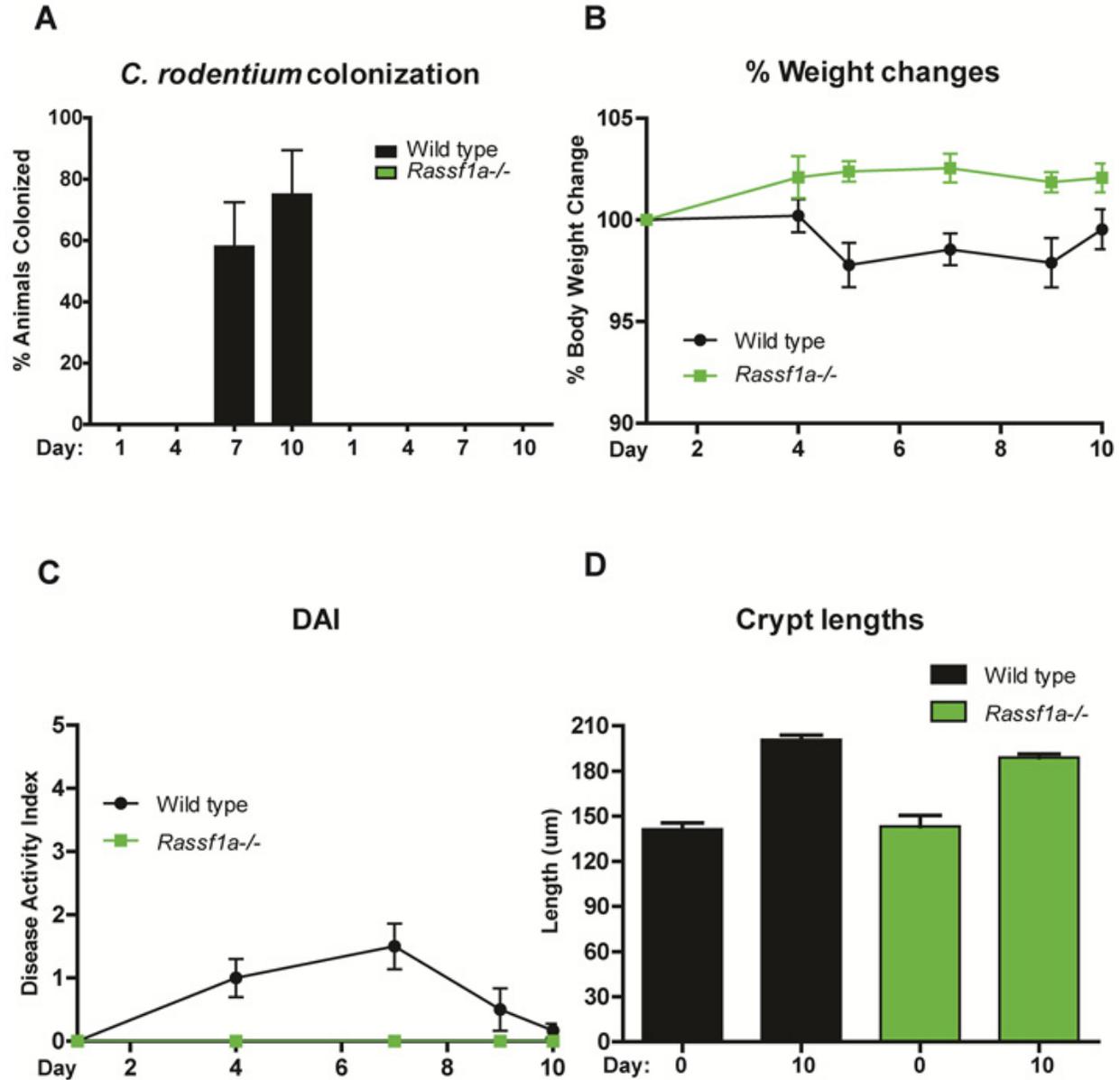
Figure A1. ***Rassf1a-/- mice are resistant to*** *Citrobacter rodentium* **infection.** (**A**) Percentage of mice postivie for *Citrobacter rodentium* cultures following rectal swab. Days indicate days post oral infection with *C. rodentium* broth. p-value<0.02 at Day 7 and <0.007 at day 10 for *Rassf1a-/-* vs WT. (**B**) *Rassf1a-/-* mice show no body weight loss following *C. rodentium infection.* p-value<0.05 at Days 5, 7, and 9 for *Rassf1a-/-* vs WT. (**C**) *Rassf1a-/-* mice show no disease symptoms following *C. rodentium* infection. p-value<0.001 at Day 7 for *Rassf1a-/-* vs WT. n=6-12 for **A-C**. (**D**) Both *Rassf1a-/-* and WT mice show crypt hyperplasia following *C. rodentium* infection. p-value<0.002 at Day for *Rassf1a-/-* vs WT, p-value<0.0001 for WT Day 0 vs Day 10, and p-value<0.0001 for *Rassf1a-/-* Day 0 vs Day 10. n=75-85 crypts measured per group.

241

A2. Dosing studies: *Rassf1a*$^{-/-}$ mice are susceptible to high doses of AOM

We have previously documented a role for RASSF1A in restricting inflammation, cell death, and DNA damage in an acute model of inflammation [3], we aimed to further characterize how RASSF1A may affect molecular mechanisms that link inflammation and cancer (see chapter four). RASSF1A loss has previously been shown to be highly associated with colorectal cancer development [89,90,347,429,430], and may also be lost in some IBD patients [88].To this end, we utilized an established model of inflammation driven carcinogenesis, whereby mice are subjected to several inflammatory episodes using the colonic irritant dextran sodium sulfate (DSS) in order to mimic a chronic inflammatory state. Mice are injected with azoxymethane (AOM), a pro-carcinogen, prior to these inflammatory episodes, as AOM exposure has been shown to decrease the time to tumor appearance using the DSS chronic model [146,156-158]. Upon review of the literature utilizing the AOM/DSS model, we noted that the majority of studies used a single IP dose of 12 mg/kg AOM prior to DSS exposure, therefore we decided to use 12 mg/kg AOM in our preliminary studies.

While wild type mice had no reaction to 12 mg/kg AOM injection, we noted that *Rassf1a*$^{-/-}$ mice showed a severe reaction and significantly decreased survival following a single 12 mg/kg injection of AOM (Figure A2 A and B). Prior to any exposure to DSS, 50% of *Rassf1a*$^{-/-}$ mice showed significantly increased DAI symptoms and died, and the remaining mice appeared to be overly sensitive to DSS, as only 12.5% of *Rassf1a*$^{-/-}$ mice survived to Day 75 of the experiment. Because of the extremely negative response of *Rassf1a*$^{-/-}$ mice to a dose of 12 mg/kg AOM, even without DSS exposure, we decided to evaluate the use of lower doses of AOM. For our dosing experiments, we utilized mice lacking both RASSF1A and MOAP-1 (*Rassf1a*$^{-/-}$*Moap1*$^{-/-}$ mice). MOAP-1 (modulator of apoptosis 1) is a putative tumor suppressor protein that cooperates with RASSF1A to promote death receptor dependent apoptosis via BAX activation, and

Rassf1a^{-/-}Moap1^{-/-} mice show similar or slightly more severe phenotypic responses compared to *Rassf1a^{-/-}* mice (unpublished observations), and were therefore used to test sensitivity to AOM dosages. We found that a dose of 10 mg/kg of AOM was also fatal to *Rassf1a^{-/-}Moap1^{-/-}* mice, while doses of 8 mg/kg and 6 mg/kg were not. Because AOM is thought to accelerate the appearance of inflammation induced carcinogenesis when used in combination with DSS [156,157,172,173], we decided to utilize a dosage of 8 mg/kg AOM for our studies in order to achieve the greatest effect within the most reasonable time frame.
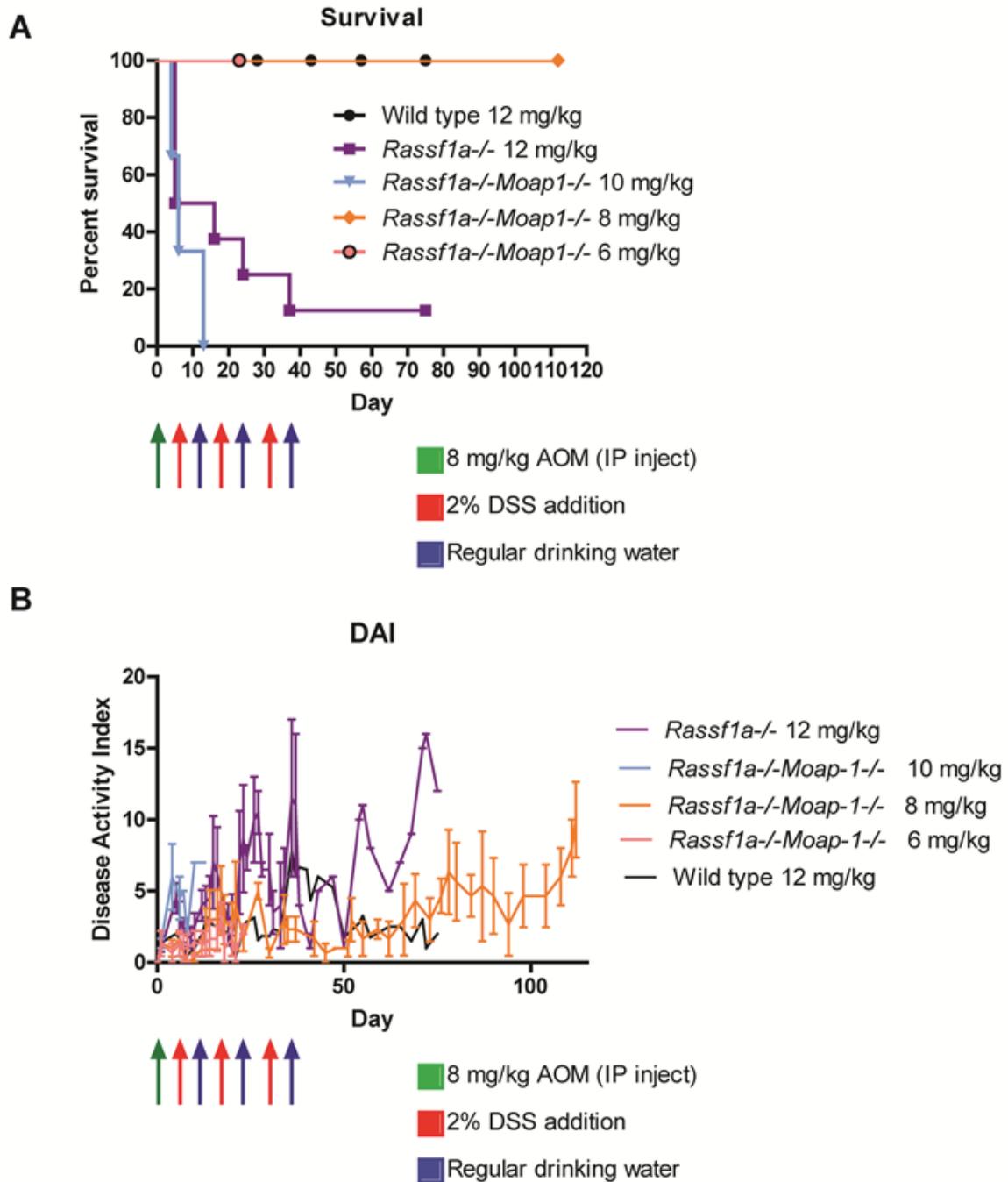
Figure A2. *Rassf1a-/-* mice are sensitive to high doses of AOM. (**A**) Mice lacking *Rassf1a* show significantly reduced survival when exposed to a single dose of AOM at doses higher than 8 mg/kg. p-value=0.0018 at 12mg/kg for *Rassf1a-/-* vs WT, p-value=0.0008 for *Rassf1a-/-Moap1-/-* 10 mg/kg vs WT 12mg/kg, and p-value=1.0000 for *Rassf1a-/-Moap1-/-* 8 mg/kg or 6 mg/kg vs WT 12 mg/kg. (**B**) Mice lacking *Rassf1a* show significantly increased disease symptoms when exposed to a single dose of AOM at doses higher than 8 mg/kg. p-value<0.05 at Days 5, 15, 16, and 54, p-value<0.01 at Days 22, 23, 26, and 75; p-value<0.001 at Days 27, 71, and 72 for *Rassf1a-/-* 12 mg/kg vs WT 12 mg/kg; p-value<0.001 at Days 6, 7, 10, 12, and 13, p-value<0.05 at Day 8 for *Rassf1a-/-Moap1-/-* 10 mg/kg vs WT 12 mg/kg; no significant differences for *Rassf1a-/-Moap1-/-* 8 mg/kg or 6 mg/kg vs WT 12 mg/kg. n=3-8 for each group. *Rassf1a-/-Moap1-/-* mice show similar or slightly more severe phenotypic responses as *Rassf1a-/-* mice and were therefore used for dosing experiments after *Rassf1a-/-* mice showed and initial sensitivity.

244

A3. Other cytokines examined in the AOM/DSS model

The balance of pro-inflammatory cytokines and anti-inflammatory cytokines is a crucial factor in the development and resolution of inflammatory bowel diseases and associated colon cancers [74,472,501]. In order to have a better understanding of how RASSF1A influences cytokine and chemokine levels and to determine which cytokines play key roles in our AOM/DSS model of inflammation driven colon cancer in our *Rassf1a*^{-/-} mice, we examined a cross section of cytokines commonly involved in IBD and/or colon cancers. In addition to the cytokines shown in Figure 4.3 (see chapter four), we also examined several other cytokines. Figure A3 shows expression patterns for IL-1α, IL-1β, IL-2, IL-17, and IL-18, and Figure A4 shows expression patterns for IFN-γ, TNF-α, CXCL10, CCL11, GM-CSF, and VEGF.

While IL-1α levels did not change throughout most of our experiment, *Rassf1a*^{-/-} showed a significant increase in serum IL-1α levels on Day 112 at the end of the experiment (Figure A3 A). IL-1α is produced by activated macrophages; however, it is rarely secreted at detectable levels into the serum except in cases of extreme inflammation [502]. Increased IL-1α has also been shown to enhance angiogenesis in colon cancers, and contribute to cancer metastases [502,503]. It is possible, therefore, that the rapid increase in IL-1α at the end of the experiment indicates a transition towards metastasis in *Rassf1a*^{-/-} mice. The most common site for colon cancer metastases is the liver [504,505], therefore histological examination of liver samples from *Rassf1a*^{-/-} mice for evidence of metastatic colon cancer will determine whether *Rassf1a*^{-/-} mice are susceptible to metastatic colon cancer following AOM/DSS induced carcinogenesis. IL-1β has been implicated as an important cytokine in IBD, with IBD patients often showing significantly elevated levels of IL-1β. Mouse models of IBD also show elevated levels of IL-1β upon inflammatory insult [501,502,506]. However, we did not observe an increase in serum IL-1β levels in either wild type or *Rassf1a*^{-/-} mice in our study, and overall levels of IL-1β were extremely low throughout the experiment (Figure A3 B).

IL-2 is a cytokine primarily associated with the adaptive immune response and regulating autoimmunity. IL-2 is secreted by T lymphocytes to promote T cell differentiation and to enhance the adaptive immune response. IL-2 replacement therapies have been suggested as potential therapeutics for IBD as well as colon cancer [507,508]. While we saw a slight initial decrease in serum IL-2 levels after the induction of inflammation and a final return to baseline levels at the end of the experiment in wild type mice, these changes were not significant (Figure A3 C). *Rassf1a*^{-/-} showed no change in IL-2 levels until an increase the end of the experiment at Day 112, however, these changes were again insignificant (Figure A3 C). IL-2 is therefore unlikely to be a key cytokine in AOM/DSS inflammation induced carcinogenesis.

IL-4 is an anti-inflammatory cytokine responsible for restricting the activation of macrophages in inflammatory settings. Decreased levels of IL-4 in IBD patients are thought to contribute to the exacerbated inflammation seen in these patients [509,510]. While overall levels of IL-4 did not change dramatically, wild type mice tended to have slightly higher levels of IL-4 compared to *Rassf1a*^{-/-} mice, particularly at Day 112 (Figure A3 D) This may represent a further inability of *Rassf1a*^{-/-} mice to restrict inflammation, as *Rassf1a*^{-/-} mice also showed significantly lower levels of anti-inflammatory IL-10 compared to wild type mice (Figure 4.3).

IL-17 is a potent pro-inflammatory cytokine regulated by IL-23. IL-17 induction results in the up-regulation of other pro-inflammatory cytokines such as TNF-α, IL-6, and IL-8, as well as up-regulation of MMPs [501,506]. IL-17 is frequently up-regulated in IBD patients and sustained IL-17 is thought to promote CRC development [511,512]. Unsurprisingly, IL-17 levels increased in both wild type and *Rassf1a*^{-/-} mice in our model system upon inflammatory stimulus (Figure A3 E). While this increase was generally not significantly different between the two genotypes, wild type mice did show significantly

higher levels of IL-17 at Days 24 and 112, suggesting that *Rassf1a*^{-/-} mice may have slightly altered IL-17 signaling. Of note, serum IL-23 levels were undetectable in our wild type and *Rassf1a*^{-/-} mice.

Another pro-inflammatory cytokine, IL-18, has also been implicated in IBD pathogenesis. IL-18 is frequently up-regulated in CD patients, and increased IL-18 has also been reported in animal models of IBD [501,506]. Conversely, IL-18 levels tend to be decreased in colon cancers and animal models of colon cancer [513]. In concurrence with *Rassf1a*^{-/-} mice showing increased symptoms of inflammatory disease, *Rassf1a*^{-/-} mice show significantly increased levels of IL-18 compared to wild type mice throughout the experiment (Figure A3 F). The substantial and sustained increase in IL-18 levels in *Rassf1a*^{-/-} mice suggest that IL-18 may be an important inflammatory driver regulated by RASSF1A, and that IL-18 is likely a major contributor to the exacerbated inflammation seen in knockout mice.

IFN-γ is another pro-inflammatory cytokine often up-regulated in IBD. IFN-γ promotes Th1 cell differentiation and activates a potent innate and adaptive immune response [501,513,514]. In our model system, IFN-γ appears to be induced only in the initial acute phase of inflammation, showing a significant increase in both genotypes at Day 14 followed by a return to baseline levels for the rest of the experiment (Figure A4 A). Despite IFN-γ being induced in both wild type animals as well as *Rassf1a*^{-/-} animals, the knockout group did show significantly increased levels of IFN-γ at Day 14 compared to wild type mice, suggesting that RASSF1A plays an important role in regulating IFN-γ levels.

TNF-α is produced by macrophages, T cells, and fibroblasts, and is a potent pro-inflammatory cytokine that is an important activator of NFκB pro-inflammatory transcription [501,506]. IBD patients often exhibit high levels of TNF-α, which drives

expression of MMPs and other pro-inflammatory cytokines which contribute to inflammation related tissue destruction [74]. TNF-α neutralizing antibodies have proven an effective treatment for IBD patients [506,515]. However, anti-TNF-α biologic use in IBD has also been linked with increased risk for CRC development in these patients, highlighting the complexity of TNF-α signaling [501,516]. We saw a significant increase in TNF-α levels in *Rassf1a*^{-/-} mice during the initial acute inflammatory stage compared to wild type mice, further strengthening our conclusion that loss of RASSF1A results in dysregulated inflammatory signaling (Figure A4 B).

CXCL10 (aka IP-10) is a chemokine induced by IFN-γ which attracts Th1 cells to sites of active inflammation. Increased levels of CXCL10 have been associated with IBD as well as several cancers [517,518]. In our mice, we saw an induction in CXCL10 levels during the first inflammatory phase, and again at the end of the experiment, suggesting that CXCL10 may be important in initiating the acute inflammatory response and possibly in sustaining established tumors in the AOM/DSS model (Figure A4 C).

Eotaxin (aka CCl11) is a pro-inflammatory chemokine implicated in the pathogenesis of IBD which is responsible for recruiting eosinophils and basophils to sites of inflammation [519,520]. *Rassf1a*^{-/-} mice tended to show elevated levels of serum eotaxin levels compared to wild type animals, suggesting that portions of the adaptive immune response are regulated by RASSF1A (Figure A4 D).

GM-CSF (granulocyte macrophage colony stimulating factor) is a cytokine that activates myeloid cell growth and differentiation. Mice lacking GM-CSF show increased susceptibility to pathogen induced colitis, and administration of GM-CSF to IBD patients has shown disease improvement [521,522]. Interestingly, we noted a complete lack of detectable GM-CSF in *Rassf1a*^{-/-} mice (Figure A4 E). As GM-CSF is a key growth factor to promote the development of white blood cells, our inability to detect GM-CSF in

Rassf1a^{-/-} mice suggests that these mice may have innate defects in white blood cell development which contribute to the aberrant inflammatory responses seen in these mice.

An important protein in initiating angiogenesis is vascular endothelial growth factor (VEGF). Overexpression of VEGF has long been associated with a variety of cancers, as hypoxic solid tumors induce VEGF in order to promote increased vascularity to the tumor and promote further growth [523,524]. More recently, increased levels of VEGF have also been implicated in IBD patients, possibly as a result of increased fibrosis resulting from chronic inflammation [525]. While VEGF levels remained relatively low throughout our experiment, mice lacking RASSF1A did show a sudden increase in VEGF levels at Day 112 (Figure A4 F). As invasive carcinoma is fully established in *Rassf1a*^{-/-} mice at this time point, it is possible that this spike represents an increased need for angiogenesis due to the increased severity of the tumors seen in these mice.

Taken together, these results show an important role for RASSF1A in regulating a variety of inflammatory cytokines, chemokines, and growth factors contributing to the pathogenesis of inflammatory diseases and related cancers. These findings further highlight the importance of RASSF1A as a multi-factorial signaling molecule.
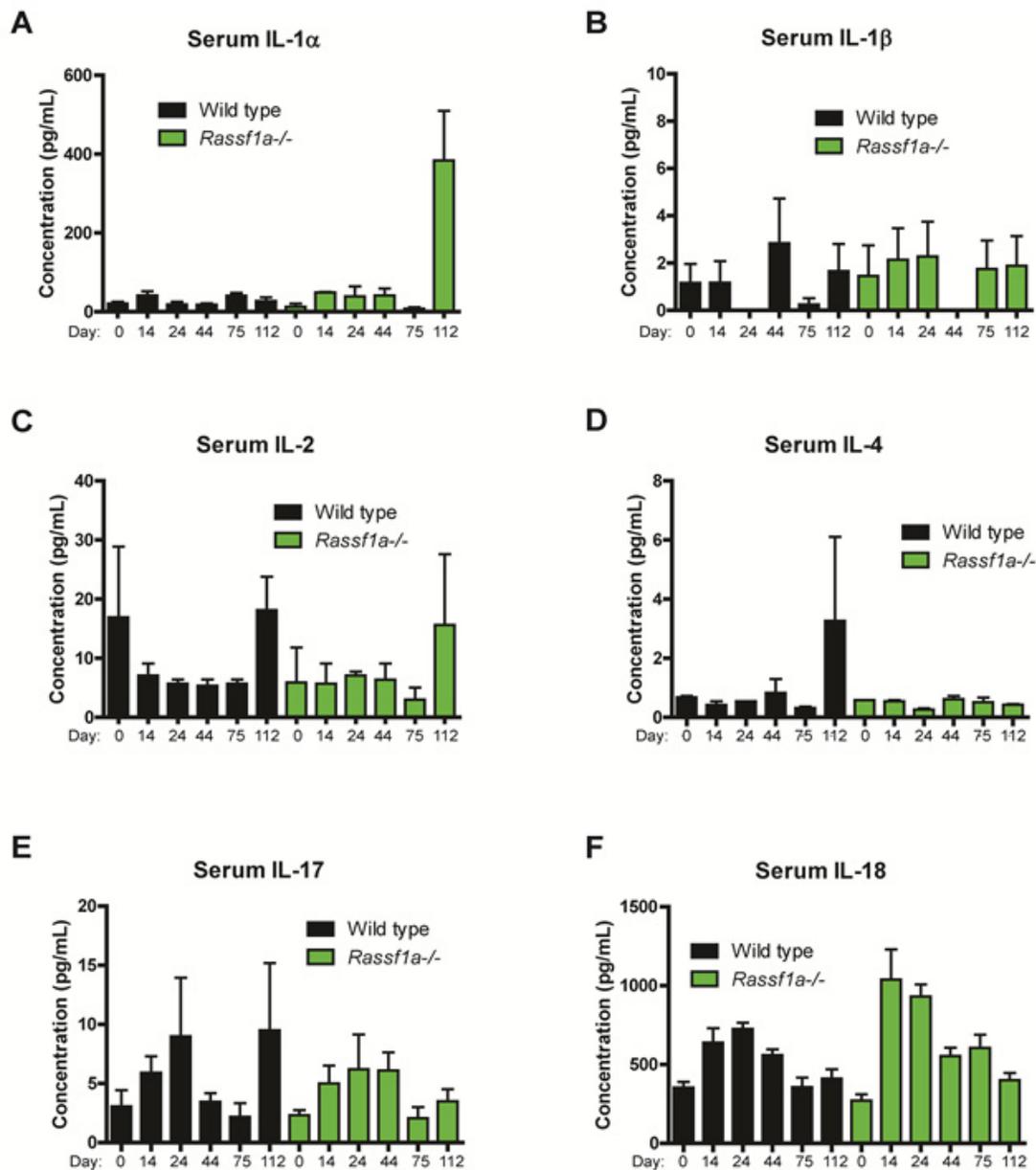
Figure A3. Other cytokines were examined. (**A**) *Rassf1a-/-* mice show increased serum levels of IL-1α at the end of the experiment. p-value>0.05 at Days 0, 14, 24, 44, and 75, and 0.0027 at Day 112 for *Rassf1a-/-* vs WT. n=2 for each time point. (**B**) Serum levels of IL-1β following inflammation induced carcinogenesis. p-value>0.05 at all time points for *Rassf1a-/-* vs WT. n=7-13 for each time point. (**C**) Serum levels of IL-2 following inflammation induced carcinogenesis. p-value>0.05 at all time points for *Rassf1a-/-* vs WT. n=2 for each time point. (**D**) *Rassf1a-/-* mice show decreased serum levels of IL-4 at the end of the experiment. p-value>0.05 at Days 0, 14, 44, and 75, <0.004 at Day 24, and 0.04 at Day 112 for *Rassf1a-/-* vs WT. n=2 for each time point. (**E**) Serum levels of IL-17 following inflammation induced carcinogenesis. p-value>0.05 at Days 0, 14, 24, and 75 <0.006 at Day 44, and <0.03 at Day 112 for *Rassf1a-/-* vs WT. n=2 for each time point. (**F**) Serum levels of IL-18 following inflammation induced carcinogenesis. p-value>0.05 at Day 0, 44, and 112, <0.03 at Days 14 and 24, and <0.01 at Day 75 for *Rassf1a-/-* versus WT. n=7-13 for each time point.
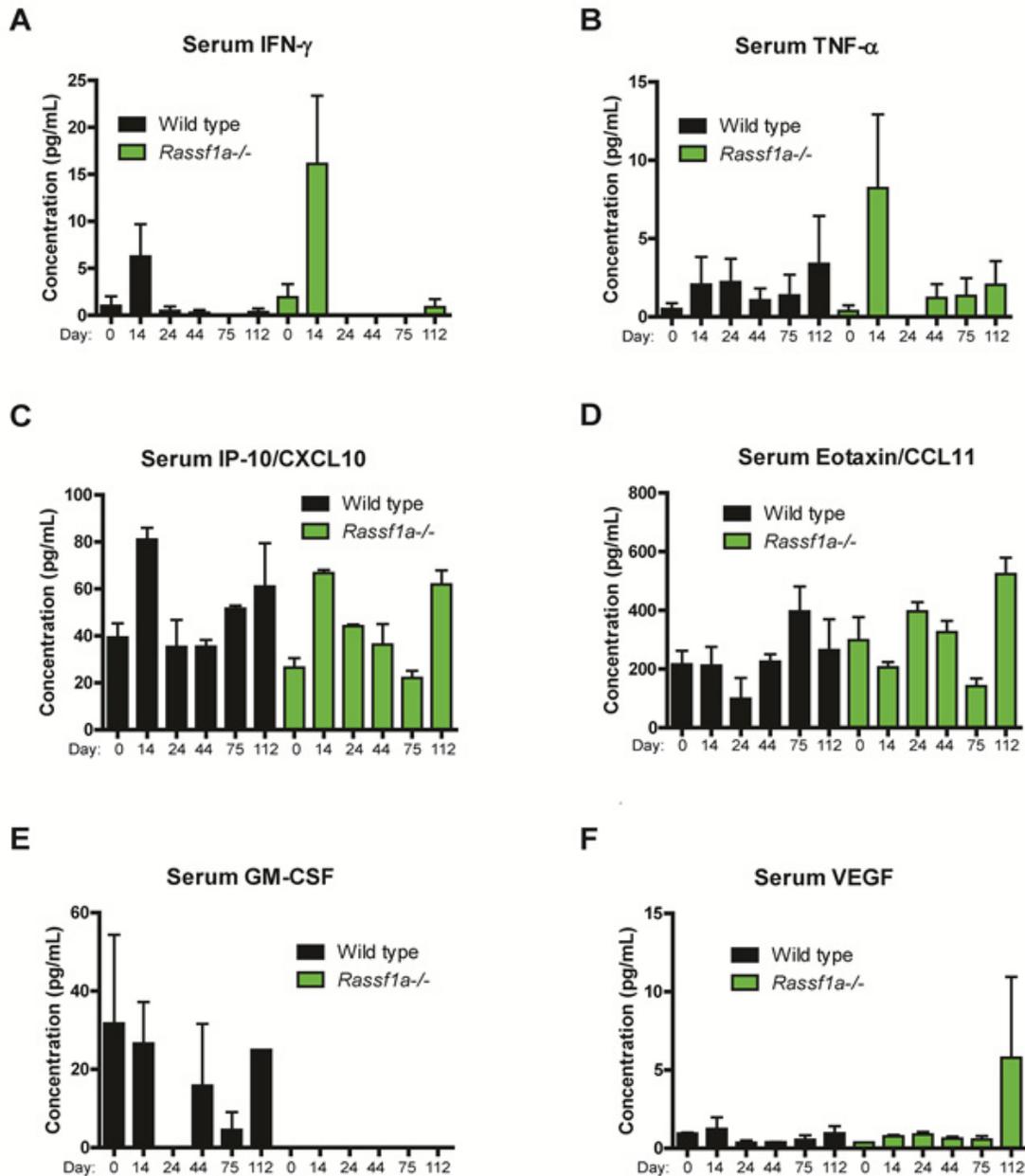
Figure A4. Other cytokines were examined. (**A**) *S*erum levels of IFN-γ following inflammation induced carcinogenesis. p-value>0.05 at Days 0, 24, 44, 75, and 112, and <0.02 at Day 14 for *Rassf1a-/-* vs WT. n=7-10 for each time point. (**B**) Serum levels of TNF-α following inflammation induced carcinogenesis. p-value>0.05 at Days 0, 24, 44, 75, and 112, and <0.02 at Day 14 for *Rassf1a-/-* vs WT. n=7-10 for each time point. (**C**) *S*erum levels of IP-10/CXCL10 following inflammation induced carcinogenesis. p-value>0.05 at Days 0, 24, 44, and 112, <0.003 at Day 14, and <0.01 at Day 75 for *Rassf1a-/-* vs WT. n=2 for each time point. (**D**) Serum levels of Eotaxin/CCL11 following inflammation induced carcinogenesis. p-value>0.05 at Days 0, and 14, <0.0006 at Day 24, <0.009 at Days 44 and 112, and <0.002 at Day 75 for *Rassf1a-/-* vs WT. n=2 for each time point. (**E**) Serum levels of GM-CSF following inflammation induced carcinogenesis. p-value<0.04 at Days 0 and 14, >0.05 at Day 24, <0.02 at Days 44 and 75, and <0.0001 at Day 112 for *Rassf1a-/-* vs WT. n=2 for each time point. (**F**) Serum levels of VEGF following inflammation induced carcinogenesis. p-value<0.0006 at Day 0, >0.05 at Days 14 and 75, <0.008 at Day 24, <0.0231 at Day 44, and <0.05 at Day 112 for *Rassf1a-/-* versus WT. n=2 for each time point.

A4. *Rassf1a^{-/-}* mice show dysregulated beta-catenin signaling and cadherin organization

In addition to the YAP signaling pathway, we would like to explore how RASSF1A may influence other pathways in an inflammation to cancer setting. As the WNT pathway is often dysregulated in many cancer types, and has also been linked to YAP signaling, we investigated whether loss of *Rassf1a* had any effect on WNT pathway components in our chronic model of inflammation induced carcinogenesis [360,361,363,382] (see also chapter four).

We observed an increase in β-catenin levels in *Rassf1a^{-/-}* mice throughout the experiment, which is not seen to the same extent in wild type controls. GSK3β is a serine/threonine kinase which constitutively phosphorylates β-catenin, targeting it for degradation in the absence of WNT ligand binding [268,383]. Phosphorylation of GSK3β inhibits its kinase activity, allowing β-catenin accumulation and nuclear translocation, and reduced pS9-GSK3β correlates with increased β-catenin levels in *Rassf1a^{-/-}* mice (Figure A5 A and B). Nuclear localization of β-catenin remains to be confirmed. Additionally, *Rassf1a^{-/-}* mice, but not wild type mice, show increasing levels of the MYC oncogene throughout the experiment, likely contributing to the enhanced tumorigenesis seen in these mice (Figure A5 A and B). MYC has previously been shown to be up-regulated in response to β-catenin/WNT signaling [526-529]. Up-regulation of MYC can then further drive pro-proliferative signaling, and when uncontrolled can result in tumorigenesis [526-528].

E-cadherin levels remain relatively stable, albeit at higher levels in *Rassf1a^{-/-}* mice than in wild type mice. Interestingly, we observed increasing levels of N-cadherin in both sets of mice, with particular prominence in *Rassf1a^{-/-}* mice, despite little change in E-cadherin levels (Figure A5 C and D). Immunohistological examination revealed that while wild type animals showed areas discretely expressing either E-cadherin or N-

cadherin at colonic epithelial junctions, *Rassf1a*^{-/-} mice appear to show co-localization of E-cadherins and N-cadherins, suggesting a general dysregulation of normal adherens junction formation (Figure A5 E).

Discussion:

We also observed an increase in β-catenin levels in *Rassf1a*^{-/-} mice throughout the experiment, which is not seen to the same extent in wild type controls. GSK3β is a serine/threonine kinase which constitutively phosphorylates β-catenin, targeting it for degradation in the absence of WNT ligand binding [268,383,384]. Phosphorylation of GSK3β inhibits its kinase activity, allowing β-catenin accumulation and nuclear translocation, and reduced pS9-GSK3β correlates with increased β-catenin levels in *Rassf1a*^{-/-} mice (Figure A5 A and B). Nuclear localization of β-catenin remains to be confirmed, and further experiments to examine β-catenin localization will give further insight to functional changes in β-catenin activity. Additionally, *Rassf1a*^{-/-} mice, but not wild type mice, show increasing levels of the MYC oncogene throughout the experiment, likely contributing to the enhanced tumorigenesis seen in these mice (Figure A5 A and B). MYC has previously been shown to be up-regulated in response to β-catenin/WNT signaling [527-530]. Up-regulation of MYC can then further drive pro-proliferative signaling, and when uncontrolled can result in tumorigenesis [487,526,528]. β-catenin is also an important component of adherens junctions, along with E-cadherin, and localization of β-catenin to adherens junctions is vital to normal epithelial integrity [531,532].

E-cadherin levels remain relatively stable, albeit at higher levels in *Rassf1a*^{-/-} mice than in wild type mice. Interestingly, we observed increasing levels of N-cadherin in both sets of mice, with particular prominence in *Rassf1a*^{-/-} mice, despite little change in E-cadherin levels (Figure A5 C and D). Immunohistological examination revealed that while wild type animals showed areas discretely expressing either E-cadherin or N-

cadherin at colonic epithelial junctions, *Rassf1a*$^{-/-}$ mice appear to show co-localization of E-cadherins and N-cadherins, suggesting a general dysregulation of normal adherens junction formation (Figure A5 E). Though at first increasing levels of N-cadherin suggests possible cadherin switching and possibly an epithelial to mesenchymal transition event (EMT), the failure of E-cadherin to be displaced by N-cadherin implies that cadherin switching and EMT are not the cause of N-cadherin up-regulation.

Typically, previous studies have associated cadherin switching, with a primarily N-cadherin rich population, with carcinoma development in the colon [533-535], with few exceptions [536-538]. Generally, increased levels of N-cadherin compared to E-cadherin have been associated with increased metastatic and invasive potential of tumors, due to the increased cellular mobility and flexibility of N-cadherin adherens junctions [539-541]. However, instances of cis-homodimers of E-cadherin and N-cadherin have previously been described, and Straub et al. [542] recently described the existence of E-N-cadherin heterodimers in a variety of endoderm derived tissues. Straub et al. importantly positively showed that E-cadherin and N-cadherin proteins were able to directly form heterodimer complexes, and revealed the presence of these complexes in both normal and cancerous tissues and cells. The bulk of their study focused on hepatic cells, and only examined a few colon-derived cell lines, CaCo2 and Colo320DM, which did not show concomitant levels of E- and N-cadherins [542]. However, results were only shown for CaCo2 cells, which have previously been shown to display inconsistent characteristics highly dependent on culturing techniques [543-545]. Because colonic tissue samples were not examined and the cell line used for immunoblot analysis may not be reliable, the possibility that E-N-cadherin heterodimers may exist in colonic tissues cannot be completely ruled out at this time. One of the most intriguing findings by Straub et al. was that E-N-cadherin heterodimers were uniquely capable of creating heterotypic junctions with the surrounding N-cadherin expressing mesenchymal stromal tissue [542]. As stromal influences are becoming increasingly recognized as crucial to neoplastic development, the development of these junctions may represent a novel method for the surrounding stroma to influence tumorous tissue [546-548].

The overall increase in N-cadherin levels in mice lacking RASSF1A, with concurrent dysregulation of adherens junction appearance suggests a potential novel role for RASSF1A in regulating these processes. Another intriguing study done by Rosivatz et al. [549] showed that up to 44% of colon cancer cases they examined showed significant increase in N-cadherin levels without concurrent reduction in E-cadherin levels. Additionally, in colon cancer samples showing increased expression of N-cadherin the authors saw no evidence of EMT (epithelial to mesenchymal transition) related transcription factors. Importantly, their study showed that increased N-cadherin levels can destabilize E-cadherin from adherens junctions and promote tumor invasion and metastases [549]. Further studies to examine whether other potential markers of EMT are up-regulated will give further insight into the possible roles that β-catenin and cadherins may be playing in our model of chronic inflammation driven carcinogenesis, and how RASSF1A may regulate these processes on a molecular level.
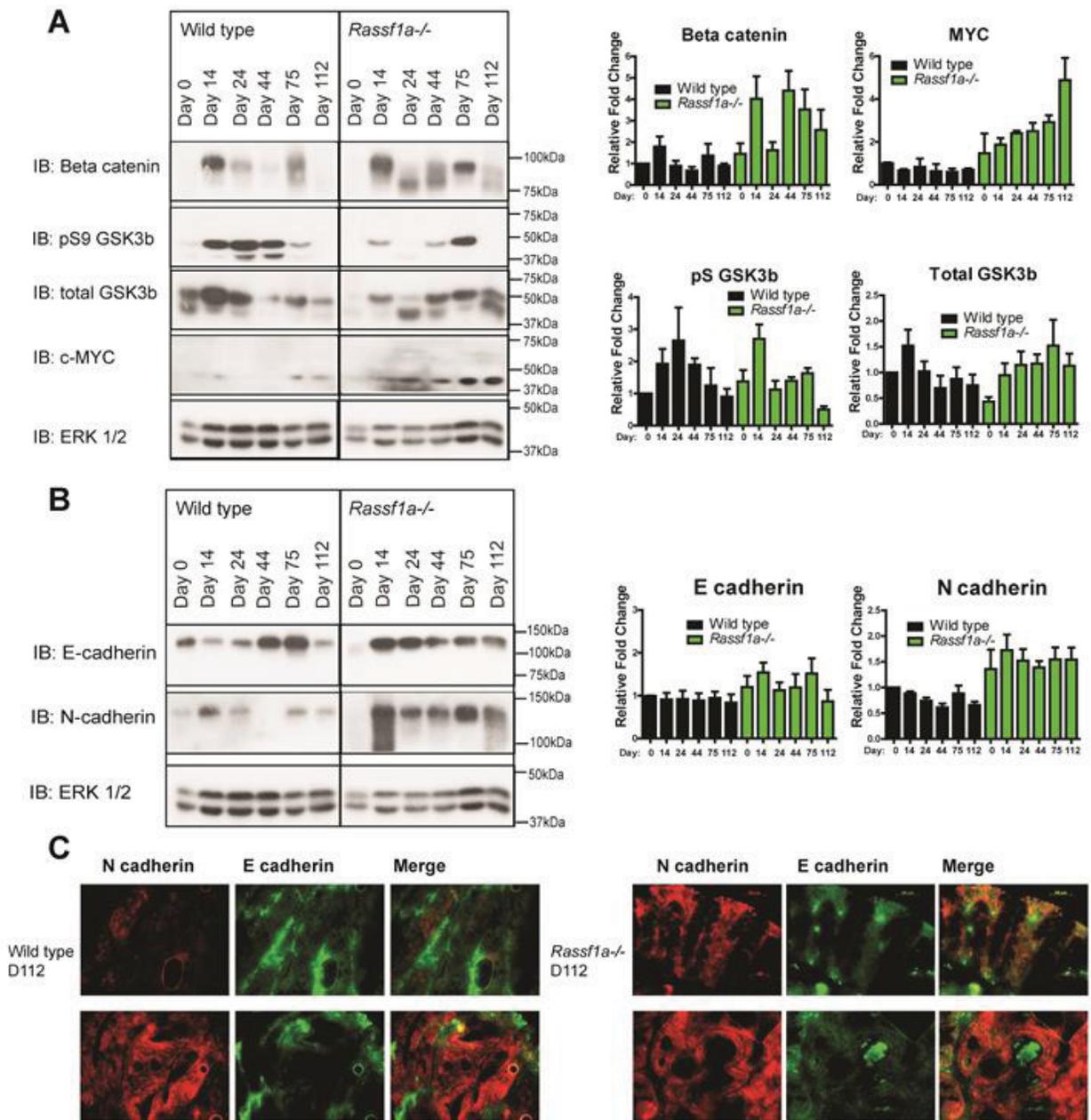
Figure A5. *Rassf1a-/-* mice show dysregulated beta-catenin signaling and cadherin organization. (**A**) Analysis for beta-catenin, pS9-GSK3b, total GSK3b, and c-MYC expression by immunoblot in colon lysates (experiment repeated four times with similar results). Right panel shows quantitations of left. For **beta-catenin**: p-value>0.05 at Days 0 and 24, <0.001 at Day 14, <0.02 at Day 44, <0.04 at Day 75, and <0.01 at Day 112 for *Rassf1a-/-* vs WT. For **c-MYC**: p-value>0.05 at Day 0, <0.02 at Day 14, <0.02 at Days 24, 44, and 112, and <0.002 at Day 75 for *Rassf1a-/-* vs WT. For **pS9-GSK3b** (Fold change is relative to total GSK3b): p-value>0.05 at Days 0, 14, 44, and 75, <0.02 at Day 24, and 0.05 at Day 112 for *Rassf1a-/-* vs WT. For **total GSK3b**: p-value<0.001 at Day 0, <0.03 at Day 14, >0.05 at Day 24, and <0.04 at Days 44, 75, and 112 for *Rassf1a-/-* vs WT. (**B**) Analysis for E-cadherin and N-cadherin expression by immunoblot in colon lysates (experiment repeated four times with similar results). Right panel shows quantitations of left. For **E-cadherin**: p-value>0.05 at Days 0, 44, 75, and 112, <0.04 at Day 14, and <0.05 at Day 24 for *Rassf1a-/-* vs WT. For **N-cadherin**: p-value>0.05 at Day 0, <0.004 at Day 14, <0.003 at Day 24, <0.0001 at Day 44, and <0.02 at Days 75 and 112 for *Rassf1a-/-* vs WT. (**C**) IHC with antibodies specific to E-cadherin or N-cadherin (as indicated) was carried out on mouse colonic sections to determine localization. Top panels show representative hyperplastic regions from Day 112, lower panels show dysplastic regions from Day 112. All images 20X.

A5. Pilot therapeutic study: Imatinib mesylate/3MA combo

In our acute and chronic models of colitis, we showed that loss of RASSF1A in mice resulted in exacerbated inflammation, increased DNA damage and oxidative damage, increased tyrosine phosphorylation of YAP, and increased cell death (see chapters three and four). The increase in disease severity was at least in part caused by the increased cell death due to increased DNA damage promoting the tyrosine phosphorylation of YAP at Y357. Further work done by other members of our lab also showed an increase in autophagy and dysregulation of components of autophagic signaling in the absence of RASSF1A (unpublished observations, see Masters thesis of Y. Fiteih, 2014). In addition to the up-regulation of pY357-YAP in our mouse model of severe colitis, we also observed a significant increase of pY357-YAP in colonic biopsies from IBD patients compared to normal controls, suggesting that pY357-YAP may be an excellent target for new IBD therapeutics.

c-ABL has been shown to induce YAP phosphorylation at Y357 in response to DNA damage, and preliminary studies suggested that imatinib, an inhibitor of the c-ABL kinase, may be somewhat effective in reducing colitis symptoms in our mouse model [3,404]. Because we were unable to fully attenuate colitis symptoms and improve survival in our acute model using imatinib alone, we decided to trial a combination therapy consisting of the PTK imatinib along with the autophagy inhibitor, 3MA [404,550]. The same protocol was used as previously described to induce inflammation-driven carcinogenesis with AOM/DSS (see Figure 2.1 and chapter four), and mice were treated with 60 mg/kg imatinib and 15 mg/kg 3MA injected intraperitoneally twice a week, starting on Day 9 (two days after DSS introduction). IP injections of imatinib and 3MA continued twice weekly until Day 51, two weeks after removing the final course of DSS. Mice were monitored for disease activity as previously described in chapters three and four.

Use of our combination therapy resulted in a slight increase in survival of our *Rassf1a*$^{-/-}$ mice, from 69% to 82%, however, wild type mice suffered a decrease in survival from 79% to 63% (Figure A6 A). While these changes were not significant, these results suggest that if imatinib and/or 3MA therapies may be useful alternatives for future therapeutics, any benefit would likely only be seen in cases showing loss of RASSF1A. Sex did not show any significant differences in responses to drug therapy, however, *Rassf1a*$^{-/-}$ males treated with imatinib/3MA showed increased survival from 52% to 71%, while wild type males treated with imatinib/3MA showed decreased survival from 63% to 43% compared to mice not receiving any therapeutics. Females in both groups showed increased survival from 96% to 100%. While the sex differences were not statistically significant, it is clear that gender-related factors, possibly hormonal, play an important role not only in the inflammatory response, but also in therapeutic treatment. Similarly, *Rassf1a*$^{-/-}$ mice showed a significant decrease in disease activity scores when treated with imatinib/3MA, and this effect was particularly significant in the male population. While wild type mice showed no significant differences in disease activity, there was a decrease in DAI scores towards the end of the experiment (Figure A6 B).

We had hoped that treatment of our mice with the imatinib/3MA combination might result in increased survival and decreased inflammatory disease, and possibly by extension, a reduction in the appearance of inflammation driven carcinogenesis. To this end, we had colonic sections from these mice scored for histological evidence of inflammation and rating of dysplasia severity as described in chapter four. Interestingly, treatment with imatinib/3MA did result in a significant reduction in histological inflammation in both wild type and *Rassf1a*$^{-/-}$ mice (Figure A6 C), suggesting that inflammation was effectively reduced using this combination treatment. Furthermore, there was a significant reduction in the appearance of dysplasia in *Rassf1a*$^{-/-}$ mice but not in wild type mice (Figure A6 D). However, while a statistically significant reduction in dysplasia scoring was seen in *Rassf1a*$^{-/-}$ mice receiving imatinib/3MA, this effect was nearly insignificant (p-value=0.480) and on a relatively small sample size. Additionally,

although the appearance of dysplasia was reduced, some animals did show evidence of intramucosal carcinoma, suggesting that the therapy can be improved either by modifying the dosages, modifying the frequency of administration, modifying the duration of the therapy, or possibly by changing the combination of drugs used.

Discussion:

As mentioned above, our pilot studies utilizing a combination therapy of imatinib/3MA showed a limited effect at improving survival and reducing disease symptoms, however this effect was only seen in our *Rassf1a* knockout mice (Figure A6 A and B). In fact, wild type mice showed aggravated symptoms and reduced survival on the therapy compared to without. This finding supports a current movement toward precision medicine, and the understanding that finding one single "magic bullet" therapy for any disease with consistent results in all patients is unlikely. Our mouse models suggest that patients lacking RASSF1A and/or showing abnormal pY357-YAP up-regulation likely have a more severe disease phenotype, and will respond in a much more favorable manner to therapies targeting signaling pathways known to be dysregulated in such cases. In fact, because wild type mice respond so poorly to this therapeutic combination when compared to *Rassf1a*$^{-/-}$ mice, this suggests that completely different signaling pathways may be affected by administration of imatinib/3MA in these mice.

Furthermore, as we see differences in responses between males and females in our model system, further research is needed to examine what factors contribute to sex based differences both in disease pathogenesis and in therapeutic response. It is possible that hormonal influences are responsible for sex based differences, or possibly differences in lipid signaling and metabolic responses. Interestingly, while wild type mice showed reduced survival and no change in disease severity, they did show a significant

reduction in histological evidence of inflammation, in a similar manner to the *Rassf1a*^{-/-} mice (Figure A6 C). This suggests that while the imatinib/3MA may be effective at reducing inflammation as intended, there may be confounding off-target effects in the wild type mice, due to their normal apoptotic and autophagic responses. The possibility of off-target side effects further strengthens the idea of using precision medicine in the future.

Finally, as discussed above, while we were able to reduce the appearance of dysplasia in *Rassf1a*^{-/-} receiving imatinib/3MA mice to some degree, this effect was nearly insignificant (p-value=0.0480) and on a relatively small sample size. Additionally, although the appearance of dysplasia was reduced, some animals did show evidence of intramucosal carcinoma, suggesting that the therapy can be improved either by modifying the dosages, modifying the frequency of administration, modifying the duration of the therapy, or possibly by changing the combination of drugs used. Further modifications will need to be tested in order to determine the best combination and administration protocol; however these results suggest that our research may be heading in the right direction for potential new IBD therapeutic targets and diagnostic biomarkers.
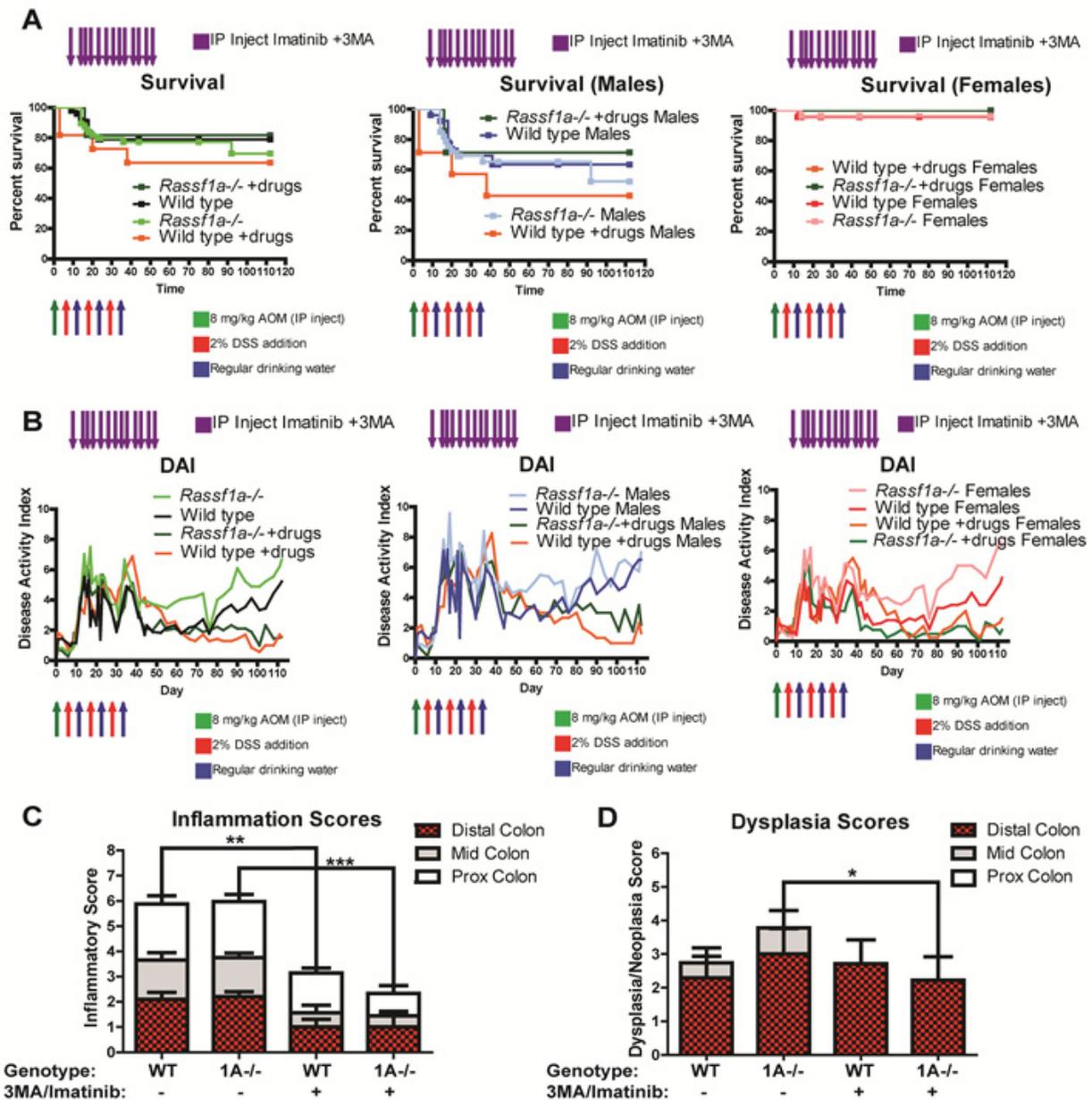
Figure A6. Pilot study using 3MA/Imatinib combination therapy in an inflammation induced carcinogenesis model. (**A**) Kaplan-Meier curve monitoring % survival following inflammation induced carcinogenesis. No significant differences in survival between mice recieving 3MA/imatib injections and those not for any groups. (**B**) Disease activity index (DAI) following following inflammation induced carcinogenesis. p-value<0.05 at Days 34 and 101, <0.01 at days 90, 108, and 111, and <0.001 at Day 112 for *Rassf1a-/-* vs *Rassf1a-/-* +drugs; p-value<0.05 at Day 112 for *Rassf1a-/-* +drugs vs WT +drugs; <0.05 at Days 17 and 112 for *Rassf1a-/-* males vs *Rassf1a-/-* males +drugs; p-value<0.001 at Day 111 and <0.01 at Day 112 for *Rassf1a-/-* females vs *Rassf1a-/-* females +drugs; p-value<0.05 at Day 14 for WT males vs WT males +drugs; no other significant differences between groups. (**C**) Inflammation scoring of colonic sections following inflammation induced carcinogenesis. p-value>0.05 for *Rassf1a-/-* vs WT at Day 112 (no drugs); p-value<0.01 for WT Day 112 vs WT D112 +drugs; p-value<0.0008 for *Rassf1a-/-* Day 112 vs *Rassf1a-/-* Day 112 +drugs; and p-value>0.05 for *Rassf1a-/-* Day 112 +drugs vs WT Day 112 +drugs. No significant male/females differences were seen. (**D**) Dysplasia scoring of colonic sections following inflammation induced carcinogenesis. p-value<0.01 for *Rassf1a-/-* vs WT at Day 112 (no drugs); p-value>0.05 for WT Day 112 vs WT D112 +drugs; p-value<0.05 for *Rassf1a-/-* Day 112 vs *Rassf1a-/-* Day 112 +drugs; and p-value>0.05 for *Rassf1a-/-* Day 112 +drugs vs WT Day 112 +drugs. No significant male/females differences were seen. For **A-D**, n=7-11 for AOM/DSS +3MA/imatinib groups, and n=24 for AOM/DSS groups. For A-D "+drugs" indicates IP injections with 15mg/kg 3MA and 60mg/kg imatinib. See also Figure 4.1.